AD-A064 143 NEW MEXICO UNIV ALBUQUERQUE BUREAU OF ENGINEERING R--ETC F/G 9/1
INVESTIGATION OF INTERFACE STATES USING METAL-OXIDE-SILICON TRA--ETC(U)
AUG 78 J WHITEFIELD, H D SOUTHWARD F29601-75-C-0036
UNCLASSIFIED EE-247(77)AF-352-1 AFWL-TR-77-140-VOL-1 NL

1 OF 4
AD A064143

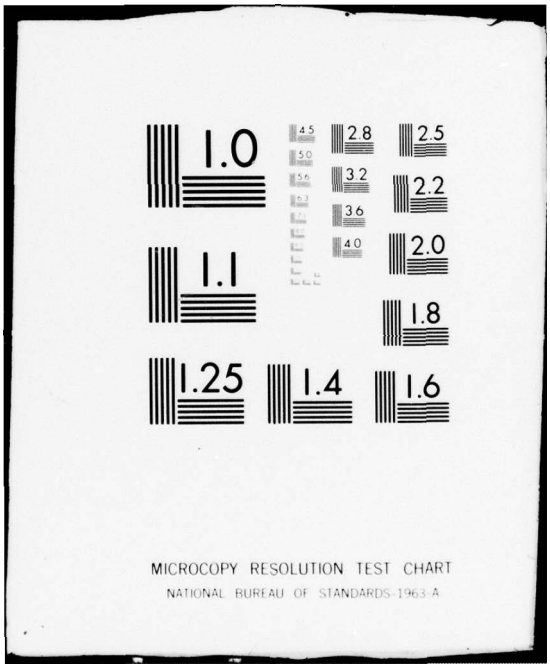
1.0
1.1
1.25
1.4
1.6
1.8
2.0
2.2
2.5
2.8
3.2
3.6
4.0
4.5
5.0
5.6
MICROCOPY RESOLUTION TEST CHART
NATIONAL BUREAU OF STANDARDS-1963-A

AFWL-TR-77-140, Vol. I

(2) LEVEL III

AFWL-TR-
77-140
Vol. I

DDC

AD A064143

DDC FILE COPY

INVESTIGATION OF INTERFACE STATES USING METAL-OXIDE-SILICON TRANSISTORS AND PULSE GATE TECHNIQUES

Volume I of II
Hall Effects Measurements

University of New Mexico
Bureau of Engineering Research
Albuquerque, NM 87131

1978 August

Final Report

Approved for public release; distribution unlimited.

AIR FORCE WEAPONS LABORATORY
Air Force Systems Command
Kirtland Air Force Base, NM 87117

AFWL-TR-77-140

This final report was prepared by the University of New Mexico, Bureau of Engineering Branch, Albuquerque, New Mexico, under Contract F29601-75-C-0036, Job Order 88091123 with the Air Force Weapons Laboratory, Kirtland Air Force Base, New Mexico. Mr. Roe J. Maier (ELP) was the Laboratory Project Officer-in-Charge.

When US Government drawings, specifications, or other data are used for any purpose other than a definitely related Government procurement operation, the Government thereby incurs no responsibility nor any obligation whatsoever, and the fact that the Government may have formulated, furnished, or in any way supplied the said drawings, specifications, or other data is not to be regarded by implication or otherwise as in any manner licensing the holder or any other person or corporation or conveying any rights or permission to manufacture, use, or sell any patented invention that may in any way be related thereto.

This report has been authored by a contractor of the United States Government. Accordingly, the United States Government retains a nonexclusive, royalty-free license to publish or reproduce the material contained herein, or allow others to do so, for the United States Government purposes.

This report has been reviewed by the Information Office (OI) and is releasable to the National Technical Information Service (NTIS). At NTIS, it will be available to the general public, including foreign nations.

This technical report has been reviewed and is approved for publication.

Roe J. Maier Jr

ROE J. MAIER
Project Officer

FOR THE COMMANDER

Aaron B. Loggins

AARON B. LOGGINS
Lt Colonel, USAF
Chief, Transient Radiation
Effects (TREE) Branch

Donald A. Dowler

DONALD A. DOWLER
Colonel, USAF
Chief, Electromagnetics Division

DO NOT RETURN THIS COPY. RETAIN OR DESTROY.

AD A064094

UNCLASSIFIED

SECURITY CLASSIFICATION OF THIS PAGE *(When Data Entered)*

REPORT DOCUMENTATION PAGE

READ INSTRUCTIONS BEFORE COMPLETING FORM

1. REPORT NUMBER: AFWL-TR-77-140, Vol I
2. GOVT ACCESSION NO.:
3. RECIPIENT'S CATALOG NUMBER:

4. TITLE *(and Subtitle)*: INVESTIGATION OF INTERFACE STATES USING METAL-OXIDE-SILICON TRANSISTORS AND PULSE GATE TECHNIQUES. Volume I. Hall Effects Measurements.

5. TYPE OF REPORT & PERIOD COVERED: Final Report.

6. PERFORMING ORG. REPORT NUMBER: EE-247(77)AF-352-1

7. AUTHOR(s): Jan Whitefield, H. D. Southward

8. CONTRACT OR GRANT NUMBER(s): AF29601-75-C-0036

9. PERFORMING ORGANIZATION NAME AND ADDRESS: University of New Mexico, Bureau of Engineering Research, Albuquerque, New Mexico 87131

10. PROGRAM ELEMENT, PROJECT, TASK AREA & WORK UNIT NUMBERS: 62601F, 88091123

11. CONTROLLING OFFICE NAME AND ADDRESS: Air Force Weapons Laboratory (EL), Kirtland Air Force Base, NM 87117

12. REPORT DATE: August 1978

13. NUMBER OF PAGES: 290

14. MONITORING AGENCY NAME & ADDRESS *(if different from Controlling Office)*: 292 p.

15. SECURITY CLASS. *(of this report)*: UNCLASSIFIED

15a. DECLASSIFICATION/DOWNGRADING SCHEDULE:

16. DISTRIBUTION STATEMENT *(of this Report)*: Approved for public release; distribution unlimited.

18. AFWL, SBIE

19. TR-77-140-Vol-1, AD-E200 923

17. DISTRIBUTION STATEMENT *(of the abstract entered in Block 20, if different from Report)*:

18. SUPPLEMENTARY NOTES:

19. KEY WORDS *(Continue on reverse side if necessary and identify by block number)*

Hardness Assurance	Radiation Hardening
Surface Effects	Total Dose Effects
Interface States	Hall Measurements
Pulsed Field Effect	Radiation Effects
Transient Radiation Effects	Nuclear Radiation Vulnerability

20. ABSTRACT *(Continue on reverse side if necessary and identify by block number)*

A single metal-oxide-silicon chip was designed containing capacitors for capacitance-voltage (C-V) and devices for Hall effect measurements on the channel region of a metal-oxide-silicon field effect transistor. These two measurements provide data to calculate interface state density (N_{ss}) in the mid gap region and near the band edges as functions of surface potential. Both Hall and conductivity mobility are calculated. It was found that N_{ss} increases with total gamma radiation dose in the mid gap region but may either increase

over

DD FORM 1 JAN 73 1473 EDITION OF 1 NOV 65 IS OBSOLETE

UNCLASSIFIED

SECURITY CLASSIFICATION OF THIS PAGE *(When Data Entered)*

or decrease near the band edges, implying that interface states may arise from different mechanisms. Dangling bond and oxygen deficiency models are discussed as pertaining to possible mechanisms. Mobility versus surface potential demonstrate consistent results. Strongly inverted device channels yield mobilities which are very insensitive to radiation, indicating predominance of carrier-carrier scattering. But lightly inverted channels demonstrate that mobility is highly dependent upon radiation, indicating predominance of carrier-interface scattering.

PREFACE

The authors would like to thank the many persons who contributed on technical problems in this work. Mr. Roe Maier of the Air Force Weapons Laboratory contributed many hours with suggestions and criticism of experiments and theory. Dr. Roy Colclaser and Dr. Shyam Gurbaxani of The University of New Mexico reviewed this report. Dr. W. D. Brown and Sandia Laboratories are thanked for their invaluable advice and technical services. Dr. J. Starner of The University of New Mexico gave much advice in analytical and computational techniques. Mr. James Southward is thanked for his versatile and untiring efforts with data acquisition, data reduction, computations, and graphical work. Mr. Anthony Giraudo is thanked for his technical criticisms while performing related work. Mr. Robert Pezzano did the work in interfacing computer routines to Air Force computers. Finally, the authors are deeply indebted to the Air Force Weapons Laboratory for making this work possible.

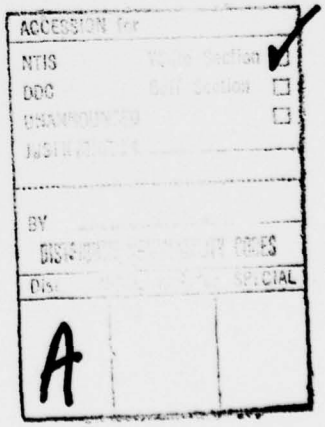

TABLE OF CONTENTS

TABLE OF CONTENTS (continued)

LIST OF FIGURES

LIST OF TABLES

CHAPTER I

INTRODUCTION

The metal-oxide-semiconductor field-effect-transistor (MOSFET) currently enjoys wide use in the electronics industry. Certain salient features of this device make it superior to its bipolar counterparts in many applications. The MOSFET can be found in virtually any type of electronic apparatus. It is used in monitoring devices, controlling devices, test equipment, home audio equipment, and is the basis for many integrated circuit devices. Interest in the influence of radiation on MOSFETs is very widespread and intense. Certainly the military is extremely concerned with how a particular instrument reacts to a radiation environment. Closer to the individual, however, is the concern for its use in nuclear power plant and hospital radiation environments. Much of today's communication is transmitted via satellites which are continuously exposed to radiation. Thus, radiation influence on electronics, and specifically MOSFETs, is of concern to a great number of diverse people.

The concern for MOSFET susceptibility to radiation is not particularly new. In 1964 Hughes and Girous (Ref. 1) submitted one of the pioneer reports in the area of radiation effects on MOSFETs. Specifically how radiation could physically affect an MOS was first inferred from some experiments on bipolar transistors. It was shown that the dc current gain and collector-base reverse leakage are both affected by ionizing radiation (Refs. 2, 3, 4, 5, 6). These changes were linked to charge trapping or charge build-up in the passivating oxide. This result was particularly important because charge trapping certainly

could occur in the gate oxide of a MOSFET and significantly affect its characteristics.

A large number of investigators then took the initiative and began to examine MOS transistors. In 1965 it was determined that, as was expected, charge buildup in gate oxides occurs during ionizing radiation bombardment. Furthermore, the amount of charge buildup is affected by the presence of an electric field in the oxide when the radiation occurs. (See Refs. 7, 8, 9, 10, and 11.)

The problem of radiation effects on MOSFETs was further complicated when Zaininger (Refs. 12, 13) discovered that along with oxide charge buildup came the production of surface states or interface states. Dennehy (Ref. 14) supplied supportive data on this point in late 1966.

These investigations along with many others led to the definition of two separate effects. First, ionizing radiation inevitably leads to a buildup of charge in the oxide. This charge is invariably positive due to the loss of mobile electrons, and its magnitude depends on the polarity and strength of the electric field in the oxide at the time of radiation. Second, an increase in the number of interface states also accompanies radiation along with possible changes in the shape of the interface state density function.

Once these two effects were defined, researchers attempted to find ways to minimize them. The trapped oxide charge was thought to be manifested by a shift in the so-called "flat-band" voltage, while changes in the interface state density are manifested by changes in the "threshold" voltage. Capacitance voltage curves (C-V curves) of an MOS capacitor are often used to characterize the oxide used in a MOSFET. Proper analysis of the C-V curves allows one to determine both the flat-band voltage and

threshold voltage. The presence of a large trapped oxide charge can be detected by a shift of the C-V curve along the voltage axis. The introduction of a large number of surface states can be determined by a change in the shape of the C-V curves.

The total charge trapped in the oxide may be reduced by controlling the fabrication processes and starting materials. Specific silicon lattice orientation, growth temperatures, and anneal temperatures, controlled growth atmospheres, and particular cleaning techniques are typical factors considered in growing high quality gate oxides. In addition, impurities can be introduced during oxide growth that can form complexes with positive ions in the oxide rendering them electrically neutral.

Optimum use of the measures mentioned above has reduced the flat band voltage shifts to a fraction of that in earlier devices. Reduction of flat band voltage shift has been accompanied by a corresponding decrease in the threshold voltage shift (Refs. 15, 16, 17).

The technology has reached a point today where the change in the interface state density (N_{ss}) is the predominant effect one sees in radiation studies. Thus, changes in N_{ss} are currently being studied. The ultimate goal in these studies is to supply enough varied physical data and trends so that some physical model can be developed to fully explain the influence of radiation on N_{ss}. Hopefully this model would lead to the fabrication of transistors which are even more resistant to radiation than those fabricated today.

Various methods for measuring N_{ss} as a function of surface potential have been devised. Each method has its inherent good points and

drawbacks. The C-V technique in one form or another enjoys the widest use. It is the easiest technique to perform, and covers the mid gap region. Using C-V techniques, Sivo et al. (Ref. 18) has demonstrated that N_{ss} increases with radiation dose regardless of the energy position in the gap. Similar confirming data were presented by Kjar and Nichols (Ref. 19) also using C-V techniques.

The C-V technique is inherently limited to studying about ±10 kT around the intrinsic Fermi level. kT is a commonly used term for thermal energy where k is Boltzmann's Constant and T is absolute temperature. The value of kT is most conveniently viewed as 0.026 electron volts (eV) for every temperature of each 300 K. The total band gap is about 42 kT at room temperature, so these data only cover about half the band gap and are limited only to the mid gap.

The primary purpose of this study is to supply data on the variation of N_{ss} with total radiation dose in the energy ranges of both the mid gap and band edge energies. The data presented here will cover about 20 kT in the mid gap and about 6 kT above the valence band down to the valence band edge. It is hoped that by examining N_{ss} at both the mid gap and band edges simultaneously, some indication of their relative contributions to device radiation susceptibility can be made.

In calculating N_{ss} using the micro-Hall conductance technique, one additional parameter that is calculated as an intermediate step is the mobility as a function of surface potential. Since mobility plays an important role in device operation, these data will be correlated to the N_{SS} data to see if any similarities exist.

CHAPTER II

DEVELOPMENT OF THE QUASI-STATIC C-V TECHNIQUE

1. INTRODUCTION

Many techniques have been developed to determine $N_{ss}(\phi_s)$. Each method has its own inherent good and bad features. Most of the techniques that have been developed utilize either an MOS transistor or an MOS capacitor as the device on which measurements are performed. The measurements made on an MOS capacitor fall into two categories. One method determines the capacitance-voltage (C-V) characteristics of the capacitor at high frequencies, low frequencies, or both. Proper handling of these data and comparisons made between theoretical data and the raw data allow one to determine the variation of the interface state density, $N_{ss}(cm^{-2}eV^{-1})$ with surface potential, ϕ_s. A second method of $N_{ss}(\phi_s)$ determination using a capacitor comes from examining the ac conductance through the capacitor at various frequencies. This is the ac conductance technique. The remaining methods for determining $N_{ss}(\phi_s)$ use measurements taken on an MOS transistor. In these techniques the dc surface conductance is measured as a function of gate voltage, and proper analysis of these data again can yield $N_{ss}(\phi_s)$. Notice that this conductance is the channel conductance and is normally a dc measurement. This should not be confused with the ac conductance technique looking at the ac conductance through a capacitor.

Terman (Ref. 20) first introduced a capacitance technique in 1962. In this technique, one determines a high frequency C-V curve and compares it to an ideal curve. The comparison of the high frequency and ideal curves allows one to determine N_{ss} as a function of applied gate

voltage, V_g, as well as the variation of the applied gate voltage with surface potential, $V_g(\phi_s)$. The frequency used in this determination is in the range of 0.1 to 1 MHz. One assumption made in this theory is that the frequency of the applied signal is high enough that the surface states cannot respond to the applied signal at high frequencies. Later data have shown that the lifetime of surface states decreases from the mid gap going toward the band edges. The high frequency used in these measurements limits the range of the band gap which can be scanned to about ±8 to 10 kT around mid gap. The main disadvantages of this technique are: (1) it is limited to about ±8 to 10 kT around mid gap, (2) theoretical curves are needed in calculations $N_{ss}(V_g)$ and $V_g(\phi_s)$, and (3) numerical differentiation of the raw data is required.

In 1967, the ac conductance technique was developed by Nicollian and Goetzberger (Ref. 21). This technique measures the ac conductance of a capacitor at different frequencies and various gate biases. These data can be analyzed to yield $N_{ss}(V_g)$. An accompanying capacitance curve still yields $V_g(\phi_s)$, so the interface state density can be characterized. This technique yields not only $N_{ss}(\phi_s)$, but also information concerning the lifetimes and cross sections of the interface states. The main disadvantages are: (1) it requires an incredible number of measurements, and (2) it is also limited to mid gap determinations.

Neither the conductance technique nor the C-V technique mentioned above yield any information about N_{ss} near the band edges. The first technique used in making this determination was proposed by Gray and Brown (Ref. 22) in 1966. This technique examines the flat band voltage shift as a function of temperature. By varying the temperature, one can move the relative position of the Fermi level to the band edges.

The flat band voltage shift is determined from a high frequency C-V curve. The limitations on how much of the energy gap can be scanned are determined by the temperature limits. At sufficiently high temperatures certain ions in the oxide became mobile, limiting the upper temperature. At lower temperatures the dopant atoms begin to deionize. This limits the Gray-Brown technique to 4 to 6 kT above the valence band and below the conduction band.

All of the above techniques involve measurements on MOS capacitors. In 1968 Fang and Fowler (Ref. 23) and E. Arnold (Ref. 24) both introduced techniques that employ measurements taken on an MOS transistor. Both of the techniques are similar in that they assume the charge induced under the gate of an MOS transistor can be split into two types; (1) charge which is trapped in the interface states and therefore does not contribute to conduction and (2) free charge which does contribute to conduction. Arnold considered the difference between the theoretical surface conductance and the actual measured surface conductance, and attributed the difference to trapped charge. On the other hand, Fang and Fowler examined the difference between the total induced charge and theoretical induced charge. Again the difference is attributed to charge trapped in N_{ss}. Both techniques scan from the band edges toward the middle. Fang and Fowler look at about 7 to 8 kT below E_c and above E_v where E_c and E_v are the conduction and valence band edges. Arnold, however, presents data for about 13 kT below E_c and above E_v. Arnold was able to extend his useful range by varying the temperature at which measurements are made. The main disadvantages of these techniques are that no mid gap information is supplied.

It can readily be seen from the above discussion that no single technique has evolved that can yield information on N_{ss} over the entire

band gap. For the purpose of this study, two techniques have been chosen for N_{ss} determination. The mid gap data are supplied using a modified C-V technique first developed by Castagne (Ref. 25) and later employed by Kuhn (Ref. 26). This technique, called the quasi-static C-V technique, uses a combination of low frequency and high frequency curves to get $N_{ss}(V_g)$. Further, $V_g(\phi_s)$ is found from comparing the high frequency curve to theoretical curves. The high frequency curve is taken at 1 MHz, while the low frequency curve is taken at 500 seconds/cycle, or 0.002 Hz. This technique allows determination of N_{ss} about ±12 kT from mid gap.

The band edge determinations are done using a modification of the Fang and Fowler technique first presented by Sakaki, et al. (Ref. 27). The Fang and Fowler technique measured the Hall carrier concentration in an MOS transistor and used this value for the free carrier density. Actually, the induced Hall carrier density differs from the surface free carrier density by the Hall mobility ratio $r = \mu_H/\mu_\sigma$ where μ_H is the Hall mobility and μ_σ is the surface conductivity mobility. Thus, Fang and Fowler assumed $r = 1$. The Sakaki technique eliminates this assumption by taking appropriate measurements that allow simultaneous determination of N_H, the Hall carrier density, and r.

The data derived from these techniques will cover ±12 kT around mid gap and 6 kT and above E_v. The total band gap is about 42 kT at 300 K, so the data presented here will cover about 71% of the total energy gap.

The next section of this chapter is devoted to reviewing semiconductor surface field effects and deriving some expressions for the space charge layer capacitance in inversion, depletion, and accumulation.

In the third section of the chapter, we consider the circuit model most used to describe MOS capacitors. By using the results of the second section we see what approximations go into the quasi-static C-V technique and develop the final model used in the C-V technique.

In the fourth section of this chapter the equations needed for the C-V analysis are reviewed. Finally, the fifth section is a summary of how the technique is implemented and what equations are actually used in the analysis.

2. A REVIEW OF SEMICONDUCTOR SURFACE FIELD EFFECTS

Before developing a model for the MOS capacitor, a brief review of some of the properties of a semiconductor surface under the influence of an electric field is presented. Some definitions stated here will be useful in the discussion modeling the MOS capacitor. This review follows one in Reference 28, but can be found in any good reference book on MOS surfaces.

Figure 1 pictures a basic semiconductor surface under the influence of different electric fields or "biasing conditions." Figures 1a and 1b represent an n-type semiconductor in accumulation and inversion, respectively. Figures 1c and 1d represent the same conditions for a p-type semiconductor. Near the surface some useful variables can be defined. Let E_i be the intrinsic Fermi level. It is parallel to E_c and E_v and lies close to mid gap. The potential ϕ can be defined by

$$q\phi = E_f - E_i \tag{1}$$

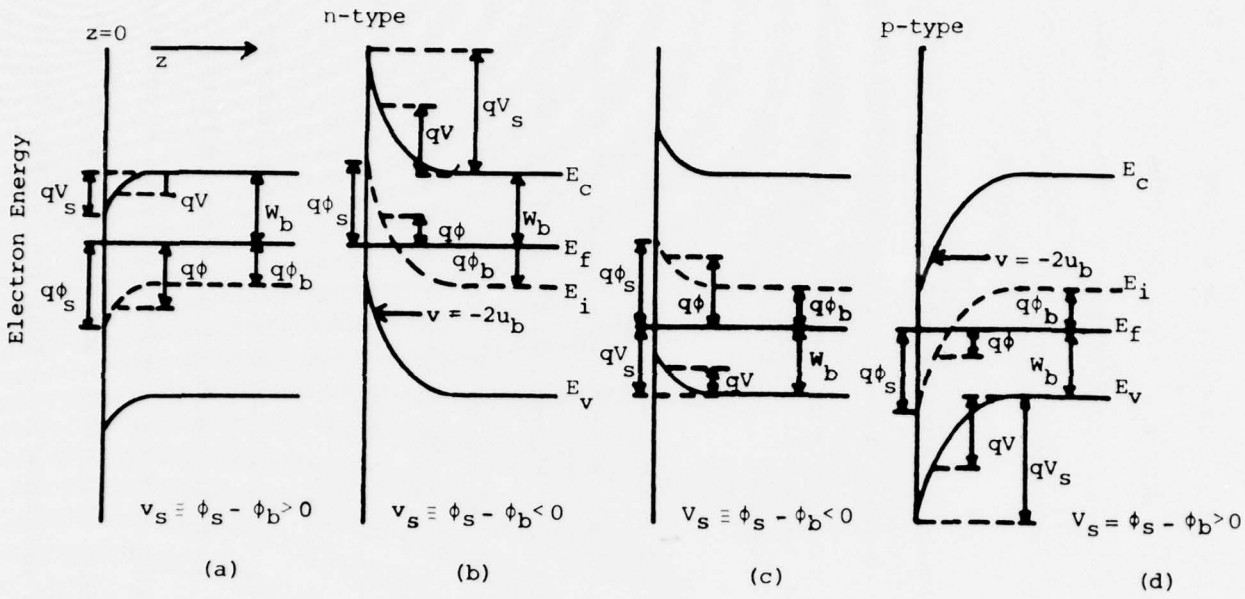

Figure 1. Energy Level diagram indicating the various energy parameters used to characterize the space charge region. (See Ref. 28).
a) n-type semiconductor, accumulation
b) n-type semiconductor, inversion
c) p-type semiconductor, accumulation
d) p-type semiconductor, inversion

where q is the absolute value of the charge on an electron. This equation defines the position of E_i with respect to the Fermi level, E_f. The exact position of E_i in nondegenerately doped semiconductors can be located in the bulk by

$$E_i = \frac{1}{2}\left(E_c + E_v\right) - \frac{1}{2} kT \left(\ell n \left(N_c/N_v\right)\right) \tag{2}$$

where

$$N_c \equiv 2\left(2\pi m_n^* kT/h^2\right)^{3/2} \tag{3}$$

and

$$N_v = 2\left(2\pi m_p^* kT/h^2\right)^{3/2} \tag{4}$$

The quantities N_c and N_v are the normally defined conduction and valence band effective density of states at the band edges.

The value of ϕ in the bulk is referred to as ϕ_b, and at the surface it is ϕ_s. Notice, if $\phi_s = \phi_b$, the bands are not bent at the surface, and the condition is referred to as flat band condition.

The potential barrier an electron sees going from the bulk to the surface is defined by

$$V(z) \equiv \phi(z) - \phi_b \tag{5}$$

where V(z) is the potential barrier referenced to the bulk. When $V_s = 0$, $\phi_s = \phi_b$ and this again corresponds to flat band conditions.

Two dimensionless potentials u and v may be defined as

$$u \equiv q\phi/kT \tag{6}$$

and

$$v \equiv qV/kT \tag{7}$$

Thus, these potentials are normalized in units of kT.

Again, for nondegenerately doped semiconductors where $E_c - E_f >> kT$ and $E_f - E_v >> kT$, the following well known relationships exist:

$$n = N_c e^{-(E_c - E_f)/kT} \tag{8}$$

and

$$p = N_v e^{-(E_f - E_v)/kT} \tag{9}$$

Using the definitions of Equations 1 through 7, the hole and electron concentrations can be written in terms of the dimensionless potentials as

$$n(z) = n_i e^{u} = n_b e^{v} \tag{10}$$

and

$$p(z) = n_i e^{-u} = p_b e^{-v} \tag{11}$$

The following definitions have been employed.

$$n_i = p_i = N_c e^{-(E_c - E_i)/kT} = N_v e^{-(E_i - E_v)/kT} \tag{12}$$

$$n_b = N_c e^{-(E_{cb} - E_f)/kT} \tag{13}$$

$$p_b = N_c e^{-(E_f - E_{vb})/kT} \tag{14}$$

The subscript b implies bulk value, so E_{cb} and E_{vb} are the conduction and valence band energies in the bulk.

Z is defined as zero at the semiconductor surface and increasing into the silicon bulk. It should be noted that both u and v are z dependent.

Some common definitions can be made now. First, note that when $u>0$, $n>p$ and when $u<0$, $p>n$. Similarly, when $v>0$, $n>n_b$ and $p<p_b$. Also, when $v<0$, $n<n_b$ and $p>p_b$.

As was mentioned before, when $v_s = 0$, the bands are flat to the surface, and we have flat band conditions. At any point where $u = 0$ the carrier densities are intrinsic. Specifically, when $u_b = 0$ the bulk is intrinsic, and when $u_s = 0$ the surface is intrinsic.

When u_b and v_s are the same sign, the majority carrier density is greater in the space charge region than it is in the bulk. This condition is termed accumulation. Here u_b and v_s must be positive for n-type material and negative for p-type material.

If u_b and v_s are of opposite sign, the space charge region is either depleted or inverted. When $v_s = -u_b$, the surface is intrinsic, as mentioned before, and the space charge region is depleted. When $v_s = -2u_b$, from the point where $v = -u_b$ to the surface, the minority carrier density is greater than the majority carrier density, but is not greater than the bulk majority carrier density. This is termed weak inversion. The condition where $v = -2u_b$ is referred to as the strong inversion point, and marks the point at which the minority carrier density is greater than the bulk majority carrier density.

Summing up these definitions, the following conditions can be stated for n-type material. Let u_b be positive

dimensionless potential v	regime
$v>0$	accumulation
$-u_b<v<0$	depletion
$-2u_b<v<-u_b$	weak inversion
$v<-2u_b$	strong inversion.

Similar restrictions on p-type material can be stated. In practice, many measurements are difficult to perform in weak inversion. The majority of literature has adopted the concept of incorporating the weak inversion region with the depletion region. Unless otherwise stated, this will be true throughout this work.

It is convenient at this time to do some analysis with the semiconductor surface and derive some results that will be useful later. Specifically, consider now Poisson's equation for the case where the bands are not sufficiently bent to cause degeneracy at the surface.

Poisson's equation in one dimension can be written as

$$\frac{d^2V}{dz^2} = - \frac{\rho(z)}{\kappa_s \varepsilon_o} \tag{15}$$

The charge density in coul/cm^3 is the sum of any ionized donor and acceptor atoms summed with the hole and electron concentrations. Using the case of constant impurity doping and complete ionization, the fixed charge density is $N_D - N_A$. Charge neutrality in the bulk means that $N_D - N_A = p_b - n_b$. Using the dimensionless potential v, Equation 15 can be written as

$$\frac{d^2v}{dz^2} = - \frac{q^2}{\kappa_s \varepsilon_0 kT} \left(n_b - p_b + p_b e^{-v} - n_b e^{v} \right) \tag{16}$$

Let us now define a parameter L, the effective Debye Length, as

$$L \equiv \sqrt{\frac{\kappa \varepsilon_o kT}{q^2 \left(n_b + p_b \right)}} \tag{17}$$

This definition is made with a little foresight. It will be seen that v will decrease with a characteristic length L, and L therefore characterizes the width of the depletion region.

Equation 16 then becomes

$$\frac{d^2v}{dz^2} = \frac{-1}{L^2} \frac{\left(n_b - p_b + p_b e^{-v} - n_b e^{v}\right)}{n_b + p_b} \tag{18}$$

which, using Equations 10 and 11, simplifies to

$$\frac{d^2v}{dz^2} = \frac{-1}{L^2} \frac{\sinh\left(u_b + v\right)}{\cosh u_b} - \tanh u_b \tag{19}$$

The boundary conditions employed here are that $v = v_s$ at $z = 0$ and $v = 0$ as $z \to \infty$. If Equation 19 is multiplied by 2 dv/dz, it can be integrated directly to yield

$$\frac{dv}{dz} = \pm \frac{F}{L} \tag{20}$$

and

$$\frac{z}{L} = \int_{v_s}^{v} \frac{dv}{\pm F} \tag{21}$$

where

$$F\left(u_b, v\right) \equiv \sqrt{2}\left[\frac{\cosh\left(u_b + v\right)}{\cosh u_b} - v \tanh(u_b) - 1\right]^{1/2} \tag{22}$$

The upper sign here refers to $v<0$ and the lower sign to $v>0$. Notice that Equation 20 is an equation for the electric field since $\xi = -\Delta V$.

In general, solutions to Equation 21 are nonanalytical, and can only be solved through numerical methods. Certain simplifications can be made, however, with instructive physical consequences. The magnitude of the space charge capacitance will be important later in this chapter, and one can obtain estimates for it through examination of Equation 21.

Let us define a space charge density Q_{sc} as the total net charge in the space charge region per unit area. Then by Gauss' law, Q_{sc} must satisfy the equation

$$Q_{sc} = \kappa_s \varepsilon_o \xi_s \tag{23}$$

where ξ_s is the electric field just inside the semiconductor surface. The value for ξ_s can be found using Equation 20.

$$\xi_s = \frac{kT}{q}\frac{dv}{dz} = \pm \frac{kT}{q}\frac{F\left(u_b, v_s\right)}{L}$$

The sign of ξ_s is chosen here to be positive when directed outward from the silicon surface. The space charge can now be written as

$$Q_{sc} = \pm q\left(n_b+p_b\right) LF\left(u_b, v_s\right) \tag{24}$$

The quantity of interest here is the space charge capacitance per unit area, and it would be convenient to express it in some form similar to a parallel plate capacitor equation. Toward that end, let an effective charge distance L_c be defined as the center of charge in the space charge region measured from the surface, or the first moment of the charge.

$$L_c \equiv \frac{\int_o^\infty \rho z dz}{\int_o^\infty \rho dz} \equiv \frac{\int_o^\infty \rho z dz}{Q_{sc}} \tag{25}$$

This can be integrated by parts to obtain

$$L_c = \frac{\left[z\int \rho dz\right]_o^\infty}{Q_{sc}} - \frac{\int\left(\int \rho dz\right)dz}{Q_{sc}} \tag{26}$$

From Equation 15, it can be seen that

$$d\left(\frac{dv}{dz}\right) = \frac{-q\rho}{\kappa_s \varepsilon_o kT}\, dz \tag{27}$$

Using Equation 20, this can be written as

$$d\left(\pm \frac{F}{L}\right) = \frac{-q}{\kappa_s \varepsilon_o kT} \rho dz \tag{28}$$

Equation 26 can now be integrated to yield

$$L_c = \frac{-\left[z\left(F\ u_b, v\right)\right]_o^\infty}{F\left(u_b, v_s\right)} + \frac{\int_o^\infty F\left(u_b, v\right) dz}{F\left(u_b, v_s\right)} \tag{29}$$

Examination of the function F reveals that as $z \to \infty$, $F \to 0$, so the first term in the right hand side of Equation 29 vanishes at both the upper and lower limits. With the help of Equation 20, this can now be written as

$$L_c = \frac{\left|v_s\right|}{F\left(u_b, v_s\right)} L \tag{30}$$

Finally, if the space charge capacitance is defined as the ratio of the space charge density to the barrier height, then the space charge capacitance per unit area can be written as

$$C_{sc} = \left|\frac{Q_{sc}}{v_s}\right| = \frac{\kappa_s \varepsilon_o}{L_c} \tag{31}$$

Equation 31 is a very important equation for future discussions, and has a simple physical interpretation. The space charge capacitance can be considered as a parallel plate capacitor with one plate at the semiconductor surface, and the other located at the center of charge. Notice that Equation 31 represents specific capacitance, or capacitance per unit area.

Using Equation 31 it is now possible to examine the approximate size C_{sc} may take in various regions of biasing.

Proceeding along these lines then, the magnitude of C_{sc} will be examined in accumulation, depletion, and inversion for an n-type semiconductor. Consider again Figure 1a. In the accumulation region, the charge is due to the hole and electron concentrations summed with the fixed ionized dopant densities as is in Equation 16. For most semiconductors one dopant density is much larger than the other. For n-type semiconductors $N_D >> N_A$, and similarly $n >> p$. Here, N_D and N_A have their usual definitions of the donor and acceptor concentrations. In the bulk, charge neutrality is maintained and $n \simeq N_D$ in this case. In accumulation, N_D cannot increase, but n does. If the surface potential is sufficiently strong, the charge in the space charge region then depends mainly on n, the majority carrier density.

The situation in strong inversion is similar. At the point of onset of strong inversion, $p \simeq N_D$. As the surface potential increases, the density of p increases and it becomes the dominant charge in the inversion region. Thus, in the inversion region the minority carrier density is dominant.

In depletion and weak inversion, $N_D > n$ and $N_D > p$. Consider, for example, the depletion region, and let the amount of band bending be about 3 kT into depletion.

Using Equation 10 the electron concentration can be written as

$$n \simeq N_D e^{-3} \simeq \frac{N_D}{20}$$

Similarly, consider the region between weak and strong inversion at a bias where the bands are bent 3 kT less than the strong inversion point, the minority carrier density can also be written as

$$p \simeq N_D e^{-3} \simeq \frac{N_D}{20}$$

Thus, in both depletion and weak inversion, the major contributor to Q_{sc} is the ionized fixed charges. This is the justification for placing weak inversion under the terminology of depletion.

Now consider what happens to the thickness of the space charge region under the influence of the electric field. If the surface is strongly accumulated, there is a lot of charge in the space charge layer, but it is concentrated at the surface because the charge is almost entirely due to n, which increases exponentially toward the accumulated surface. Thus, the greater v_s, the smaller L_c. If the electric field magnitude is decreased, L_c increases. The effective charge depth therefore increases. In terms of capacitance, the capacitance at strong accumulation is greater than weak accumulation.

If the electric field now is reversed, and a depletion region begins to form, the charge is predominantly due only to the fixed ionized donors. As the electric field increases, the depletion region continues to widen to incorporate more ionized dopants to compensate. The effective charge length continues to increase up to some maximum. During this period, C_{sc} is continuously decreasing.

Finally, at the point of strong inversion, the charge center begins to again recede toward the silicon surface because the dominant charge becomes the minority charge in the inversion region. Thus C_{sc} again begins to increase, and continues to do so as the applied electric field increases.

Thus, C_{sc} decreases with decreasing accumulation strength, and continues to decrease through depletion, reaching a minimum near the strong inversion point. At this time, C_{sc} begins to increase again with increased inversion strength.

One further point can be mentioned here. Consider the semiconductor under accumulation, and let the electric field have a very small ac component. The accumulation region will accommodate the ac component of frequency as long as charge can be injected from the bulk into the accumulation region to compensate for the small ac signal component. For the n-type semiconductor under study, this means injecting majority charge from the bulk into the accumulation region.

In the depletion region, an ac component of charge is compensated by varying the width of the depletion region. The charge is commuted from the depletion region-semiconductor interface to the semiconductor.

In the inversion region, however, the situation is quite different. If an ac signal is applied to a semiconductor under inversion, two distinct cases arise. If the frequency of the ac signal is very low, the variation in the electric field is reflected in a change in the total charge in the inversion region. The width of the depletion region does not change. The additional holes needed for the inversion region are generated in the depletion region. The generation-recombination rate in the depletion region thus limits how quickly an inversion region can respond to an ac signal. If the frequency of the signal is sufficiently high, charge cannot be generated and recombined fast enough to follow the signal, and the depletion region again reacts with a varying width.

Thus, for high and low frequency signals, C_{sc} appears the same in depletion and accumulation. For inversion, however, C_{sc} looks like the minimum depletion capacitance at high frequencies and the inversion

capacitance at low frequencies. This phenomenon is very important in modeling an MOS capacitor.

By solving Poisson's equation for nondegenerate semiconductors, it is possible to express the space charge capacitance in terms of the effective charge length L_c in Equation 31. To get a more accurate estimate of the relative sizes of C_{sc}, Seiwatz and Green (Ref. 29) actually did calculations similar to those just described. The bulk of the semiconductor is normally nondegenerate, but the surface can quite easily be made degenerate with modern devices. Seiwatz and Green calculated C_{sc} considering the bulk to be nondegenerate and the surface degenerate. Their results are reviewed here so that they may be referred to later in the chapter. They define one more parameter, w_b, which is the difference between the Fermi level and majority carrier band edge in the bulk. (See Figure 1.)

Figures 2 and 3 are the results of their calculations normalized in units of L, defined by Equation 17. It should be noted that the definition of L_c that appears in Equation 25 is valid for degenerate statistics; and as long as ρ is expressed in degenerate statistics, Equation 31 remains valid. This is precisely what Seiwatz and Green did. Figures 2 and 3 can thus be used to estimate the accumulation and depletion capacitances.

Consider, for example, an n-type semiconductor doped to a background density of 10^{15} cm^{-3}. This corresponds to a value for L of about 1300 $\mathring{A}$. Assuming total ionization, this corresponds to a value of $u_b \simeq 11$ kT, and a value of E_i of 0.55 eV $\simeq$ 21 kT. Thus $w_b \simeq 21\text{-}11 \simeq$ 10 kT. At the point of onset of accumulation then, C_{sc} is about

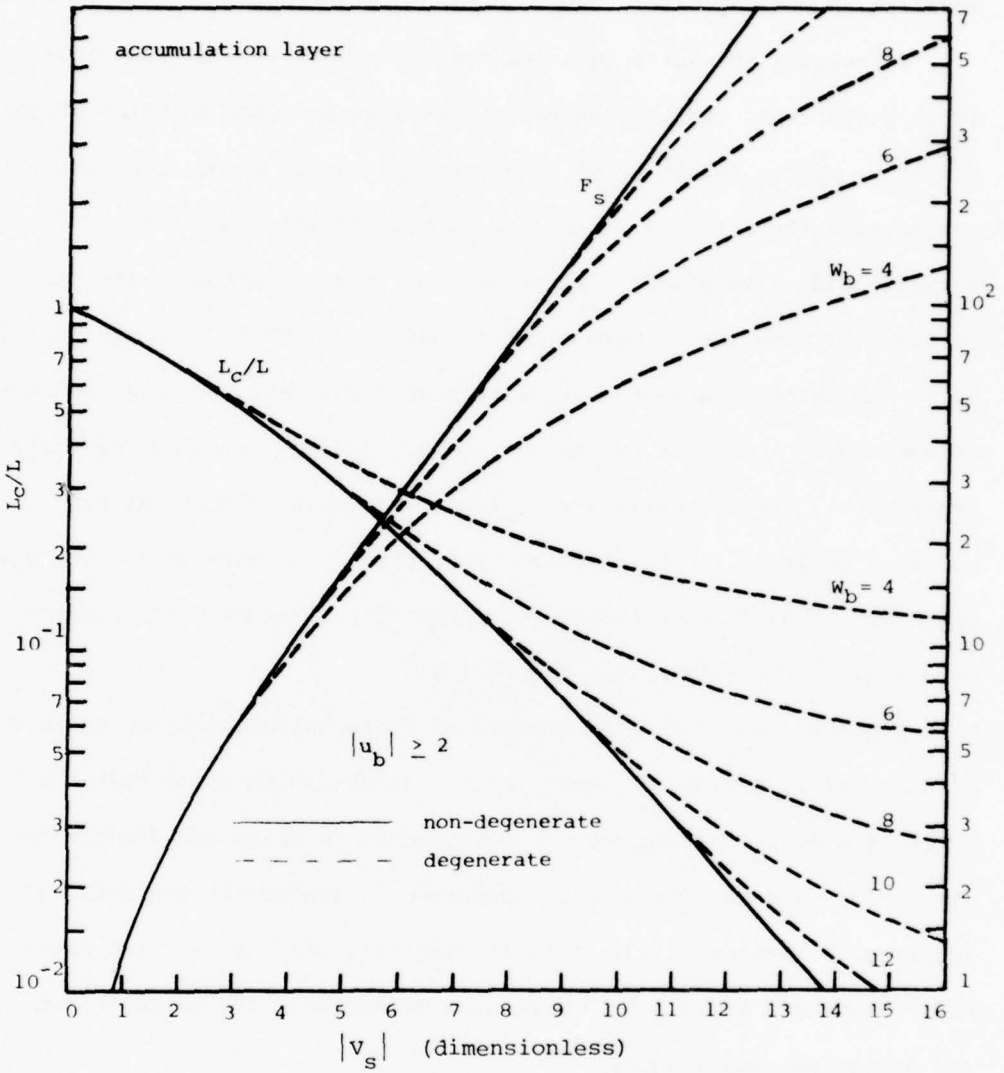

Figure 2. The functions $F(u_b, v_s)$ and L_c/L plotted for various values of $|v_s|$ in accumulation. The dashed curve represents degenerate surfaces (Ref. 29).

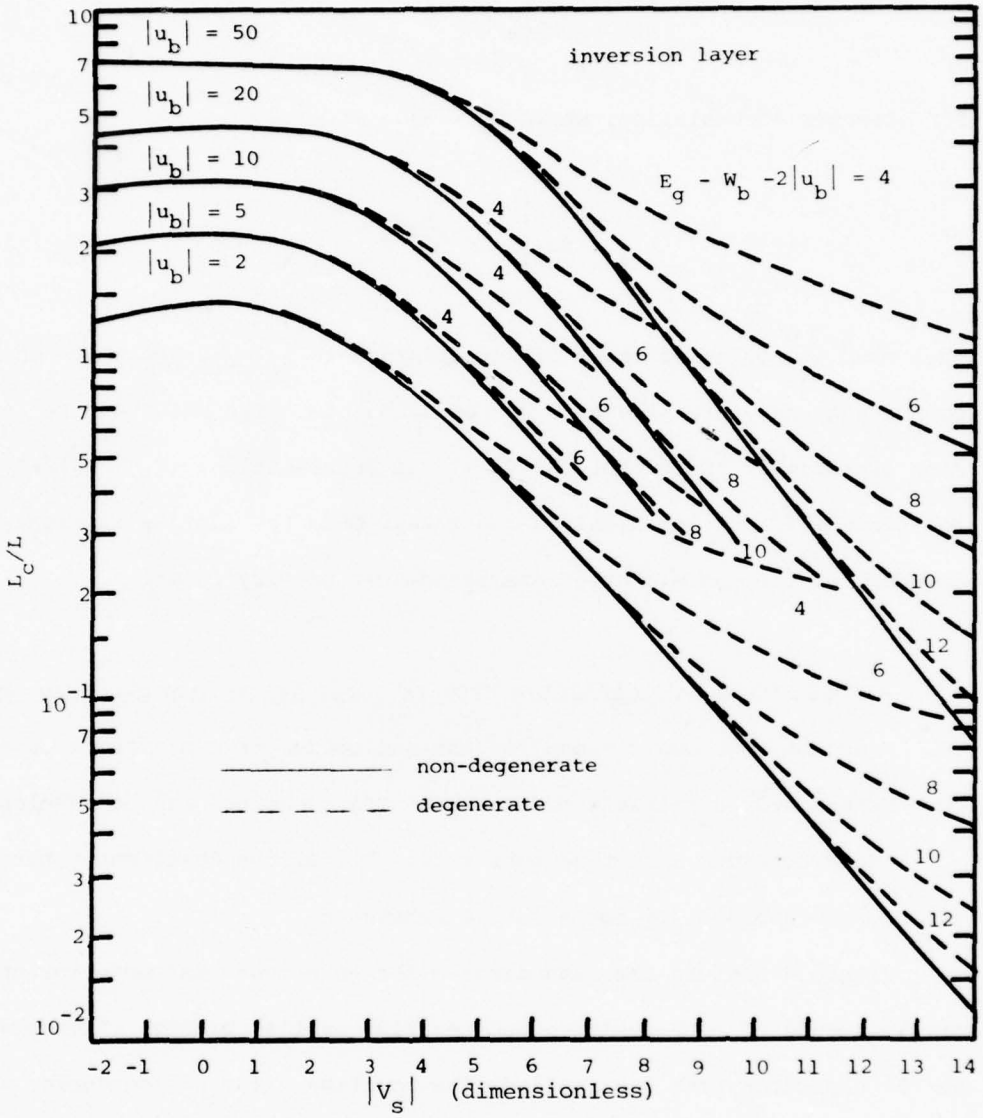

Figure 3. The function L_c/L plotted for various values of $|v_s|$ in strong inversion. The dashed lines represent degenerate surface conditions for different values of $E_g - W_b - 2|u_b|$ (Ref. 29).

$$C_{sc}\Big|_{v_s=0} \simeq \frac{K_s \varepsilon_o}{L}$$

For stronger accumulation, where $v_s \simeq 8$,

$$C_{sc}\Big|_{v_s=8} \simeq \frac{K_s \varepsilon_o}{0.1\ L}$$

Thus from the point of onset of accumulation to $v_s = 8$, the space charge capacitance has increased an order of magnitude. The situation in inversion is similar. Note that for $v_s = 8$ in accumulation, $(E_c - E_f)/kT \simeq 3$, the surface is not yet highly degenerate. Once the surface is highly degenerate, the space charge capacitance can be very large.

3. A MODEL OF AN MOS CAPACITOR USED IN QUASI-STATIC C-V CALCULATIONS

Now that some expressions for the semiconductor capacitance have been determined, a suitable model for an MOS capacitor can be developed.

Again consider an n-type substrate. All of the development here can be done analogously for a p-type substrate.

Figure 4 depicts the band diagram for an n-type semiconductor under the influence of both positive and negative applied biases. Figure 4a is the capacitor with the applied bias positive. The semiconductor is accumulated. The figure also shows a hypothetical surface state distribution N_{ss}. In accumulation almost all of the interface states are full. As the applied voltage decreases and becomes negative, the silicon Fermi level goes below the metal Fermi level, and the silicon surface goes from depletion to inversion. Notice that the Fermi level changes relative position with respect to the band edges. Toward inversion, fewer interface states are filled.

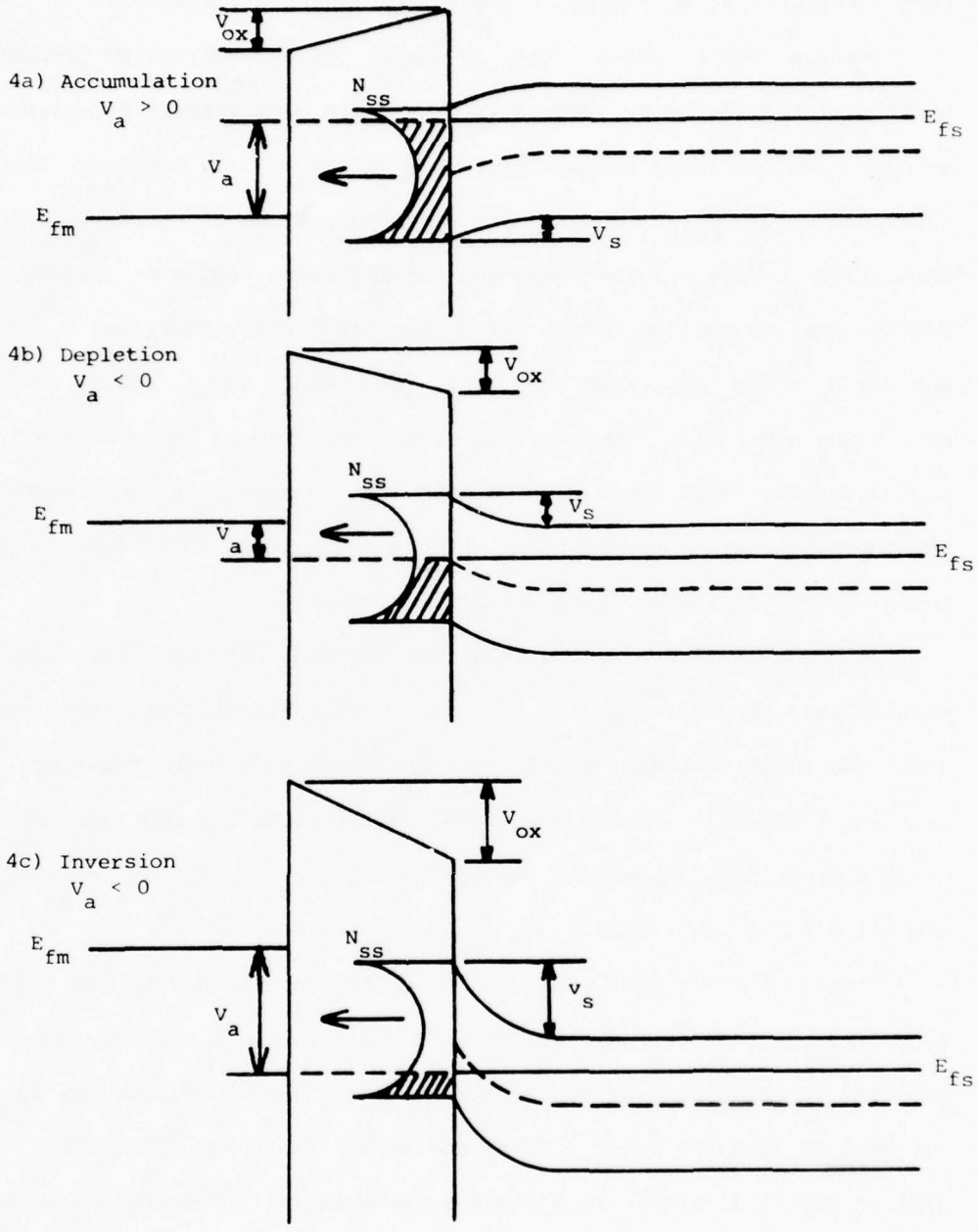

Figure 4. Band diagram of a n-type MOS capacitor biased into a) accumulation, b) depletion and c) inversion. A hypothetical surface state distribution, N_{ss} is depicted, and the filling of the states relative to the Fermi level is indicated.

Thus, by changing the applied bias on an MOS capacitor one can change the occupation status of some of the interface states.

Consider now Figure 5. This is a model of the MOS system proposed by Lehovec and Slobodsky (Ref. 30). The oxide capacitance is designated as C_{ox}. The remaining circuitry represents the silicon surface. The capacitances C_a, C_d, C_i and C_{ss} are capacitances due to charge in accumulation, depletion, inversion and the interface states or surface states. Notice that C_a cannot exist simultaneously with C_d and C_i. However C_i and C_d can exist together. The resistances R_c and R_v represent the generation-recombination mechanisms through which the surface states interact with the valence and conduction bands. R_g represents the thermal generation-recombination from the valence to conduction bands, and R_s is the series substrate resistance.

In order to determine the interface state density from this model, considerable simplification is in order. The approach taken is to consider the model in Figure 5 under the influence of a high frequency signal and a very low frequency signal (quasi-static). One can next examine inversion, depletion, and accumulation and find that certain simplifications are valid.

First, consider the model under the influence of a very low frequency signal such that all the circuit time constants are very short compared to the period of the applied signal. This condition can be achieved at frequencies of 0.01 Hz and less. In such a case, the applied signal is always in a quasi equilibrium with the semiconductor. For this case, the time constants associated with thermal generation-recombination and the time constants associated with the interface states' exchange or communication of charge with the valence and conduction bands are very short compared to the applied signal period.

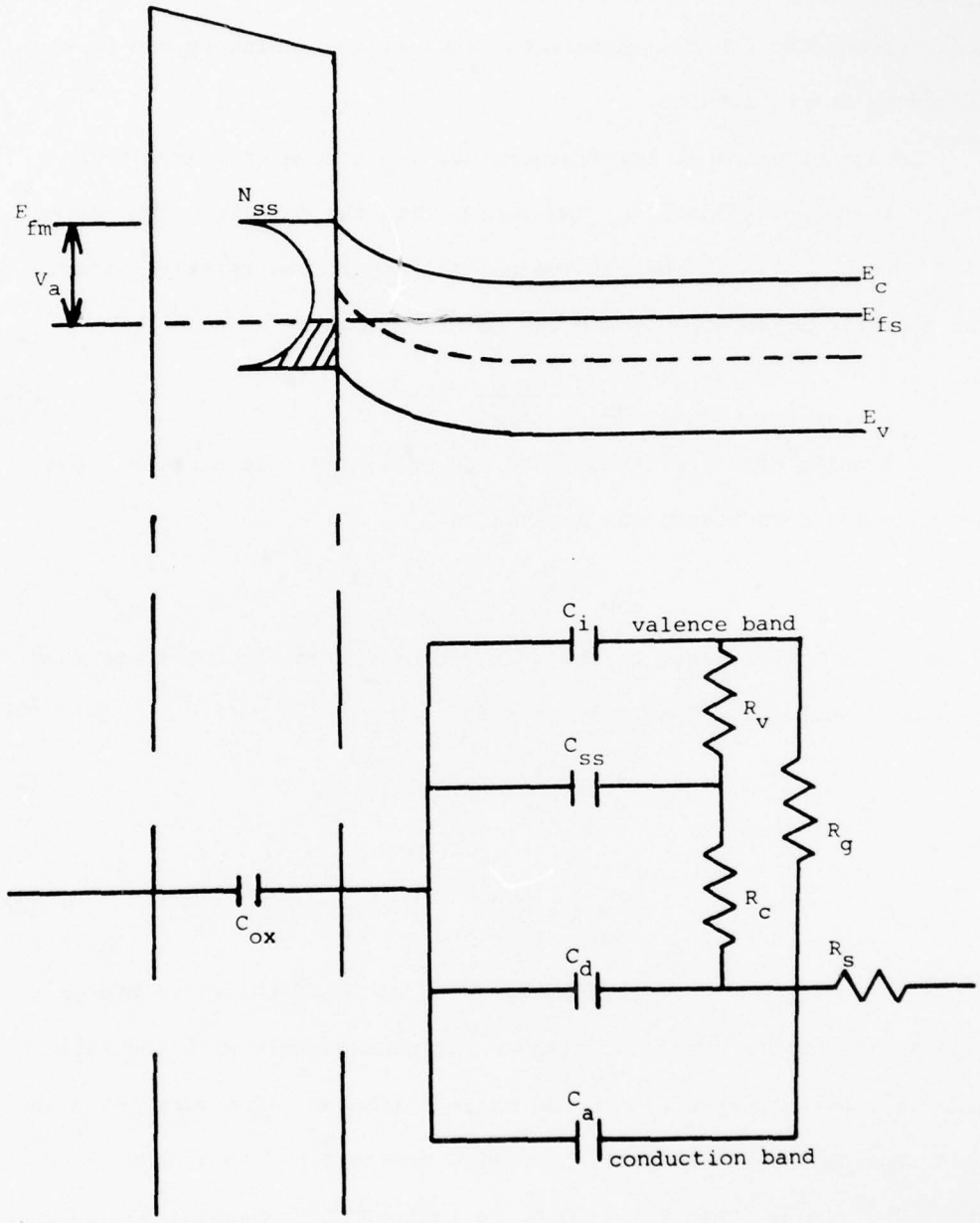

Figure 5. A model of the MOS capacitor. The oxide capacitance is designated C_{ox}. The remaining circuit is a model of the semiconductor.

Then the entire current through the circuit can be considered displacement current through the capacitors, and all the resistors can be replaced by short circuits.

In accumulation at low frequencies, the equivalent circuit is simply the combination of C_{ox} in series with the parallel combination of C_a and C_{ss}. It is instructive now to compare the relative sizes. The specific oxide capacitance can be written as

$$C_{ox} = \frac{\kappa_{ox}\varepsilon_o}{t_{ox}} \tag{32}$$

The units here are capacitance per unit area. In Section 2 the accumulation capacitance was derived as

$$C_{sc} = \frac{\kappa_s\varepsilon_o}{L_c}$$

where L_c is the distance to the charge center from the interface (semiconductor surface). The ratio is then

$$\frac{C_{sc}}{C_{ox}} = \frac{t_{ox}}{\kappa_{ox}} \cdot \frac{\kappa_s}{L_c} \tag{33}$$

or

$$\frac{C_{sc}}{C_{ox}} = 3\,\frac{t_{ox}}{L_c} \tag{34}$$

since $\kappa_{ox} = 3.9$ and $\kappa_s = 11.7$. Thus, the ratio of the space charge capacitance to the oxide capacitance varies inversely with the ratio of effective charge depth L_c and the oxide thickness. Consider again in this section, as in the last, an n-type device doped to a density of about 10^{15} cm^{-3}. Then $L \simeq 1300$ Å. A typical MOS capacitor has an oxide thickness of 700 to 1000 Å. At the point of the onset of accumulation the ratio of L_c to L can be determined from Figure 2. At the point $v_s = 0$, $L_c = L$, so at this point $C_{sc}/C_{ox} \simeq 1.62$ if t_{ox} is chosen as 700 Å. At the point where $v_s = 8$, $L_c/L \simeq 0.1$. Thus,

$$\left.\frac{C_a}{C_{ox}}\right|_{v_s=8} = \left.\frac{C_{sc}}{C_{ox}}\right|_{v_s=8} \simeq 16$$

It is plainly seen then that the stronger into accumulation this capacitor is biased, the larger the ratio of the accumulation capacitance to oxide capacitance becomes. Since C_{ss} is in parallel with C_a, regardless of the size of C_{ss}, $C_{ss} + C_a >> C_{ox}$ in strong accumulation. Thus, the measured capacitance in strong accumulation is C_{ox}.

The situation in inversion at low frequencies is quite similar. In inversion, with all the resistors shorted, the circuit becomes the series combination of C_{ox} with the parallel combination of C_i, C_{ss}, and C_d. The parallel combination of C_i and C_d in inversion is equivalent to C_{sc} in inversion derived in the preceding section. Again, from Figure 3 it can be seen that if $|v_s| - 2|u_b| \simeq 8$, $L_c/L \simeq 0.35$. Thus

$$\left.\frac{C_d+C_i}{C_{ox}}\right|_{|v_s|-2|u_b|=8} = \left.\frac{C_{sc}}{C_{ox}}\right|_{|v_s|-2|u_b|=8} \simeq 4.6$$

The stronger into inversion, the larger this ratio. Again, since C_{ss} is in parallel with C_i and C_d at low frequencies and in inversion, no matter what value C_{ss} has, $C_d + C_i >> C_{ox}$. Thus, at strong inversion the measured capacitance is again the oxide capacitance at low frequencies.

In depletion, neither C_i nor C_a are present, and the equivalent circuit for low frequencies becomes the series combination of C_{ox} with the parallel combination of C_d and C_{ss}. The three measured equivalent capacitances in strong accumulation, depletion, and strong accumulation are depicted in Figure 6a.

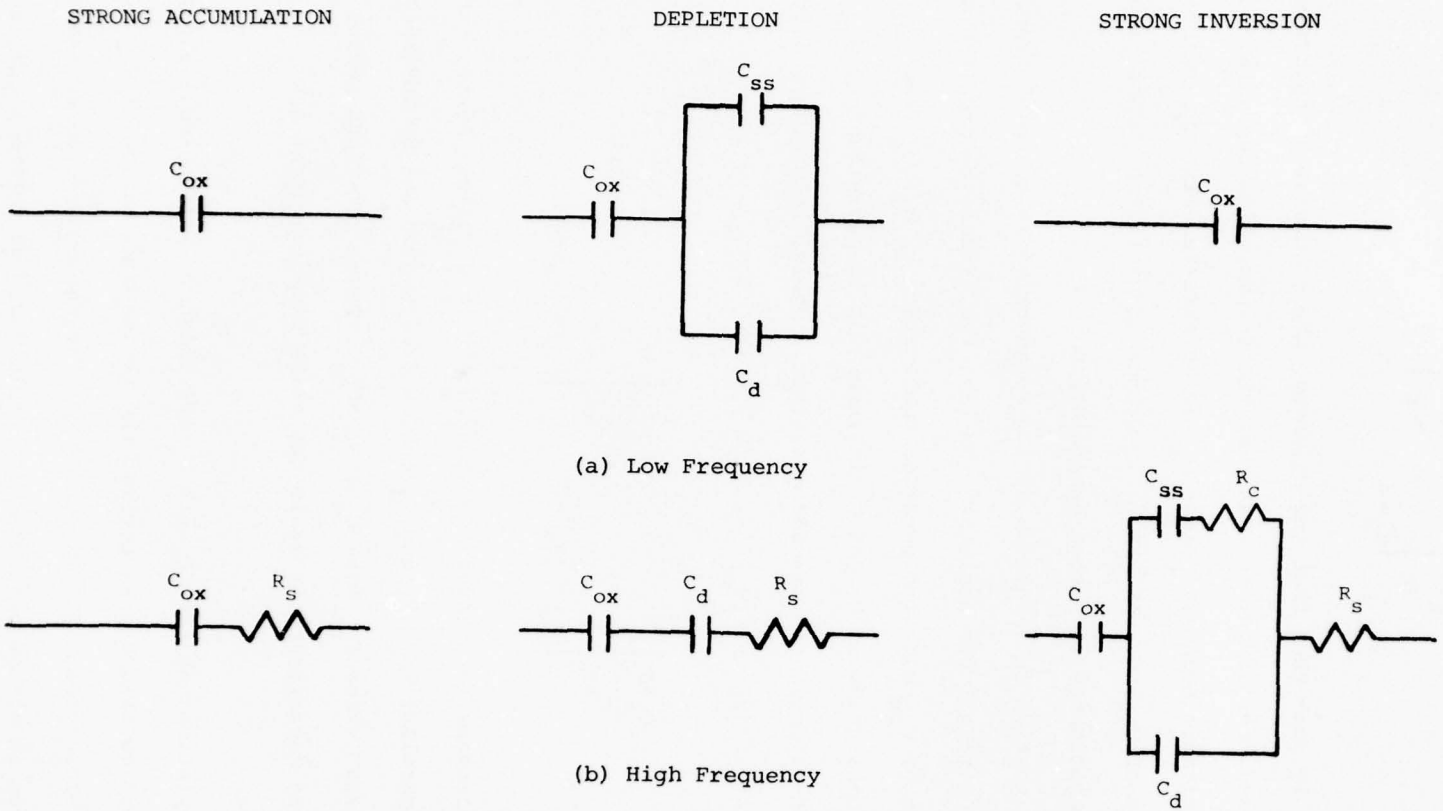

Figure 6. The equivalent circuit for an MOS capacitor in accumulation, depletion, and inversion at (a) low frequency and (b) high frequency.

Next consider the high frequency case, and again examine the capacitance of the network in Figure 5 in accumulation, depletion, and inversion. Through information supplied by the conductance technique for measuring N_{ss} (see Reference 21), it is known that the lifetime of interface states near mid gap is $\sim 10^{-2}$ second. The lifetime of the interface states decreases as the energy positions progress toward the band edges. (See Figure 7.) Thus, if the impressed ac signal is of the order of 1 MHz, the surface states in strong inversion and strong accumulation can react. It is known, however, that the time constants associated with minority carrier generation of charges needed for the inversion region are of the order of a second in reasonably pure silicon (Ref. 26). Thus C_i cannot respond to the high frequency signal.

Consider now strong accumulation. Again, as in the low frequency case, $C_{ss} + C_a >> C_{ox}$. Thus the series combination of C_a and $C_{ss} + C_a$ is effectively C_{ox}. At 1.0 MHz, for a typical capacitance of about 300 pf, $X_c \simeq 530\Omega$, where X_c is the capacitive reactance. The resistance R_s is the bulk wafer resistance and can be calculated to an order of magnitude by

$$R_s \sim \rho \frac{t}{A}$$

where ρ is the bulk resistivity, t is the wafer thickness, and A is the capacitance area (see Ref. 31). For 10^{15} cm^{-3} impurity doping, $\rho \sim 5\Omega$-cm. A typical wafer is about 10 mil thick and a typical capacitor dot size is about 30 mils. For these figures, $R_s \sim 90\Omega$. Thus, R_s cannot be ignored in the model. Since R_s is in series with C_{ox}, the effective impedance is greater than the impedance due to C_{ox} alone, and the measured capacitance in accumulation would appear to be less than C_{ox}. This turns out to be the case in practice, and R_s can be evaluated by examining

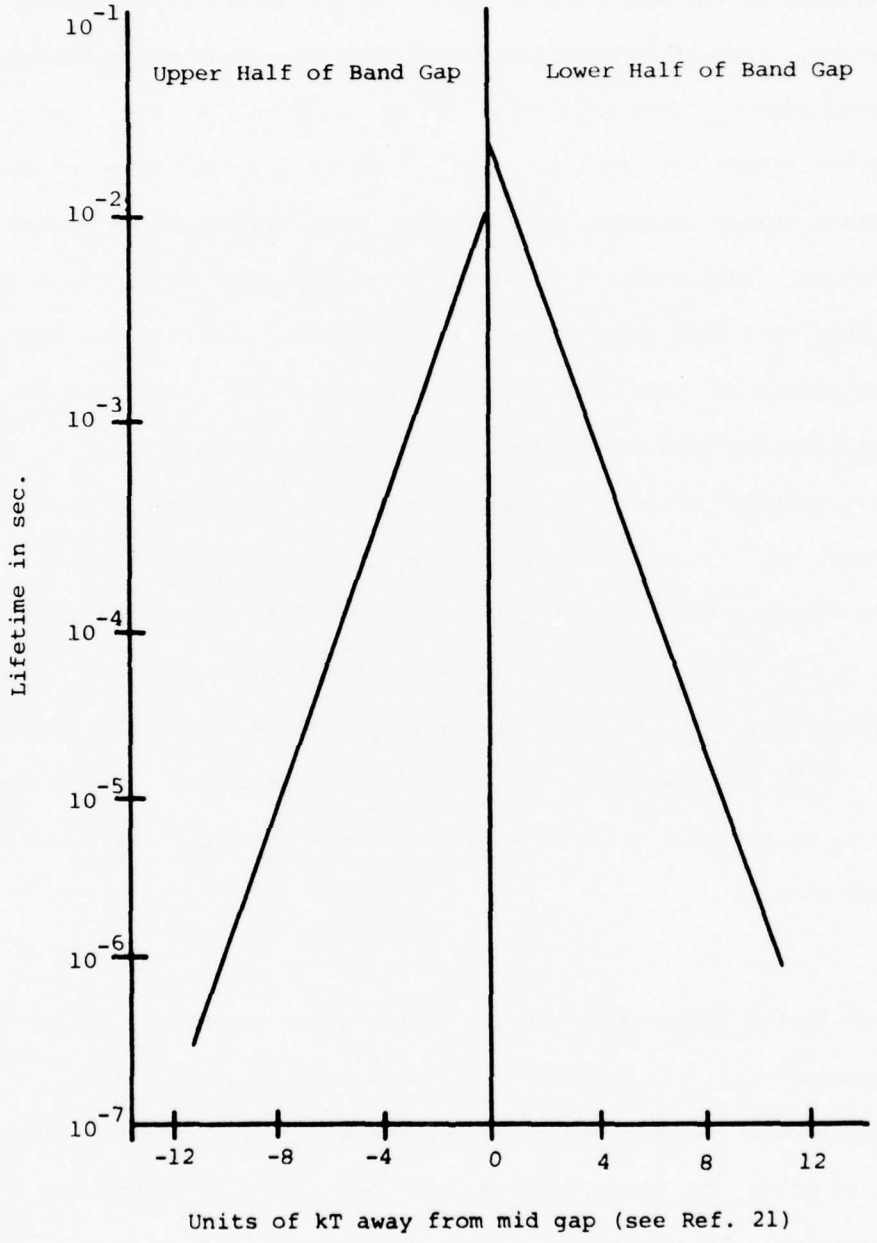

Figure 7. A plot of interface state density lifetime vs. energy. The energy is measured in units of kT away from mid gap.

the measured high and low frequency capacitances under conditions of strong accumulation.

In the depletion region, C_{ss} cannot respond because the lifetimes of the surface states are longer. This is true as long as the intrinsic Fermi level does not bend more than 10 kT away from the Fermi level. (See Figure 7.)

In inversion, C_{ss} can again respond, but C_i is limited by the thermal generation rate. The depletion capacitance region can also respond because its charge is supplied by majority carriers directly from the conduction band.

Figure 6b depicts the high frequency models. Keep in mind that C_d in depletion is greater than C_D in accumulation.

Figure 8 is a plot of actual high and low frequency curves run on one of the capacitors made in this project. In accumulation the curve levels off to C_{ox} at low frequencies. At high frequencies the measured capacitance is lower due to R_s.

In depletion, both the high and low frequency curves decrease as the depletion region widens. When the depletion region reaches its maximum width, the low frequency curve again progresses toward C_{ox}. The high frequency curve remains at a minimum value. Since the high frequency curve does in fact remain at a minimum value corresponding to the maximum depletion region width, this indicates that, in practice, there is no noticeable contribution from C_{ss} in strong inversion. If C_{ss} did get large, or at least large compared to C_d, the inversion high frequency curve would begin to rise. Thus, the branch containing C_{ss} and R_c can be eliminated in practice as long as the high frequency curve stays flat into strong inversion.

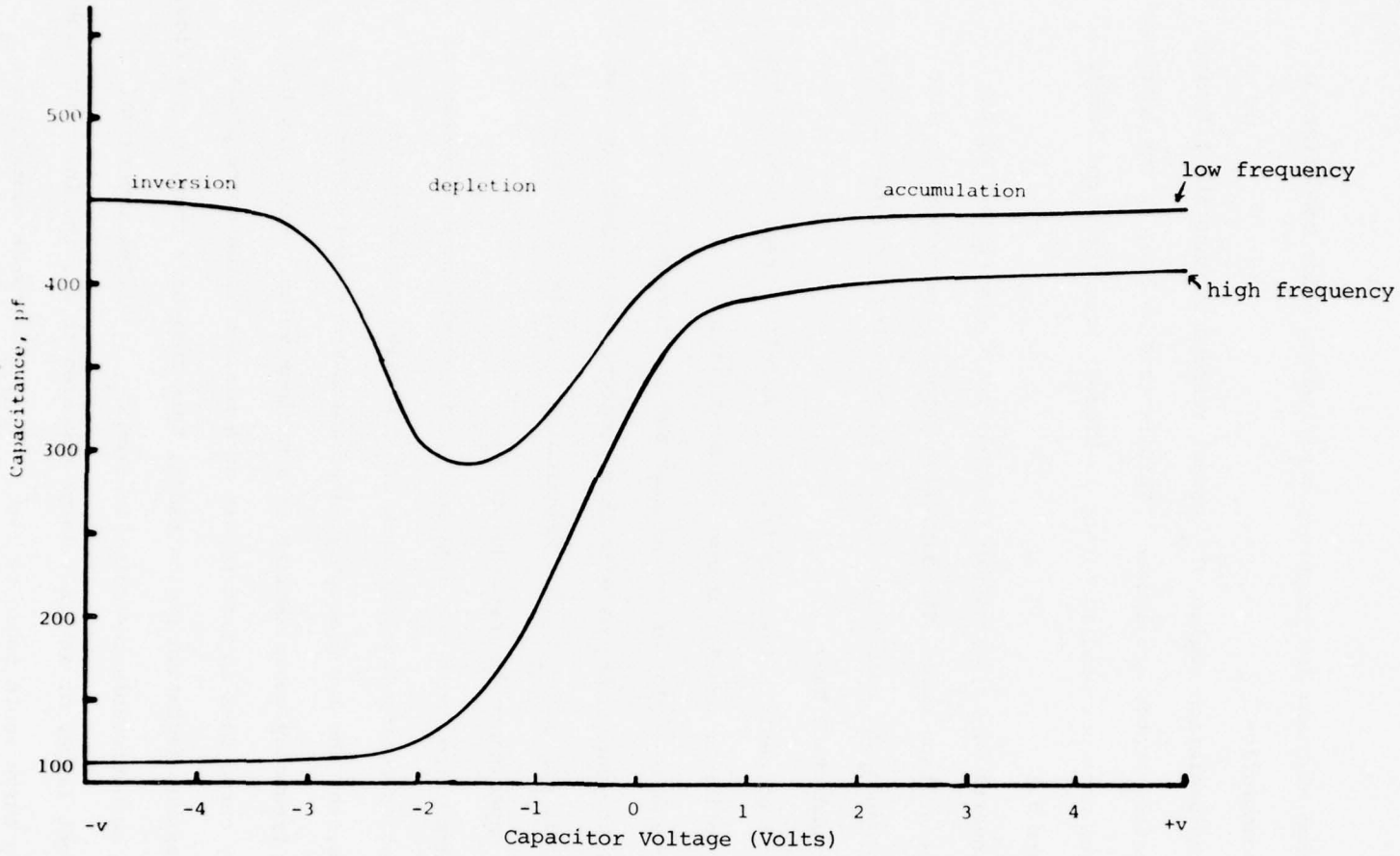

Figure 8. A plot of an actual low and high frequency curve for an n-channel device.

Before progressing to the next section, one point should be again emphasized. These models are good only in strong inversion, strong accumulation, and depletion. The depletion model specifically is only useful up to the point where the interface states begin to react substantially. This sets a fundamental limit to a region in the center of the band gap which can be scanned by the C-V technique.

4. DERIVATION OF THE EQUATIONS USED IN THE QUASI-STATIC TECHNIQUE

The purpose of this section is to show how to derive $N_{ss}(\phi_s)$ from C-V data. The procedure progresses in three steps. First, by comparing the high frequency and low frequency data, one can obtain $N_{ss}(V_a)$ where V_a is the applied voltage across the MOS device. Next, a numerical integration of the low frequency curve is performed, which yields $V_a(\phi_s)$ to within an integration constant. Finally, the high frequency flat band capacitance is determined theoretically. This value is located on the high frequency C-V curve yielding the flat-band voltage. The flat-band voltage determines the integration constant in the $V_a(\phi_s)$ relationship. Each of these steps is considered in the following subsection.

a. Determination of $N_{ss}(V_a)$

The approach to this measurement is straightforward. In the depletion region, the measured high and low frequency capacitances differ by an amount that can be attributed to C_{ss}. In order to retrieve C_{ss} from the measured data, R_s, C_{ox}, and C_d must be eliminated in some fashion. A value for C_{ox} can be obtained directly from the low frequency C-V curve in strong accumulation. The quantity R_s can then be obtained from the high frequency curve in the following manner. In high frequency accumulation the series circuit of C_{ox} and R_s can be

transformed into its equivalent parallel circuit. (See Figure 9.) The transformation is done through the definition of admittance.

$$Y = \frac{1}{Z} = G + jB \tag{35}$$

where Z is impedance, G is conductance, and B is susceptance. In this case, $B = \omega C_{HF}$ where C_{HF} is the measured high frequency capacitance. The input impedance of the high frequency series circuit is

$$Z = R_s - jX_c$$

Using the definition of admittance and the input impedance of the high frequency model, the following expression can be derived.

$$C_{HF} = \frac{C_{ox}}{\omega^2 C_{ox}^2 R_s^2 + 1} \tag{36}$$

This expression can be solved for R_s since C_{ox} and ω are known, and C_{HF} is the measured high frequency capacitance in accumulation.

Having determined R_s, the depletion region can now be examined. Let the quantity C'_{HF} be defined by the following equation:

$$\frac{1}{C'_{HF}} = \frac{1}{C_{ox}} + \frac{1}{C_d} \tag{37}$$

Then C'_{HF} is the equivalent series capacitance of C_{ox} and C_d. Using this definition the measured high frequency capacitance, C_{HF}, can be related to C'_{HF} by another equivalent parallel circuit. (See Figure 9b.) This development leads to the following relationship

$$C_{HF} = \frac{C'_{HF}}{\omega^2 C'^2_{HF} R_s^2 + 1} \tag{38}$$

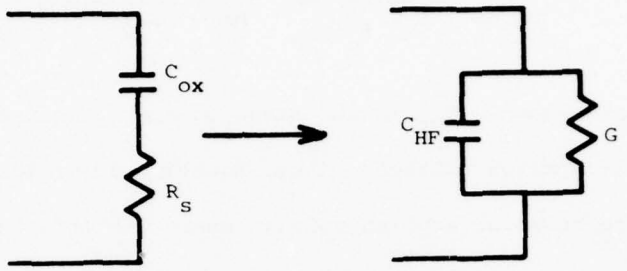

(a) accumulation

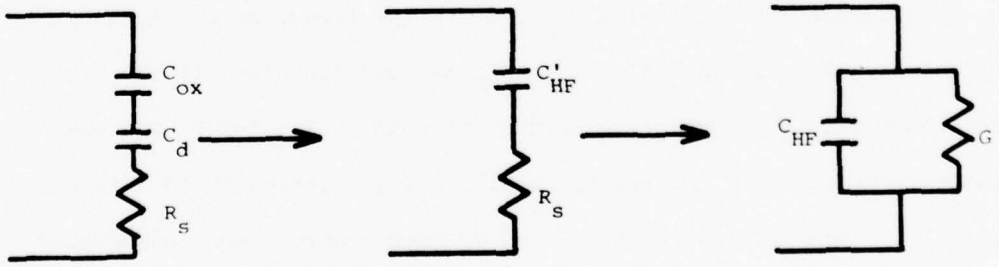

(b) depletion

Figure 9. The equivalent parallel circuit transformation for the high frequency accumulation region and depletion region.

Equation 38 can be solved for C'_{HF}.

$$C'^{2}_{HF} - \frac{1}{\omega^2 R_s^2 C_{HF}} C'_{HF} + \frac{1}{\omega^2 R_s^2} = 0 \qquad (39)$$

Both R_s and ω are known. C_{HF} is the measured high frequency capacitance as a function of applied voltage. Thus, Equation 39 yields a new function C'_{HF} as a function of applied voltage where the effects of R_s are scaled out. Note that in accumulation, C_d is not present, and $C_a >> C_{ox}$, so Equations 37 through 39 can be used in accumulation as well as depletion. When this is done, $C'_{HF} = C_{ox}$ in accumulation.

In the last section it was demonstrated that if the high frequency curve stayed constant in inversion, the $C_{ss}R_c$ branch in the high frequency inversion equivalent circuit could be ignored. (See Figure 6b.) If it is ignored, then Equations 37 through 39 can also be used in inversion. By using the C'_{HF} curve scaled by Equation 39, the effects of R_s can be eliminated in all regions. In practice, this is done.

In Figure 10, the data in Figure 8 are used to determine C_{ox} and R_s in accumulation by reading C_{ox} off the low frequency curve, and calculating R_s using Equation 36. C_{HF} is read directly off the high frequency strong accumulation curve. Once the value for R_s was obtained, the entire C_{HF} curve was scaled using Equation 39 to obtain $C'_{HF}(V_a)$. Then both the high and low frequency curves were normalized by a factor of C_{ox}. Figure 10 is a plot of these results.

Next, consider the low frequency depletion region equivalent circuit. We can write

$$\frac{1}{C_{LF}} = \frac{1}{C_{ox}} + \frac{1}{C_{ss} + C_d} \qquad (40)$$

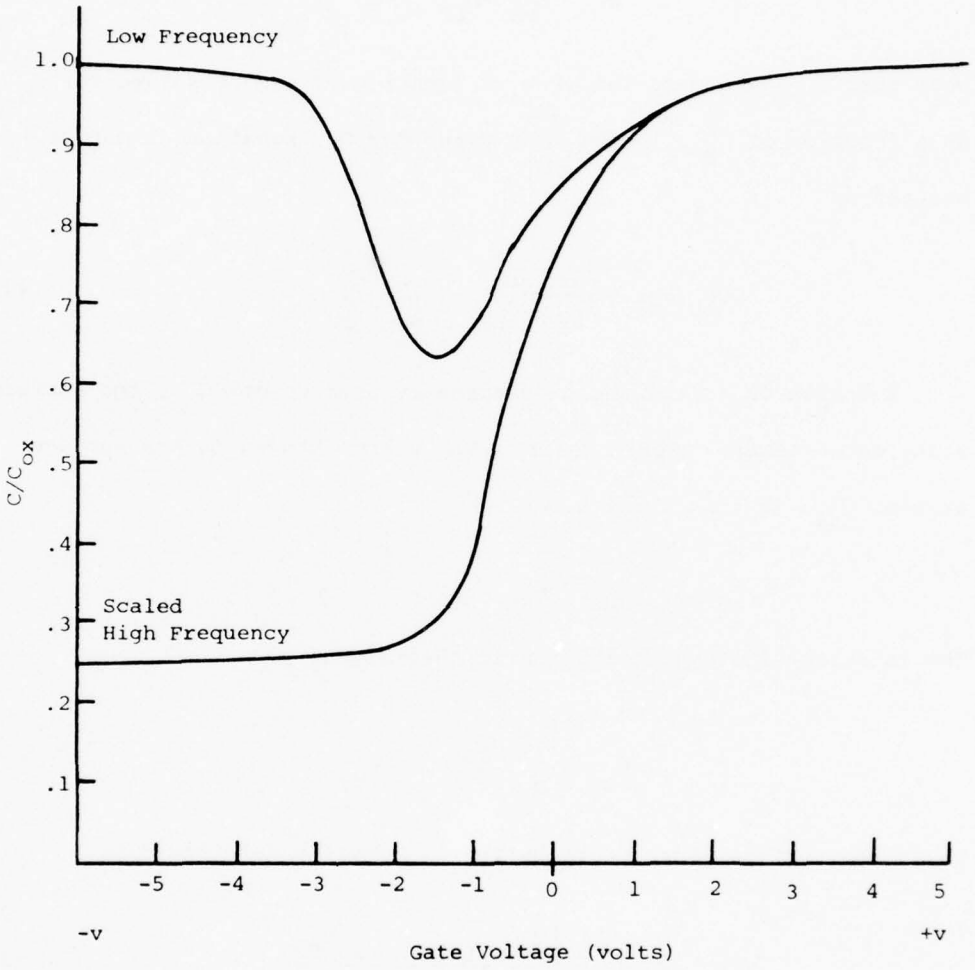

Figure 10. The low frequency and scaled high frequency curves obtained from the data in Figure 8. The high frequency curve is scaled using Equation 39, and is C'_{HF}/C_{ox}. The low frequency curve is C_{LF}/C_{ox}.

which can be solved for C_{ss} to yield

$$C_{ss} = \frac{C_{ox}\, C_{LF}}{C_{ox} - C_{LF}} - C_d \tag{41}$$

Note that C_{LF} is a function of V_a. Equation 37 can be solved for C_d as a function of C'_{HF}. Using that value for C_d, Equation 41 can be written as

$$C_{ss}\left(V_a\right) = \frac{C_{ox}\, C_{LF}}{C_{ox} - C_{LF}} - \frac{C_{ox}\, C'_{HF}}{C_{ox} - C'_{HF}} \tag{42}$$

Equation 42 is the equation actually used to get C_{ss}, the surface state capacitance, experimentally. The charge stored in the surface states, Q_{ss}, is in general given by

$$Q_{ss} = C_{ss}\, V_{ss}$$

The interface state distribution is then given by

$$N_{ss} = \frac{1}{q}\,\frac{\partial Q_{ss}}{\partial V_{ss}} = \frac{1}{q}\, C_{ss}$$

Thus, the surface state distribution is actually determined by

$$N_{ss} = \frac{1}{q}\left[\frac{C_{ox}\, C_{LF}}{C_{ox} - C_{LF}} - \frac{C_{ox}\, C'_{HF}}{C_{ox} - C'_{HF}}\right] \tag{43}$$

The capacitances here are all specific capacitances, or capacitance per unit area.

If Equation 43 is multiplied by $\left(\frac{C_{ox}}{C_{ox}}\right)^2$, the equation can be put in a normalized form.

$$N_{ss} = \frac{C_{ox}}{q}\left[\frac{C_{LF}/C_{ox}}{1 - \left(C_{LF}/C_{ox}\right)} - \frac{C'_{HF}/C_{ox}}{1 - \left(C'_{HF}/C_{ox}\right)}\right] \tag{44}$$

The examination of Figure 10 will reveal that the data are already in a normalized form here and can readily be analyzed by Equation 44.

Thus, after the data are scaled to eliminate the effects of R_s, then either Equation 43 or 44 can be used to determine N_{ss}. If the data are not normalized in units of C_{ox}, Equation 43 is used. If the data are normalized in units of C_{ox}, Equation 44 is used.

b. Determination of $V_a(\phi_s)$ to Within an Integration Constant

Consider Equation 5 again, and Figure 1. The quantity V_s is a measure of the total amount of band bending referenced to the bulk. Any differential applied voltage must be split across the oxide and the space charge region. Thus, (Ref. 32)

$$dV_a = dV_{ox} + dV_s \tag{45}$$

The differential voltage applied will give rise to charge transferred to the metal-insulator interface, and the magnitude of this charge, dq will be given by

$$dq = CdV_a \tag{46}$$

where C is the measured capacitance. In order for N_{ss} to have an effect in Equation 46, the measured capacitance at low frequency must be used. Thus, Equation 46 becomes

$$dq = C_{LF}\, dV_a \tag{47}$$

The incremental charge on the gate of the oxide, however, is given by $C_{ox}dV_{ox}$, so dq can also be written as

$$dq = C_{ox}\, dV_{ox} \tag{48}$$

Thus,

$$\frac{C_{LF}}{C_{ox}} = \frac{dV_{ox}}{dV_a} \tag{49}$$

This result can be combined with Equation 45 to yield

$$\frac{dV_s}{dV_a} = 1 - \frac{C_{LF}}{C_{ox}} \tag{50}$$

where

$$C_{LF} = C_{LF}(V_a)$$

Therefore, integration of Equation 50 yields an equation that expresses the amount of band bending, V_s, as a function of the applied voltage V_a. Integration of Equation 50 from $V_a = V_{a1}$ to $V_a = V_{a2}$ yields

$$V_s(V_{a2}) - V_s(V_{a1}) = \int_{V_{a1}}^{V_{a2}} \left[1 - \frac{C_{LF}(V_a)}{C_{ox}}\right] dV_a \qquad (51)$$

Equation 51 then relates the applied gate voltage to the relative position of the Fermi level in the band gap. Using Equation 5, this can in turn be written as

$$\phi_s(V_{a2}) - \phi_s(V_{a1}) = \int_{V_{a1}}^{V_{a2}} \left[1 - \frac{C_{LF}(V_a)}{C_{ox}}\right] dV_a \qquad (52)$$

This is precisely what was to be derived in this section. Normally V_{a1} is chosen in strong accumulation, and V_{a2} is a running variable.

c. Determination of the Integration Constant for the $V_g(\phi_s)$ Equation

The last quantity needed to completely characterize $N_{ss}(\phi_s)$ is the integration constant in Equation 52. One way to do this is to calculate the theoretical MOS capacitance at some known value of ϕ_s. By examining the actual C-V curve for the value of capacitance, the voltage corresponding to this ϕ_s can be determined. This one boundary condition would allow integration of Equation 52.

The value chosen for capacitance here is the flat-band capacitance for the high frequency curve because it can easily be theoretically

calculated. At flat band, $\phi_s = \phi_b$, and the needed integration constant can be determined.

Recall Equation 24 which gives the value for the space charge density at the surface of the wafer. It is repeated again here for continuity.

$$Q_{sc} = \pm q(n_b+p_b)L\ F(u_b,v_s) \tag{24}$$

where L is defined by Equation 17 and F is defined by Equation 22. In general, the space charge capacitance can be written as

$$C_{sc} = \frac{\partial Q_{sc}}{\partial V_s} = \frac{\partial Q_{sc}}{\partial v_s}\frac{\partial v_s}{\partial V_s} = \pm \frac{\kappa_s \varepsilon_o}{LF(u_b,v_s)}\left[\frac{\sinh(u_b + v_s)}{\cosh u_b} - \tanh u_b\right] \tag{53}$$

At flat band, $v_s = 0$. If Equation 53 is expanded about $v_s = 0$ using the hyperbolic trigonometric expansions, one obtains

$$C_{sc}(\text{flat band}) = \frac{\kappa_s \varepsilon_o}{L} \tag{54}$$

The actual measured capacitance at flat band would be the series combination of C_{ox} and $C_{sc}(\text{flat band})$. Recalling that $C_{ox} = \kappa_{ox}\ \varepsilon_s/t_{ox}$, the measured capacitance at flat band is

$$C_{meas}\ (\text{flat band}) = \frac{\left(\frac{\kappa_{ox}\varepsilon_o}{t_{ox}}\right)\left(\frac{\kappa_s\varepsilon_o}{L}\right)}{\left(\frac{\kappa_{ox}\varepsilon_o}{t_{ox}}\right)+\left(\frac{\kappa_s\varepsilon_o}{L}\right)} \tag{55}$$

This simplifies to

$$C_{meas}\ (\text{flat band}) = \frac{\kappa_{ox}\varepsilon_o}{t_{ox} + \left(\frac{\kappa_{ox}}{\kappa_s}\right)L} \tag{56}$$

By definition this is the value of the measured flat-band capacitance at $v_s = 0$, $\phi_s = \phi_b$. So Equation 52 should be integrable uniquely.

As is often the case, there is one physical quantity which prevents using this equation directly. Recall Equation 17

$$L = \sqrt{\frac{\kappa_s \varepsilon_o kT}{q^2\left(n_b+p_b\right)}} \tag{17}$$

For most normal semiconductors the majority carrier density far exceeds the minority carrier density. Considering a p-type wafer for instance, $p_b >> n_b$. Further, for all practical purposes $p_b = N_A$ in nondegenerate wafers at room temperature. Under these conditions, L can be calculated and C_{meas} (flat band) can also be calculated.

Two problems encountered in practice are that, when a gate oxide is grown, the oxide has a tendency to either leach out boron atoms from the bulk, or push phosphorous atoms ahead as it grows ("snowplowing" effect). As a result the effective surface concentration of N_A decreases with oxide growth and N_D increases. Thus, a method must be devised for calculating an effective or average $\langle N_A \rangle$ to use in calculating L.

This can be accomplished conveniently by examining at the high frequency C-V curve in strong inversion. The width of the depletion region reaches a maximum in strong inversion, so C_d reaches a minimum. Since in inversion at high frequency, the MOS capacitor looks like C_{ox} in series with C_d, and since the width of the depletion region depends on the doping density, this affords a way to find the depletion region maximum width.

Poisson's equation can be solved in depletion to derive an expression for the maximum depletion region/width. In depletion, charge in the space charge region is effectively entirely due to the ionized dopants. Consider the depletion region of a p-type semiconductor with N_A acceptors. If the surface is depleted, the charge in the depletion

region is given by $-qN_A$. As long as $N_A >> N_D$, and N_A is much larger than the free carrier concentration in the depletion region (a rather good assumption), then Poisson's equation becomes

$$\frac{d^2V}{dz^2} = \frac{-qN_A}{\kappa_s \varepsilon_o} \tag{57}$$

This is good only in depletion. If the depletion region is considered to be of width L_D, and further note that there are two boundary conditions, (1) $\xi = 0$ at $z = L_D$ and (2) $V = 0$ at $L = L_D$, then Equation 57 can be integrated.

The first integration yields

$$\frac{dV}{dz} = \frac{qN_A L_D}{\kappa_s \varepsilon_o}\left(1 - \frac{X}{L_D}\right) \tag{58}$$

and the second yields

$$V = V_s\left(1 - \frac{X}{L_D}\right)^2 \tag{59}$$

where

$$V_s = \frac{qN_A L_D^2}{2\kappa_s \varepsilon_o} \tag{60}$$

As the applied voltage increases, V_s does also. Accordingly then, L_D also increases. This phenomenon continues only until strong inversion occurs, however. At strong inversion the minority bands near the surface begin to approach the Fermi level. At such a point, very small changes in the energy difference between the bulk minority carrier band edge and the Fermi level reflect large changes in the inversion layer charge density. Thus at strong inversion, L_D ceases to increase. This occurs when $qV_s/kT \approx 2|u_b|$. Thus, Equation 60 can be solved for L_{Dmax} as

$$L_{Dmax} = \sqrt{\frac{4\kappa_s \varepsilon_o kT\, u_b}{q^2 N_A}} \tag{61}$$

At room temperature and for nondegenerate doping densities

$$u_b = \ell n \left(N_A/n_i\right) \tag{62}$$

so the maximum depletion region width can be written as

$$L_{Dmax} = \sqrt{\frac{4\kappa_s \varepsilon_o \; kT \; \ell n\left(N_A/n_i\right)}{q^2 \; N_A}} \tag{63}$$

In strong inversion, the measured high frequency capacitance is C_{ox} in series with C_d, where $C_d = \kappa_s \varepsilon_o / L_{Dmax}$. Thus, the minimum high frequency capacitance can be expressed as

$$C_{HF}(min) = \frac{\kappa_{ox} \varepsilon_o}{t_{ox} + \left(\frac{\kappa_{ox}}{\kappa_s}\right) L_{Dmax}} \tag{64}$$

This can be normalized in terms of the oxide capacitance as

$$\frac{C_{HF}(min)}{C_{ox}} = \frac{1}{1 + \left(\frac{\kappa_{ox}}{\kappa_s}\right) L_{Dmax}} \tag{65}$$

The high frequency capacitance minimum used here is the one where the effects of R_s are scaled out (Eq. 39).

If the data have already been scaled, as in Figure 10, $C_{HF}(min)$ can be read directly off the high frequency curve.

The procedure for determining the value for V_a(flat band) at $\phi_s = \phi_b$ goes as follows:

1) Pick off C_{min}(flat band) from the scaled high frequency curves.
2) Use Equation 64 to determine L_{Dmax}.
3) Use Equation 63 to determine $\langle N_A \rangle$, the average doping density at the surface.

4) Use $\langle N_A \rangle$ in Equation 17 to determine L by using $\langle N_A \rangle$ for the majority carrier density and ignoring the minority carrier density.

5) Use this value of L to determine C_{meas} (flat band) in Equation 56.

6) Go back to the actual high frequency curve and locate C_{meas}(flat band). The applied gate voltage that corresponds to this capacitance is the flat band voltage. This is the voltage at $\phi_s = \phi_b$, $v_s = 0$ and supplies the necessary integration constant for Equation 51.

This is the procedure used in this study.

Once V_a(flat band) has been found, $N_{ss}(\phi_s)$ has been uniquely characterized. Notice that other things which have been determined are R_s - the series wafer resistance, V_a(flat band) - the applied voltage at flat band, $\langle N_A \rangle$ - the average doping density, C(flat band), L_{Dmax} - the maximum depletion region width, as well as the $V_a(\phi_s)$ curve. The $V_a(\phi_s)$ curve allows determination of the threshold voltage, which is V_a at the point where $v_s = -2u_b$, or $\phi_s = -\phi_b$.

5. LOW AND HIGH FREQUENCY MEASUREMENTS

Before concluding this chapter, something should be said about how the low and high frequency curves are obtained since all of the previous data come strictly from these two curves.

The high frequency data are quite easily obtained. The procedure is simply to bias the MOS capacitor into various regions and measure the capacitance with a small impressed ac signal. In practice this signal is usually 1 MHz, and the measuring apparatus is a high grade capacitance bridge. A block diagram of this is shown in Figure 11.

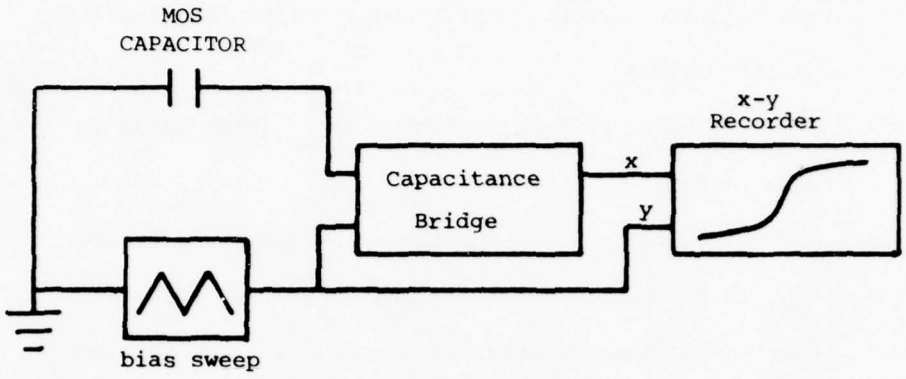

a) High Frequency Block Diagram

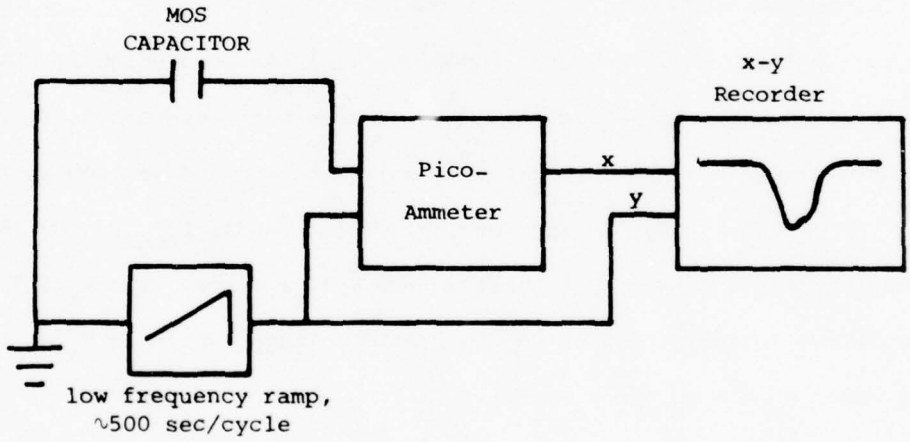

b) Quasi Static (low frequency)

Figure 11. Block diagrams for (a) HF and
(b) LF or quasi-static measurements.

The low frequency curves are usually obtained with a more sophisticated method. Very low frequency ac signals are hard to use. Often phase lock amplifiers must be employed between the driving signal and picked up signals. This difficulty can be eliminated by using a quasi-static C-V setup. Again, it is a simple apparatus. Figure 11b shows a typical quasi-static setup. The MOS capacitor is charged with a very slow varying ramp generator. Typical sweep rates are on the order of 100 mv/sec.

The charging current is measured with a sensitive ammeter. If the ramp voltage is very linear, it can be expressed as

$$V(t) = V_o + at \tag{65a}$$

where a is the sweep rate. The charge on the capacitor is given by $Q = CV$, and the differential capacitance is defined by $C = dQ/dV$. The applied voltage is time varying, so it can be written as

$$i = \frac{dQ}{dt} = \frac{dQ}{dV(t)} \frac{dV}{dt} = C(t) \frac{dV}{dt} \tag{66}$$

Using Equation 65a for the applied voltage, it can be seen

$$C_{LF}(t) = \frac{1}{a} i(t) \tag{67}$$

Thus, the output of the ammeter is a direct measurement of the quasi-static or low frequency capacitance.

6. SUMMARY

In this chapter the surface of a semiconductor has been considered and its space charge capacitance in accumulation, depletion, and inversion has been examined. Using these considerations, one is able to derive approximate values for the space charge capacitance in strong accumulation and strong inversion.

Next the metal-oxide-semiconductor capacitor system was modeled. By using the relationships and numbers derived in Section 1, it was possible to simplify this model into a usable form.

Once a reasonable model was established, it was then possible to derive equations that allow calculation of N_{ss} when the space charge region is in the depletion mode. It was found that both high and low frequency curves were needed for this determination. Also, it was noted that some of the parameters needed in the N_{ss} determination actually came from the strong accumulation and strong inversion regions. Thus, when obtaining C-V curves, care should be taken to see that both the high and low frequency curves are taken into those regions.

Finally, a brief note was included as to how the high and low frequency curves can be obtained. The actual setup used in this study is discussed later in Chapter V.

Table 1 summarizes the necessary steps that must be taken to determine $N_{ss}(\phi_s)$. The appropriate curves used at each step and/or equations used are noted. The abbreviations are LF, HF, QS and scaled HF for low frequency, high frequency, quasi-static, and scaled high frequency, respectively. In this work, low frequency and quasi-static are synonymous.

TABLE 1

A Summary of the Steps Used in Determining $N_{ss}(\phi_s)$ Using the Quasi-Static (QS) Technique

STEP NUMBER	EQUATION OR GRAPH USED	COMMENTS
1	Figure 8	Obtain HF and quasi-static curves (QS).
2	QS, Figure 10	Determine $C_{ox} = C_{QS}$(acc.).
3	HF, Figure 10	Determine C_{HF}(acc.)
4	Equation 36	Calculate R_s.
5	Equation 39	Scale HF curve obtaining C'_{HF} curve.
6	Equation 43, QS of Figure 10, scaled HF of Figure 10	Calculate $N_{ss}(V_a)$.
7	Equation 52, QS of Figure 8	Numerically integrate getting $\phi_s(V_a)$ to within a constant Δ.
8	Equation 64, scaled HF of Figure 10	Calculate L_{DMAX}.
9	Equation 63	Calculate $\langle N_A \rangle$.
10	Equation 17	Calculate L.
11	Equation 56	Calculate C_{meas}(flat band).
12	Scaled HF of Figure 10	Determine V(flat band) and therefore Δ needed in step 7.

NOTE: 1. The quasi-static curve used here is the same as the low frequency curve discussed in the text.

2. The abbreviations are LF, HF, QS, AND scaled HF for low frequency, high frequency, quasi-static, and scaled high frequency, respectively. In this work, low frequency and quasi-static are synonymous.

CHAPTER III

THE DEVELOPMENT OF THE MICRO-HALL CONDUCTANCE TECHNIQUE

1. INTRODUCTION

The basic idea of determining N_{ss} through conductance techniques was introduced in 1968 by Fang and Fowler (Ref. 23) and Arnold (Ref. 24), as was mentioned previously. Conceptually the two conductance techniques are quite similar. Consider Figure 12, an MOS system under the influence of a bias voltage V_g. There exists some interface state density N_{ss} at the oxide-semiconductor interface as shown in the figure.

The approach taken in the conductance technique is as follows (see Ref. 27). If some voltage is applied to the gate of an MOS transistor, a portion of that voltage appears across the oxide, and the rest of that voltage appears across the semiconductor space charge region. Since part of the applied gate voltage appears across the space charge region, the Fermi level must have changed its relative position in the band gap. Consider the case where the transistor is going from depletion toward inversion, as shown in Figure 12. The applied gate voltage has induced charge in the space charge region. If the surface is already at strong inversion, this increase in charge within the space charge region is not used to increase the depletion region width because the depletion region is already at its maximum width.

Consequently, the charge induced at the surface due to the applied voltage can be assumed to fall into two categories: (1) free charge carriers at the surface, and (2) immobile or fixed charges trapped in the interface states. This is only true when the device is already "turned on," or at the point where $v_s = -2u_b$.

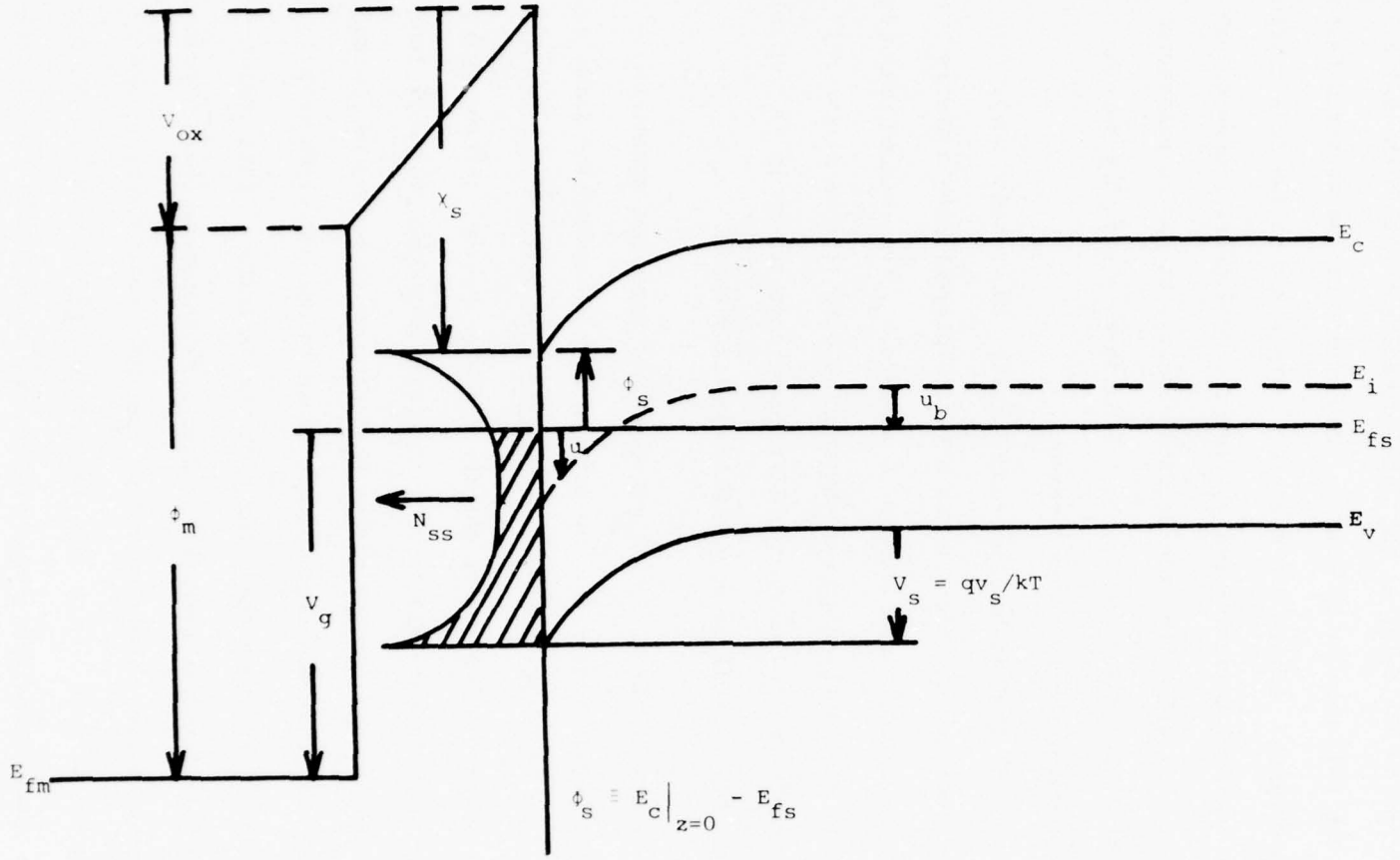

Figure 12. MOS interface under the influence of an applied gate voltage, V_g.

The approach taken to finding N_{ss} then is as follows. The total charge induced on the oxide is the oxide capacitance times the oxide voltage. The Hall carrier density at the surface can be measured using the Hall technique. If one can measure r, the ratio of the free carrier density to the Hall carrier density, then the free carrier density can be determined. Knowing the free carrier density, it can be subtracted from the total charge induced across the oxide to yield that portion which is accounted for by trapped charge.

Conceptually that is how the conductivity measurements work. In the next section the equations necessary to implement such a theory are derived. The basic technique is to measure N_H, the induced Hall carrier density as a function of V_g, the applied gate voltage at two different temperatures. By using two different temperature, it is possible to determine N_{ss} as well as r, the Hall mobility ratio.

2. DEVELOPMENT OF THE MICRO-HALL CONDUCTANCE TECHNIQUE EQUATIONS

Consider again Figure 12. To develop this technique the first equation needed is an expression for the applied gate voltage in terms of (a) the free charges induced in the space charge region, (b) the charge trapped in the interface states, (c) the metal-semiconductor work function differences, and (d) any charge that happens to be trapped permanently in the gate. This development follows close to one in Reference 27.

Consider first the actual charge on the capacitor. This charge comes from bulk minority carriers induced into the space charge region, bulk majority carriers repelled out of the space charge region, and finally charge trapped in the interface states, Q_t. Let N_i and N_d represent the induced and depleted charge in cm^{-2}, and also let Q_t be the

charge trapped in coul/cm^{-2}, then the total number of charges existing at the oxide-semiconductor interface including their sign is

$$\pm N_i \pm N_d + \frac{Q_t}{q} \text{ cm}^{-2} \tag{68}$$

The upper sign is for p-channel and the lower sign is for n-channel. The quantities N_i and N_d have the dimensions of cm^{-2} and represent states. The sign has to be supplied to these terms. The quantity Q_t actually implies charge, however, and inherently has a sign associated with it. For p-channel devices, some surface states are emptied and Q_t is inherently positive. For n-channel devices, some surface states fill, and Q_t is inherently negative. The induced and depleted states are both positive for p-channel and negative for n-channel. Thus, all three terms are additive for a p or n-channel device.

The total voltage drop across the oxide will contain two terms. The first is the voltage drop due to the charges in Equation 68. The second has to do with any charge trapped in the oxide itself. During fabrication or irradiation, charge can be incorporated in the oxide which is fixed. It does not change its magnitude with Fermi level variations, and therefore is constant with respect to V_g. It is further assumed that this trapped oxide charge does not vary with temperature or become mobile with temperature. This last assumption limits how high the temperature may be set when taking measurements. If the temperature is too great, some trapped charge can become mobile; and, while its total magnitude may not change, its proximity to the surface may change. Redistribution of this charge at elevated temperatures can cause it to affect the underlying silicon in some varying fashion. Thus, the measurements must be taken at some temperature range where fixed oxide charge is immobile.

If the voltage drop across the oxide due to the preexistence of some fixed charge is designated as V'_{ox}, the oxide voltage becomes

$$V_{ox} = \left(\mp N_i \mp N_d - \frac{Q_t}{q}\right) \frac{q}{C_{ox}} + V'_{ox} \tag{69}$$

The signs chosen here render V_{ox} as positive.

The applied gate voltage, V_g, can now be expressed as

$$\phi_m + V_{ox} = \chi_s - \phi_s + V_g$$

or

$$V_g = \phi_s + V_{ox} + \left(\phi_m - \chi_s\right) \tag{70}$$

Using Equation 69, the gate voltage is

$$V_g = \phi_s - \left(\pm N_i \pm N_d + \frac{Q_t}{q}\right) \frac{q}{C_{ox}} + V_{go} \tag{71}$$

Here, the following definitions apply:

ϕ_s = Fermi potential at the interface measured in volts

N_i = induced carrier concentration (cm^{-2})

N_d = depleted carrier concentration (cm^{-2})

Q_t = trapped charge at the interface ($coul/cm^2$)

C_{ox} = oxide capacitance (f/cm^2)

V_{go} = gate zero bias voltage measured relative to the silicon which is $(\phi_m - \chi) + V'_{ox}$. Note that V_{go} is not a function of temperature and surface potential.

ϕ_m = Fermi level of the metal

χ_s = semiconductor electron affinity. Notice that $\phi_m = \chi_s - \phi_s$.

In writing Equation 70 notice that all the electronic potential quantities increase downward in the figure (indicating increasing electronic potential) and electronic energies increase in the upward direction with the exception of ϕ_s, which has been selected as positive in the

other direction. Again the upper sign stands for p-channel, the lower for n-channel.

An examination of Equation 71 will point out some of its fundamental features. First of all, Φ_s is a function of the temperature T because as the temperature varies, the relative position of Φ_s changes within the band gap. The total amount of charge trapped depends on the relative position of Φ_s, so Q_t is a function of Φ_s and T. Similarly, the induced and depleted charge carrier densities are functions of Φ_s and T. Thus, the following expressions indicate what types of relations exist here:

$$\Phi_s = \Phi_s(T) \tag{72a}$$

$$Q_t = Q_t(\Phi_s, T) \tag{72b}$$

$$N_i = N_i(\Phi_s, T) \tag{72c}$$

$$N_d = N_d(\Phi_s, T) \; . \tag{72d}$$

It is possible to derive exact relationships for Equations 72a, 72c, and 73d in the cases of either Boltzmann Statistics (nondegenerate semiconductors) or Fermi Dirac Statistics (degenerate semiconductors). Such relationships will be necessary to do the entire analysis, and will be derived in Chapter IV.

Equation 71 can be differentiated with respect to Φ_s holding T constant.

$$\left.\frac{\partial V_g}{\partial \Phi_s}\right|_T = 1 - \left(\pm \left.\frac{\partial N_i}{\partial \Phi_s}\right|_T \pm \left.\frac{\partial N_d}{\partial \Phi_s}\right|_T + \frac{1}{q} \left.\frac{\partial Q_t}{\partial \Phi_s}\right|_T \right) \frac{q}{C_{ox}} \tag{73}$$

which can be rearranged as

$$-\frac{1}{q} \left.\frac{\partial Q_t}{\partial \Phi_s}\right|_T = \frac{C_{ox}}{q} \left.\frac{\partial V_g}{\partial \Phi_s}\right|_T \pm \left.\frac{\partial N_i}{\partial \Phi_s}\right|_T - \frac{C_{ox}}{q} \pm \left.\frac{\partial N_d}{\partial \Phi_s}\right|_T \tag{74}$$

By defining the following quantities,

$$N_{ss} \equiv -\frac{1}{q}\frac{\partial Q_t}{\partial \Phi_s}\bigg|_T \tag{75}$$

$$w = \frac{\partial N_H}{\partial N_i}\bigg|_T \tag{76}$$

$$\alpha = \frac{C_{ox}}{q}\frac{\partial V_g}{\partial N_H}\bigg|_T \tag{77}$$

and further, noting that at constant T

$$\frac{\partial V_g}{\partial \Phi_s}\bigg|_T \frac{\partial \Phi_s}{\partial N_i}\bigg|_T = \frac{\partial V_g}{\partial N_i}\bigg|_T$$

and

$$\frac{\partial N_H}{\partial N_i}\bigg|_T \frac{\partial V_g}{\partial N_H}\bigg|_T = \frac{\partial V_g}{\partial N_i}\bigg|_T$$

then Equation 74 becomes

$$N_{ss} = \left[\frac{\partial N_i}{\partial \Phi_s}\bigg|_T (\alpha w \pm 1)\right] - \frac{C_{ox}}{q} \pm \frac{\partial N_d}{\partial \Phi_s}\bigg|_T \tag{78}$$

It is important to bear in mind that $\partial N_i/\partial \Phi_s\big|_T$ and $\partial N_d/\partial \Phi_s\big|_T$ are both equations that are theoretically obtainable as functions of Φ_s and T. Also, the quantity α is the slope of a curve of N_H vs V_g where N_H is the induced Hall carrier density. Thus, if data are found relating N_H to V_g experimentally, then α is also known. It will not be known as a function of Φ_s and T, but will be known as a function of either V_g or N_H. Thus, functional forms for all the variables in Equation 78 can be found either theoretically or experimentally; figure 13 shows a typical plot of N_H vs V_g at two different temperatures. These values can easily be measured experimentally, as described in the next chapter.

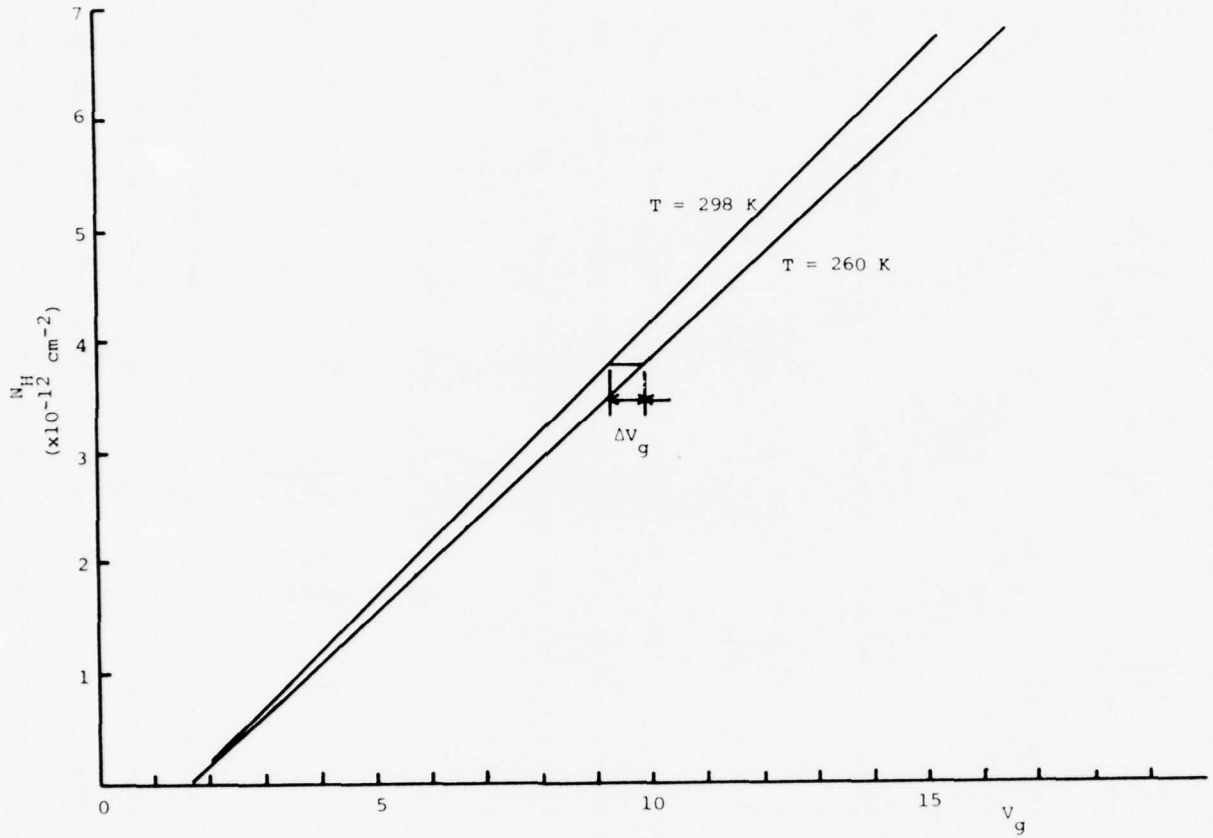

Figure 13. A typical plot of the induced Hall carrier concentration, N_H vs. applied gate voltage, V_g for two different temperatures. The quantity α comes from the slope of one curve. The quantity β must be determined using both curves (see text).

Next consider Equation 71 again, and differentiate it with respect to temperature holding N_i constant.

$$\left.\frac{\partial V_g}{\partial T}\right|_{N_i} = \left.\frac{\partial \Phi_s}{\partial T}\right|_{N_i} - \left(0 \pm \left.\frac{\partial N_d}{\partial T}\right|_{N_i} + \frac{1}{q}\left.\frac{\partial Q_t}{\partial T}\right|_{N_i}\right)\frac{q}{C_{ox}} \tag{79}$$

Further, define a constant β_o by

$$\beta_o \equiv \frac{C_{ox}}{q}\left.\frac{\partial V_g}{\partial T}\right|_{N_i} \tag{80}$$

Using this definition and rearranging Equation 79, the following results

$$-\frac{1}{q}\left.\frac{\partial Q_t}{\partial T}\right|_{N_i}\left.\frac{\partial T}{\partial \Phi_s}\right|_{N_i} = \left.\frac{\partial T}{\partial \Phi_s}\right|_{N_i}\left(\beta_o \pm \left.\frac{\partial N_d}{\partial T}\right|_{N_i}\right) - \frac{C_{ox}}{q} \tag{81}$$

From Equation 72a, it is known that $Q_t = Q_t(\Phi_s, T)$, and, from Equation 72c, it is known that $N_i = N_i(\Phi_s, T)$. By assuming that Equation 73c can be inverted to $\Phi_s = \Phi_s(N_i, T)$, then the variation of Q_t or N_i can in theory be written as

$$Q_t = Q_t\left(\Phi_s\left(N_i, T\right), T\right)$$

Then

$$\left.\frac{\partial Q_t}{\partial T}\right|_{N_i} = \left.\frac{\partial Q_t}{\partial \Phi_s}\right|_{T}\left.\frac{\partial \Phi_s}{\partial T}\right|_{N_i} + \left.\frac{\partial Q_t}{\partial T}\right|_{\Phi_s} \tag{82}$$

Equation 81 is valid as long as Equation 72c does not have a singularity in its derivative with respect to Φ_s. It can be shown that this is a quite reasonable assumption. Actually, in inversion it can be shown that as the semiconductor goes into strong inversion, N_i increases monotonically as Φ_s decreases, so this assumption is valid over the region of interest.

Equation 82 can be simplified to the following:

$$\left.\frac{\partial Q_t}{\partial T}\right|_{N_i} \simeq \left.\frac{\partial Q_t}{\partial \Phi_s}\right|_{T} \left.\frac{\partial \Phi_s}{\partial T}\right|_{N_i} \tag{82a}$$

This is true as long as the following assumption can be made:

$$\left|\left(\left.\frac{\partial Q_t}{\partial \Phi_s}\right|_{T} \left.\frac{\partial \Phi_s}{\partial T}\right|_{N_i}\right)\right| >> \left|\left(\left.\frac{\partial Q_t}{\partial T}\right|_{\Phi_s}\right)\right| \tag{83}$$

Equation 83 can be rewritten using cyclic derivatives and further simplified to

$$\left|\left(\left.\frac{\partial Q_t}{\partial N_i}\right|_{T}\right)\right| >> \left|\left(\left.\frac{\partial Q_t}{\partial N_i}\right|_{\Phi_s}\right)\right| \tag{84}$$

In the actual experiment the induced Hall carrier concentration, N_H, and the Hall ratio r are measured at two different temperatures. Actually, r does not vary much with T, but N_H does. The amount of charge trapped, Q_t, is a function of Φ_s. In Equation 84, we can fix Φ_s such that Q_t is the same on both the right and left side of the inequality, and the problem then becomes one of examining ΔN_i at constant T and Φ_s. The approach used here is to make the assumption, perform the calculations, and see if this inequality in fact holds. Using this approach some typical numbers are listed below for device number S127R000.

$$\Phi_s = -37\ kT \qquad \left.\frac{1}{\Delta N_i}\right|_{T} \simeq 11 \times 10^{-11} \qquad \left.\frac{1}{\Delta N_i}\right|_{\Phi_s} \simeq 0.47 \times 10^{-11}$$

$$\Phi_s = -44\ kT \qquad \left.\frac{1}{\Delta N_i}\right|_{T} \simeq 5 \times 10^{-11} \qquad \left.\frac{1}{\Delta N_i}\right|_{\Phi_s} \simeq 0.217 \times 10^{-11}$$

In both cases the assumption then is reasonable. Using the approximation in Equation 84, Equation 81 then becomes

$$N_{ss} = \left.\frac{\partial T}{\partial \Phi_s}\right|_{N_i} \left(\beta_o \pm \left.\frac{\partial N_d}{\partial T}\right|_{N_i} \right) - \frac{C_{ox}}{q} \tag{85}$$

It is now possible to make the last assumption and final simplification. The Hall mobility ratio, r, can be written as

$$r = N_i/N_H \tag{86}$$

where N_H is the induced Hall carrier concentration graphed in Figure 13 against V_g. Equation 86 implies that $N_H = N_H(r,N_i)$. It is possible for r to depend on temperature. Finally, by curve fitting the original data plotted in Figure 13 it is possible to derive an expression for $V_g = V_g(N_H,T)$. The dependence of this chain then can be expressed as

$$V_g = V_g\left(N_H,T\right) = V_g\left[N_H\left(r,N_i\right),T\right] \tag{87}$$

Taking the partial derivative of this with respect to T and holding N_i constant one obtains

$$\left.\frac{\partial V_g}{\partial T}\right|_{N_i} = \left.\frac{\partial V_g}{\partial N_H}\right|_T \left.\frac{\partial N_H}{\partial r}\right|_{N_i} \left.\frac{\partial r}{\partial T}\right|_{N_i} + \left.\frac{\partial V_g}{\partial T}\right|_{N_H} \tag{88}$$

If the dependence of r on T is not very large, this can be written as

$$\left.\frac{\partial V_g}{\partial T}\right|_{N_i} \simeq \left.\frac{\partial V_g}{\partial T}\right|_{N_H} \tag{89}$$

The assumption here is that

$$\left| \left.\frac{\partial V_g}{\partial N_H}\right|_T \frac{N_i}{r^2} \left.\frac{\partial r}{\partial T}\right|_{N_i} \right| << \left.\frac{\partial V_g}{\partial T}\right|_{N_H} \tag{90}$$

which can be expressed as

$$\frac{r^2\beta}{N_i\alpha} >> \left.\frac{\partial r}{\partial T}\right|_{N_i} \tag{91}$$

where

$$\beta \equiv \frac{C_{ox}}{q} \left.\frac{\partial V_g}{\partial T}\right|_{N_H} \tag{92}$$

By looking at one device at two separate temperature ranges, r can be determined and $\Delta r/\Delta T$ found. This was done, and it was found that in general

$$\frac{r^2\beta}{N_i\alpha} \simeq 4 \left.\frac{\partial r}{\partial T}\right|_{N_i}$$

Thus, the second assumption is justifiable.

Equation 85 can now be written in its final form,

$$N_{ss} = \left.\frac{\partial T}{\partial \Phi_s}\right|_{N_i} \left(\beta \pm \left.\frac{\partial N_d}{\partial T}\right|_{N_i} \right) - \frac{C_{ox}}{q} \tag{93}$$

In Equation 92, the partial derivatives can be found as functions of Φ_s and *T through space charge theory. The quantities* β *and* C_{ox} *can be* determined experimentally. The unknown here is N_{ss}.

Finally, the definition of w in Equation 76 gives us a way to evaluate r as a function of N_H, the measured Hall carrier density, and N_i, the induced carrier concentration.

$$r = \frac{N_i}{\int_0^{N_i} w dN_i} \tag{94}$$

All of the equations used in the micro-Hall conductance technique have now been developed.

In an effort to put these equations into proper prospective, a few of them will be repeated here and grouped to show how this system is solved.

Consider again Equations 78, 93, and 94.

$$N_{ss} = \left.\frac{\partial N_i}{\partial \Phi_s}\right|_T \left(\alpha \cdot w \pm 1\right) - \frac{C_{ox}}{q} \pm \left.\frac{\partial N_d}{\partial \Phi_s}\right|_T \tag{78}$$

$$N_{ss} = \left.\frac{\partial T}{\partial \Phi_s}\right|_{N_i} \left(\beta \pm \left.\frac{\partial N_d}{\partial T}\right|_{N_i}\right) - \frac{C_{ox}}{q} \tag{93}$$

$$r = \frac{N_i}{\int_0^{N_i} w dN_i} \tag{94}$$

All of the partial derivatives as well as N_i are functions for which expressions can be derived through basic surface theory. All of them are functions of Φ_s, the surface potential, and T, the temperature. Also, the quantities α and β can be determined experimentally. The quantity α is the slope of one of the curves in Figure 13, and β can be found by differencing the two curves in Figure 13. Thus, β can be approximated by

$$\beta \cong \frac{C_{ox}}{q} \left.\frac{\Delta V_g}{\Delta T}\right|_{N_H} \tag{95}$$

Therefore Equations 78, 93, and 94 constitute a set of three equations in the three unknowns r, w, and N_{ss}.

In order to simplify these three equations, the following quantities can be defined.

$$C_1 \equiv \left.\frac{\partial N_i}{\partial \Phi_s}\right|_T \tag{96}$$

$$C_2 \equiv \pm \left.\frac{\partial N_i}{\partial \Phi_s}\right|_T - \frac{C_{ox}}{q} \pm \left.\frac{\partial N_d}{\partial \Phi_s}\right|_T \tag{97}$$

$$C_3 \equiv \left.\frac{\partial T}{\partial \Phi_s}\right|_{N_i} \tag{98}$$

$$C_4 \equiv \pm \left.\frac{\partial T}{\partial \Phi_s}\right|_{N_i} \left.\frac{\partial N_d}{\partial T}\right|_{N_i} - \frac{C_{ox}}{q} \tag{99}$$

Then Equations 78, 93, and 94 can be rewritten as

$$N_{ss} = C_1 \alpha w + C_2 \tag{100a}$$

$$r = \frac{N_i}{\int_0^{N_i} w dN_i} \tag{100b}$$

$$N_{ss} = C_3 \beta + C_4 \ . \tag{100c}$$

All four quantities C_1, C_2, C_3, C_4 are functions of Φ_s and T. Their exact expressions are derived in the next chapter.

Notice that w can be expressed as a function of α and β by solving Equation 100c for N_{ss} and substituting into Equation 100a.

$$w = \frac{C_3 \beta + C_4 - C_2}{C_1 \alpha} \tag{101}$$

The quantities α and β are functions of N_H, so they are also functions of N_i through r. Thus, Equation 101 really expresses w as a function of N_i.

The method chosen to solve this system is as follows. First, a value for r is chosen. A good choice is r = 1. This value for r allows α and β to be determined as functions of N_i instead of N_H. Next, Φ_s and T are fixed, and C_1, C_2, C_3, C_4, and the upper limit in the integral Equation 100b are calculated. Using Equation 101 for w, Equation 100b is numerically integrated yielding a new r. This process is repeated until r converges at some value. After this value for r is determined, a new Φ_s and T are chosen, and the whole process is repeated.

3. SUMMARY

In this chapter the micro-Hall conductance technique has been examined. The equations used in determining $N_{ss}(\Phi_s)$ have been developed.

The types of input data or measurements needed for this technique have been discussed. Figure 13 is a typical plot of the curves needed for this analysis.

While the basic equations peculiar to this particular technique have been developed here, all the equations necessary to perform the analysis have not been presented. The next chapter provides the additional equations needed for this analysis.

Finally, Table 2 summarizes the step taken to obtain $N_{ss}(\Phi_s)$ following this technique.

TABLE 2

A Summary of the Major Steps Used in Finding $N_{ss}(\Phi_s)$ in the Micro-Hall Conductance Technique

STEP NUMBER	EQUATIONS OR GRAPHS USED	COMMENTS
1	See Chapter IV and Step 2, Table 1	Measure $N_H(V_g)$ at two distinct temperatures. Measure C_{ox}.
2	Figure 13 or raw data, Appendix B	Curve fit analytical expressions for $V_g(N_H)$ at both temperatures.
3	Appendix B	Calculate analytical curves for α and β as functions of N_H.
4	Appendix C	Select initial values for Φ_s,T.
5	Equations 96-99 and Chapter IV	Calculate C_1, C_2, C_3, C_4, N_i.
6		Select an initial value for r. This allows determination of α and β in terms of N_i.
7	Equations 100b, 101	Integrate Equation 100b. This yields a new r value of r'. If (r-r') is less than some error limit proceed onto step 8. If not, set r=r' and go back to step 6.
8	Equations 100a or 100c	Determine N_{ss}, r at this value of Φ_s.
9		Select another Φ_s, and go back to step 5.

CHAPTER IV

DEVELOPMENT OF THE HALL EQUATIONS AND SURFACE FIELD EQUATIONS NEEDED FOR THE MICRO-HALL CONDUCTANCE TECHNIQUE

1. INTRODUCTION

In the last chapter the micro-Hall conductance technique was developed. It was demonstrated that if one could calculate $N_H(V_g)$ at two separate temperatures, and if C_1, C_2, C_3, C_4, and N_i all could be evaluated theoretically as functions of the surface potential, Φ_s, and T, temperature, then $N_{ss}(\Phi_s)$ could be determined. The intent of this chapter is to develop the actual equations that are used to calculate N_H from the experimental data and develop the equations used to calculate the other quantities from Φ_s and T. Thus, the chapter is divided into two main sections. The first section deals with the Hall technique, while section two deals with the electric field theory.

The theory in Chapter III needs a determination of $N_H(V_g)$. In taking experimental data to determine N_H, data can quite readily be taken to determine μ_H, the Hall mobility, and $\sigma_\square$, the sheet conductivity of the surface. The units of μ_H and $\sigma_\square$ are cm^2/v-sec and mho/square, respectively. It was decided to calculate these additional parameters as part of the experiment. Therefore, the equations necessary for determining them are also described. One of the outputs of the program which determines $N_{ss}(\Phi_s)$ is a plot of $V_g(\Phi_s)$. Thus, N_H, μ_H, and $\sigma_\square$ can be conveniently examined as a function of surface potential.

The experimental quantities are N_H, μ_H and $\sigma_\square$, all as functions of V_g. Data are obtained at two temperatures. From these measurements, α and β as defined by Equations 77 and 92 are calculated.

In addition $V_g(\Phi_s)$ is determined, so the quantities μ_H and $\sigma_\square$ can also be related to Φ_s.

2. CALCULATION OF μ_H, $\sigma_\square$ AND N_H

A number of techniques and geometries have been developed for the measurement of the Hall voltage. (Refs. 33 and 34.) L. J. van der Pauw has developed a theory for measuring the specific resistivity and Hall mobility of discs of arbitrary shape (Ref. 35) under certain restrictions. The four assumptions are that (1) the contacts are at the circumference of the sample, (2) the contacts are small, (3) the sample is homogeneous in thickness, and (4) the surface is singly connected. This analysis can be used on an MOS transistor to explore its inversion region by designing the transistor properly.

Consider Figure 14. This depicts a circular MOS transistor with four symmetrically positioned sources (or drains) S_1, S_2, S_3, and S_4. The sources have small "fingers" that protrude under a gate oxide. When the surface is inverted, conduction can occur between the respective sources. Practically speaking, if the width of the fingers of the sources is much smaller than the device circumference, then criterion (2) above can be satisfied. The first and fourth criteria are easily satisfied also. The only one which is not easily satisfied is criterion (3). This particular criterion can be circumvented by considering the sheet resistance of the inverted region instead of the specific resistivity. This is the approach taken here.

The circular geometry transistor has been used by several investigators in the past as a method for examining inversion layers in MOS transistors (Refs. 36, 37, 27). The basic Hall technique allows

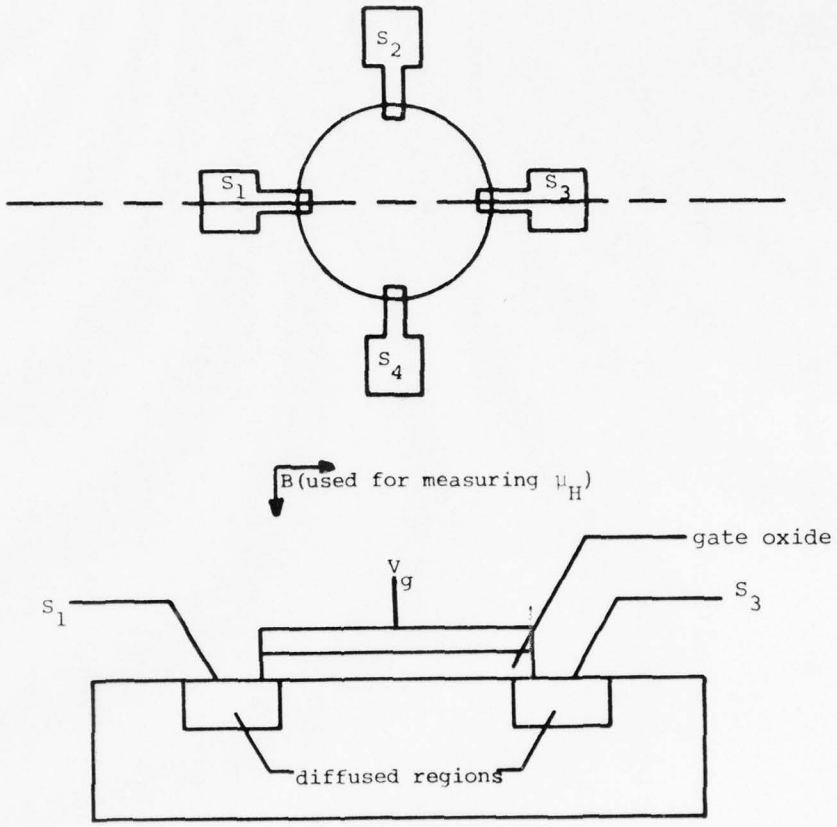

Figure 14. a) A circular MOS transistor with four symmetrical sources or drains labeled S_1, S_2, S_3, and S_4 respectively.
b) A section view of the MOS transistor.

calculation of μ_H, $\sigma_\square$ and N_H directly from current voltage measurements combined with the magnetic field strength.

No attempt will be made here to derive the actual equations used in the Hall measurements. The derivations are straightforward and are quoted in most of the references. Reference 35 contains the actual solutions to the electric field problem from which these equations arise. The only significant variation here is to realize that with the inverted silicon layer the resistivity is sheet resistance, and is in ohms per square. In van der Pauw's original article he deals with device resistivity in ohm-cm, so if the sample thickness is divided out, the resulting equations are in ohms per square.

The transistor in Figure 14 has four symmetrical sources, as has already been mentioned. Consider the following definition,

$$R_{ij,kl} = \frac{V_l - V_k}{I_{ij}} \tag{102}$$

The resistance $R_{ij,kl}$ is the potential difference between the l and k^{th} electrodes divided by the current going through the i-j electrode path. Using this definition, the sheet resistivity of the sample can be found by

$$\rho_s = \frac{\pi}{\ln 2} \frac{(R_{ij,kl} + R_{jk,li})}{2} f\left(\frac{R_{ij,kl}}{R_{jk,li}}\right) \tag{103}$$

Thus, if a current is applied to the i and j terminals, and the voltage across terminals k and l is measured, and if then current is applied to the j and k terminals, and the voltage across terminals l and i is measured, then ρ_s, the sheet resistivity, is given by Equation 103. The function f is defined by

$$\frac{R_{ij,kl} - R_{jk,li}}{R_{ij,kl} + R_{jk,li}} = f \cosh^{-1}\left[\frac{\exp \ln 2/f}{2}\right]$$

A plot of f vs ($R_{ij,kl}/R_{jk,li}$) is shown in Figure 15. The function f is a correction factor that allows one to take into account any lack of symmetry in the electrode placement around the device. Notice that if the device is totally symmetric, $R_{ij,kl} = R_{jk,li}$, and Equation 103 would become

$$\rho_s = \frac{\pi}{\ell n\ 2} R_{ij,kl} \tag{105}$$

or

$$\rho_s = \frac{\pi}{\ell n\ 2} \frac{V_l - V_k}{I_{ij}} \tag{106}$$

In Equations 102 through 106, it is assumed that ijkl are cyclic permutations of 1, 2, 3, 4. Thus, current is applied only to two adjacent electrodes, and the voltage across the other two adjacent electrodes is measured. For the devices used in this experiment, in general the four possible measured values of $R_{ij,kl}$ differed by less than 5%. Examination of Figure 15 shows that the value for f in this case is greater than 0.99. Thus, the f function was ignored in these calculations. Instead, $R_{ij,kl}$ was measured for all four cases and the average was used. Thus, letting $\langle R_{ij} \rangle$ be the average defined by

$$\langle R_{ij} \rangle \equiv \left(R_{12,34} + R_{23,41} + R_{34,12} + R_{41,32}\right)/4 \tag{107}$$

then the sheet resistivity was found by

$$\rho_s = \frac{\pi}{\ln\ 2} \langle R_{ij} \rangle \tag{108}$$

Only the first two subscripts are used here indicating that adjacent terminals are stimulated. The units for ρ_s are ohms/square here. It should be noted that if the simulating voltage is held constant, and if the gate voltage is varied, ρ_s will vary with it. Thus, the value for ρ_s in Equation 108 varies with the applied gate voltage. The sheet conductivity, $\sigma_\square$ is given by

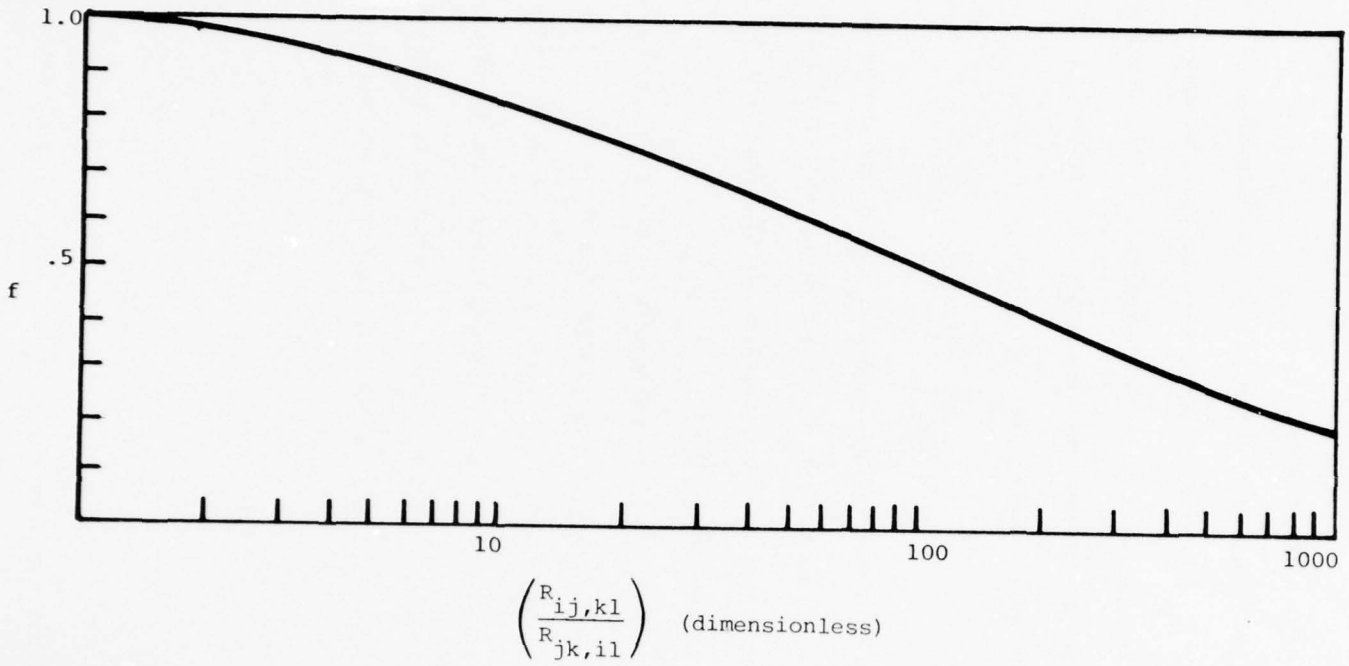

Figure 15. A plot of the function f used in the van der Pauw theory.

$$\sigma_{\square} = \frac{1}{\rho_s} \tag{109}$$

The units for $\sigma_{\square}$ here are mho/square.

The Hall mobility comes from a similar set of measurements. Notice, however, that $\sigma_{\square}$ and ρ_s can be determined without the influence of a magnetic field applied perpendicular to the surface of the device. The Hall mobility must be determined with the aid of an applied field. The equation for the Hall mobility is

$$\mu_H = \frac{10^8}{B} \frac{\Delta R_{j1,ik}}{\rho_s} \tag{110}$$

where ρ_s is defined by Equation 108, and $\Delta R_{j1,ik}$ is the change in the resistance $R_{j1,ik}$ with and without the applied magnetic field B. The units of B are Gauss. Again, the derivation of this equation is in Reference 35 and is only quoted here.

Notice that the Hall mobility measurements are taken by looking at a voltage across two <u>opposite</u> electrodes when the remaining two electrodes are stimulated with a current. For instance, a current may be pumped through terminals 1 and 3, and the voltage measured over 2 and 4, or the opposite may be done. In this experiment, both sets of measurements were done, and the average was used. Thus, defining $\langle R_{j1} \rangle$ as

$$\langle \Delta R_{j1} \rangle = (\Delta R_{13,24} + \Delta R_{24,13})/2 \tag{111}$$

then

$$\mu_H = \frac{10^8}{B} \frac{\langle \Delta R_{j1} \rangle}{\rho_s} \tag{112}$$

Again, only the first two subscripts remain indicating that the measurements are taken across opposite electrodes while the remaining two electrodes are stimulated. Notice that again, $\langle \Delta R_{j1} \rangle$ is dependent on the applied gate voltage. The units of μ_H are cm^2- $volt^{-1}$ sec^{-1}.

Finally, once the Hall mobility and sheet resistivity are known, these can be used to calculate N_H, the Hall carrier concentration.

$$N_H = \frac{\sigma_\square}{q\ \mu_H} = \frac{1}{q\ \rho_s\ \mu_H} = \frac{B}{10^8\ q\ \langle \Delta R_{jl} \rangle} \tag{113}$$

This yields the density of the Hall carriers in cm^{-2}.

The approach to the measurements taken in this project was to build a transistor similar to the one shown in Figure 14. This transistor was put into a 10 pin flat package, placed within the poles of an electromagnet, and measurements were taken in it. First, all four pairs of adjacent terminals were stimulated as in Equation 107 and both pairs of opposite terminals were stimulated, as in Equation 111. This was done at several values of applied gate voltage, and two different temperatures. From the measurements it was possible to calculate $\sigma_\square$, μ_H, and N_H all as functions of V_g.

Before going on to the next set of derivations, a brief mention of some other effects that can affect our measurements should be made. In any series of Hall effect measurements, four other effects are present. They are (1) the transverse magnetoresistive effect, (2) the Ettinghausen effect, (3) the Nernst effect, and (4) the Righi-Leduc effect.

The transverse magnetoresistive effect is the increase in the effective resistance of a conducting channel due to the introduction of curvature to the paths traveled by charge carriers under the influence of a transverse magnetic field. The magnetic field causes the charge particles to travel effectively in helical paths, and decreases their apparent mobility.

Consider next some carriers moving in an x-direction under the influence of a magnetic field in the y-direction. The carriers will be

displaced toward the z-direction, and the faster carriers will be displaced the most. This results in a temperature gradient along the z-direction and is called the Ettinghausen effect.

Next consider a conductor that is hot at one end and cool at the other. This thermal gradient will give rise to charge transfer from the hot to the cold end. Under the influence of a magnetic field, this gives rise to a voltage transverse to the direction of flow of the electrons. This is referred to as the Nernst effect. Since there is a flow of charge from the hot to cold end of the bar, and since there is a magnetic field present, an effect similar to the Ettinghausen effect is present in this case also. It is referred to as the Righi-Leduc effect.

By taking a proper set of measurements, all of these effects can be eliminated except the Ettinghausen effect. The special measurements involve changing the direction of the magnetic field and current flow during the experiment. These specific measurements are reviewed in References 33, 38, and 39. The transverse magnetoresistive effect is eliminated using a constant current. The Nernst effect and Righi-Leduc effect are eliminated by voltage reversals.

Since the Ettinghausen effect cannot be eliminated, its approximate value is calculated here using the equations from Reference 38 after they have been put in a form useful to inversion regions. The numbers used here are from a typical MOS transistor.

To a first approximation, the Hall coefficient R_s is given by

$$R_s \simeq \frac{1}{nq} \tag{114}$$

where n is the induced charge carrier density in m^{-2}. For a typical device, $n \sim 1 \times 10^{16}\ m^{-2}$, so

$$R_s \sim \frac{1}{1 \times 10^{16} \times 1.6 \times 10^{-19}}$$

$$R_s \sim 624\ m^2\ coul^{-1}$$

The Hall voltage is then given by

$$V_H \sim R_s BI \tag{115}$$

The currents used in this experiment were of the order of 1μa, and B is about 4.5 kG or 0.45 Tesla, so

$$V_H \sim (624)\ (0.45)\ (1 \times 10^{-6})\ \text{volts}$$

$$V_H \sim 280\ \mu V$$

The Ettinghausen coefficient, P_s, is given as

$$P_s = \frac{T}{\kappa_s} \frac{1}{2} \left(\frac{k}{q} \right) R_s \tag{116}$$

where

T = temperature, K

κ_s = thermal conductivity of silicon, 30 watts m^{-1} K^{-1}.

k/q = ratio of Boltzmann's constant to the electronic charge, 8.63×10^{-5} volts/K

The Ettinghausen temperature gradient, $\Delta T/\Delta y$ where Δy is normal to the current flow and in the plane of the inversion region, is given by

$$\frac{\Delta T}{\Delta y} = \frac{P_s IB}{w} \tag{117}$$

where w is the effective conduction width of the channel.

The Seebeck coefficient is determined by the relation of the Fermi level to the conduction band, and is the number u_s given in Figure 12 For these devices, $u_s \simeq 11$. The Seebeck coefficient is defined by

$$\theta = -\left(\frac{k}{q} \right) \left(2 - u_s \right) \tag{118}$$

Using Equations 116, 117, and 118, the Ettinghausen/Seebeck voltage is given by

$$V_E = \Theta w \frac{\Delta T}{\Delta y} \tag{119}$$

If the appropriate values are substituted into Equation 119, an approximate value for V_E can be found as

$$V_E \sim 2.8 \times 10^{-8} \text{ volt}$$

If this is compared to the theoretical Hall voltage, it is seen to be some four orders of magnitude less, and was consequently ignored.

One problem that experimentally arose was that when the magnet was energized, a pulse was induced in the input lines to the refrigerator of sufficient magnitude to break down the gate oxides. This phenomenon was eventually overcome by slowly energizing the magnets with a programmer. However, initially it was desirable to use as few readings as possible where the magnet had to be turned on and off. As a result, instead of doing the standard eight measurements as described in Reference 39, it was decided to use only two measurements involving the magnetic field, which are the measurements referred to in Equation 111.

It was also mentioned that the transverse magnetoresistive effect could be eliminated using a constant current. The currents used in this experiment were on the order of 1μA. Approximately 240 individual current measurements were made per device per dose level (480 I-V measurements). Because of the number of measurements needed, a constant current source would have been convenient so that external adjustment of the current would not have been necessary. However, such a constant current source was not available, and a stable constant voltage source was available that would handle the needed dynamic range. The source is described

in the next chapter. As a result, it was decided to take the measurements at a constant voltage.

To determine if the two compromises mentioned above would limit the results to any extent, one device was analyzed using the entire set of eight reversing measurements driven with a hand adjusted current source. The results are summarized in Table 3. Notice that the average difference is 0.9%, and the maximum is 2.9%. This is certainly within experimental error.

TABLE 3

Comparison of the Values of $\langle \Delta R_{j1} \rangle$ defined in Equation 111 Calculated by the Present Technique and the 8 Measurement Technique of Cusack (Ref. 39). The Average % Difference is 0.90%, and maximum is 2.9%.

Gate Voltage	Present Technique	Eight Measurement Technique Plus Constant Current	% Difference
- 2.5	690.1	689.4	0.105
- 3.0	430.9	425.9	1.17
- 3.5	314.9	309.8	1.63
- 4.0	249.2	244.3	1.96
- 4.5	205.5	202.1	1.64
- 5.0	175.4	172.4	1.71
- 5.5	154.5	150.0	2.9
- 6.0	135.0	133.1	1.37
- 6.5	121.4	119.8	1.39
- 7.0	110.1	108.9	1.14
- 8.0	92.8	91.5	1.4
- 9.0	80.1	80.0	0.17
-10.0	70.8	70.4	0.62
-11.0	63.1	63.0	0.07
-12.0	57.0	56.8	0.33
-13.0	51.9	52.1	0.426
-14.0	47.7	47.8	0.059
-15.0	44.02	43.88	0.678
-16.0	41.1	40.8	0.44
-17.0	38.2	38.4	0.523

3. CALCULATION OF C1, C2, C3, C4, and N_i AS FUNCTIONS OF Φ_s AND T

a. Introduction

In Chapter III a set of expressions that yield $N_{SS}(\Phi_s)$ was derived. (See Equations 78, 93 and 94.) In solving these equations certain quantities must be supplied through the theory of space charge regions. The quantities needed are N_i, $\partial N_i/\partial \Phi_s|_T$, $\partial N_d/\partial \Phi_s|_T$, $\partial T/\partial \Phi_s|_{Ni}$, and $\partial N_d/\partial T|_{Ni}$. The purpose of this section is to derive these quantities as functions of Φ_s and T.

Consider Figure 17, which depicts the surface of a semiconductor under the influence of an electric field. In general, the bulk semiconductor for most devices is nondegenerate where nondegenerate is taken to mean the Boltzmann approximation is valid. However, at the surface the situation is clearly different. By applying an appropriate gate bias, the surface can easily become degenerate where degenerate is taken to mean that Fermi-Dirac statistics must be used. As a result, the derivations developed in the next section consider the bulk as nondegenerate, but the surface as degenerate.

The approach used here is to first solve Poisson's equation using the appropriate charge density. The quantities ΔN and ΔP will be defined as the excess electron and hole densities above those in the bulk, expressed in units of cm^{-2}. Thus, they represent excess surface densities, and the inversion region thickness variation is integrated out. Once ΔN and ΔP are known as functions of Φ_s and T, the partial derivatives needed can be determined because ΔN and ΔP are N_i and N_d. In p-channel devices, $N_i = \Delta P$ and $N_d = \Delta N$. The situation is reversed in n-channel.

NOTE: FIGURE 16 - DELETED.

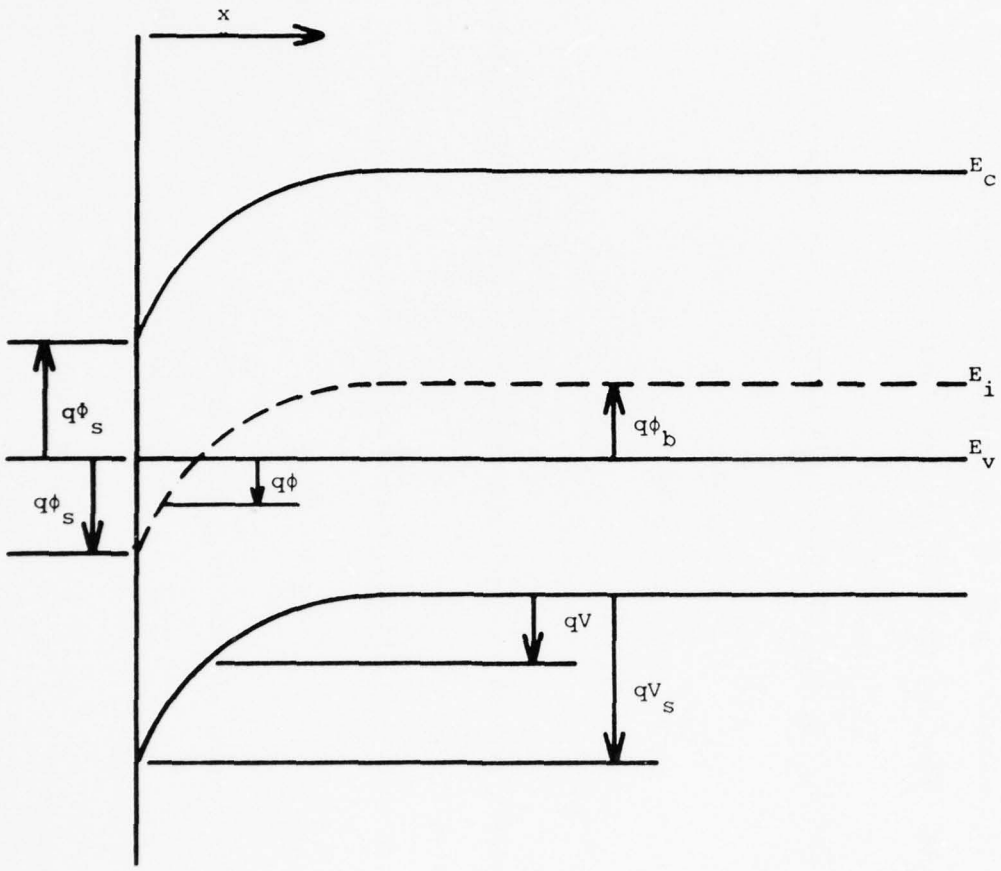

Figure 17. Semiconductor surface under the influence of an electric field.

b. Determination of N_i and N_d as Function of Φ_s and T

This treatment follows closely to one presented in Reference 40. The subscript b represents a bulk value for a variable, and an s represents a surface value for a variable.

Again, consider Figure 17, and some definitions presented in Chapter II. They are repeated here for clarity

$$q\phi = E_F - E_i \tag{1}$$

Notice that $E_i = E_i(z)$. The dimensionless potentials u and v are defined by

$$u = q\phi/kT \tag{6}$$

$$v = qV/kt \tag{7}$$

where

$$V = \phi - \phi_b \tag{5}$$

Notice that u, v, and V are all functions of z where z is the distance into the silicon.

Using these definitions, Poisson's equation can be written as

$$\frac{d^2u}{dz^2} = \frac{q\rho(z)}{\kappa_s \varepsilon_o kT} \tag{120}$$

The charge density $\rho(z)$ can be written as

$$\rho(z) = \rho_D + \rho_A + q(p-n) \tag{121}$$

where

ρ_D = ionized donor density, cm^{-3}

ρ_A = ionized acceptor density, cm^{-3}

p = hole concentration, cm^{-3}

n = electron concentration, cm^{-3}

Here, it is desirable to express all of these functions in their Fermi-Dirac degenerate forms. The boundary conditions used here are that $u = u_s$ at $z = 0$. This system will be solved for ΔN and ΔP as

functions of u, and converted to Φ_s dependence at the end. The dimensionless parameter u is more convenient to use here.

The hole and electron concentrations can be easily expressed as

$$n = 2\int_{E_c}^{\infty} D_c(E)\ f(E)\ dE \tag{122}$$

and

$$p = 2\int_{-\infty}^{E_v} D_v(E)\ \left[1-f(E)\right]\ dE \tag{123}$$

where

$D_c(E) \equiv$ the density of states function in the conduction band

$D_v(E) \equiv$ the density of states function in the valence band

and

$f(E) =$ the Fermi-Dirac occupation probability. (124)

In the present case, f(E) has the form

$$f(E) = \left\{1 + \exp\left[(E-E_f)/kT\right]\right\}^{-1}$$

Also, it is assumed here that both $D_c(E)$ and $D_v(E)$ take the common parabolic forms of

$$D_c(E) = 2\pi\left(2m_n^*/h^2\right)^{3/2}\left(E-E_c\right)^{1/2} \tag{125}$$

and

$$D_v(E) = 2\pi\left(m_p^*/h^2\right)^{3/2}\left(E_v-E\right)^{1/2} \tag{126}$$

Using these standard forms for $D_c(E)$, $D_v(E)$, and f(E), then n and p can be written as

$$n = 4\pi\left(2m_n^*/h^2\right)^{3/2}\int_{E_c}^{\infty} \frac{\left(E-E_c\right)^{1/2}\ dE}{1 + \exp\left[\left(E-E_f\right)/kT\right]} \tag{127}$$

AD-A064 143 NEW MEXICO UNIV ALBUQUERQUE BUREAU OF ENGINEERING R--ETC F/G 9/1
INVESTIGATION OF INTERFACE STATES USING METAL-OXIDE-SILICON TRA--ETC(U)
AUG 78 J WHITEFIELD, H D SOUTHWARD F29601-75-C-0036
UNCLASSIFIED EE-247(77)AF-352-1 AFWL-TR-77-140-VOL-1 NL

2 OF 4
AD A064143

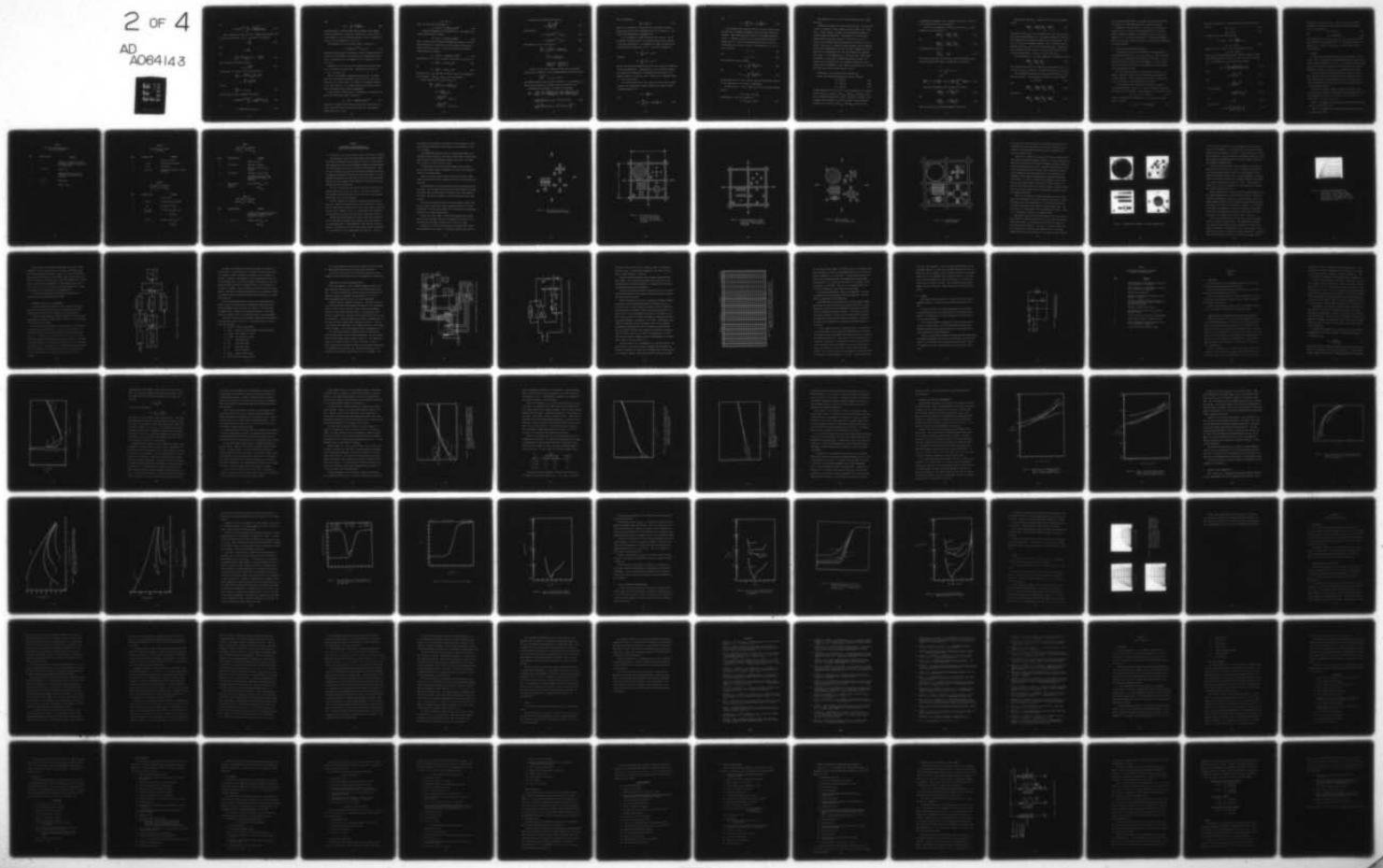

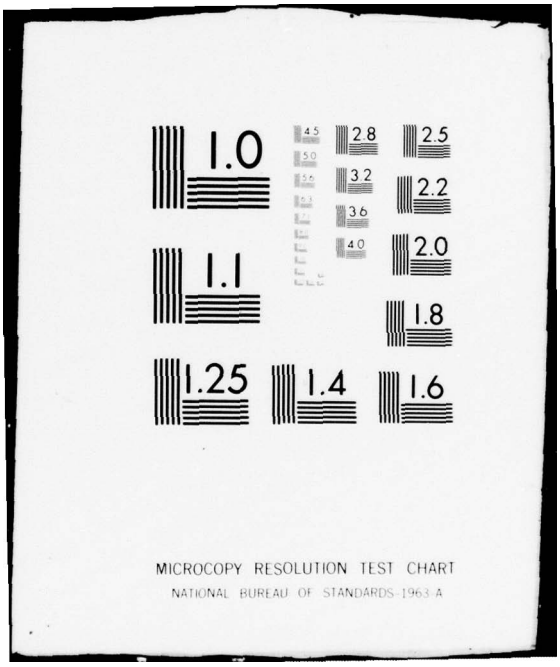
1.0
1.1
1.25
1.4
1.6
1.8
2.0
2.2
2.5
2.8
3.2
3.6
4.0
4.5
5.0
MICROCOPY RESOLUTION TEST CHART
NATIONAL BUREAU OF STANDARDS-1963-A

and

$$p = 4\pi\left(2m_p^*/h^2\right)^{3/2} \int_{-\infty}^{E_v} \frac{\left(E_v - E\right)^{1/2}}{1 + \exp\left[\left(E_f - E\right)/kT\right]} \tag{128}$$

These equations can be put into a more standard and convenient form as follows. Notice that $E = E(z)$. Now define a new variable

$$\xi \equiv \frac{E - E_c}{kT} \tag{129}$$

Then,

$$d\xi = \frac{dE}{kT}$$

and

$$\frac{E - E_f}{kT} = \frac{E - E_c + E_c - E_f}{kT} = \xi - \frac{\left(E_f - E_c\right)}{kT} \tag{130}$$

Next, also define the general quantity

$$w_{P,Q} = \frac{E_P - E_Q}{kT} \tag{131}$$

Using Equation 131, Equation 130 can be rewritten as

$$\frac{E - E_f}{kT} = \xi - \frac{\left[\left(E_f - E_i\right) - \left(E_c - E_i\right)\right]}{kT}$$

$$= \xi - \frac{\left[q\phi - \left(E_c - E_i\right)\right]}{kT}$$

Finally,

$$\frac{E - E_f}{kT} = \xi - \left(u - w_{c,i}\right) \tag{132}$$

Then Equation 127 can be expressed very simply as

$$n = 4\pi\left(2m_n^* \, kT/h^2\right)^{3/2} \int_0^{\infty} \frac{\xi^{1/2} \, d\xi}{1 + \exp\left[\xi - \left(u - w_{c,i}\right)\right]} \tag{133}$$

or

$$n = 4\pi\left(2m_n^* \, kT/h^2\right) F_{1/2}\left(u - w_{c,i}\right) \tag{134}$$

where

$$F_j(\eta) \equiv \int_0^\infty \frac{\xi^j \, d\xi}{1 + \exp(\xi-\eta)} \tag{135}$$

The quantity $F_j(\eta)$ is the so-called "Fermi-integral" and in general cannot be evaluated in a closed form. However, for a given value of j and argument η, this can be easily tabulated. Notice in Equation 134 that $w_{c,i}$ is not a function of z, but u is.

An expression for p can be stated similar to Equation 134.

$$p = 4\pi \left(2m_p^* \, kT/h^2\right)^{3/2} F_{\frac{1}{2}}\left(w_{v,i}-u\right) \tag{136}$$

The quantities m_n^* and m_p^* are the density of states effective masses for electrons in the conduction band and holes in the valence band respectively. Notice again that u in Equation 136 is a function of z, but $w_{v,i}$ is not.

Equations 134 and 136 can be placed directly into Poisson's equation as the values for n(z) and p(z). Specifically notice that if $u = u_b$, $n = n_b$ and $p = p_b$.

Next, it is necessary to determine $\rho_A(z)$ and $\rho_D(z)$. The model used here for the donor and acceptor states is that all of the donor states are at one energy level, E_D, and all of the acceptor states are at one energy level E_A. It is further assumed that the donor and acceptor concentrations are N_D and N_A respectively.

A donor state is neutral when it is occupied by an electron so the density of neutral donor states is given by

$$N_D = N_D \left\{1 + \tfrac{1}{2} \exp\left[\left(E_D-E_f\right)\right]/kT\right\}^{-1} \tag{137}$$

The factor of one-half arises from the fact that the electron that occupies a donor site can be of either spin (Ref. 41). The number of ionized donor sites is then

$$n_D^+ = N_D - n_D$$

Thus, the charge due to the donors is

$$\rho_D = qN_D \left\{1 + 2 \exp\left[(E_f - E_D)/kT\right]\right\}^{-1} \tag{138}$$

A similar development can be presented for N_A. The number of occupied acceptor sites is given by

$$n_A^- = N_A \left\{1 + 2 \exp\left[(E_A - E_f)/kT\right]\right\}^{-1} \tag{139}$$

Here, an acceptor site is negatively charged when occupied. The occupation factor here is 2 instead of one-half because the electrons in question here must be paired. Thus, the total static charge due to ionized acceptors is given by

$$\rho_A = -qN_A \left\{1 + 2 \exp\left[(E_A - E_f)/kT\right]\right\}^{-1} \tag{140}$$

Using Equations 1, 6, and 131, Equations 138 and 140 can be written as

$$\rho_D = qN_D\left[1 + 2 \exp\left(u - w_{D,i}\right)\right]^{-1} \tag{141}$$

and

$$\rho_A = -qN_A\left[1 + 2 \exp\left(w_{A,i} - u\right)\right]^{-1} \tag{142}$$

Notice that here, as in Equations 134 and 136, the only z dependence is in the variable u. Both $w_{D,i}$ and $w_{A,i}$ are fixed numbers.

Poisson's Equation 120 can now be written as

$$\frac{d^2u}{dz^2} = \frac{-q^2}{\kappa_s \varepsilon_o kT} \left\{ \frac{N_D}{1 + 2 \exp\left(u - w_{D,i}\right)} - \frac{N_A}{1 + 2 \exp\left(w_{A,i} - u\right)} + 4\pi\left(\frac{2m_p^* kT}{h^2}\right)^{3/2} F_{\frac{1}{2}}\left(w_{v,i} - u\right) - 4\pi\left(\frac{2m_n^* kT}{h^2}\right)^{3/2} F_{\frac{1}{2}}\left(u - w_{c,i}\right) \right\} \tag{143}$$

By defining the intrinsic Debye length as

$$L_D \equiv \left[\frac{\kappa_s \varepsilon_o \, kT}{2q^2 \, n_i}\right]^{1/2} \tag{144}$$

and noting that

$$n_i = 4\pi \left(2m_n^* \, kT/h^2\right)^{3/2} F_{1/2}\left(w_{i,c}\right) \tag{145}$$

$$= 4\pi \left(2m_p^* \, kT/h^2\right)^{3/2} F_{1/2}\left(w_{v,i}\right) \tag{146}$$

then Equation 144 can now be written as

$$\frac{d^2u}{dz^2} = \frac{1}{2 \, L_D^2} \left\{ \frac{N_D}{n_i} \frac{1}{1 + 2 \exp\left(u - w_{D,i}\right)} \right. \tag{147}$$

$$- \frac{N_A}{n_i} \frac{1}{1 + 2 \exp\left(w_{A,i} - u\right)}$$

$$\left. + \frac{F_{1/2}\left(w_{v,i} - u\right)}{F_{1/2}\left(w_{v,i}\right)} - \frac{F_{1/2}\left(u - w_{c,i}\right)}{F_{1/2}\left(w_{c,i}\right)} \right\}$$

In order to get ΔN and ΔP, Equation 147 must now be integrated. Actually, this integration is quite straightforward using the fact that

$$\frac{\partial F_j(\eta)}{\partial \eta} = j \, F_{j-1}(\eta) \quad \text{for } j>0$$

The boundary condition here is that in the bulk, $u = u_b$ and $du/dz\big|_{u_b} = 0$. This is true because the net electric field in the bulk is zero.

Performing the integration, one obtains the following.

$$\frac{du}{dz} = \pm \frac{1}{L_D} \left\{ \frac{N_D}{n_i} \ln\left[\frac{1 + \tfrac{1}{2} \exp\left(w_{D,i} - u\right)}{1 + \tfrac{1}{2} \exp\left(w_{D,i} - u_b\right)}\right] + \frac{N_A}{n_i}\left[\frac{1 + \tfrac{1}{2}\left(\exp u - w_{A,i}\right)}{1 + \tfrac{1}{2}\left(\exp u_b - w_{A,i}\right)}\right] \right.$$

$$- \frac{1}{F_{1/2}\left(w_{v,i}\right)} \left[\frac{2}{3} F_{3/2}\left(w_{v,i} - u_b\right) - \frac{2}{3} F_{3/2}\left(w_{v,i} - u\right)\right] \tag{148}$$

$$\left. + \frac{1}{F_{1/2}\left(w_{i,c}\right)} \left[\frac{2}{3} F_{3/2}\left(u - w_{c,i}\right) - \frac{2}{3} F_{3/2}\left(u_b - w_{c,i}\right)\right] \right\}^{1/2}$$

This is simplified as

$$\frac{du}{dz} = \pm \frac{1}{L_D} G(u) \tag{149}$$

where G(u) is defined as the square root of the quantity in braces. Notice again that the only z dependence seen in G is caused by u. All of the other quantities are independent of z.

It is now possible to define expressions for ΔN and ΔP. Let ΔN be defined, as stated earlier, as the excess electron carrier density in the space charge region. It represents the number of electrons over the bulk electron concentration in cm^{-2}. This can be expressed as

$$\Delta N \equiv \int_{z=0}^{\infty} \left(n(z) - n_b\right) dz$$

Similarly,

$$\Delta P = \int_{z=0}^{\infty} \left(p(z) - p_b\right) dz$$

The hole and electron concentrations p(z) and n(z) are given by Equations 134 and 136 respectively. Unfortunately, to get an analytical expression, Equation 149 would have to be integrated one more time. For n-channel devices, $N_i = \Delta N > 0$, $N_d = \Delta P < 0$. Similarly, for p-channels device, $N_i = \Delta P > 0$, and $N_d = \Delta N < 0$.

If one notices that at z=0, $u=u_s$, and as $z \to \infty$, $u=u_b$, then the above integrals can be expressed in terms of Equation 149 without actually integrating Equation 149.

$$dz = - \frac{L_D}{\pm G(u)} du$$

Thus,

$$\Delta N = - \int_{u=u_s}^{u_b} \left[n(u) - n_b\right] \frac{L_D}{\pm G(u)} du \tag{150}$$

and

$$\Delta P = - \int_{u=u_s}^{u_b} \left[p(u) - p_b \right] \frac{L_D}{\pm G(u)} \, du \tag{151}$$

If one examines these equations closely, it can be seen that these equations are of fundamental importance to the micro-Hall conductance technique. These equations relate ΔN and ΔP to the dimensionless potential u. Equation 6 relates u to ϕ, and can be easily related to Φ through Figure 17. Thus, in essence Equations 150 and 151 give the relationships of N_i and N_d to Φ_s and T. From Equations 5, 6, and 7 it can be said that

$$v = u - u_b \tag{152}$$

and

$$v_s = u_s - u_b \tag{153}$$

Thus, Equations 150 and 151 become

$$\Delta N = - L_D \int_{v_s}^{o} \frac{n(v) - n_b}{\pm G(v)} \, dv \tag{154}$$

and

$$\Delta P = - L_D \int_{v_s}^{o} \frac{p(v) - p_b}{\pm G(v)} \, dv \tag{155}$$

The expressions for n(v), p(v), and G(v) come from substituting Equation 152 into Equations 134, 136, and 148, respectively.

Consider Figure 17. One can relate v_s and Φ_s to each other through $(E_c - E_f)_b$.

$$-q\Phi_s + qV_s = \left(E_c - E_f \right)_b$$

Using Equation 7, this can be written as

$$v_s = \left(w_{c,f} \right)_b - q\phi_s/kT \tag{156}$$

Thus, Equations 154, 155, and 156 are equations that yield $\Delta N(\Phi_s)$ and $\Delta P(\Phi_s)$.

Consider for a moment how ΔN and ΔP could be found. If a value for Φ_s and T is selected or fixed, Equation 156 can be used to get a value for v_s. Notice that $w_{c,f}$ is simply the bulk difference between the conduction band and Fermi level. This quantity can be found quite readily using nondegenerate statistics. Similarly u_b, $w_{c,i}$, $w_{v,i}$, and $w_{D,i}$ are all readily found using nondegenerate statistics and field theory. Thus, once v_s is fixed, the lower and upper limits on Equations 154 and 155 (or Equations 150 and 151) are fixed. Equation 148 can be made into G(v) using Equation 152, and can be numerically integrated quite easily. If one tabulates $F_{1/2}(\eta)$ and $F_{3/2}(\eta)$ for a large number of arguments, η, then having fixed the upper and lower limits, the argument of the integrand, G(v), can be simply evaluated as an integration dummy is incremented. Thus, numerical integration can be readily performed to get ΔN and ΔP after Φ_s and T are set.

c. Determination of the Necessary Partial Derivatives

Notice that functionally speaking, we have the following

$$\Delta N = \Delta N(v_s, T) \tag{157}$$

$$\Delta P = \Delta P(v_s, T) \tag{158}$$

$$v_s = v_s(\Phi_s, T) \tag{159}$$

through Equations 154, 155, and 156. In the introduction it was pointed out that $\partial N_i/\partial \Phi_s\big|_T$, $\partial N_d/\partial \Phi_s\big|_T$, $\partial T/\partial \Phi_s\big|_{N_i}$, $\partial N_d/\partial T\big|_{N_i}$, $\partial N_d/\partial T\big|_{N_i}$, and N_i are all needed as functions of Φ_s and T. Since $N_i = \Delta N$ and $N_d = \Delta P$ for n-channel, and the opposite is true for p-channel, then the desired quantities are $\partial(\Delta N)/\partial \Phi_s\big|_T$, $\partial T/\partial \Phi_s\big|_{\Delta N}$, $\partial(\Delta P)/\partial T\big|_{\Delta N}$, and ΔN and the

corresponding ΔP parameters, all as functions of Φ_s and T. Notice ΔN and ΔP were derived in the last subsection.

Consider now the quantities $\partial(\Delta N)/\partial\Phi_s\big|_T$ and $\partial(\Delta P)/\partial\Phi_s\big|_T$. These quantities can be obtained from

$$\left.\frac{\partial(\Delta N)}{\partial\Phi_s}\right|_T = \left.\frac{\partial(\Delta N)}{\partial v_s}\right|_T \left.\frac{\partial v_s}{\partial\Phi_s}\right|_T \tag{160}$$

and

$$\left.\frac{\partial(\Delta P)}{\partial\Phi_s}\right|_T = \left.\frac{\partial(\Delta P)}{\partial v_s}\right|_T \left.\frac{\partial v_s}{\partial\Phi_s}\right|_T \tag{161}$$

From Equation 156 we see that

$$\left.\frac{\partial v_s}{\partial\Phi_s}\right|_T = -\frac{q}{kT} \tag{162}$$

The values of $\partial(\Delta N)/\partial v_s\big|_T$ and $\partial(\Delta P)/\partial v_s\big|_T$ can be established through the use of Leibnitz Rule, which is stated here for reference.

If

$$F(t) = \int_{\phi}^{\psi} f(t,\xi)\, d\xi$$

then

$$\frac{dF(t)}{dt} = f\big(t,\psi(t)\big)\frac{d\psi(t)}{dt} - f\big(t,\phi(t)\big)\frac{d\phi(t)}{dt} + \int_{\phi(t)}^{\psi(t)} \frac{\partial f(t,\xi)}{\partial t}\, d\xi \tag{163}$$

Using this relationship, the following can be written

$$\left.\frac{\partial(\Delta N)}{\partial v_s}\right|_T = +L_D \frac{n(v_s) - n_b}{\pm G\, v_s} \tag{164}$$

and

$$\left.\frac{\partial(\Delta P)}{\partial v_s}\right|_T = +L_D \frac{p(v_s) - p_b}{\pm G(v_s)} \tag{165}$$

where $n(v_s)$ and $p(v_s)$ are given by Equations 134 and 136.

Consider next $\partial(\Delta N)/\partial T\big|_{\Phi_s}$. Equations 157 and 159 can be combined to yield

$$\left.\frac{\partial(\Delta N)}{\partial T}\right|_{\Phi_s} = \left.\frac{\partial(\Delta N)}{\partial v_s}\right|_{T} \left.\frac{\partial v_s}{\partial T}\right|_{\Phi_s} + \left.\frac{\partial(\Delta N)}{\partial T}\right|_{v_s} \tag{166}$$

The quantity $\partial(\Delta N)/\partial v_s\big|_T$ is given by Equation 164, and $\partial v_s/\partial T\big|_{\Phi_s}$ can be easily found through Equation 156. The remaining derivative, $(\Delta N)/\partial T\big|_{v_s}$, can be obtained by again applying Leibnitz rule to Equation 154. However, this result is exceedingly unwieldy. Thus, the method chosen to determine $\partial(\Delta N)/\partial T\big|_{v_s}$ was to hold v_s constant and vary T. Equation 154 can be integrated for both values of T, and then differencing is used to obtain the derivative. The same is true for $\partial(\Delta P)/\partial T\big|_{v_s}$.

Consider Equation 157. The cylic permutation of derivatives yields

$$\left.\frac{\partial(\Delta N)}{\partial T}\right|_{\Phi_s} \left.\frac{\partial \Phi_s}{\partial(\Delta N)}\right|_{T} \left.\frac{\partial T}{\partial \Phi_s}\right|_{\Delta N} = -1 \tag{167}$$

Using the differenced value for $\partial(\Delta N)/\partial T\big|_{\Phi_s}$ and Equations 160, 162, and 164, then $\partial T/\partial \Phi_s\big|_{\Delta N}$ is evaluated. The same is again true for $\partial T/\partial \Phi_s\big|_{\Delta P}$.

The final partial derivatives, $\partial(\Delta N)/\partial T\big|_{\Delta P}$ and $\partial(\Delta P)/\partial T\big|_{\Delta N}$, can be derived as follows. In theory Equation 158 can be inverted to yield

$$\Phi_s = \Phi_s(\Delta P, T) \tag{168}$$

then

$$\left.\frac{\partial(\Delta N)}{\partial T}\right|_{\Delta P} = \left.\frac{\partial(\Delta N)}{\partial \Phi_s}\right|_{T} \left.\frac{\partial \Phi_s}{\partial T}\right|_{\Delta P} + \left.\frac{\partial(\Delta N)}{\partial T}\right|_{\Phi_s} \tag{169}$$

and similarly

$$\left.\frac{\partial(\Delta P)}{\partial T}\right|_{\Delta N} = \left.\frac{\partial(\Delta P)}{\partial \Phi_s}\right|_{T} \left.\frac{\partial \Phi_s}{\partial T}\right|_{\Delta N} + \left.\frac{\partial(\Delta P)}{\partial T}\right|_{\Phi_s} \tag{170}$$

All of the partial derivatives on the right hand side have previously been obtained, so these expressions can be directly evaluated.

By keeping in mind then that $N_i = \Delta N$ and $N_d = \Delta P$ for n-channel devices, and $N_i = \Delta P$ and $N_d = \Delta N$ for p-channel devices, all of the partial derivatives necessary for calculating C_1, C_2, C_3, and C_4 in Equations 78, 93, and 94 have been derived. It should be remembered that once Φ_s and T are chosen, then all of the above partial derivatives are uniquely defined.

d. Pertinent Bulk Semiconductor Equations

In evaluating ΔN and ΔP it is necessary to evaluate Equation 147. This expression involves $w_{D,i}$, $w_{A,i}$, $w_{v,i}$, and $w_{c,i}$. Also, to evaluate $\partial v_s/\partial T|_{\Phi_s}$, it is necessary to have $\partial w_{c,i}/\partial T|_{\Phi_s}$ in the bulk. Thus, expressions for these quantities must be available. All of the expressions are evaluated in the bulk, so the expressions for them can come from nondegenerate statistics.

All of the above quantities can be expressed in terms of T, N_D, and N_A. References 28 and 42 can be consulted for the derivations of these equations. They will simply be stated here for convenience, and no justification or derivations will be mentioned.

In the program itself, the valence band energy is used as the zero reference energy. Thus, $E_v = 0$. Then the conduction band energy is given by E_g, the energy gap. From Reference 42, it can be written that

$$E_c = E_g = 1.551 - 0.00023\ T \tag{171}$$

where T is temperature in K, and E_g is in eV. The intrinsic Fermi level is given by

$$E_i = E_g/2 - 0.75\ kT\ \ell n(m_n^*/m_p^*) \tag{172}$$

where kT is in units of eV. The effective masses are given by (see Ref. 42)

$$m_n^* = 1.1\ m_o \tag{173}$$

$$m_p^* = 0.59\ m_o \tag{174}$$

The Fermi level in the bulk is given by

$$E_f = E_g/2 - 0.75\ kT\ \ell n\left(\frac{m_p^*}{m_p^*}\right) + kT\ u_b$$

$$E_f = E_i + kT\ u_b \tag{175}$$

where kT is again in units of eV. The expression for u_b is

$$u_b = \left(E_f - E_i\right)/kT$$

where u_b is the dimensionless potential difference between the Fermi level and intrinsic Fermi level. For n-type, $u_b > 0$, and for p-type, $u_b < 0$. An expression for u_b can be written as follows

$$u_b = \sinh^{-1}\left[\frac{\left(N_D - N_A\right)}{2\sqrt{N_c\ N_v}\ \exp\left(-E_g/2\ kT\right)}\right] \tag{176}$$

where

$$N_c = 2\left(\frac{2\pi m_n^*}{h^2}\ kT\right)^{3/2} \tag{177}$$

and

$$N_v = 2\left(\frac{2\pi m_p^*}{h^2}\ kT\right)^{3/2} \tag{178}$$

If the definitions

$$\xi \equiv 2\left(\frac{2\pi k}{h^2}\right)^{3/2}\left(m_n^*\ m_p^*\right)^{3/4} \tag{179}$$

and

$$\gamma \equiv E_g/2k \tag{180}$$

are given, then

$$u_b = \sinh^{-1}\left[\frac{\left(N_D - N_A\right)}{2\xi T^{3/2}\ \exp(-\gamma/T)}\right] \tag{181}$$

So Equations 181 and 175 yield E_f. Thus, E_c, E_f, and E_i have been established as functions of T, N_D, and N_A. The donor and acceptor levels can be obtained by

$$E_D = 0.9506\ E_g \tag{182}$$

and

$$E_A = 0.041398\ E_g \tag{183}$$

Using Equation 172 for E_i, $w_{D,i}$, $w_{A,i}$, $w_{v,i}$, and $w_{c,i}$ have been determined through the use of Equations 171, 182, 183 and the reference potential $E_v = 0$. Similarly, $\partial w_{c,f}/\partial T\Big|_{\Phi_s}$ is easily obtained from the above equations.

4. SUMMARY

In this chapter two separate areas have been discussed at great length. First, the equations were developed through which one can take the raw data and determine N_H, $\sigma_\square$, and μ_H. The current voltage data are taken at various levels of gate bias, and therefore each of the above quantities is known as a function of V_g, the applied gate voltages.

Next, the theoretical equations necessary to complete the micro-Hall conductance technique were derived for a semiconductor surface under strong inversion using degenerate statistics. The partial derivatives derived in the third section are the ones actually used in the data reduction program.

Finally, the equations needed to characterize the bulk silicon were stated but not derived. These equations have been developed using the assumption of nondegenerate conditions, and can be found in any common text on bulk silicon properties.

Table 4 is a summary of the steps that one must perform to put the raw data into some useful form.

Table 5 is a summary of the steps taken in determining the pertinent partial derivatives.

TABLE 4

Steps Used in Determining N_H, $\sigma_\square$, μ_H from the Raw Data

STEP	EQUATIONS USED	COMMENTS
1		Choose a V_g, stimulate adjacent electrodes, measure voltage across the remaining two.
2	107, 108	Determine ρ_s
3		Stimulate opposite electrodes and measure voltage across the other two.
4	111, 112	Determine μ_H
5	113	Choose a new V_g

TABLE 5a

Steps Taken to Calculate
N_i and N_d

STEP	EQUATIONS USED	COMMENTS
1		Choose a Φ_s and T
2	171-183	Calculate bulk parameter
3	156	Calculate v_s
4	154, 155	Numerically integrate to obtain N_i and N_d

TABLE 5b

Steps Taken to Calculate
$\partial N_i/\partial \Phi_s|_T$ and $\partial N_d/\partial \Phi_s|_T$

STEP	EQUATIONS USED	COMMENTS
1		Fix Φ_s and T
2	171-183	Calculate bulk parameters
3	162	Calculate $\partial v_s/\partial \Phi_s|_T$
4	134, 136 164, 165	Calculate $\partial N_i/\partial v_s|_T$ and $\partial N_d/\partial v_s|_T$
5	160, 161	Calculate $\partial N_i/\partial \Phi_s|_T$ and $\partial N_d/\partial \Phi_s|_T$

TABLE 5c

Steps Taken to Calculate

$\partial T/\partial \Phi_s|_{N_i}$ and $\partial T/\partial \Phi_s|_{N_d}$

STEP	EQUATIONS USED	COMMENTS
1		Choose a Φ_s and T
2	See Table 5a	Calculate N_i and N_d
3		Choose a new T but hold v_s constant
4	See Table 5a	Calculate a new N_i and N_d
5		Difference the values for N_i and N_d getting $\Delta N_i/\Delta T|_{v_s}$ and $\Delta N_d/\Delta T|_{v_s}$
6	166, 167 and results of Table 5b	Calculate $\partial T/\partial \Phi_s|_{N_i}$ and $\partial T/\partial \Phi_s|_{N_d}$

TABLE 5d

Steps Taken to Calculate

$\partial N_i/\partial T|_{N_d}$ and $\partial N_d/\partial T|_{N_i}$

STEP	EQUATIONS USED	COMMENTS
1		Calculate all pertinent derivatives in Equations 169 and 170 using Tables 5a, 5b, and 5c.
2	169, 170	Determine $\partial N_i/\partial T|_{N_d}$ and $\partial N_d/\partial T|_{N_i}$

CHAPTER V

DESCRIPTION OF THE DEVICES USED IN THIS STUDY AND THE EXPERIMENTAL SETUPS

1.. DESCRIPTION OF THE DEVICES AND THE GENERAL EXPERIMENTAL PROCEDURES

This particular study uses an MOS capacitor and a special geometry MOS transistor equipped with Hall probes to do all the required work. Some simultaneous work is being performed to examine the pulse response of an MOS transistor to see how it varies with radiation dose. Thus, the chip contained not only the MOS transistor and capacitor, but also a standard MOS transistor that does not contain Hall probes. The standard MOS transistor was not very large in size, and a gate controlled junction diode was included on that quadrant of the chip for tutorial purposes more than anything else.

The size of the silicon chip within which all these devices were made was chosen as 0.100 in. by 0.100 in. This area was sectioned into quadrants and three devices were put into three of the quadrants and two went into the fourth quadrant.

The Hall transistor is circular in geometry as was described in Figure 14. Actually, two different Hall transistors were in the chip. They are geometrically similar, but one had a gate diameter of 0.020 in. and the other a diameter of 0.005 in. The geometry of the transistor was modeled after similar devices described in References 43 and 36.

The MOS capacitor consisted of a circular gate oxide surrounded by the field oxide and covered with aluminum. Many investigators do not put bonding pads on the MOS capacitor. They probe the capacitors directly. The devices used in this study sometimes had to be packaged, so it was decided to put a bonding pad on the capacitor. Therefore,

the diameter of the capacitor was chosen as large as possible to minimize any stray effects due to the bonding pad. The capacitor is 0.040 in. in diameter.

The standard MOS transistor used in the pulse measurements has a symmetrical source and drain. The length of the channel is much shorter than the width to keep the measured current values high. The channel here is 0.002 in. long and 0.028 in. wide.

In fabricating these devices certain general steps are taken. These are described in detail in Appendix A. Briefly, the fabrication occurs in four general steps.

First, a very thick oxide is grown over the entire wafer (about 10,000 Å) and the source drain openings are cut into the oxide using the first mask.

After diffusing in the source and drain, the field oxide must again be etched. This etch opens the areas where the gate oxide will be grown. At the same time the scribe paths are etched and the contact openings are etched. This mask is referred to as the second mask or gate oxide cut mask.

Once the gate opening has been cut, the gate oxide is grown. When the gate oxide is growing, the contact openings reoxidize, as do the scribe paths. The third mask reopens the contact holes and scribe paths. This mask is the contact opening mask.

Finally, the entire wafer is coated with aluminum and the metal plates used for the gates and contact connections are etched. This is the fourth and final mask, referred to as the metal etch mask.

Figure 18, 19, 20 and 21 are drawings of the masks used to fabricate the devices in this study. It is readily apparent from Figure 22,

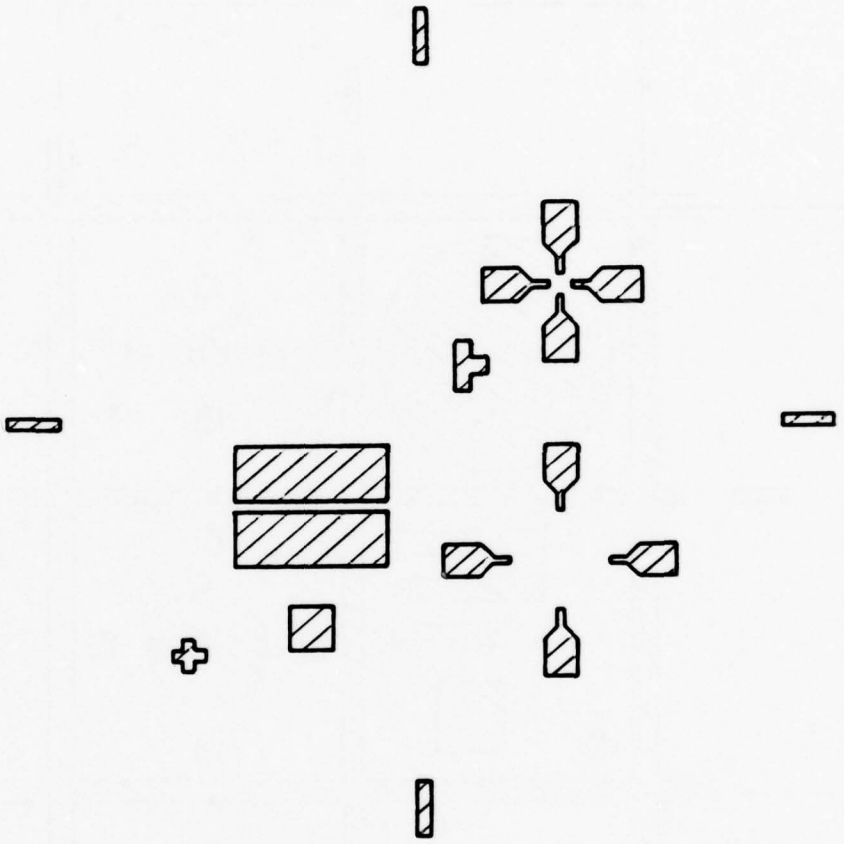

Figure 18. Source-drain diffusion cut.
The hatched area is removed.

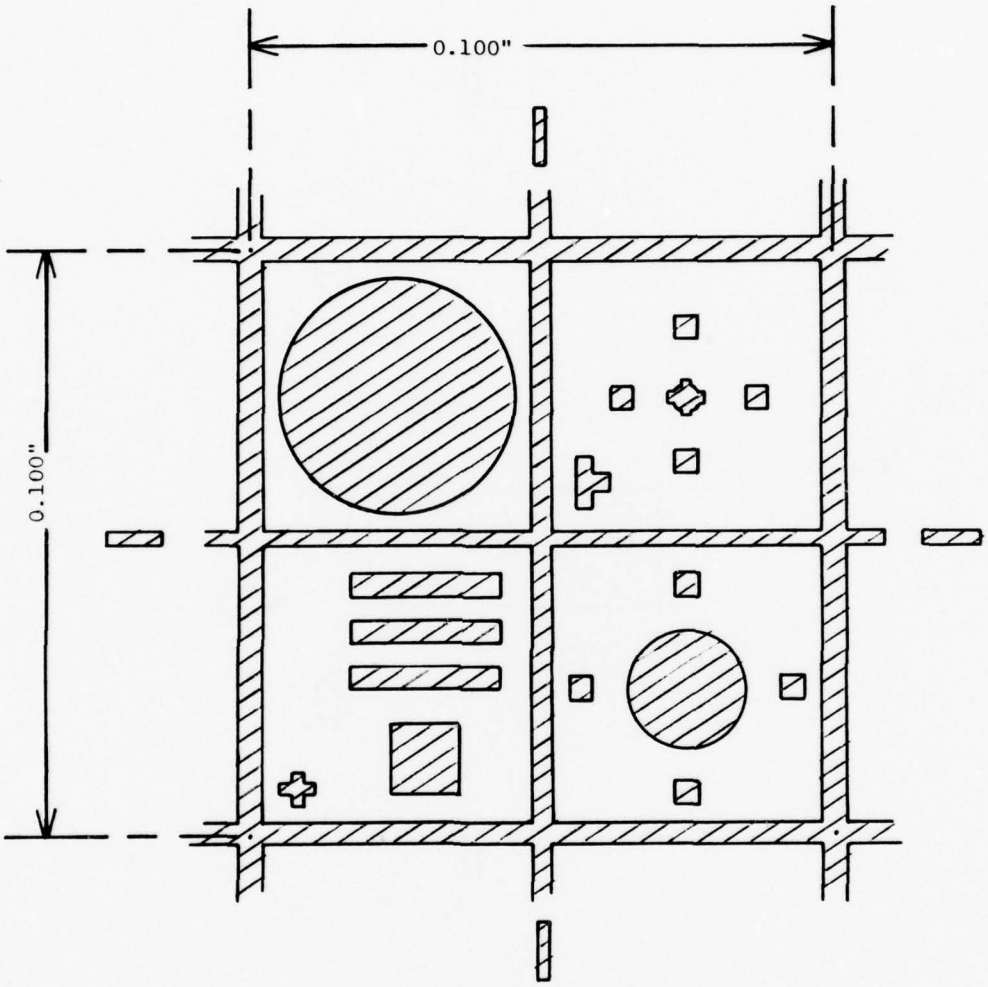

Figure 19. Gate oxide cut. Notice the contact openings and scribe streets are opened here also. The hatched area is removed.

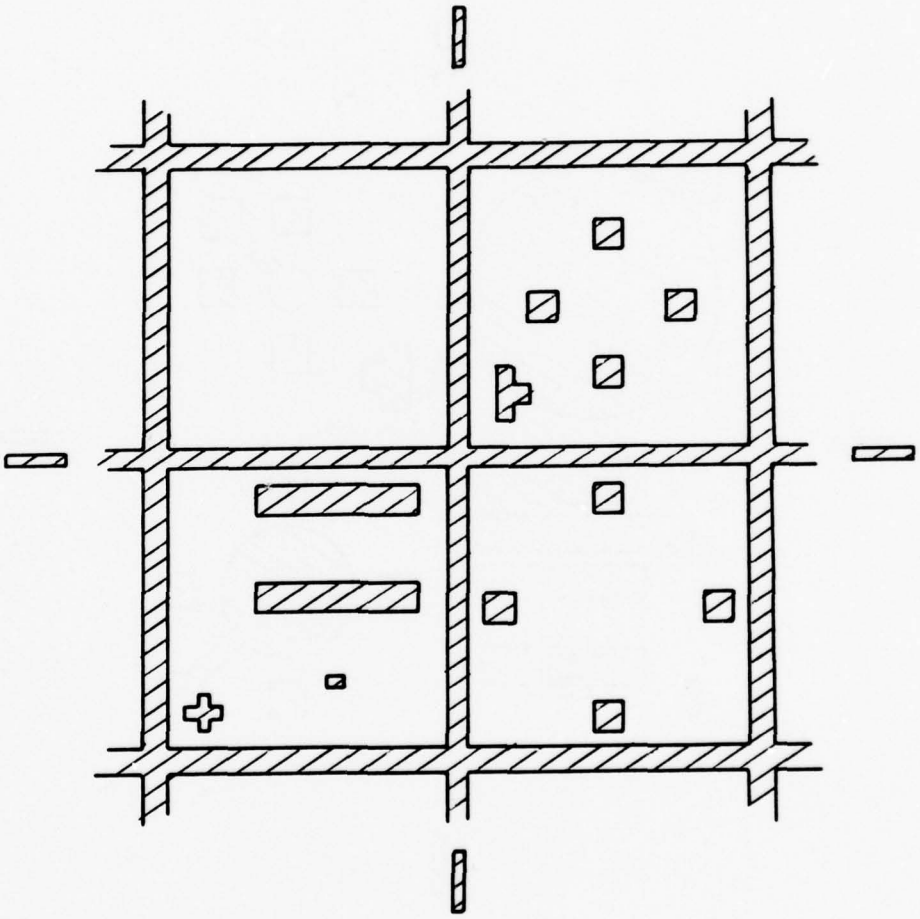

Figure 20. Contact Opening Cut. Notice the scribe streets are again opened here. The hatched area is removed.

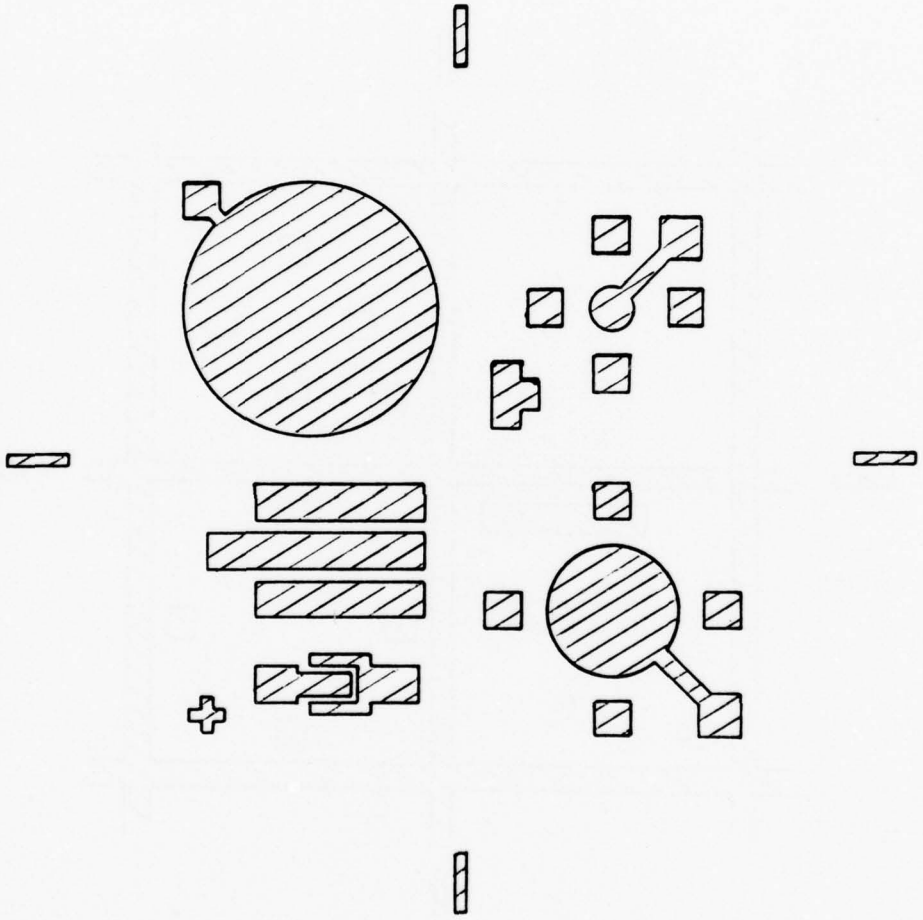

Figure 21. Metal etch mask.
The hatched area remains.

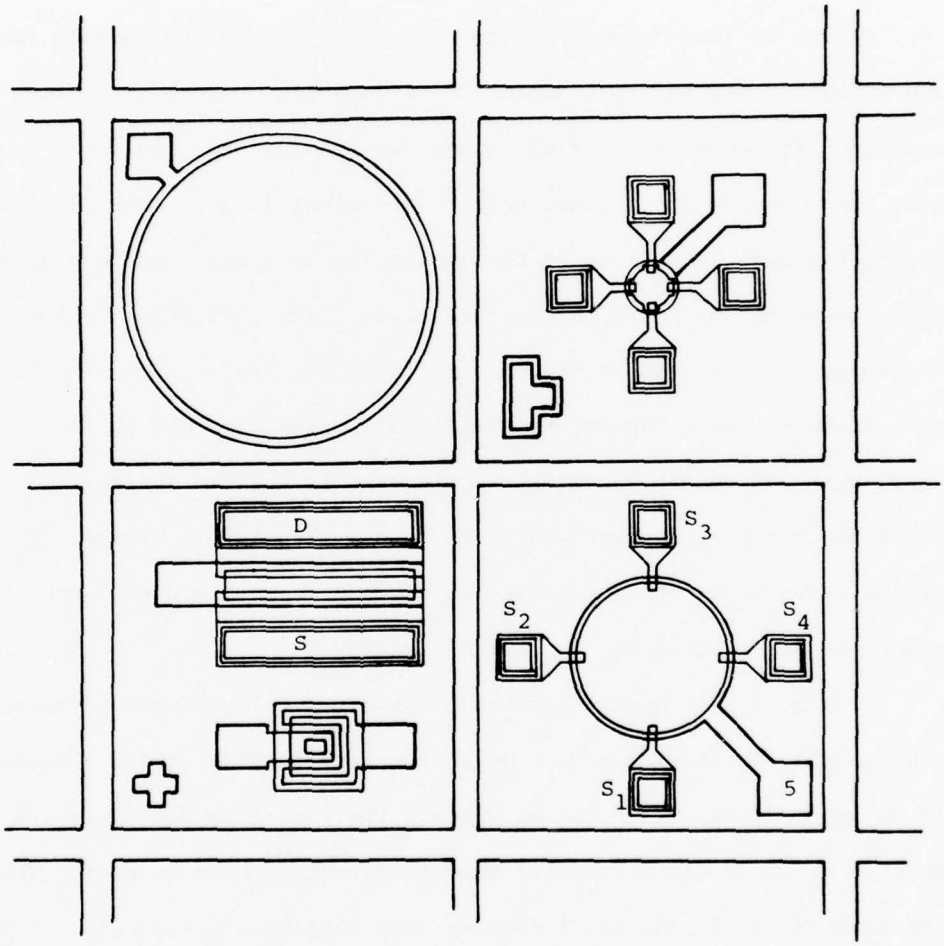

Figure 22. A composite overlay of all the masks.

the overlay of Figures 18 through 21, that the circular geometry MOS transistors have four equivalent sources or drains, labeled S_1 to S_4. Similarly, the standard MOS transistor also has a symmetric source and drain, labeled S and D.

Figure 18 is a drawing of the mask used to open the initial oxide and allow the source/drain dopant to diffuse in. Figure 19 depicts the mask used for opening the field oxide for growing the gates, and at the same time opening the contact holes. The small diameter MOS Hall transistor has some extensions of the gate oxide to assure that the gate oxide overlaps the four source/drain areas. The resolution of the alignment systems used at the University of New Mexico necessitated this feature. As a result, the small Hall transistor was to be used only as a last resort because the gate area is hard to define. In practice this device never had to be used. Finally, in Figures 20 and 21 one can see the contact holes and scribe streets reopened, and the metal pattern delineated.

Figure 22 is a drawing of the composite overlay of all the masks used in the fabrication of the devices tested in this study. Figures 18 through 22 are all scaled drawings. The actual device sizes are not given here because it would make the drawings hard to read. The critical sizes of individual devices were mentioned previously. Figure 23 is a photograph of sections of a completed wafer.

The starting material for these devices was n-type (111) silicon wafers doped to a uniform resistivity of 4.0 Ω-cm. There was no epitaxial layer present. A preliminary oxide of 6400 Å or greater was initially grown and etched off. (See Ref. 16.) This so-called "etch back" oxide seems to eliminate some mechanical faults in the wafer generated during the wafer fabrication. This oxide is grown at 1100°C.

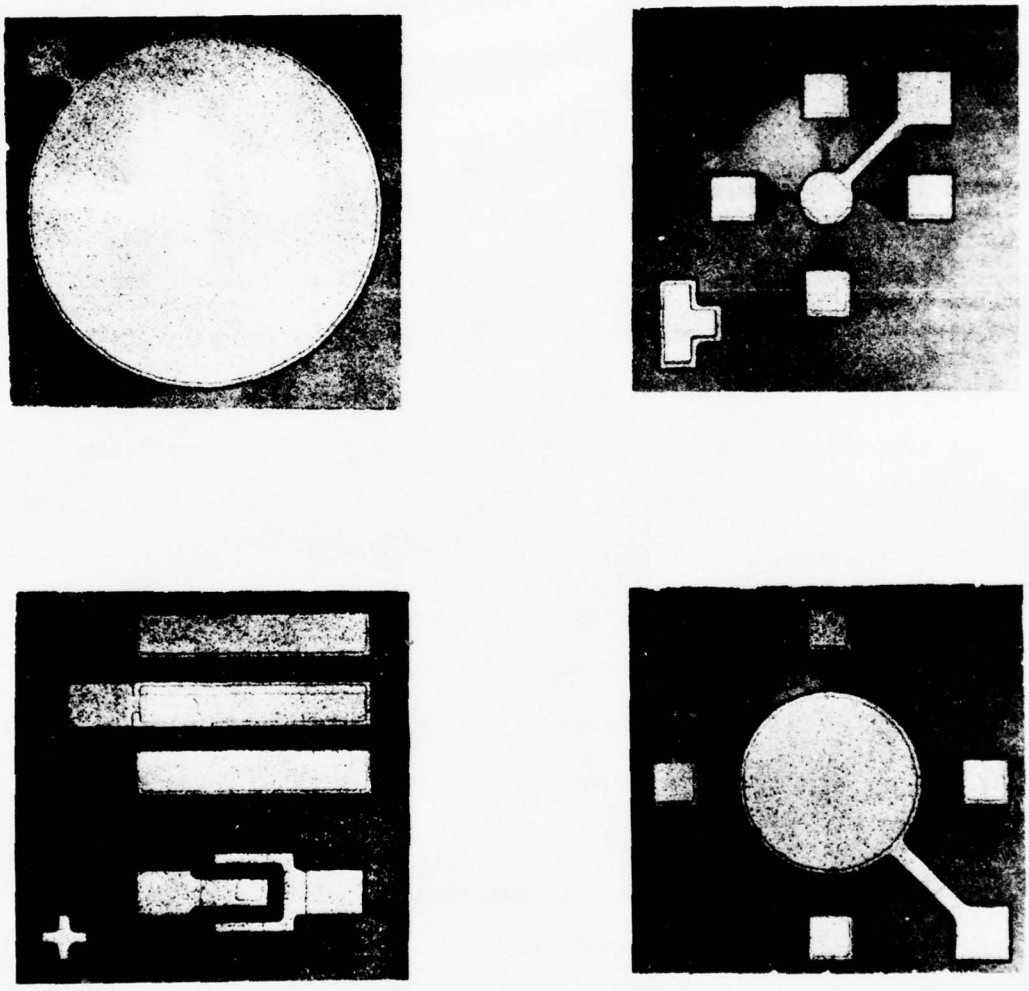

Figure 23. Photographs of sections of a Sandia supplied wafer.

The first 15 minutes is grown in a dry atmosphere and the remainder is grown in a wet atmosphere. It is believed that the initial dry oxide somehow prevents propagation of certain structural faults into the wafer during oxidation. The steam oxide then successfully allows one to strip off the upper few thousand angstroms of silicon, thereby reducing the total number of defects present.

After this first "etch-back" oxide is removed, a field oxide is grown at 1100°C in steam to about 10,000 Å. Following the gate oxide cuts, the gate oxide is grown at 1000°C in a dry atmosphere, and annealed for 90 minutes at 850°C under a nitrogen atmosphere. After the contacts are opened, the aluminum is thermally evaporated and sintered in a nitrogen atmosphere for 20 minutes at 500°C. These particular temperatures, times, and atmospheres are those recommended by Aubuchon (Ref. 44) and Derbenwick (Ref. 16).

After the devices were fabricated they were randomly probed. The two things examined were the leakage current, and basic shape of the transistor characteristic curves, I_{SD} vs V_{SD} for various values of V_g. Typical leakage currents for Sandia supplied p-channel devices were less than 1×10^{-11} amp on the capacitors, or about 1.2×10^{-9} amp/cm^2. Low leakages in these devices are important because the currents measured in the low frequency C-V curves are of the order of 10^{-9} amp. A typical set of characteristic curves is shown in Figure 24.

After it was determined that a given wafer contained acceptable devices, the wafer was scribed apart. The standard MOS transistors were mounted in TO-5 headers for pulse measurements, the Hall transistors were mounted in Tekform #40179 ten pin flat packages, and the capacitors were sent in a chip form to Sandia Laboratories. The mounted chips had aluminum leads attached to them with an ultrasonic bonder.

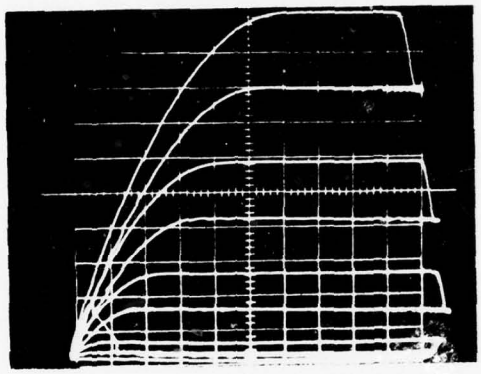

Figure 24. A typical set of characteristic curves from device #S162PA. The vertical axis is I_{SD}, and horizontal axis is V_{SD}. This is taken at various gate voltages. The settings are 1 volt/step gate pulse, 2 volts/div. horizontal, and 20 μa/div. vertical.

Once the devices were packaged, measurements were taken at Sandia Laboratories on the capacitors using a C-V setup to determine $N_{ss}(\Phi_s)$ and the other parameters described in Chapter II. The Hall transistors were analyzed at The University of New Mexico (UNM) using the Hall technique to determine $N_{ss}(\Phi_s)$ and $N_H(\Phi_s)$. After the preirradiation data were taken, the devices were irradiated with a ^{60}Co gamma radiation source to 5×10^5, 1×10^6, 5.5×10^6, and 1×10^7 Rad (Si) total dose. After each irradiation the devices were then recharacterized.

In the next two sections we briefly describe the experimental apparatus used at Sandia Laboratories and UNM.

2. EXPERIMENTAL SETUP FOR C-V MEASUREMENTS

It will be recalled from Chapter II that to characterize $N_{ss}(\Phi_s)$ and the other parameters derivable from C-V measurements, one needs measurements taken at both high frequencies and low frequencies.

A system has been developed at Sandia Laboratories for taking these measurements on a capacitor automatically. Figure 25 is a block diagram of the system used at Sandia.

This particular system impresses a ramp voltage on an MOS capacitor. The resulting dc current charging the capacitor is measured with an electrometer and is directly related to the low frequency capacitance. The dc bias is applied to the capacitor through a capacitance bridge. The bridge measures the MOS capacitance directly, as shown in the figure. An internal oscillator in the capacitance bridge sets the ac measurement frequency at 1 MHz. The outputs of the capacitance bridge, electrometer, and ramp generator are all constantly monitored by three digital voltmeters. The outputs of these voltmeters are fed directly into a computer.

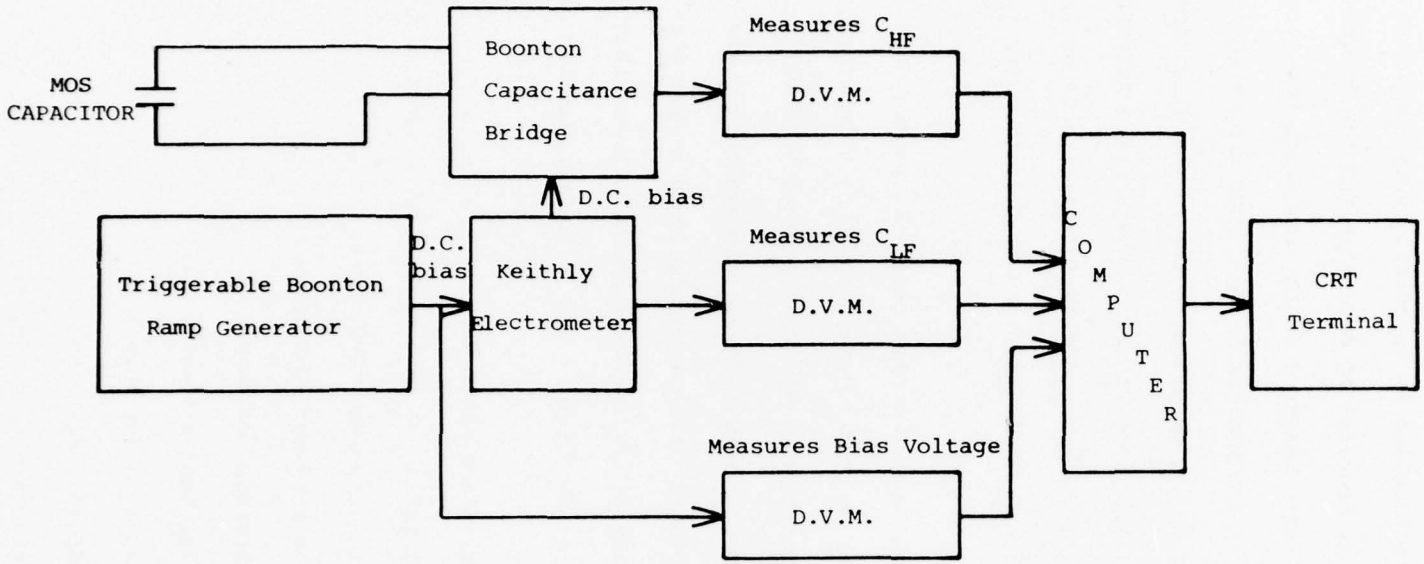

Figure 25. A block diagram of an automated C-V measuring system.

Although this system may look relatively simple, one significant problem arises. The electrometer is in general very sensitive to noise in the ranges in which it operates to determine the low frequency capacitance. Typical currents measured in the low frequency setup are in the low nanoamp range. A new Boonton bridge, when connected in the configuration shown in Figure 25, generates noise in the electrometer on the order of nanoamps. Thus, the signal to noise ratio renders the data useless. Initially, considerable modifications to the capacitance bridge were needed in order to reduce the noise in the electrometer to a useful level (Ref. 45).

Once the proper modifications were made, the experimental setup shown in Figure 25 could be used to simultaneously generate both low and high frequency curves on a given MOS capacitor. These data were fed directly into a computer and analyzed automatically. The output from such a system is fed to a CRT terminal, where it was photographed.

The overall accuracy of the measurements made using this system are on the order of 1 percent (Ref. 45). The following data are supplied using this technique:

(1) $N_{ss}(\phi_s)$ interface state density

(2) $V_g(\phi_s)$ variation of gate voltage with surface potential

(3) $C_{HF}(V_g)$ high frequency C-V curve

(4) $C_{LF}(V_g)$ low frequency C-V curve

(5) V_{th} threshold voltage

(6) V_{fb} flat band voltage

(7) C_{ox} oxide capacitance

(8) R_s series resistance

(9) L_{Dmax} depletion region width

(10) N_A or N_D average impurity density

All of these quantities were derived in Chapter II and the method for determining them from the raw data have been established.

All of the C-V data used in this study were supplied by Sandia Laboratories and were generated on such an automated data taking system.

3. DESCRIPTION OF THE HALL MEASUREMENT SETUP

Recall from Chapter IV that the Sakaki technique or Hall conductance technique requires $N_H(V_g)$ which can be determined from the raw data. In order to determine N_H, various currents and voltages must be measured in the Hall transistor (see Equations 107, 111, and 113). These measurements must also be done at various temperatures.

The basic system is depicted in Figure 26. The device is housed in an Air Products WMX-2 Joule-Thompson refrigerator. The refrigerator tip lies within the pole pieces of a Varian V-3704-1 electromagnet driven by a Varian Model 6030 power supply. The temperature of the system is measured using a gold (with 0.07% atomic weight iron) vs. copper thermocouple. This thermocouple can be read on a potentiometer, but also feeds an Artronix Model 3501-E temperature controller. The controller detects the temperature in the system and drives a 2-watt heater within the system. This system routinely holds the temperature to ±1 K.

The source-drain voltage is supplied using a constant voltage source designed around a Union Carbide S1034 op-amp. The basic source-drain constant voltage supply is shown in Figure 27. This system was chosen so the ammeter (Keithly 171 digital multimeter) could be used to measure the source-drain current, but the terminal voltage drop of the ammeter would not affect V_{SD}. This system holds V_{SD} at ±100 microvolts over a delivery current range of 0 to 15 microamps. The

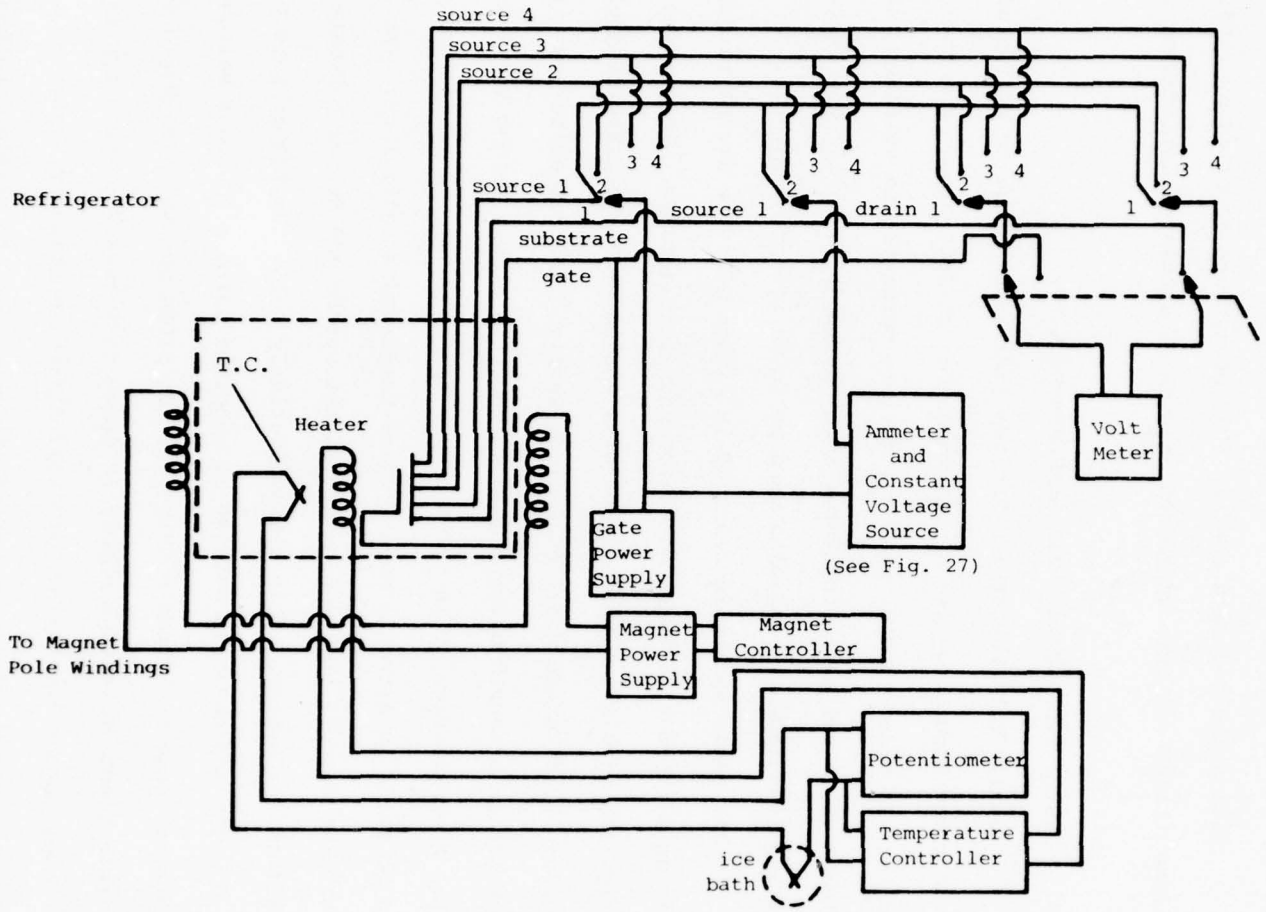

Figure 26. The basic experimental setup for Hall measurements.

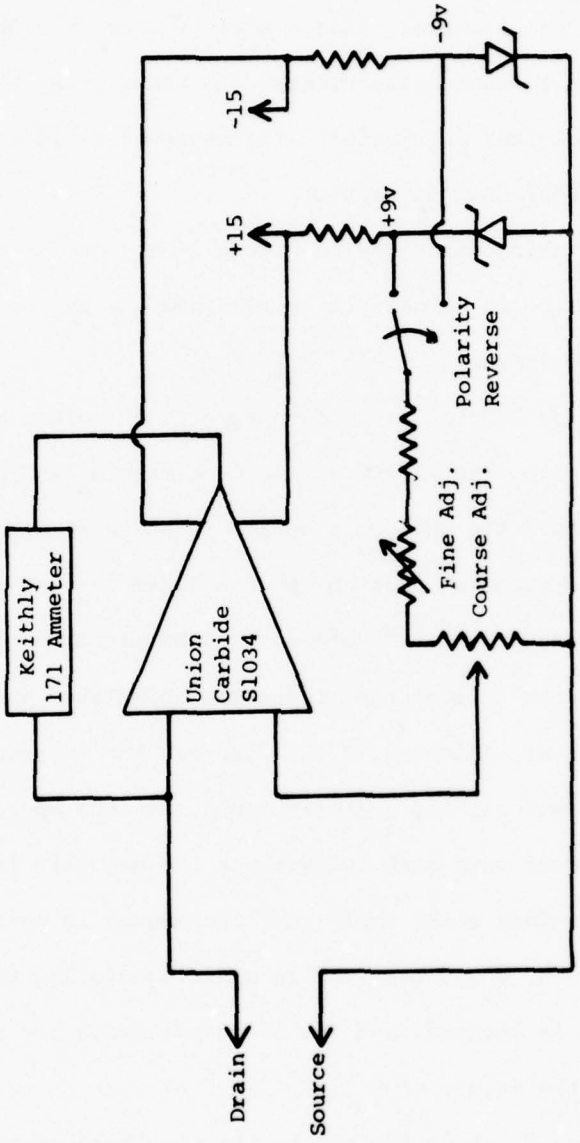

Figure 27. Constant voltage source used in the Hall measurements.

resistors R_1 and R_2 can be used to adjust V_{SD}, while S_1 changes the polarity of V_{SD}. The source-drain voltage for this series of experiments was held constant at 0.250 volt.

The gate voltage was supplied using a Hewlett Packard 6206B dc power supply. All the voltage measurements were taken using a Data Technology Model 351 digital multimeter. The magnetic field strength was measured using a Bell 610 Gaussmeter.

By using the switching described in Figure 26 any one of the four source-drain terminals could be made the source and any of the remaining three could be the drain.

Recall from Chapter IV that it is necessary to stimulate adjacent electrodes as well as opposite electrodes to determine N_H and μ_H. A data sheet used to record the data on a device is shown in Figure 28. The gate voltage is adjusted so that the source-drain current is just above turn on. This was arbitrarily chosen as 0.05 microamp or more. Then, with V_{SD} fixed, the various electrodes are stimulated and resulting voltages measured, as indicated in the figure. The adjacent electrodes are stimulated without any magnetic field, but the opposite electrodes are stimulated both with and without the magnetic field. The $\bar{V}_{13}$ and $\bar{V}_{24}$ on the data sheet imply that the magnet is energized. Thus, at a given value of V_g, a total of 14 measurements are taken. Then the gate voltage is changed, and the 14 measurements are repeated. This is done for all the values of V_g.

The lower limit on V_g is determined by the threshold current. The upper limit on V_g was set such that the maximum value derived for N_H through the raw data was larger than the maximum value of N_H called for by the computer program. Experience with the data reduction program

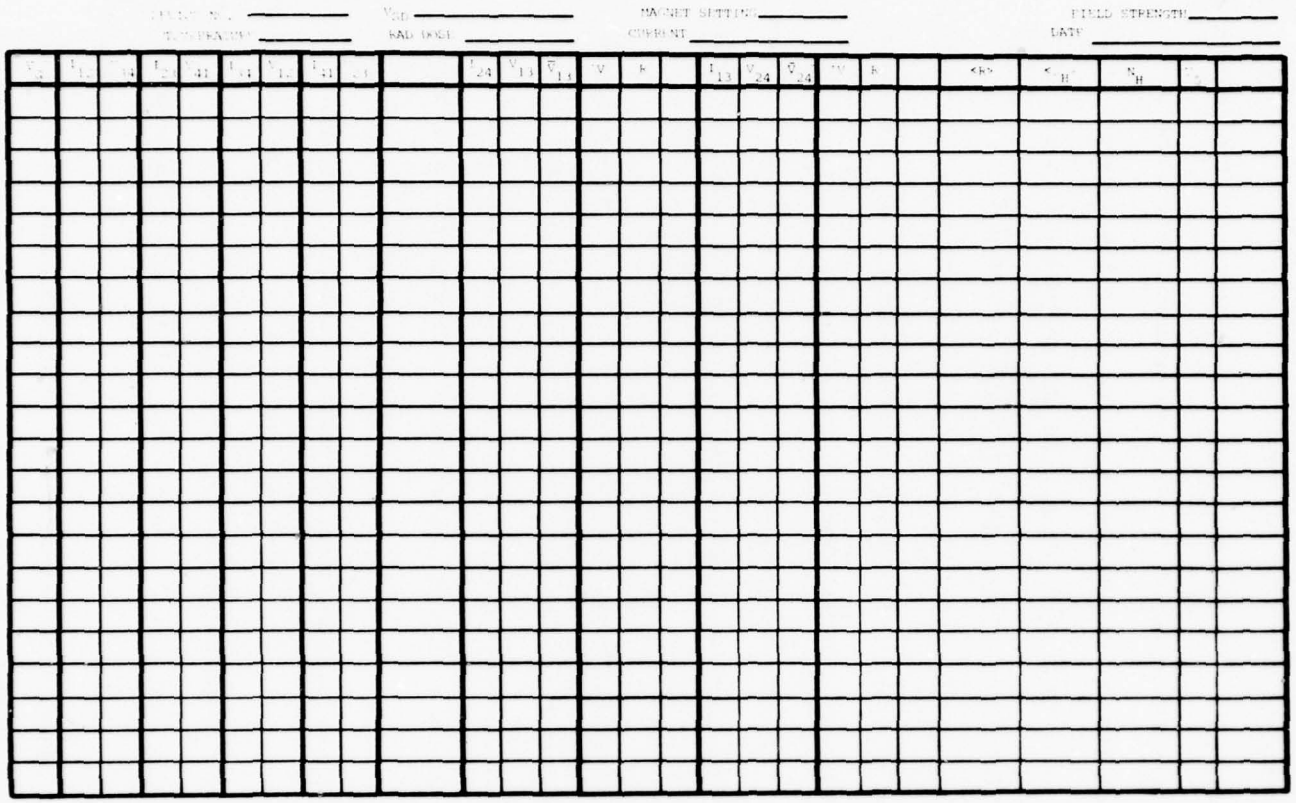

Figure 28. Data sheet used for Hall measurements. All voltages are entered in millivolts, and currents in microamps. The subscripts refer to the source numbers defined in Figure 21.

set this upper limit at about $6 \times 10^{12}/cm^2$, which sets the upper voltage limit from about -16 volts for unirradiated devices up to -22 volts for devices irradiated to 1×10^7 Rad (Si). The actual cutoff point for a given device was determined while the measurements were being made. Using Equation 113, it can be seen that for B = 4.5 kilogauss, $\Delta R \sim 45\Omega$ to yield $N_H \sim 6 \times 10^{12}$ cm^{-2}. Thus, one can calculate ΔR near -16 or -17 volts to determine if more values for V_g are needed.

Once these measurements are taken at one temperature, the device is cooled and they are repeated at the other temperature. One data sheet is used per device per temperature.

The MOSFETs used in this project have no gate protection diodes, and extreme care must be exercised when handling the devices. Static buildup on a counter top or an individual's clothes must be avoided since it could easily break down the gate. In this study, all four source-drain terminals, the gate, and the substrate are all shorted to ground when a device is being mounted or dismounted. Similarly, all leads from any equipment are grounded before being connected to the device.

One last complication arose in taking the data. The input wires to the refrigerator are rather long, and wrap around the refrigerator internally as a means of preventing heat conduction into the refrigerator through the lead wires. These wires act as antenna pickups when the magnet is energized. If the magnet is turned on via the switches on the front panel, large electromagnetic pulses could be generated which could break down the gate oxide. This problem was solved as follows. The Varian controller has a programmer in the back that turns on the magnet to varying degrees if a voltage is impressed across two

of the back input terminals. Using the voltage specifications for the programmer terminals, a circuit was constructed that would turn on the magnet such that the magnetic current increased according to a capacitor charging rate. The programmer used is shown in Figure 29. The magnet turn on time is determined by a time constant R_1C_1. In our unit, the magnet turns on in about 3 seconds. Thus, the large induced electromagnetic pulse was limited to a value that would not destroy the gate oxides.

4. SUMMARY

This chapter has been devoted to an overall view of the physical appearance devices, how they are made, and the steps taken to test them.

In the first section, the various masks used in the production were presented along with the characteristics of the parent starting material. Following this, an overall discussion of the major processing steps was presented.

In the second section the automated C-V analysis system was described in a general manner. A block diagram showing the pertinent equipment was presented, and mention was made of the parameters actually calculated with these measurements.

Finally, the micro-Hall conductance technique was described briefly. The particular equipment used here was also described, along with schematics of two prototype circuits actually used in this work. Table 5 is a summary of the basic step performed in obtaining the micro-Hall data.

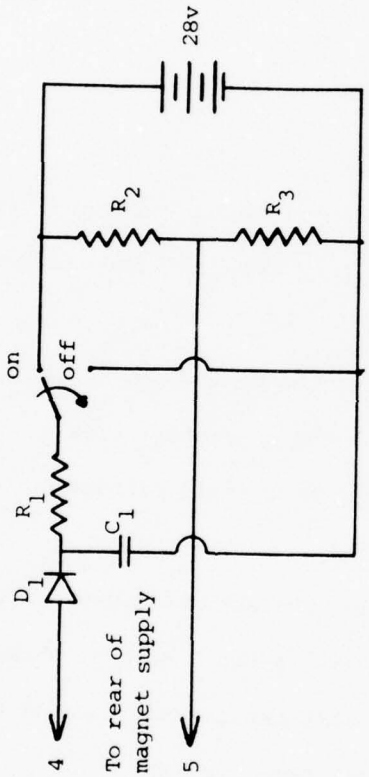

Figure 29. Magnet programming circuit for energizing the magnet slowly.

TABLE 6

Basic Summary of the Steps Performed
in Taking the Micro-Hall Data

STEP	COMMENTS
1	Mount the device in the refrigerator and place the refrigerator in the magnet.
2	Take a picture of the characteristic curves to see if the device is functional.
3	Evaluate the refrigerator.
4	Measure the temperature, and magnetic field strength. Fix V_{SD}.
5	Increase V_g toward threshold and monitor I_{SD}. When I_{SD} reaches turn on, take 7 sets of readings (14 readings).
6	Increment V_g and go back to step 5.
7	Continue this until sufficient $N_H(V_g)$ data have been taken.
8	Turn on the cooling and reduce the temperature.
9	Repeat steps 2 through 7, skipping step 3.
10	Turn off cooling and allow the system to come back to atmospheric temperature.
11	Vent the system and change the sample.

CHAPTER VI

RESULTS

1. INTRODUCTION

In this chapter some of the problems encountered in interpreting the micro-Hall data are presented and discussed.

After discussing these problems, typical results of the micro-Hall measurements are presented for one device.

Next, the data supplied by the C-V curves are presented. Both the C-V technique and micro-Hall technique yield more useful information than is used in this study.

Finally, some comparisons between some of the parameters obtained in the C-V technique and the micro-Hall technique are made.

2. PROBLEMS ARISING IN INTERPRETING THE MICRO-HALL MEASUREMENTS

Recall from Chapter IV that the micro-Hall measurements are taken at two different temperatures. The data fed into the data reduction program are various gate voltages along with the permutations of the source-drain voltages and source-drain currents described in Figure 28, Chapter V. These permutations of the source-drain voltages and currents are all used to find $N_H(V_g)$ at both temperatures through Equation 113, $\mu_H(V_g)$ at the upper temperature through Equation 111, $\sigma_{\square}(V_g)$ at the upper temperature through Equation 108, and the sheet resistance defined by Equation 107.

Figure 13, Chapter III, is a typical plot of $N_H(V_g)$. This figure is actually a plot of the data from device number S160 before it was irradiated. These two sets of data points are fit by a fourth order

polynomial in order to determine β as defined by Equation 92. The data points at the upper temperature were also curve fit by a basis set of tension splines to determine β defined by Equation 77. Both of the curve fitting schemes are discussed in depth in Appendix B.

If all of the data looked like Figure 13, there would be no problem. However, this was not the case. Figure 30 is a plot of what is called a leaky device. These data are from device S150 after a total dose exposure of 10^7 Rad (Si). All of the devices, when unirradiated, exhibited curves similar to those in Figure 13. As the total irradiation dose progressed, some devices began to develop some curvatures near their turn-on voltages. Many of the devices exhibited very little of this phenomenon. The plot shown in Figure 30 is the worst case.

This anomaly in the curvature certainly presents a problem in the data reduction. Recall the real quantities of interest are $V_g(N_H)$, $(\partial V_g/\partial T)\big|_{N_H}$ and $(\partial V_g/\partial N_H)\big|_T$. Figure 30 is actually a plot of the inverse function $N_H(V_g)$. For the data sets represented in Figure 30, the quantities of interest are not unique. That is to say, for a certain range of N_H, more than one value of V_g exists. This is also true for the two derivatives.

The origin of the impulse in N_H at low values of V_g is thought to be explainable in the following fashion. Consider again Equation 113, the equation for N_H.

$$N_H = \frac{B}{10^8 \, q\langle \Delta R_{j1} \rangle} \tag{113}$$

For the sake of this discussion, assume that the device has total symmetry, so an average is not necessary to find $\langle \Delta R_{j1} \rangle$. Also assume the current through the device does not change measurably with and without

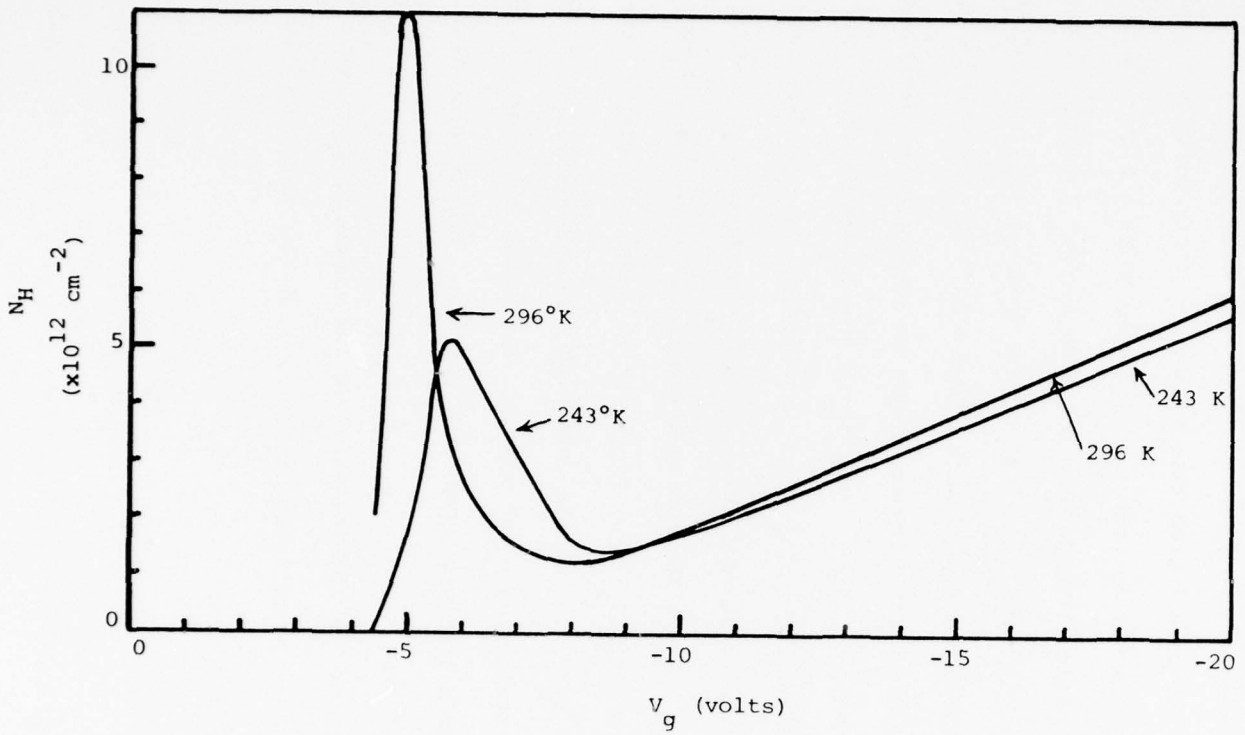

Figure 30. A plot of $N_H(V_g)$ at two separate temperatures for device S150R107, irradiated to $1x10^7$ Rad (Si).

the application of the magnetic field, and let it have a value I_{13}. Next, let V_{24} and $\bar{V}_{24}$ represent the voltage across sources 2 and 4 while sources 1 and 3 are being stimulated with the current I_{13}. In this case,

$$R = \frac{V_{24} - \bar{V}_{24}}{I_{13}} \tag{184}$$

Then N_H can be expressed as

$$N_H = \frac{B}{10^8 q} \frac{I_{13}}{V_{24} - \bar{V}_{24}} \tag{185}$$

The current I_{13} is the current in the inversion region. This current physically passes through the inversion region past sources 2 and 4. This current in the inversion region past sources 2 and 4 gives rise to the Hall voltage, $V_H = V_{24} - \bar{V}_{24}$. If any leakage path is established that gives rise to a component of current that is measured by the ammeter as part of I_{13}, and if this component of current does not pass sources 2 and 4, this current would then increase the value of I_{13}, but would not give rise to a Hall voltage.

Consider what would happen if such a leakage path exists, and is independent of whether or not the device itself is in operation. As the gate voltage is being applied, if this leakage current is flowing but the device is not turned on, the Hall voltage should be zero, or near zero, and according to Equation 185 a very large but erroneous value for N_H would be calculated. As the gate voltage increases and the channel current increases, the credibility of the results coming from Equation 185 increases because the relative magnitude of the leakage current becomes small when compared to the true channel current. The more the device turns on, the more accurate the calculated value of N_H becomes. The actual channel current when these devices

are turned on hard is between 5 and 10 microamps, and as long as the leakage current is less than 0.5 microamp, the N_H determination will be sufficiently accurate. However, the leakage current can be very small and still give rise to a large error in N_H because the apparent Hall voltage would be very small when the device is operating below or near threshold.

After noticing these peaks in the data, some measurements on the devices were made to try to detect any such possible leakage paths. These measurements were taken both across the possible gate to source contacts, and source to source without an applied gate bias. In certain devices the gate to source exhibited such leakage, and in other cases source-to-source leakage was found.

Evidently portions of the gate oxide are susceptible to irradiation so that the oxide begins to conduct. *This gate-source leakage current* is measured because the ammeter measures terminal current, but this leakage current may or may not give rise to a corresponding Hall voltage.

The source-to-source leakage presents a somewhat more baffling problem, however. Whether this current is carried on the oxide upper surface, or leakage paths at the oxide semiconductor interface, it should seemingly pass the Hall terminals. One possible explanation for this component is that the epoxy used to cement the lid on the device may touch the bonding wires or the package bonding pads, and serve as a possible leakage path. Most epoxies degrade significantly with gamma irradiation, and this leakage path would be radiation dependent.

In both cases, the leakage currents were under 0.5 microamp at 10 volts, so when the device is turned on hard, they did not constitute a significant portion of the measured terminal current.

Having assumed the peak is due to leakage currents, a method must be selected either to minimize or eliminate that problem in the data reduction. The fourth-order polynomial curve fitting scheme and the tension splines, however, both inherently contain sufficient flexibility to allow quite laudable attempts to fit Figure 30.

One possibility is to simply eliminate all data points concerned with the anomaly. This is not a particularly desirable solution, however. Almost any curve fitting scheme that has the flexibility of tension splines and fourth-order polynomials would exhibit some rather unpredictable properties if used to describe such a large region without any data points supplied in that region to tie it down.

One scheme that is possible, however, is to least squares fit $V_g(N_H)$ by a straight line, and throw away any data in the anomalous region. By using a straight line least squares fit, unwanted oscillations could not occur in the region where no data points are supplied. This straight line fit could be used to determine both β and α. If this approach is used, α would then be a constant.

Consider Figure 31. This is a plot of both α and β vs N_H for device S160. Two plots for β are shown. The curved figure is evaluated using a fourth-order polynomial. The straight lined plot is a least squares first order fit. The plots for α are evaluated using tension splines (curved plot) and a constant value from the first-order polynomial fit of $V_g(N_H)$. It can be seen that for small values of N_H the first order fit does not give very good approximations to either α or β. As N_H increases, the fits become better.

A better evaluation of the linear fit of $V_g(N_H)$ can be obtained if one examines Equations 100a, b, c and 101. Note that the function w

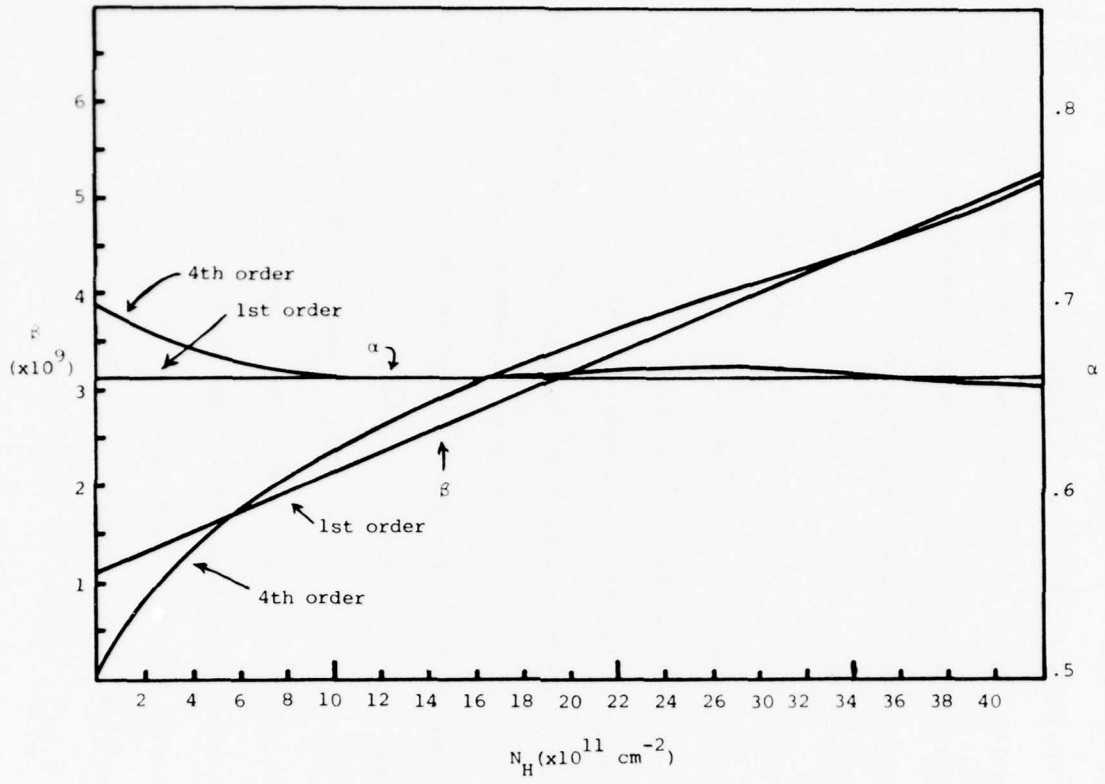

Figure 31. Plots of $\alpha(N_H)$ and $\beta(N_H)$ for device S160R000 using the 1st order and 4th order polynomial for β, and the 1st order polynomial and tension splines for α. In both cases, the straight line represents the 1st order fit.

must be integrated in Equation 100b to determine r in the contraction steps. The value for w is given by Equation 101 in terms of the raw data functions α and β. The accuracy of r depends on the integral of w, and not the values of α and β directly.

Recall, the variables C_1, C_2, C_3, and C_4 are functions of Φ_s and T, and they can be printed out for each value of Φ_s if one chooses to do so when running the data reduction program. Also, the data reduction program prints out $V_g(\Phi_s)$. Knowing these functions, it is possible to plot $w(N_H)$. Such a plot is shown in Figures 32 and 33. These data are from device S160, which showed negligible leakage. In Figure 32, w is plotted as a function of N_H for the unirradiated device using a fourth order fit and a first order fit. Since the area under the curve is what is important, significant error occurs up to $N_H = 6 \times 10^{11}$ for this device, and the error rapidly decreases after that.

Figure 33 is a similar plot, but the data come from device S160 irradiated to 10^7 Rad (Si). The same general characteristics are shown. An approximation to the area under these curves is possible by integrating from zero toward the right, and using a trapezoid formula to calculate the area. If this is done, the following figures result:

N_H (cm^{-2})	Area (arbitrary units) 1st Order	4th Order	Difference (%)
8×10^{11}	17.8	14.8	20
12×10^{11}	27.6	23.8	16
20×10^{11}	49	44	11

The smallest data point supplied in this case after the data in the anomalous region were eliminated was 1×10^{12}. Thus, at a value of

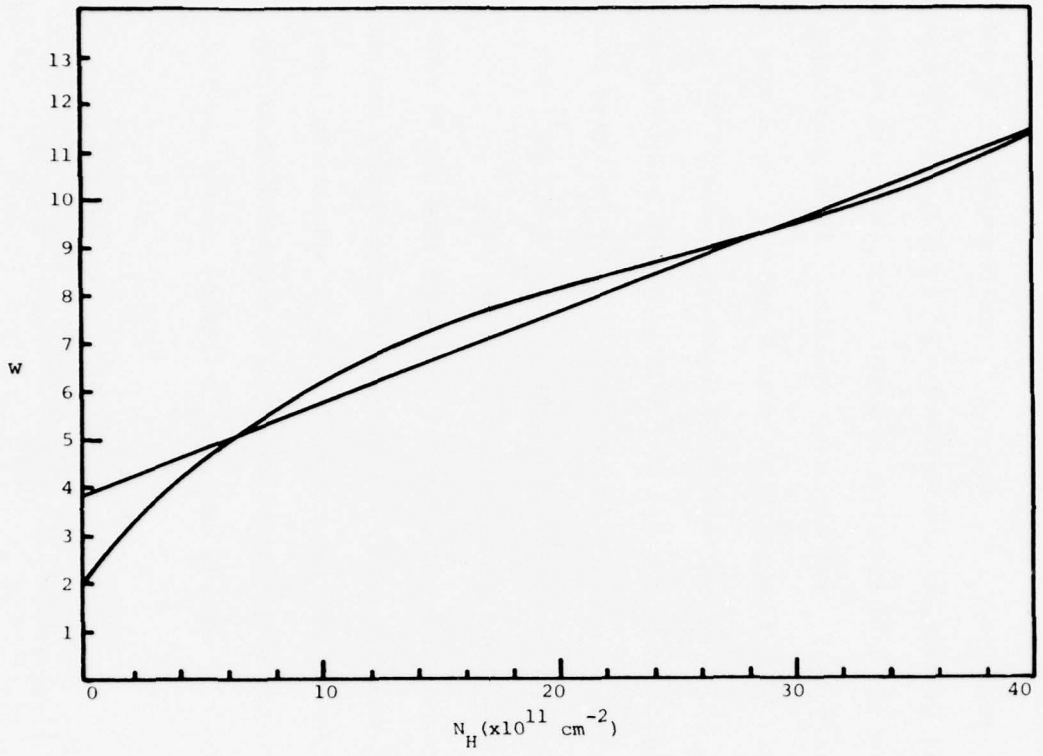

Figure 32. A plot of w vs. N_H calculated using both 1st and 4th order curve fits. The straight line comes from the 1st order curve fit. This is for S160R000, very good original data.

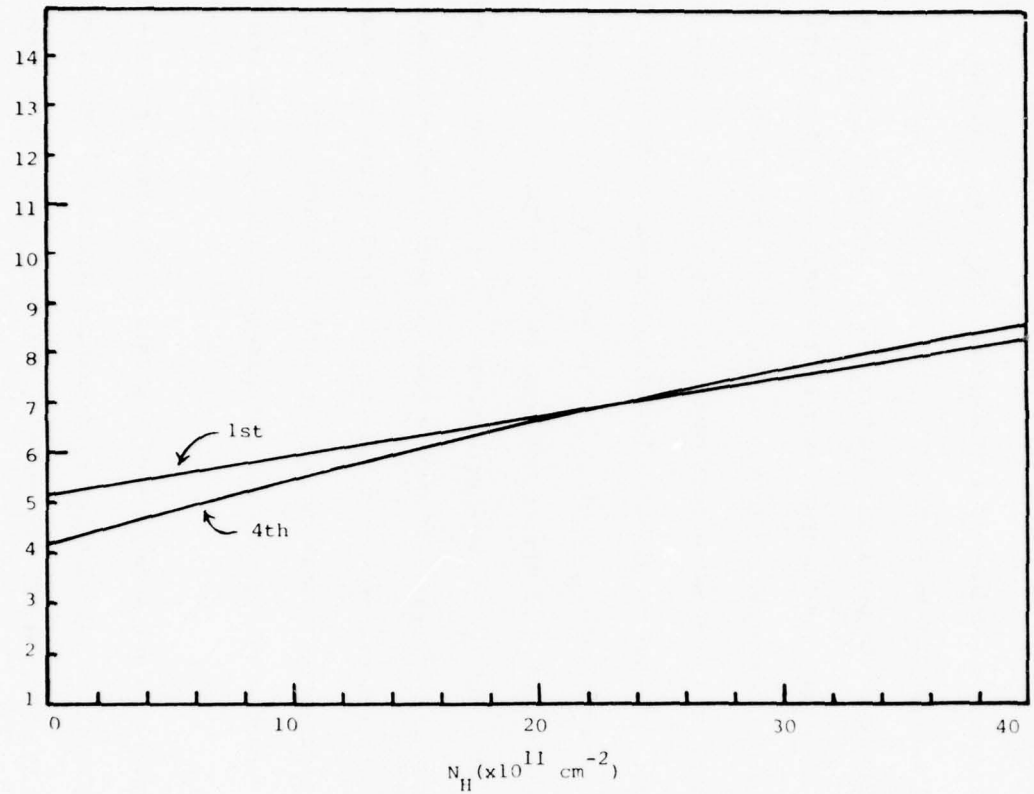

Figure 33. Another plot of w vs. N_H fit by both a 1st order and 4th order fit. This is the same device plotted in Figure 32, after $1x10^7$ Rad(Si) irradiation. Note the lowest value for N_H actually calculated from the data is marked.

N_H equal to about twice the smallest supplied datum point, the error here was about 11%. For a value of N_H near the smallest supplied datum point, the error in w is about 20%. Keeping this in mind, no values of any variable calculated in the data reduction program are used if they were calculated solely on values of w evaluated at N_H less than the smallest actual supplied datum point.

This is easy to do in practice. Figure C-4 in Appendix C shows a typical output listing. The program lists on the last page of the printout the value of N_H corresponding to the values of Φ_s and V_g currently being used. Thus, on the final output page, one simply needs to look at the N_H column, and exclude all calculated outputs where the value of N_H is less than the minimum N_H supplied by the raw data. This minimum value is found in column 3 of the second page of the output.

In this study, the $N_H(V_g)$ data were visually inspected for any peaks near the turn on gate voltage. If such a peak existed, these data were eliminated at both temperatures. If more than a third of the data were thrown out, a first order approximation was used to determine β and α. The amount of output actually used was determined by the criteria mentioned above.

It is possible to get some idea of how this first order approximation would affect the calculations by examining Equation 100a, b, and c, and Figures 31, 32, and 33. In general, the area under the w curve is larger for the first-order polynomial than for the fourth-order. Thus, r would be estimated too small in Equation 100b. Similarly, consideration of β in Figure 31 shows that for small N_H, the first order estimate of β is too large, and N_{ss} calculated by the first order polynomial would be too large. In the mid gap range of N_H, the N_{ss} value

would be too small. In very strong turn-on, both methods give about the same answers.

3. RESULTS OF THE MICRO-HALL MEASUREMENTS

Many different quantities are calculated in the process of reducing the micro-Hall data. Some of these parameters could be very interesting to examine, but are not too relevant for this study. The main quantities of interest calculated by the Hall program are $N_{ss}(\Phi_s)$, $V_g(\Phi_s)$. Recall that the Hall mobility is calculated from the experimental data directly, so an additional plot of interest that can be generated by using the data $\mu_H(V_g)$ along with $V_g(\Phi_s)$ is the function $\mu_H(\Phi_s)$. These specific results are the ones considered in this study.

Figures 34 and 35 are plots of $N_{ss}(\Phi_s)$ for two separate devices, S160 and S161. Two curves have been selected here because they represent the changes displayed by other devices in general. Ncte that these plots are $N_{ss}(\Phi_s)$ at different levels of total dose irradiation. The general trends that these curves demonstrate are somewhat surprising. In Figure 34 it can be seen that in general $N_{ss}(\Phi_s)$ decreases with total radiation dose, but it does not do this consistently. Examination of Figure 35 leaves little doubt that N_{ss} near the band edges can either decrease or increase as a function of total dose.

This result demonstrates two surprises. The first is that $N_{ss}(\Phi_s)$ decreases at all. Recall (Refs. 18, 19) that in the mid gap energy range $N_{ss}(\Phi_s)$ increases for the entire energy range at all dose levels. The second surprise is that it may either increase or decrease as a function of total dose. This seems to imply that possibly two separate mechanisms may account for N_{ss} at the band edges, and that they compete with each other as a function of total dose.

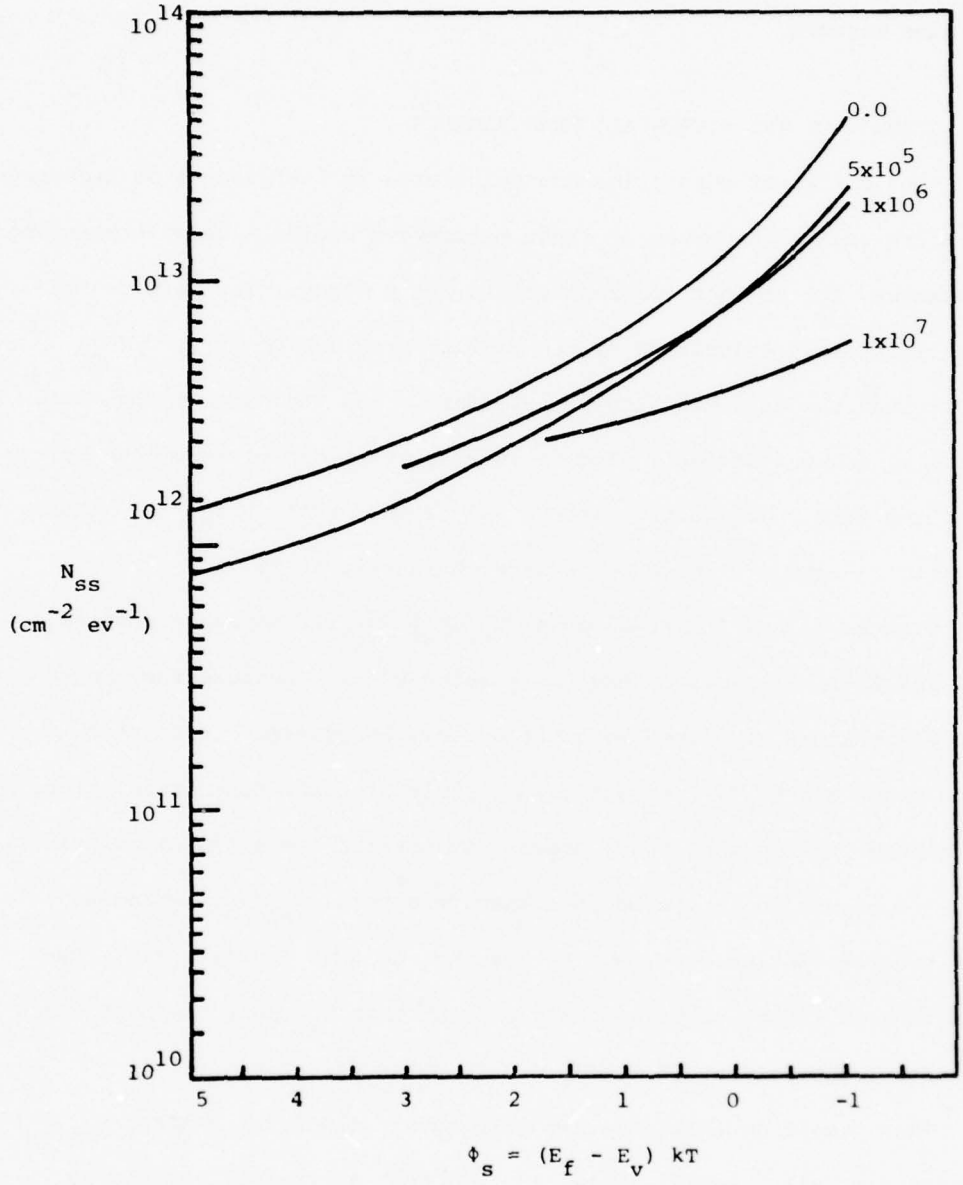

Figure 34. $N_{SS}(\Phi_S)$ at four different radiation levels. Here, Φ_S is measured in units of kT and is equal to (E_f-E_v).

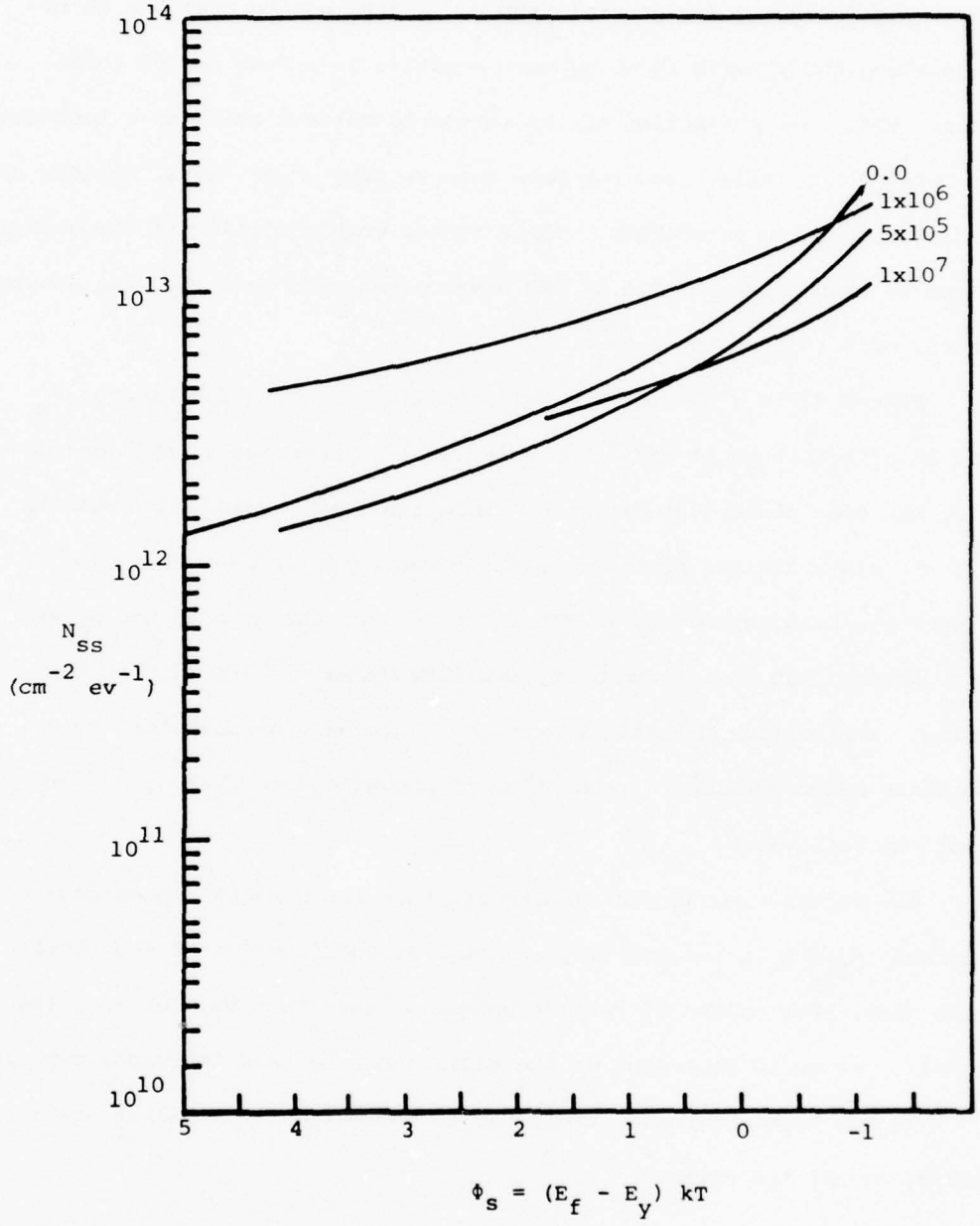

Figure 35. $N_{SS}(\Phi_S)$ at four different radiation levels. Here, Φ_S is measured in units of kT and is equal to (E_f-E_v).

Figure 36 is a plot of $V_g(\Phi_s)$ at all of the dose levels. These curves again show a few general trends. First, notice that the intercept along the V_g axis is going more negative as a function of total dose. This is a reflection of the threshold voltage shift as a function of total dose. This trend has been seen in many other investigations of radiation effects on MOSFETs. There is not much variation in the general shape of these curves. All of the devices measured show the same general trends of $V_g(\Phi_s)$ on total dose.

Figure 37 is a plot of the Hall mobility, μ_H as a function of Φ_s and at different total radiation dose levels. Once again, only one device has been plotted at different radiation dose levels. Essentially all the other devices demonstrate these characteristics. This same figure has been reproduced in Figure 38, except the plot is now μ_σ vs. Φ_s. Notice that the conductivity mobility measured here is that for holes. For surface potentials very near turn-on, the conductivity mobility measured before irradiation is around 430 cm^2/V-sec, or very near the bulk value.

The features worth noting here are that for a highly degenerate surface ($E_f \approx E_v$), the mobility is not a strong function of the radiation dose. For values of surface potential near turn-on, however, the mobility is quite dependent on the radiation dose, and decreases rapidly.

As has been mentioned, these basic trends for the mobility are displayed by all the devices.

4. RESULTS OF THE C-V MEASUREMENTS

The results of the C-V measurements supplied by Sandia Laboratories were all photographs taken from the computer graphics terminal. These

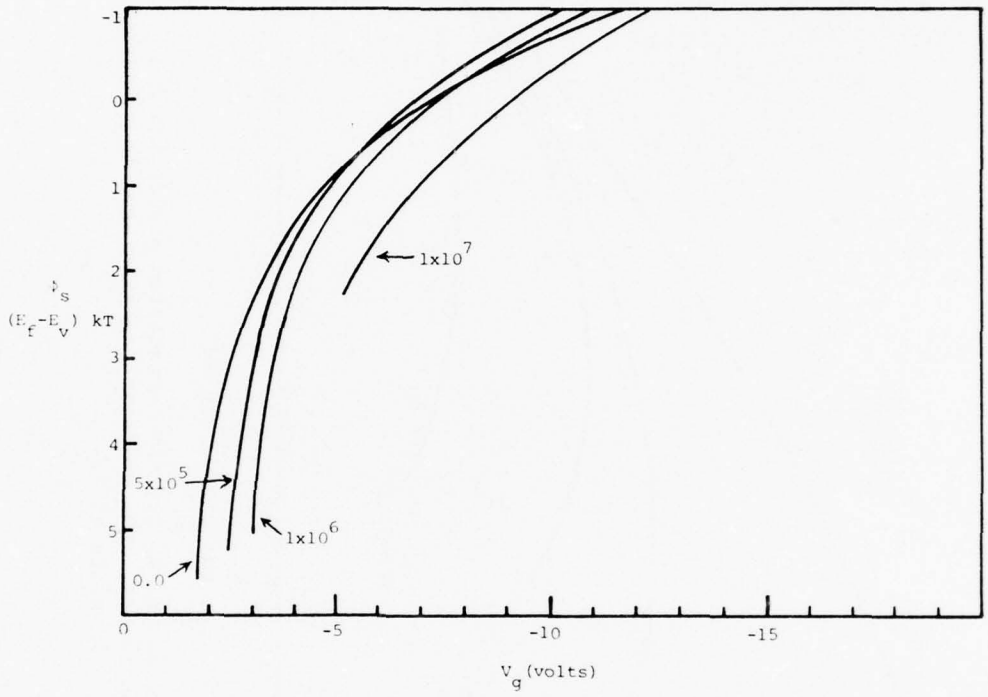

Figure 36. $V_g(\Phi_s)$ determined by micro-Hall calculations. Note this can only cover the range where the device is turned on.

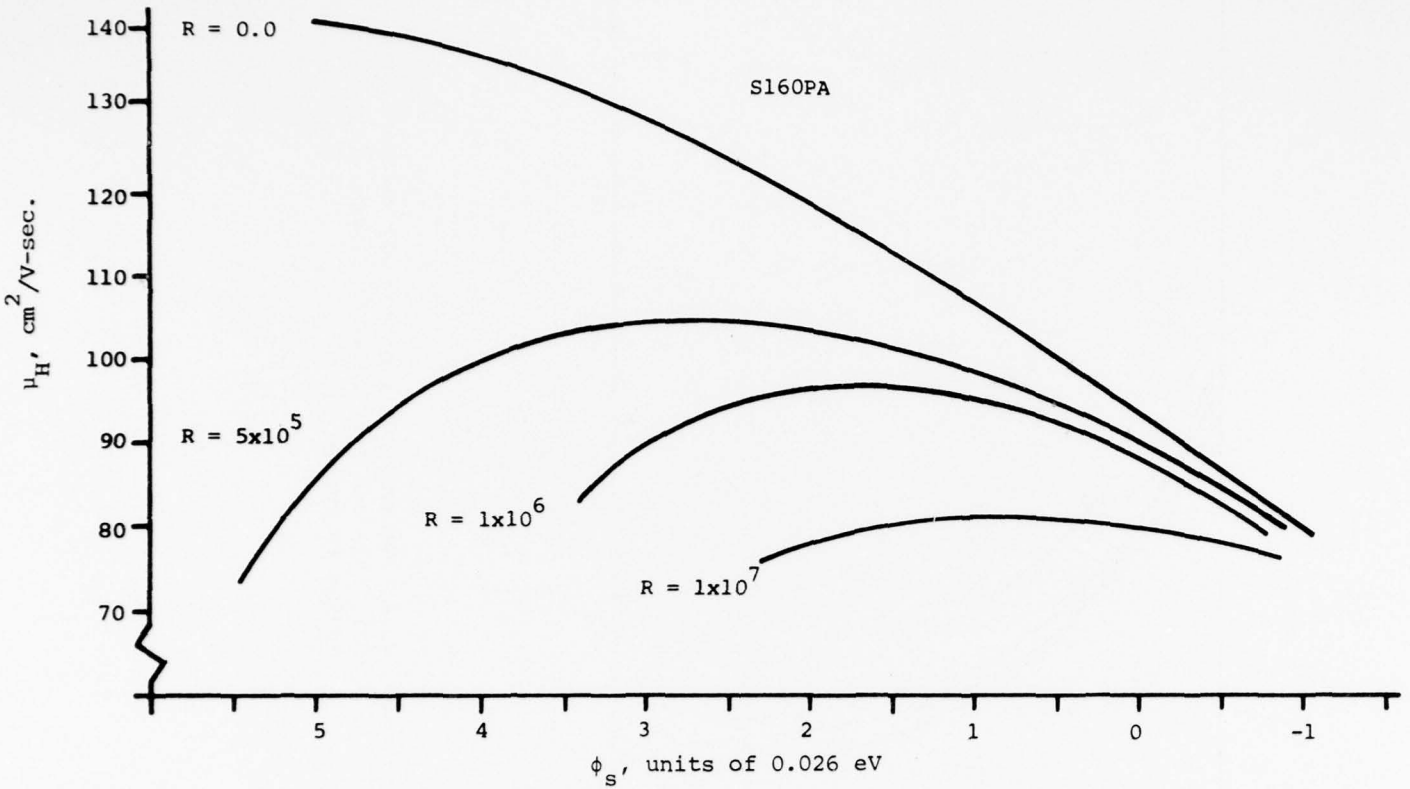

Figure 37. A plot of μ_H vs. Φ_S for an unirradiated device and four radiation levels. The surface potential here is measured as $E_f - E_v$ in units of kT.

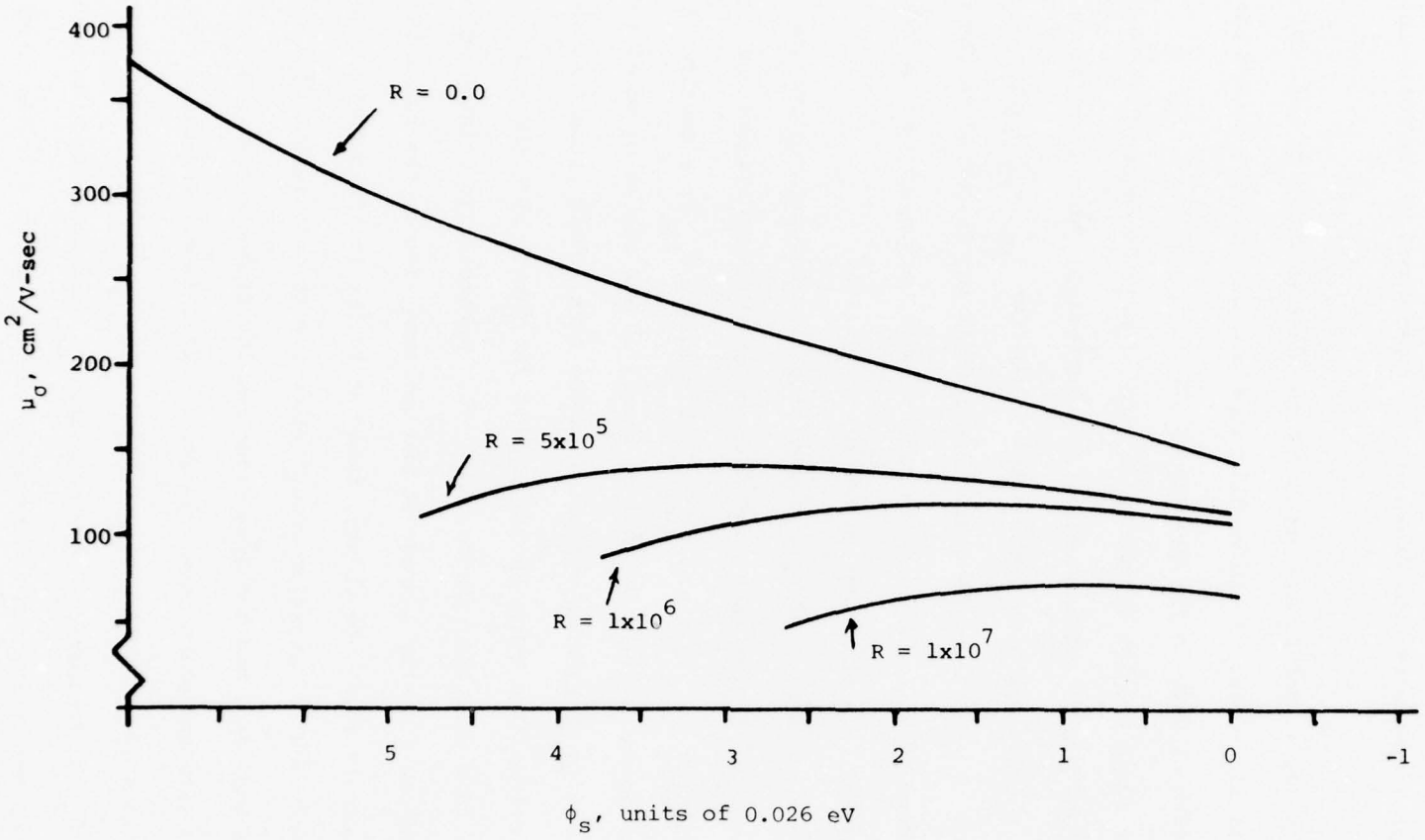

Figure 38. A plot of μ_σ vs. ϕ_s at the various dose levels. The surface patented is measured in $E_f - E_i$ in units of kT.

pictures did not duplicate well enough to make printing masters, so some typical curves were hand drawn and are reproduced in the following figures.

Figures 39, 40 and 41 are graphs of the data supplied on one device for one radiation dose. It is readily apparent that the C-V curves can yield a wealth of data in the mid gap range.

Figure 39 is the low frequency and scaled high frequency C-V curves normalized and put on the same axis, as described in Table 1. Along the top of the picture are also written the values for C_{FB}, V_{FB}, N_A, w_D, T_{ox}, C_{ox}, and R_s. These values have all been defined and discussed in Chapter II. The quantity T_{ox}, the oxide thickness, must be supplied as an input to the program. All the other values are calculated.

Figure 40 is a plot of $V_g(\Phi_s)$ resulting from integrating the low frequency curve. Notice that along the top of this are printed the three quantities Φ_{s_o}, V_{th}, and $\Phi_{s_{th}}$. The quantity Φ_{s_o} is a measure of the maximum amount of band bending in inversion and should be equal to (E_f-E_v) in units of eV when evaluated in the bulk. This means that in strong inversion, the bands should be bent far enough that the Fermi level coincides with the valence band. This parameter is printed out so that one can visually inspect it and get some idea of the reliability of these calculations. In theory, integrating the low frequency curve from accumulation to inversion should allow one to calculate $V_g(\Phi_s)$ over the entire band gap, and the area under the low frequency curve should not change with radiation dose. In reality this is not the case. The area decreases as a function of radiation dose and limits the accuracy of the $V_g(\Phi_s)$ determination. The quantity Φ_{s_o} describes the area under the low frequency curve and is therefore printed out to allow the user to get a quick feel for the accuracy of the data.

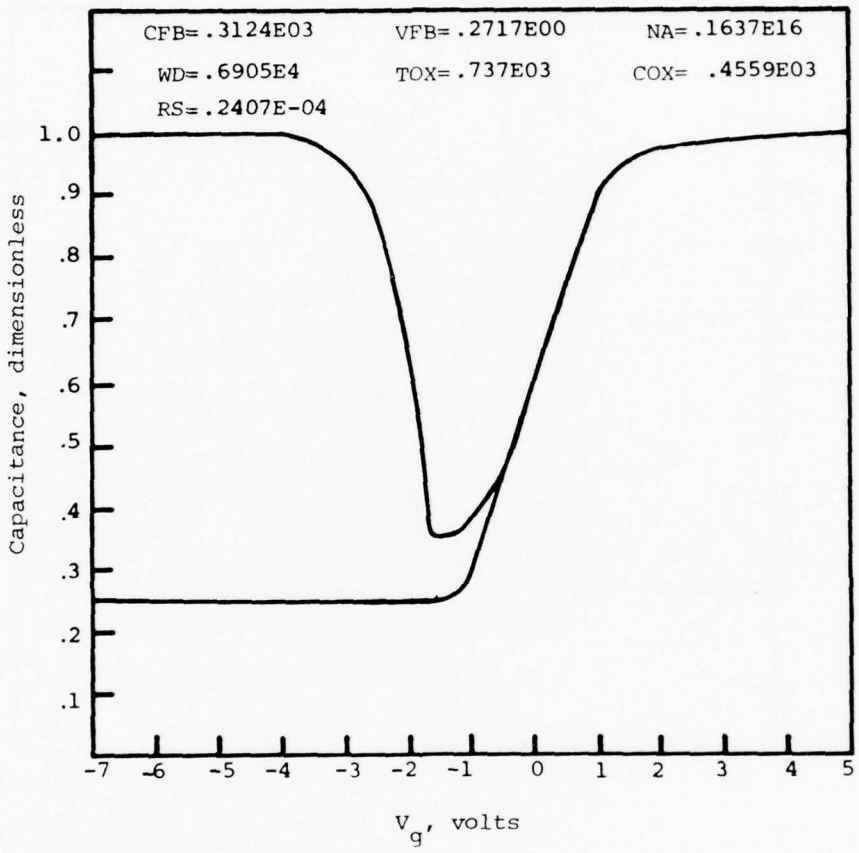

Figure 39. The first output of the C-V program, the high frequency and low frequency curves on the same scales.

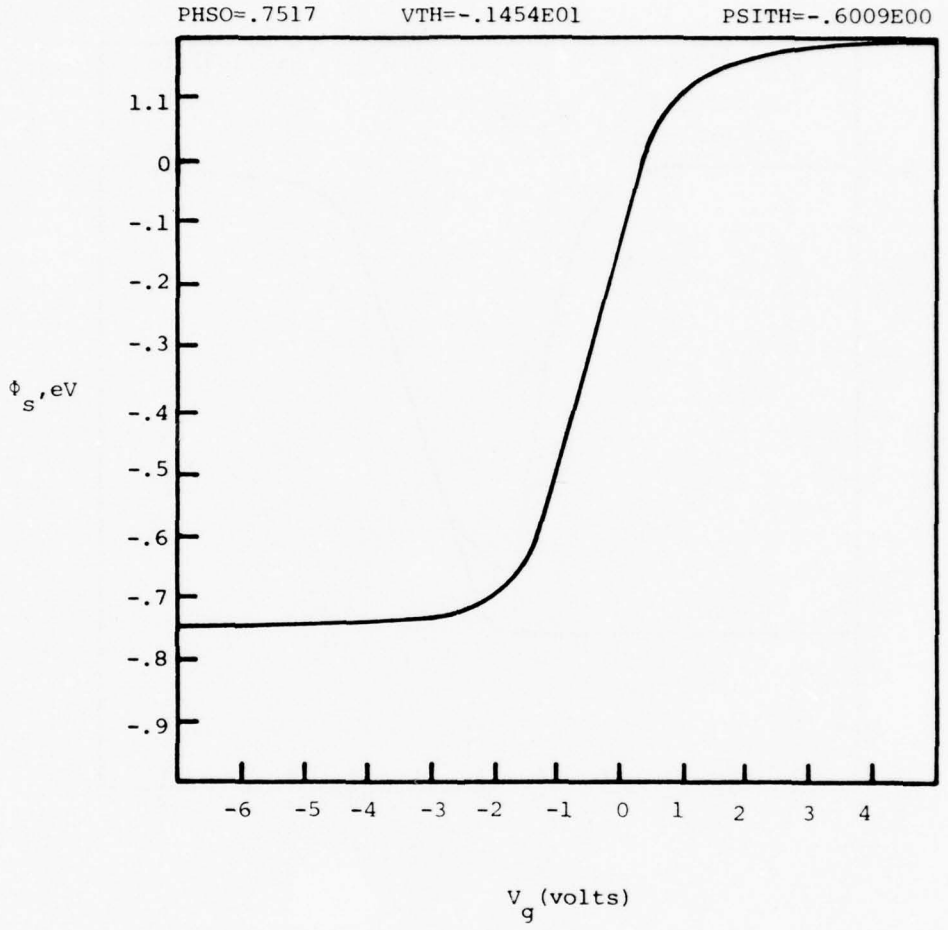

Figure 40. Plot of $V_g(\Phi_s)$ from the C-V program.

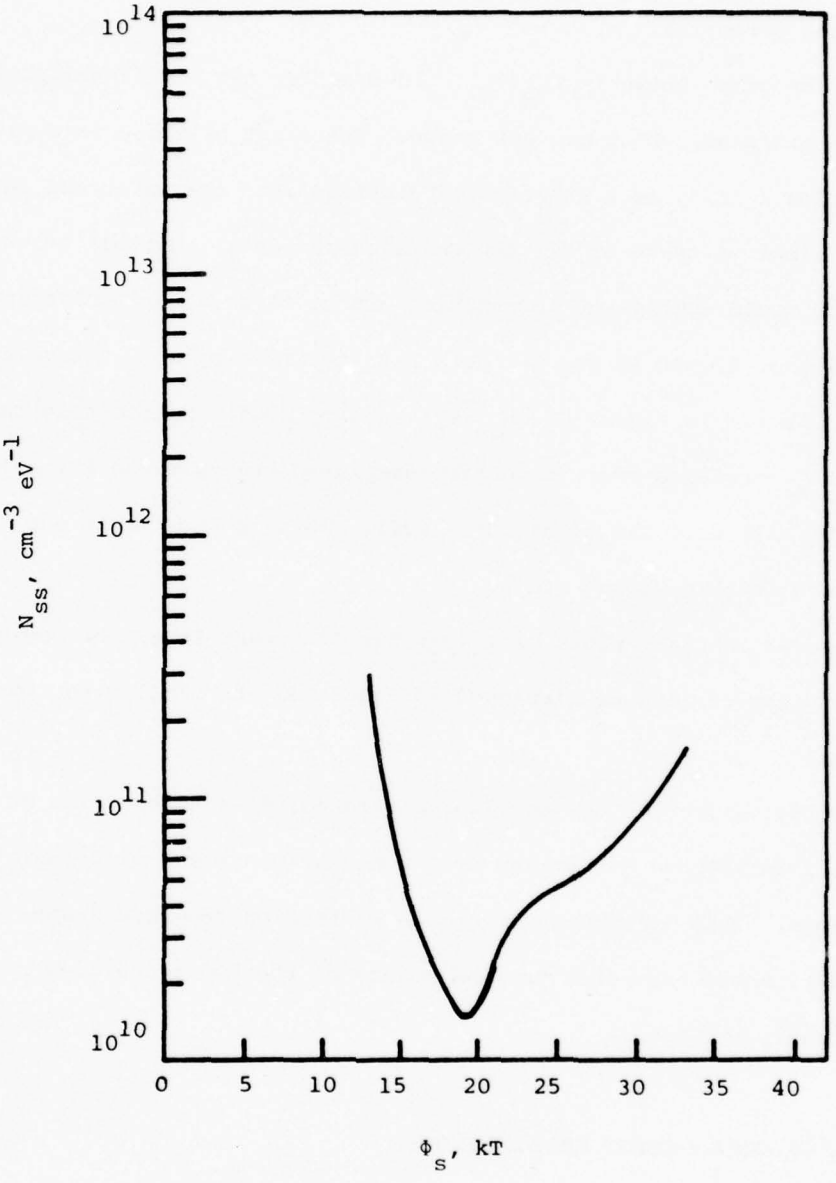

Figure 41. N_{ss} vs. Φ_s from a typical device. Results derived from C-V analysis.

The other two parameters are the threshold gate voltage and threshold surface potential.

The last graph shown is $N_{ss}(\Phi_s)$. In practice two additional photographs are produced, which are not shown. The first of these is a plot of the doping density as a function of distance into the wafer and the second is simply a table of all the unscaled raw data. Neither of these photographs would supply any information useful to this particular study.

In Figures 42 and 43 the C-V data results are displayed for various radiation doses. In Figure 42, $N_{ss}(\Phi_s)$ is displayed. Notice that the value of N_{ss} increases over the entire displayed energy range for all consecutive values of the total dose level. This is the result one would expect in this energy range.

Figure 43 contains plots of $V_g(\Phi_s)$ for different levels of radiation dose. The variations displayed in Figure 43 are similar to those in Figure 36.

The final graph in this section, Figure 44, is a combination of the $N_{ss}(\Phi_s)$ variations determined by C-V measurements and micro-Hall measurements. This is Figures 42 and 34 plotted on the same graph. It should be noted here that the end points of the two techniques compare favorably.

5. PLOT OF SOURCE-DRAIN CHARACTERISTICS

In order to get an overall idea of the effect of the total dose irradiation on the device performance, in addition to measuring $N_{ss}(\Phi_s)$ at the different dose levels, the MOS transistors were also mounted in a holder, and the standard source-drain characteristics were examined using a curve trace.

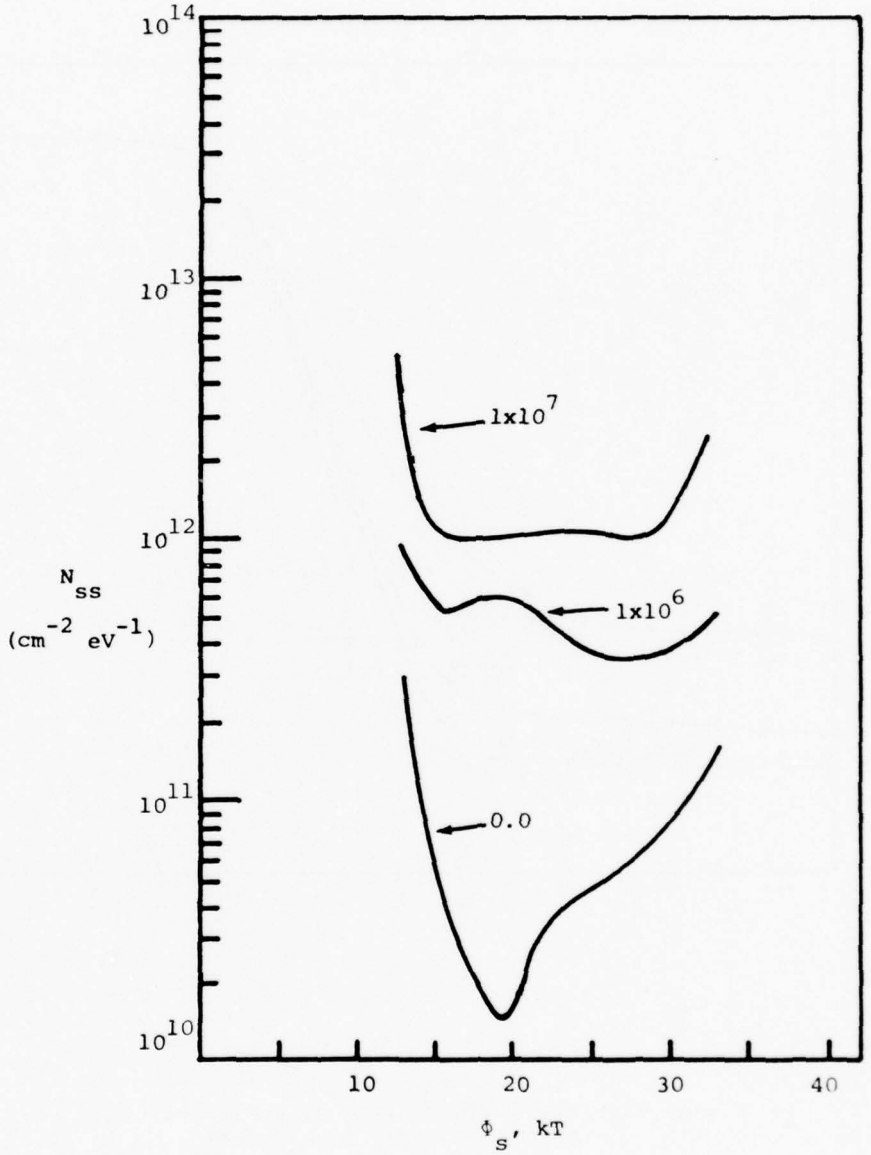

Figure 42. N_{SS} vs. Φ_S determined using the C-V technique at three different dose levels.

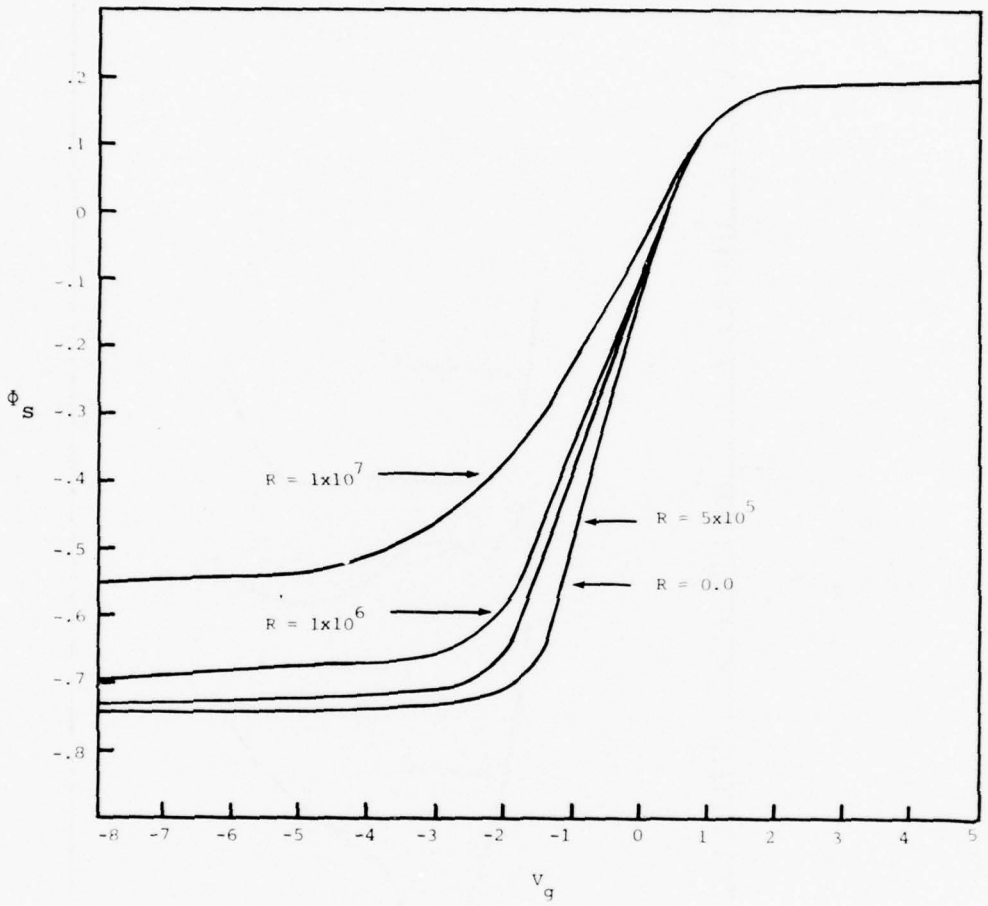

Figure 43. $V_g(\Phi_s)$ determined by C-V curves for different total dose levels. V_g is in volts. Φ_s is in eV measured from E_f in the bulk.

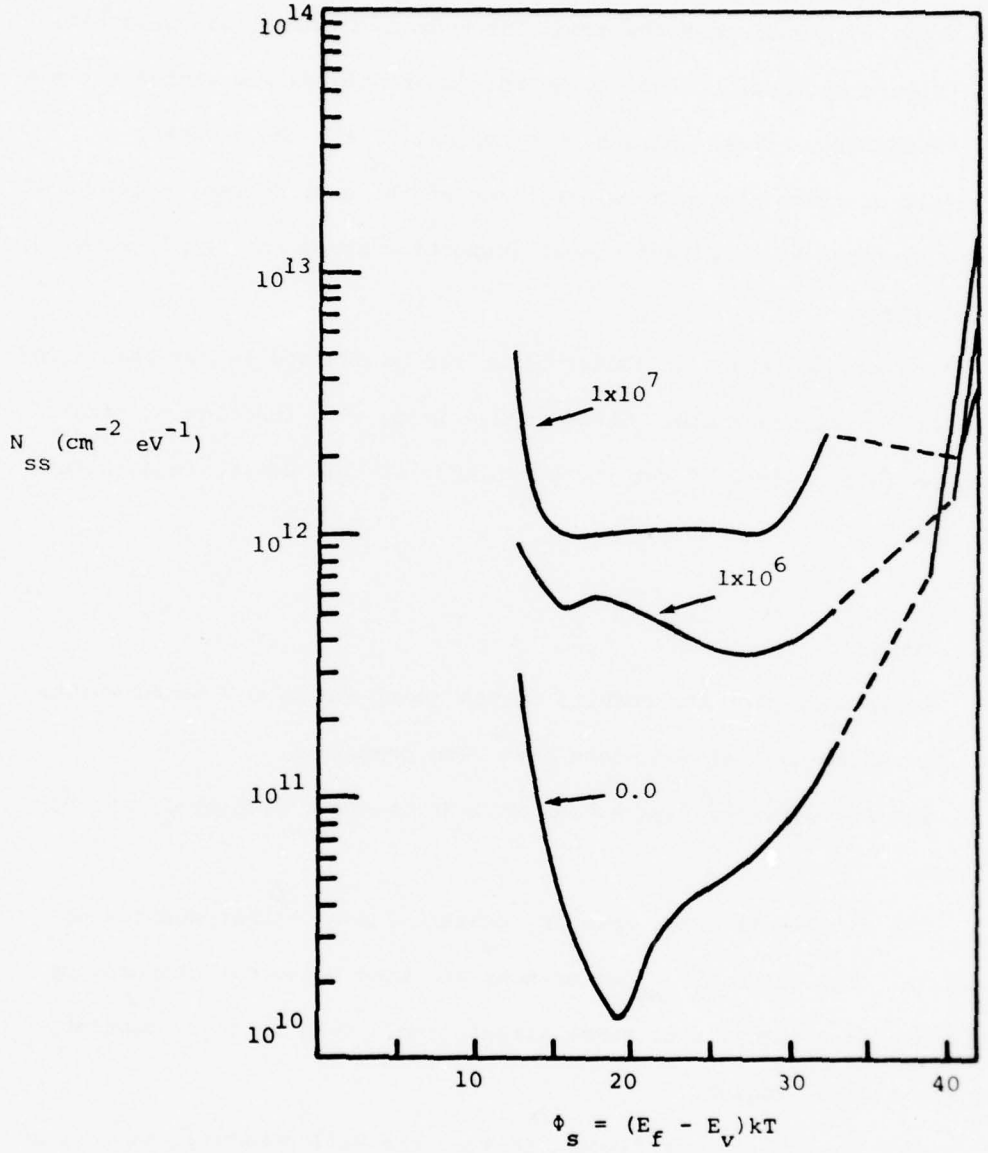

Figure 44. $N_{ss}(\Phi_s)$ constructed using both C-V technique and micro-Hall technique.

The specific characteristics measured each time were plots of the source-drain current vs. the source-drain voltage at varying gate voltage steps. In each case the same source-drain terminal was selected.

Figure 45 shows the way these characteristic curves varied for one of the devices. These changes were typical of all the devices.

All of these photographs are taken at the same control settings of the curve tracer, so direct visual inspection shows the trends with total dose.

The most outstanding feature that can be noticed is the change in g_m, the transconductance. The decrease in g_m as a function of total dose would certainly affect the usefulness of this device in an actual circuit.

6. SUMMARY

In this chapter the results of the quasi-static C-V measurements and the micro-Hall measurements have been presented.

The C-V data displays trends similar to those displayed in other places.

The micro-Hall data, however, exhibited some rather surprising results. The value of N_{ss} at or near the band edges can decrease or increase as a function of gamma irradiation. This is quite contrary to the mid gap region.

Another significant finding is that the Hall mobility, as well as conductivity mobility both decrease as a function of total radiation dose. For electric fields near device turn-on, the mobility variation depends quite strongly on the radiation dose. However, if the surface electric field is very strong causing extreme degeneracy at the surface, the mobility is not a particularly strong function of the radiation dose.

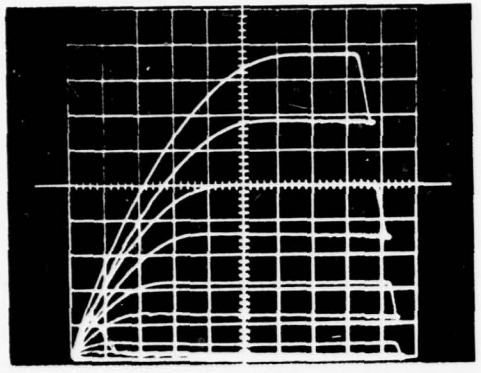

(a) R = 0.0

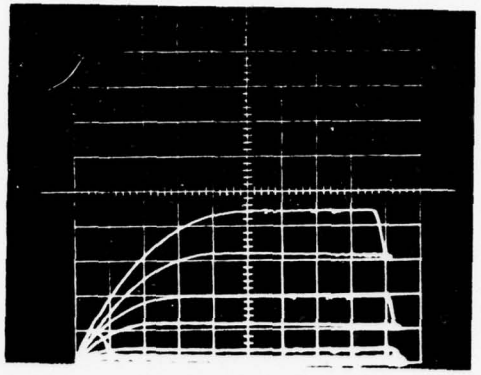

(c) R = $1x10^7$ Rad(Si)

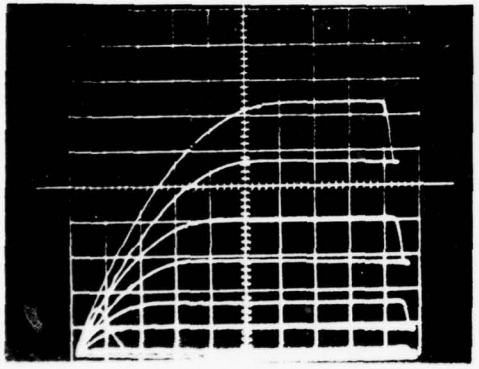

(b) R = $1x10^6$ Rad(Si)

Figure 45. Typical MOS transistor characteristics under the influence of radiation dose. The curves are I_{SD} vs. V_{SD} for various values of V_g. Figure a, b, and c are at three separate dose levels. The curve tracer settings are the same in all three photographs.

Finally, some photographs of the drain current vs. the source-drain voltage at various gate voltages are shown for different total dose levels of irradiation. It is evident from these photographs that the transconductance of the transistor is decreasing with total dose.

CHAPTER VII

DISCUSSION AND CONCLUSIONS

1. INTRODUCTION

In this chapter some general statements are made about the data in an attempt to physically explain or model the results observed. No attempt is made to do any mathematical modeling. The results shown in Chapter VI are discussed in terms of some previously hypothesized models, and an attempt is made to correlate the variation of g_m with the radiation dose level.

In examining the data, they are considered on the whole and not broken into subsections. This is done because all the measured results are probably physically interdependent, and any attempt to look at one result without the others would be incomplete.

2 GENERAL DISCUSSION OF THE RESULTS

As was noted in Chapter VI, one of the more surprising results of the N_{ss} determination is that it can decrease or oscillate as a function of radiation dose at the edge region. The variation of $N_{ss}(\Phi_s)$ with radiation dose at the band edges has never before been reported.

The existence of mid gap states has been attributed to several mechanisms. One of the most comprehensive explanations was given by Gwyn (Ref. 46). The essence of Gwyn's model is the existence of "dangling-bonds" in the gate oxide. In a pure oxide such as quartz, a very repetitive stoichiometric structure is established according to the crystalline pattern of the material. When an oxide of silicon

grows on the silicon surface, a completely different situation exists. The lattice distances of SiO_2 are such that no perfect interface could ever exist between the SiO_2 and the silicon host. Also, any imperfections in the original host such as stacking faults, slip planes, screw dislocations, or, in general, any crystalline imperfection might manifest itself as nonstoichiometry of an oxide grown on the substrate. In addition, any impurity present in the oxidizing gases or growth system could cause lattice strain in an oxide if it were included in the oxide during its formation.

Thus, there are many ways in which imperfections could arise in an oxide. These imperfections would result in strained bonds in the oxide, and could serve as traps for charge or sources for charge depending on the exact mechanisms involved with the imperfection formation.

This model has been used to explain the positive oxide charge build-up during irradiation. If a radiation pulse releases an electron from one of these imperfections, or for that matter from a stoichiometric portion of the oxide, and if this free electron successfully diffuses to either the gate electrode or semiconductor bulk before it is captured, an uncompensated immobile charge is left behind. If this charge is in the oxide to such a depth that an electron cannot tunnel from the gate electrode or the semiconductor to the charge site and neutralize it, no matter what the Fermi level position is with respect to the band edges, this charge comprises a fixed charge in the oxide.

If the charge is near the $Si\text{-}SiO_2$ interface and is not so deep that an electron cannot tunnel to it, the occupancy of such a state would be determined by its relative energy in the forbidden region as compared to the position of the Fermi level relative to the band edges.

By observing the time constants for emptying and filling of surface states, it has been estimated that these states must be within 20Å of the $Si-SiO_2$ interface (Ref. 47). Such states can be considered interface states.

This model explains to some extent both the trapped positive oxide charge and interface state production under the influence of radiation. The relative position of a given interface state would be determined by the exact physical mechanism from which it was generated. The relative strength of the trap to electron bond would establish the relative position of the interface state in the band gap.

Experimental evidence for another explanation of interface states was supplied by Hughes, et al. (Ref. 48). This is really quite similar to the Gwyn model for interface states. The evidence here indicates that impurities in the oxide may migrate toward the interface during irradiation. If they get sufficiently close, they become traps which can communicate charge with the semiconductor. The term "communicate charge" means that charge is either trapped in a given state or released from that state as the Fermi level sweeps across it. Communicable charge states would be interface states, while incommunicable charge states would represent the fixed charge trapped in the oxide.

While either of the two above mentioned effects or a combination of the two explains the variation of $N_{ss}(\phi_s)$ at the mid gap region, neither seems to shed any light on the band edge region. An explanation of the edge effects has been proposed by Maier (Ref. 49). The foundations of this explanation ultimately are similar to the Gwyn theory. Maier considers the condition of the oxide during growth. As an oxide grows, the oxygen must diffuse in from the outer surface to the $Si-SiO_2$ interface.

The outer surface is oxygen rich, while the $Si-SiO_2$ interface will be oxygen deficient. The inherent oxygen gradient across the oxide accounts for the oxygen diffusion according to Fick's law. When the wafer is removed from a furnace after growth of an oxide, this oxygen gradient is "frozen in" the oxide. The only way in which oxygen can now diffuse toward the interface is if some energy of sufficient magnitude is supplied to make the oxygen mobile. Under the influence of radiation, an oxygen atom could gain such energy; and since an oxygen gradient exists, it would diffuse toward the silicon-oxide interface. If it diffused to a physical location to allow it to bond with silicon instead of existing interstitially and if in the process of bonding it relieved some strained bonds at the interface, then N_{ss} could, in fact, reduce as a function of radiation dose. Certainly, this is not the only explanation, but it fits the evidence. An inherent assumption here is that the energy associated with the relaxation of strained bonds when the oxygen arrives is near the band edge. Again Maier points out that such energy levels have been observed near the band edge (Ref. 49).

These data seem to indicate, therefore, that the physical mechanisms which lead to the formation of interface states near the mid gap are different from the mechanisms which account for the interface states near the band edge. More accurately, the mechanisms near the band edge are probably compound. Some of the mechanisms may be the same as the mid gap mechanisms, and others are not. The particular way in which $N_{ss}(\Phi_s)$ varies with radiation dose must be due to some competing mechanisms. Whether the density distribution moves up or down depends on which mechanisms are dominant at that dose level and for that device.

It seems significant that the mid gap interface state density increases with radiation dose, but the edge states do not follow any apparent predictable pattern. The mobility also varies consistently with radiation dose, decreasing in each case.

The particular shape of the mobility curve has been observed by others (Refs. 23, 50, 51). This is the first time the variation of $\mu_H(\Phi_s)$ with total radiation dose has been reported. The overall shape of the mobility curve has been explained as follows (Refs. 23, 52). Consider Figure 37 or Figure 38. Let the regions of 0 to 1 kT be referred to as strong field and the regions of 3 to 6 kT be referred to as weak field.

For the weak field region Stern and Howard (Ref. 52) have hypothesized that the existence of positive charge near the Si-SiO_2 interface trapped in the oxide results in bound states. These bound states could trap electrons or serve as scattering centers for holes or electrons. In either case, as the free carrier density in the inversion region increases when the electric field goes from weak toward strong, the effect of the bound states is screened due to the increase in free charge. At very weak fields, these potential wells then decrease the mobility. As the carrier concentration increases, the effect of the potential wells or scattering centers is screened, and the mobility increases. This trend only continues to a certain maximum, however. At some critical value, the free carrier density becomes sufficiently large, and carrier-carrier scattering of the free charge carriers begins to become important. The greater the free carrier density beyond this critical value, the more effect carrier-carrier scattering has on the mobility. Thus, the mobility begins to decrease again.

In the weak field region, where the scattering mechanism is due to the trapped positive charge scattering, the basic mechanism can be thought of as carrier-interface scattering because a scattering "well" exists at the $Si-SiO_2$ interface. In the strong field region, the basic scattering mechanism is carrier-carrier scattering, or Coulomb scattering.

The basic theory quite nicely accounts for the salient features seen in Figures 37 and 38. The mobility variation at a given dose level has already been examined. As the device is exposed to radiation, both interface states and states which are uncommunicable with the silicon bulk are introduced. Both of these sites will act as scattering centers to decrease the mobility for weak fields. At strong fields, however, the dominant process is still carrier-carrier scattering, and is relatively unaffected by the radiation dose.

This generally predicts and explains the mobility variations observed here. It is believed that the radiation has produced scattering centers at the $Si-SiO_2$ interface that increase the amount of carrier interface scattering at weak fields and results in the decrease in the mobility with radiation dose. The large decrease in the mobility indicates that the number of scattering centers introduced must have been on the order of the number of scattering centers initially present. It does not seem reasonable to assume that a few percent increase in the number of scattering centers could be responsible for a 35% to 40% decrease in mobility as seen in Figure 37 for $\Phi_s = 5.5$.

The mobility decrease at strong fields is still present, but not as pronounced as it is for weak fields. Thus, while carrier-carrier scattering is still the dominant process, some net effect of the carrier-interface scattering is still seen at strong fields.

Since the weak field mobility is such a strong function of the radiation dose, any attempt to correlate the mobility variations with the $N_{ss}(\Phi_s)$ variations on total radiation dose immediately leads to the conclusion that the interface states near the mid gap are ultimately the ones which affect the mobility. The mid gap variations are the only ones of sufficient magnitude and consistent variation that could explain the phenomenon. The band edge states do not seem to vary in a large enough magnitude nor with sufficient consistency to correlate with the mobility.

The mobility variation with total dose has significant effects on the overall device performance. In any general treatment of the theory of operation of an MOS transistor, the mobility is one of the fundamental parameters (Refs. 53, 54, 55). Both small and large signal theories of MOS transistor operation predict a direct variation of g_m with the mobility. The characteristic curves displayed in Figure 45 indicate that g_m does, in fact, decrease with total dose. Thus, the presence of physical scattering centers can be used to explain mobility decrease, and ultimately the degradation of an important device parameter, the transconductance.

3. SUMMARY

In this chapter an attempt has been made to unify all the observed results.

First, examination of the $N_{ss}(\Phi_s)$ curves led to the conclusion that the band edge states are probably due to several competing mechanisms, and the dominant mechanisms at the band edge are different than the ones in the mid gap region.

The decrease in mobility as a function of radiation dose has been explained in terms of the generation of scattering centers near the mid-gap region which causes an increase in carrier-interface scattering at weak electric fields. This basic trend coupled with the $N_{ss}(\phi_s)$ data allows one to conclude that the mid gap states are the ones most likely responsible for device degradation.

Finally, the decrease in transconductance is, in turn, attributed to the mobility decrease. Thus, the ultimate transistor degradation has been linked back to the introduction of scattering centers at the $Si\text{-}SiO_2$ interface.

Since the mid gap surface states are the ones which seem to be dominant in determining the device characteristics, any future study that is concerned with device performance should probably concentrate on mid gap surface state determination. On the other hand, if some basic research is performed to examine scattering mechanisms at the surface, both mid gap state and band edge state determinations should be considered.

REFERENCES

1. Hughes, H. L. and Giroux, R. A., "Space Radiation Effects on MOS FETs," Electronics, Vol. 37, December 1964, p. 58.

2. Peden, J., "Gamma-irradiation of some Silicon Planar Transistors," paper presented at the IEEE Nuclear and Space Radiation Effects Conference, Seattle, Washington, July 1964.

3. Peck, S. and Schmid E., quoted in "Surface Effects of Space Radiation on Semiconductor Devices," by J. P. Mitchell and D. K. Wilson, Bell Systems Technical Journal, Vol. 46, January 1967, p. 1.

4. Green, D., Sandor, J. E., O'Keeffe, T. W., and Matta, R. K., "Reversible Changes in Transistor Characteristics Caused by Scanning Electron Microscope Examination," Applied Physics Letters, Vol. 6, January 1, 1965, p. 3.

5. Brucker, G. J., Dennehy, W. J., Holmes-Siedle, A. G., "Electron Induced Surface Damage in Silicon Transistors," Proceedings IEEE (correspondence), Vol. 53, November 1965, p. 1800.

6. Brucker, G. J., Dennehy, W. J., Holmes-Siedle, A. G., "High Energy Radiation Damage in Silicon," IEEE Transactions on Nuclear Science, Vol. NS-12, October 1965, p. 69.

7. Szedon, J. R. and Sandor J. E., "The Effect of Low Energy Electron Irradiation of Metal-Oxide-Semiconductor Structures," Applied Physics Letters, Vol. 6, May 1965, p. 181.

8. Speth, A. J. and Fang, F. F., "Effects of Low Energy Electron Irradiation on Si-Insulated Gate FETs," Applied Physics Letters, Vol. 7, September 1965, p. 145.

9. Messenger, G. C., Steele, E. J. and Neustadt, M., "Displacement Damage in MOS Transistors," IEEE Transactions on Nuclear Science, Vol. NS-12, October 1965, p. 78.

10. Kooi, E., "Effects of Ionizing Irradiations on the Properties of Oxide-Covered Silicon Surfaces," Philips Research Reports (Netherlands), Vol. 20, Oct. 1965, p. 595.

11. Hughes, H., "Gamma Radiation Effects on Some MOS Transistors," presented at the IEEE Conference of Nuclear and Space Radiation Effects," Ann Arbor, Michigan, July 1965.

12. Zaininger, K. H., "Electron Bombardment of MOS Capacitors," Applied Physics Letters, Vol. 8, March 1966, p. 140.

13. Zaininger, K. H., "Irradiation of MIS Capacitors with High Energy Electrons," IEEE Transactions on Nuclear Science, Vol. NS-13, December 1966, p. 237.

14. Dennehy, W., Brucker G. and Holmes-Siedle, A. G., "A Radiation-Induced Instability in Silicon MOS Transistors," IEEE Transactions on Nuclear Science, Vol. NS-13, December 1966, p. 273.

15. Aubuchon, K. G., "Radiation Hardening of P-MOS Devices by Optimization of the Thermal SiO_2 Gate Insulator," IEEE Transactions on Nuclear Science, Vol. NS-18, No. 6, December 1971, p. 117.

16. Derbenwick, G. F., and Gregory, B. L., "Process Optimization of Radiation-Hardened CMOS Integrated Circuits," IEEE Transactions on Nuclear Science, Vol. NS-22, No. 6, December 1975, p. 2151.

17. Gregory, B. L., "Process Controls for Radiation-Hardened Aluminum Gate Bulk Silicon CMOS," IEEE Transactions on Nuclear Science, Vol. NS-22, No. 6, December 1975, p. 2295.

18. Sivo, L. L., Hughes, H. L., and King, E. E., "Investigation of Radiation-Induced Surface States Utilizing Gated-Bipolar and MOS Structures," IEEE Transactions on Nuclear Science, Vol. NS-19, No. 6, December 1972, p. 313.

19. Kjar, R. A. and Nichols, D. K., "Radiation-Induced Surface States in MOS Devices," IEEE Transactions on Nuclear Science, Vol. NS-22, No. 6, December 1975, p. 2193.

20. Terman, L. M., "An Investigation of Surface States at a Silicon/Silicon Dioxide Interface Employing Metal-Oxide-Semiconductor Diodes," Solid State Electronics, Vol. 5, 1962, p. 285.

21. Nichollian, E. H. and Goetzberger, A., "The Si-SiO_2 Interface-Electrical Properties as Determined by the MIS Conductance Technique," Bell Systems Technical Journal, Vol. 46, July-August 1967, p. 1055.

22. Gray, P. V. and Brown, D. M., "Density of SiO_2-Si Interface States," Applied Physics Letters, Vol. 8, 1966, p. 31.

23. Fang, F. F. and Fowler, A. B., "Transport Properties of Electrons in Inverted Silicon Surfaces," Physical Review, Vol. 169, No. 3, May 1968, p. 619.

24. Arnold E., "Surface Charges and Surface Potential in Silicon Surface Inversion Layers," IEEE Transactions on Electron Devices, Vol. ED-15, No. 12, December 1968, p. 1003.

25. Castagné, R., "Determination de la densité d'e'tats lents d'une capacité métal-isolant-semi-conducteur par l'etude de al charge sous une tension croissant linéairement," C. R. Acad. Sc. Paris, t167, Series B, October 1968, p. 866.

26. Kuhn, M., "A Quasi-Static Technique for MOS C-V and Surface State Measurements," Solid State Electronics, Vol. 13, 1970, p. 873.

27. Sakakih, Hoh K., and Sugano, T., "Determination of Interface State Density and Mobility Ratio in Silicon Surface Inversion Layers," IEEE Transactions on Electron Devices, Vol. ED-17, No. 10, October 1970, p. 892.

28. Many, A., Goldstein, Y., Grover, N. B., Semiconductor Surfaces, American Elsevier Publishing Co., New York, 1971.

29. Seiwatz, R. and Green, M., "Space Charge Calculations for Semiconductors," Journal of Applied Physics, Vol. 29, No. 7, 1958, p. 1034.

30. Lehovec, K., Slobodsky, A., "Impedance of Semiconductor-Insulator-Metal Capacitors," Solid State Electronics, Vol. 7, 1964, p. 59.

31. Ghandi, S. K., The Theory and Practice of Microelectronics, John Wiley and Sons, Inc., New York, 1968.

32. Berglund, C. N., "Surface States at Steam-Grown Silicon-Silicon Dioxide Interfaces," IEEE Transactions on Electron Devices, Vol. ED-13, No. 10, October 1966, p. 701.

33. Putley, E. H., The Hall Effect and Semiconductor Physics, Dover Publications, New York, 1960.

34. Beer, A. C., "Galvanametric Effects in Semiconductors," Solid State Physics, Supplement 4, Academic Press, New York, 1963.

35. van der Pauw, L. J., "A Method of Measuring Specific Resistivity and Hall Effect of Discs of Arbitrary Shape," Philips Research Reports, Vol. 13, No. 1, February 1958, p. 1.

36. Johansson, N. G. E., Mayer, J. W., Marsh, O. J., "Technique Used in Hall Effect Analysis of Ion Implanted Si and Ge," Solid State Electronics, Pergamon Press, Vol. 13, pp. 317-335.

37. Fowler, A. B., Fang, F., Hochberg, F., "Hall Measurements on Silicon Field Effect Transistor Structures," IBM Journal, September 1964.

38. Colclaser, R. A., Southward, H. D., "The Silicon Micro-Hall Device--Design, Fabrication and Applications," Bureau of Engineering Research, The University of New Mexico, Technical Report EE-173(70)ONR-005, 1970.

39. Cusack, N., The Electrical and Magnetic Properties of Solids, Longmans, London, 1958.

40. Seiwatz, R., Green, M., "Space Charge Calculations for Semiconductors," Journal of Applied Physics, Vol. 29, No. 7, July 1958, p. 1034.

41. Landsberg, P. T., "A Note on the Theory of Semiconductors," Proceedings, Physical Society (London), Vol. A65, 1952, p. 604.

42. Wolf, H., Semiconductors, John Wiley & Sons, 1971.

43. Fowler A. B., Fang, F., Hochberg, F., "Hall Measurements on Silicon Field Effect Transistors," IBM Journal, September 1964, p. 427.

44. Aubuchon, K., "Radiation Hardening of P-MOS Devices by Optimization of the Thermal SiO_2 Gate Insulator," IEEE Transactions on Nuclear Science, NS-18, 1971, p. 117.

45. Dubenweick, G., Sandia Laboratories, Private Communication, July 1976, Summary of system to be published.

46. Gwyn, C. W., "Model for Radiation-Induced Charge Trapping and Annealing in the Oxide Layer of MOS Devices," Journal of Applied Physics, Vol. 40, No. 12, November 1969, p. 4886.

47. Holmes- Siedle, A. G., and Zaininger, K. H., "The Physics of Failure of MIS Devices Under Radiation," IEEE Transactions on Reliability, Vol. R-17, No. 1, March 1968, p. 34.

48. Hughes, H. L., Baxter, R. D., Phillips, B., "Dependence of MOS Device Radiation-Sensitivity on Oxide Impurities," IEEE Transactions on Nuclear Science, Vol. NS-19, No. 6, December 1972, p. 256.

49. Maier, R. J., "Silica Lattice Constraints on the Structure of Interface States," Proceedings, IEEE Nuclear and Space Radiation Effects Conference, July 1976.

50. Kassabov, J., Velchev, N., Gancheva, V., "On the Effect of Gate Oxide Thickness Upon the Hall Mobility and Other Magneto-Electrical Characteristics in MOST Structures," Solid State Electronics, Vol. 17, 1974, pp. 41-45.

51. Colman, D., Bate, R. T., Mize, J. P., "Mobility Anisotropy and Piezoresistance in Silicon p-Type Inversion Layers," Journal of Applied Physics, Vol. 39, No. 4, March 1968, p. 1923.

52. Stern F. and Howard, W. E., "Properties of Semiconductor Inversion Layers in the Electric Quantum Limit," Physical Review, Vol. 163, No. 3, November 1967, p. 816.

53. Neumark, G. F., "Theory of the Influence of Hot Electron Effects on Insulated Gate Field Effect Transistors," Solid State Electronics, Vol. 10, March 1967, pp. 169-175.

54. Das, M. B., "Physical Limitations of MOS Structures," Solid State Electronics, Vol. 12, May 1969, p. 305.

55. Cobbald, R. S., Theory and Applications of Field Effect Transistors, Wiley-Interscience, New York, 1970.

56. Forsythe, G. E., Malcolm, M. A. Maler, C. B., "Computer Methods for Mathematical Computations," Prentice Hall, in press.

57. Pruess, S., "Properties of Splines in Tension," Technical Report No. 296, Dept. of Mathematics and Statistics, The University of New Mexico, Albuquerque, New Mexico, August 1974.

APPENDIX A

DEVICE FABRICATION

1. INTRODUCTION

The first devices used in this study were fabricated at the University of New Mexico. As the study progressed, other devices were supplied by Sandia Laboratories, and these devices were also studied. The majority of the work done here was performed on Sandia made devices.

The particular fabrication steps used at UNM were modeled after the processing steps used at Sandia. The only significant differences in the processing steps occur in the initial wafer cleaning process. The Sandia initial wafer cleaning process does not include a chromic acid step. The rest of the cleaning process described here is the actual process recommended by Sandia.

In the following sections, various steps in the processing are described in some detail. Although these steps are listed in rather extensive detail, it should be noted that they are not exact steps which were duplicated every time. The cleaning steps were all kept constant; but different dopants have been used, as well as different oxide growth temperatures and times.

In fabricating MOS transistors, several general steps must be performed. At each step, the device must be cleaned frequently. The initial cleaning differs somewhat from the other cleaning steps. In the remainder of this appendix, the following steps are described in detail:

(1) initial clean

(2) basic clean

(3) photo process

(4) oxide growths

(5) source and drain diffusion

(6) metal deposition

(7) metal removal

2. THE INITIAL CLEANING

The preliminary cleaning of the wafer differs in some extent from the basic cleaning step used in the remainder of the processing. The initial clean involves several steps where the purpose is to entirely remove any organics on the surface left from wafer fabrication. This can be done by using a soap solution, strong oxidizing agents, and heat. The following set of steps has been used to perform the initial clean. Note that all the reagents, when called for, are to be used undiluted directly from electronic grade bottles. Also notice that any numbers in parenthesis indicates ratios by volume.

When a wafer is cycled through the transistor washer, it should be done in 2 minutes per bath until the last bath. The wafer should remain in the last bath until the resistivity of the water returns to its maximum value. This can be facilitated by spray washing the wafer in deionized (D.I.) water for about 10 seconds before it is placed in the washer. This initial spray removes much of the liquid adhering to the wafer surface and thus prevents gross contamination of the water in the transistor washer. Therefore, anytime "cycle through the transistor washer" is referred to, it implies an initial spray rinse, as well as 2 minutes per bath until the last bath. The wafer remains in the

last bath until the resistivity returns to 18 Meg-Ω.

It should also be noted that two hydrofluoric acid (HF) dips are used here. The deglassification step involves buffered HF which does not etch silicon, but does etch SiO_2. The other solution is 10% HF, which is 10% by volume HF plus 90% by volume water when the HF comes straight from the electronic grade bottle. This particular solution slowly etches silicon as well as SiO_2. Often 10% HF is used to etch or clean any quartzware and is followed by an extensive D.I. water rinse.

The chromic acid used in these steps is made by making a dilute mixture of CrO_3 and water. The following steps are the ones used in the initial clean.

Initial Clean

1) NH_4OH (1), H_2O (4) → H_2O_2 (1) at 80°C for 10 minutes.
2) Cycle through transistor washer.
3) Place in chromic acid at 80°C for 10 minutes.
4) Cycle through transistor washer.
5) Place in HNO_3 at 80°C for 10 minutes.
6) Cycle through transistor washer.
7) H_2SO_4 (1) → H_2O_2 (1) for 10 minutes. This mixture is exothermic, and care must be exercised in its use.
8) Cycle through transistor washer.
9) H_2SO_4(1) → H_2O_2 (1) for 10 minutes. This should be a fresh solution every time.
10) Cycle through transistor washer.
11) Etch in 10% HF to remove all oxide.
12) Cycle through transistor washer.
13) Store wafer in D.I. water.

This series of steps is designed to remove any organics on the face left by the wafer manufacturing, and to give a standard startin point. Notice that steps 7 and 9 use exceptionally strong oxidizing agents which actually oxidize the silicon surface. This oxide is re moved in Step 11.

3. BASIC CLEAN

The basic cleaning procedure is simpler than the initial clean. It is assumed that by this time the major impurities due to manufact ing have been eliminated. This clean relies on the strong oxidizing properties of H_2SO_4 mixed with H_2O_2 to oxidize and organics on the s face coming from the photo resist steps, and the dissolving power of H_2SO_4 to dissolve nonorganics obtained from the dopant step.

Basic Clean

1) Place in HNO_3 at 80°C, 10 minutes.
2) Cycle through the transistor washer.
3) H_2SO_4 (l) → H_2O_2 (l), 10 minutes.
4) Cycle through transistor washer.
5) H_2SO_4 (l) → H_2O_2 (l), 10 minutes.
6) Cycle through transistor washer.
   Note: This clean stops here when it precedes a photo process.
7) Dip in 10% HF and etch off oxide formed in steps (3) and (5). This takes about 8 seconds.
   Note: This step is done prior to any oxide growth to assure that the oxide is growing on bare silicon.
8) Cycle through transistor washer.
9) Store in D.I. water.

4. PHOTO PROCESSING

The basic photo processing done at UNM and Sandia is different. Sandia uses an entirely automated coater, mask aligner, exposer and developer. The system at UNM is all manual. The basic processing steps used at UNM are as follows:

1) Clean the wafer with a basic clean.

2) Spin and blow dry wafers on the spinner for 30 seconds at 3500 RPM.

3) Dry wafers in an oven at 230°C for 2½ minutes.

4) Apply photo resist using a glass syringe.

5) Spin the wafer at 3500 RPM for 30 seconds.

6) Prebake the wafer at 230°C for 1 minute.

7) Align the mask and expose for 10 seconds.

8) Develop the wafer for 15 seconds and rinse for 10 seconds.

9) Blow dry with N_2.

10) Check pattern for completeness of development. Redevelop if necessary.

11) Place the wafer on a quartz boat, and post-bake for 10 minutes at 200°C.

12) Remove and cool.

13) Apply wax to back side of wafer.

Note: This step is only used for the source/drain opening cut. At this step, removal of this oxide could allow the source/drain dopant to form a p-n junction on the back side of the wafer.

14) Etch openings in buffered HF. This takes about 200 seconds for the field oxide.

15) Dip into trichlorethylene to remove wax.

Note: Only necessary if (13) was performed.

16) Place in J-100 at 95°C for 10 minutes to remove photo resist.

17) Rinse in two methanol baths.

18) Perform basic cleaning.

The photo resist used at UNM was a Transene product, PKP Type III. Similarly, the developer and rinse were Kodak Thin Film Developer and Kodak Thin Film Rinse. The black wax was a trichloroethylene soluble Apiezon wax.

5. OXIDE GROWTHS

Four distinctly separate oxides are grown during the fabrication of an MOS wafer. Two oxides, the etch-back oxide and field oxide are grown under identical conditions. The other two oxides, the gate oxide and oxide formed during drive in, are done at the same temperatures but different atmospheres.

The etch-back and field oxides are grown in a two step process. The first step is done dry, and the second is wet. All the steam used for wet oxides in this process were produced by mixing ultra high purity oxygen and hydrogen in the proper ratios in the furnace tubes. They spontaneously ignite at growth temperatures to form steam.

The dry oxides are grown in an atmosphere of ultra high purity oxygen mixed with a carrier gas, ultra high purity nitrogen.

A summary of the various oxide growths follows:

a. Etch Back and Field Oxide Growths

1) Perform basic clean.
2) Cycle through transistor washer.
3) Spin dry at 3500 RPM for 30 seconds, blow with N_2.
4) Place wafers on boats. Grow a dry oxide for 15 minutes at 1100°C.
5) Switch to a steam growth, and grow a pure wet oxide for 1 hour at 1100°C.
6) Pull quartz boat to end of tube and cool.
7) Store in D.I. water.

In this furnace operation, as in all furnace operations, the boat and pull rod should be cleaned in 10% HF and rinsed in D.I. water prior to placing them in the furnace.

The above steps should yield oxides about 7500Å thick.

b. Gate Oxide Growth

1) Perform basic clean.

2) Spin at 3500 RPM for 30 seconds and blow dry with N_2.

3) Place wafer on quartz boat and insert into oven.

4) Oxidize in a dry atmosphere at 1000°C for 2 hours to get a 750Å gate oxide or 5 hours for a 1200Å gate oxide.

5) Pull quartz boat to the end of tube and reduce tube temperature to 850°C.

6) After temperature has stabilized, reinsert the wafer and anneal it in an N_2 atmosphere for 90 minutes.

7) Cool, remove, store in D.I. water.

c. Dopant Drive-In/Oxide Growth

After a predeposit has been placed on a wafer, it has to be driven in. At this time an oxide is simultaneously grown in steam according to the following steps:

1) Perform basic clean.

2) Place wafers on a quartz boat and insert into the tube.

3) Grow wet oxide for 5 minutes at 1000°C.

4) Cool and remove wafers.

5) Store in D.I. water.

6. SOURCE AND DRAIN DIFFUSIONS

Although both n and p channel devices have been tested in this study, the p channel wafers were all supplied by Sandia Laboratories.

At UNM, so far the majority of wafers made has been n channel. The method for depositing n channel sources and drains is listed below. Two separate dopants have been used for the n-channel diffusion; one was Accuspin P-120, and the other was Emulsitone N-250.

a. N-Type Diffusion Using Accuspin P-120

1) Perform basic clean.

2) Dry wafer at 232°C for 2½ minutes.

3) Apply P-120 using a presterilized plastic syringe.

4) Spin at 3000 RPM for 10 seconds.

5) Bake for 10 minutes at 200°C.

6) Place on quartz boat and insert into furnace.

7) Drive the predeposit onto the surface for 15 minutes at 1000°C under N_2.

8) Pull to end of tube and cool for 2 to 3 minutes.

9) Strip Accuspin P-120 doped oxide in buffered HF. This should take about 30 to 90 seconds, but is readily apparent when the water "breaks" on the wafer surface.

10) Perform a basic clean.

11) Grow a drive in oxide.

12) Cool and remove.

13) Store in D.I. water.

b. N-Type Diffusion Using Emulsitone N-250

1) Perform basic clean.

2) Dry at 232°C for 2½ minutes.

3) Clean the syringe filter in isopropyl alcohol ultrasonically.

4) Dry filter with N_2.

5) Using a presterilized syringe and the filter, apply N-250 to the wafer surface.

6) Spin at 3000 RPM for 10 seconds.

7) Dry at 200°C for 15 minutes.

8) Place on a quartz boat and drive in for 15 minutes at 1000°C under an N_2 atmosphere.

9) Pull to end of tube and cool.

10) Strip the N-250 doped oxide in buffered HF

11) Perform a basic clean.

12) Grow a dopant drive in oxide.

13) Cool, remove.

14) Store in D.I. water.

7. METAL DEPOSITION

Once the various oxides and diffusions are performed, the metal used in making the gate and source drain contacts must be applied. In addition, if the facilities are available chrome can be deposited on the back of the wafer to improve gold adhesion and retard gold diffusion, then a layer of gold applied on top of this. These metals make die bonding easier and insure high reliability of the substrate connection when the wafer is probed. Since chrome oxidizes so rapidly at normal atmospheric conditions, the gold and chrome must both be applied in one vacuum pump down.

At UNM, facilities for chrome/gold deposition are not available. Thus, only the aluminum deposition is described here.

The method chosen for depositing the aluminum is vacuum evaporation. Experience has shown that both electron beam evaporation and sputtering seem to increase the amount of charge trapped in the gate oxide. The filaments used here are tungsten helical filaments with low sodium content supplied by Materials Research Corporation. The aluminum is actually "alusil," or a 97% aluminum--3% silicon alloy also available from Materials Research Corporation.

It has been determined that a brand new filament has surface impurities on it that degrade MOS properties. These impurities can be greatly reduced if the filament is used for at least two dummy evaporations before it is actually used in making a device. This procedure has been adopted at UNM.

Metal Deposition

1) Vent the vacuum system.
2) Install a new filament.
3) Evacuate the system to 5×10^{-6} torr or less.
4) Raise the filament temperature much higher than evaporation temperatures and leave it there for 5 minutes.
5) Cool the filament for 15 minutes.
6) Vent the vacuum system with N_2.
7) Install 5 "hooks" of aluminum.
8) Reevacuate the vacuum system to 5×10^{-6} torr or less.
9) Evaporate this aluminum.
10) Let filament cool for 15 minutes.
11) Revent the vacuum system with N_2.
12) Install 5 more aluminum hooks and the prepared wafers.
13) Reevacuate the vacuum system to less than 5×10^{-6} torr.
14) Evaporate aluminum onto the wafers.
15) Let the system cool for 45 minutes.
16) Revent the system with N_2.
17) Remove the wafers, store in a dry carrier.
18) Reevacuate the vacuum system.

8. SELECTIVE METAL REMOVAL

Once the aluminum has been deposited, the excess metal must be etched off. The following steps are performed in the metal removal.

1) Cycle wafer through a cold transistor washer at 2 minutes per bath.

2) Spin at 3500 RPM for 30 seconds and blow dry.

3) Heat at 200°C for 10 minutes.

4) Using a glass syringe, apply photo resist.

5) Spin at 3500 RPM for 30 seconds.

6) Dry for 1 minute at 232°C.

7) Align mask and expose for 10 seconds.

8) Develop for 15 seconds and rinse for 10 seconds.

9) Check development under a microscope.

10) Dry at 200°C for 15 minutes.

11) Mix the aluminum etch: 80 ml phosphoric acid
18 ml D.I. water
4 ml nitric acid

12) Heat mixture to 80°C.

13) Etch metal.

Note: This takes about 8 seconds for our aluminum process.

14) Dip in 10% HF for 10 seconds to remove any aluminum diffused into the surface of the field oxide.

15) Rinse in D.I. water.

16) Put in J-100 at 95% for 10 minutes.

17) Rinse twice in methanol.

18) Spray in transistor shower.

19) Blow dry with N_2.

9. SUMMARY OF STEPS USED IN FABRICATING THE MOS WAFERS

Now that all of the individual steps have been described, it is appropriate to list the steps performed in fabricating a wafer from beginning to end.

1) Perform initial clean.

2) Grow etch back oxide to about 7000Å.

3) Etch off etch back oxide entirely in 10% HF.

4) Perform basic clean.

5) Grow a field oxide.

6) Open source/drain openings with the first photo processing step.

7) Perform basic clean.

8) Perform source/drain diffusion (which includes pre-deposit and drive in).

9) Perform basic clean.

10) Open gate oxide areas, source/drain contact openings, and scribe streets with the second photo processing step.
NOTE: Insure that the oxide on the reverse side of the wafer is entirely removed at this step.

11) Perform basic clean.

12) Grow gate oxide.

13) Open contact holes and scribe streets using the third photo processing step.

14) Perform basic clean.

15) Deposit aluminum.

16) Etch away excess metal using the fourth photo processing step.

17) Probe the wafer if one desires to do such.

Following the above listed procedures a complete wafer of MOS devices can be fabricated. At step 17 the wafer is ready for scribing apart and packaging.

10. SUMMARY OF GAS FLOW SETTINGS FOR OXIDE GROWTHS

The oxides grown at UNM are all grown in a tube that is supplied by a Tylan Corporation gas handling system. This system is hard plumbed with stainless steel tubing from the tanks to the system, then from the system to the tube. The gas handling system controls the following gases, O_2, H_2, N_2, and HCl. The N_2 and HCl flow rates are monitored by rotameters. The O_2 and H_2 flow rates are controlled by mass flow controllers. The system is a model GP-181-2 controller.

Figure (A-1) is a block diagram of the gas handling system. The gases can all be turned on and off using electric solenoid valves controllable from the front panel of this rack mount unit.

The nitrogen and hydrogen chloride are controlled in the normal fashion using rotameters.

The hydrogen and oxygen are controlled in quite a different fashion. In Figure A-1, the units designated FC 200 are active in measuring and controlling the H_2 and O_2 gases. The actual flow rate is determined by the measurement of heat transfer along a capillary tube. Since this transfer rate is really proportional to the specific heat of a gas and its mass flow rate, these controllers actually measure mass flow rate. The mass flow rate is converted to a volume flow rate, and displayed on a 5 in. wide faced meter calibrated in standard cubic centimeters per minute (SCCM).

Another unique feature of this system is that a small valve is in each controller that can vary the flow rate of the gas through the controller. This valve controls flow rate by a thermal expansion design. The actuator of the valve is a small thin walled tube with a ball welded on the end. The seat is a cone. Inside the tube is a

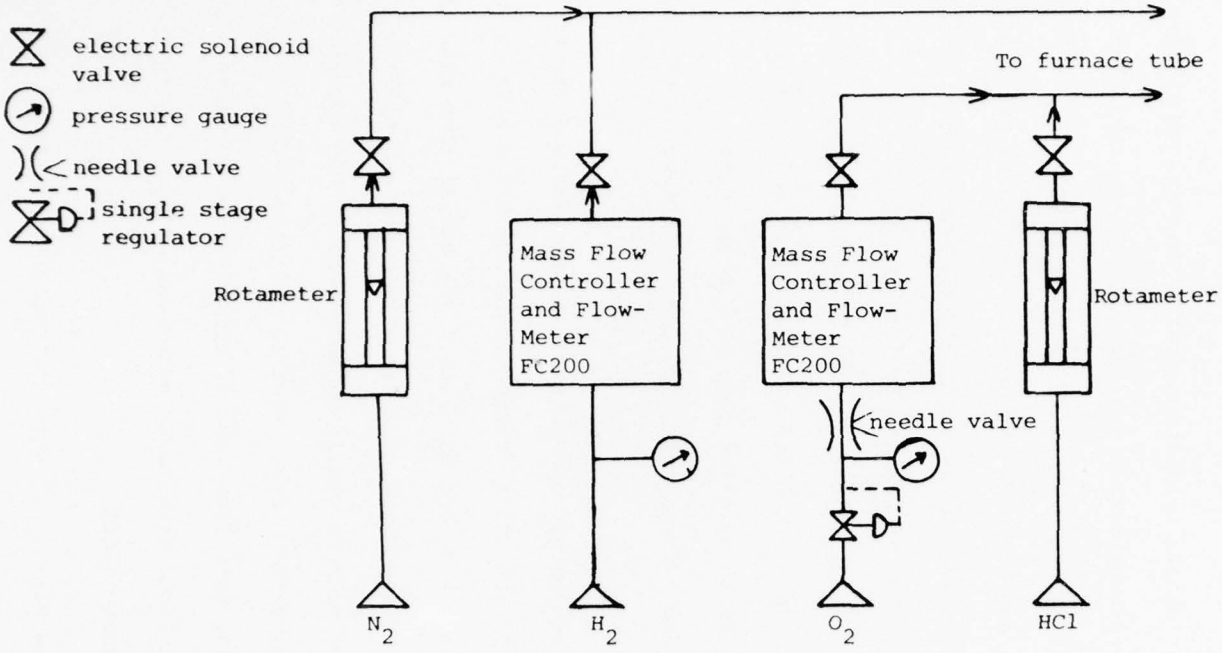

Figure A-1. The Tylan gas handling system.

heater wire that causes the tube to expand relative to the outer shell, thus modulating the flow.

In practice, the flow of oxygen is the one normally adjusted. There is a needle valve in series with the oxygen flow meter/flow controller. This needle valve can be used to adjust the oxygen flow from zero to 5 standard liters per minute. The flow rate is detected by the FC 200 unit and displayed on the front panel.

Also on the front panel is a potentiometer with a 0 to 1000 accumulator on it. This adjusts the ratio of H_2 to O_2. At a setting of 000, no H_2 flows. At settings of 500 and 1000 the molar ratios of H_2 to O_2 are 1:1 and 2:1 respectively. Thus, at 1000, if the output gas mixture is burned, pure water should be formed.

The oxygen mass flow is monitored by means of the oxygen FC 200 unit. This flow is electrically compared to the desired ratio of H_2 to O_2 set by the potentiometer on the front panel, and the hydrogen flow is controlled through the hydrogen FC 200 controller to the desired ratio. If the oxygen flow rate is adjusted by means of the needle valve, the hydrogen flow rate automatically follows it in the proper ratio desired.

Using this system, dry oxides, wet oxides, wet/dry oxides, and oxides grown with the inclusion of HCl are possible. All of the etch-back oxides, field oxides, gate oxides, and diffusion drive in oxides were grown using this system.

Potentially this system could be dangerous because of possible free hydrogen buildup. Certain safeguards are built into the system. The unit has its own thermocouple input from the furnace tube. If the tube ever goes below 590°C, the flash point of the H_2/O_2 mixture, the

hydrogen gas is automatically shut off and cannot be manually restarted unless the malfunction is fixed. Similarly, if an oxygen tank runs out of gas due to inattentiveness, the hydrogen again shuts off. When the hydrogen is shut off by either of these two mechanisms, the nitrogen is automatically turned on to whatever value is set on the N_2 rotameter.

The following gas settings were used for the oxide growths.

Etch Back and Field Oxides: (1100°C)

a) Dry: O_2 : 1500 SCCM
N_2 : 1000 SCCM

b) Wet: H_2 : 3000 SCCM
O_2 : 1500 SCCM

Gate Oxide: (1000°C)

a) Dry: O_2 : 1500 SCCM

b) Anneal: N_2 : 1000 SCCM

Diffusion Drive In Oxide: (1000°C)

a) Wet: H_2 : 3000 SCCM
O_2 : 1500 SCCM

11. SUMMARY

In this appendix we have presented the various processing steps used at the University of New Mexico to fabricate MOS devices. Some of the devices tested here were made with the UNM facilities. Others were supplied by Sandia Laboratories. The particular processing steps used at UNM were modeled after those at Sandia Laboratories.

Although certain differences exist between the processes at the two places, it should be noted that the most critical processing parameters have been kept identical. In References 16 and 44 some

basic steps in processing have been identified that have a definite effect on device hardness. These steps are listed below, and are considered the most important steps necessary in obtaining reasonably hard gate oxides assuming no gross contamination exists anywhere in the growth facilities.

(1) Always grow and strip an etch-back oxide of at least 6400Å.

(2) Be sure the basic clean involves the double H_2SO_4/H_2O_2 steps. Never use an $NH_4OH/H_2O_2/H_2O$ clean or $HCl/H_2O_2/H_2O$ clean after the sulphuric steps.

(3) Rinse until the water reaches 18 Meg-Ω.

(4) Avoid overnight storage, if possible.

(5) Prior to oxidation, clean the furnace tubes for two hours. The cleaning gases should be set at 60 CC/min. HCl, 500 CC/min. O_2, and 2000 CC/min. N_2.

(6) Anneal the oxide at 850°C in N_2 for 90 min.

(7) Sinter the aluminum at 450°C in N_2 for 20 min.

These steps seem to be the most critical in growing hardened MOS devices.

AD-A064 143 NEW MEXICO UNIV ALBUQUERQUE BUREAU OF ENGINEERING R--ETC F/G 9/1
INVESTIGATION OF INTERFACE STATES USING METAL-OXIDE-SILICON TRA--ETC(U)
AUG 78 J WHITEFIELD, H D SOUTHWARD F29601-75-C-0036
UNCLASSIFIED EE-247(77)AF-352-1 AFWL-TR-77-140-VOL-1 NL

3 OF 4
AD A064143

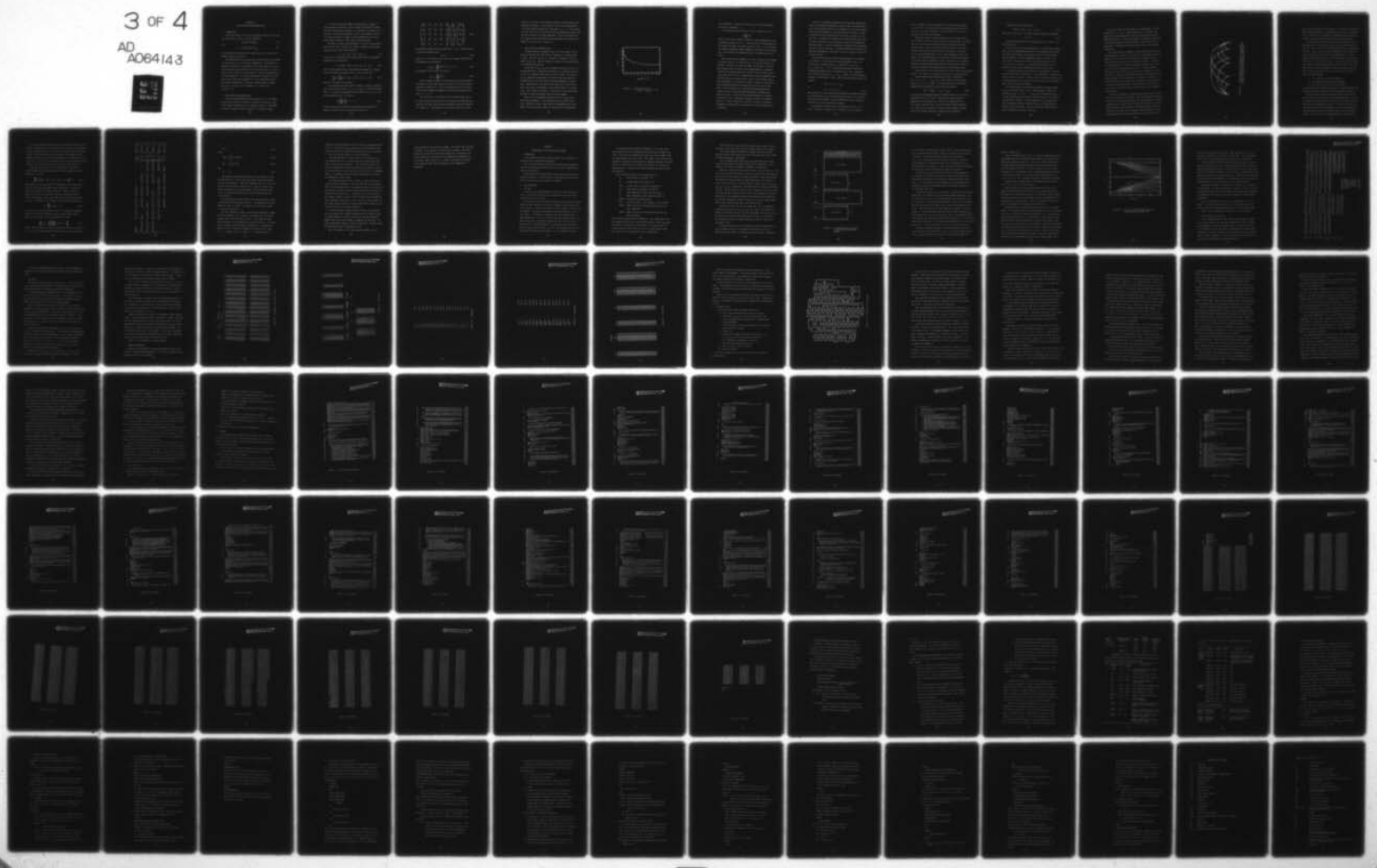

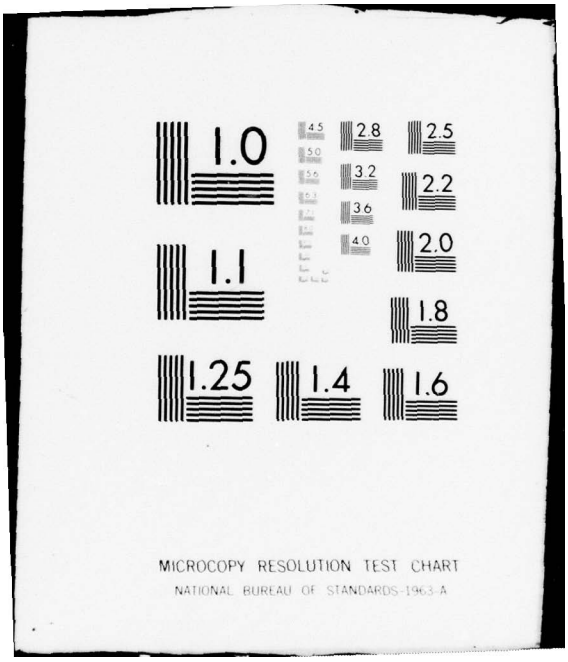
1.0
1.1
1.25
1.4
1.6
1.8
2.0
2.2
2.5
2.8
3.2
3.6
4.0
4.5
5.0
5.6
MICROCOPY RESOLUTION TEST CHART
NATIONAL BUREAU OF STANDARDS-1963-A

APPENDIX B

CURVE FITTING THE EXPERIMENTAL DATA

1. INTRODUCTION

Recall from Chapter III that the experimental data are used to supply two functions, α and β. They are defined by

$$\alpha \equiv \left(C_{ox}/q\right)\left(\partial V_g/\partial N_H\right)\Big|_T \tag{77}$$

and

$$\beta \equiv \left(C_{ox}/q\right)\left(\partial V_g/\partial T\right)\Big|_{N_H} \tag{92}$$

In this appendix the methods used to derive both α and β from the experimental data are developed.

The experimental data from which these two functions are calculated are plots of N_H vs V_g at two distinct temperatures. The quantity α is determined by forcing a curve through a set of data points at one temperature and taking the derivative of the analytical curve. To find β, first a curve is fitted to the data points at the upper temperature and the lower temperature. This allows calculation of $V_g(N_H)$ for an arbitrary value of N_H at both temperatures. The necessary derivative is then found by differencing. Because the function needed is $V_g(N_H)$, when $y(x)$ is used later in this appendix, x is assumed to be N_H, and y is V_g.

2. CURVE FITTING TO DETERMINE $\beta(N_H)$

The most straightforward quantity to determine is β. The experimental data are given in the form of a sequence of points $\left\{V_{g_i}, N_{H_i}\right\}$ at two separate temperatures, as is graphed in Figure 13. The graphs are shown as $N_H(V_g)$, but the real quantity of interest is $V_g(N_H)$.

It can be seen from the graph that either $N_H(V_g)$ or $V_g(N_H)$ is almost linear for good data. There is always some curvature in these plots near device turn on, however, so to determine an accurate fit to the data, a fourth order polynomial is used. When leakage in the device causes bad values to appear in the N_H determinations, the polynomial order is reduced to first order to smooth the data.

The fifth (or first) order polynomial is fit in the least squares sense for this work. Consider for a moment a sequence of data points $\{x_i, y_i\}$, and the fourth order polynomial

$$y = \lambda_1 x^4 + \lambda_2 x^3 + \lambda_3 x^2 + \lambda_4 x + \lambda_5 \tag{B-1}$$

Let the error in determining the y_i^{th} data point using the polynomial evaluated at x_i be defined as

$$E_i = \left(\lambda_1 x_i^4 + \lambda_2 x_i^3 + \lambda_3 x_i^2 + \lambda_4 x_i + \lambda_5 - y_i\right) \tag{B-2}$$

Then the total squared error in determining the sequence of y_i points using the polynomial evaluated at the x_i values is given by

$$\sum_{i=1}^{M} E_i^2 = \sum_{i=1}^{M} \left(\lambda_1 x_i^4 + \lambda_2 x_i^3 + \lambda_3 x_i^2 + \lambda_2 x_i + \lambda_1 - y_i\right)^2 \tag{B-3}$$

where M is the number of data points.

This expression now can be used to determine a system of equations that can be solved to yield, λ_1, λ_2, λ_3, λ_4 and λ_5 in the least squares sense. To minimize the squared error with respect to λ_j, j = 1, 5, the following equation must be satisfied,

$$\frac{\partial}{\partial \lambda_j}\left(\sum_{i=1}^{M} E_i^2\right) = 0, \quad j = 1, \tag{B-4}$$

By taking these partial derivatives and putting the resultant five equations in matrix form, the system can be written as

$$\begin{pmatrix} \Sigma x_i^8 & \Sigma x_i^7 & \Sigma x_i^6 & \Sigma x_i^5 & \Sigma x_i^4 \\ \Sigma x_i^7 & \Sigma x_i^6 & \Sigma x_i^5 & \Sigma x_i^4 & \Sigma x_i^3 \\ \Sigma x_i^6 & \Sigma x_i^5 & \Sigma x_i^4 & \Sigma x_i^3 & \Sigma x_i^2 \\ \Sigma x_i^5 & \Sigma x_i^4 & \Sigma x_i^3 & \Sigma x_i^2 & \Sigma x_i \\ \Sigma x_i^4 & \Sigma x_i^3 & \Sigma x_i^2 & \Sigma x_i & M \end{pmatrix} \begin{pmatrix} \lambda_1 \\ \lambda_2 \\ \lambda_3 \\ \lambda_4 \\ \lambda_5 \end{pmatrix} = \begin{pmatrix} \Sigma x_i^4 \, y_i \\ \Sigma x_i^3 \, y_i \\ \Sigma x_i^2 \, y_i \\ \Sigma x_i \, y_i \\ \Sigma y_i \end{pmatrix} \tag{B-5}$$

All the sums in Equation B-5 are taken from i = 1, M. This can be put in the more convenient form of

$$AX = B \tag{B-6}$$

where A is a (5 x 5) matrix and X and B are 5 element column vectors. The elements of A are given by

$$\left(a_{i,k}\right) = \sum_{i=1}^{M} x_i^{10-j-k}, \; j, \; k = 1, \; 5 \tag{B-7}$$

The elements of the B vector are given by

$$\left(b_j\right) = \sum_{i=1}^{M} x_i^{5-j} \, y_i \tag{B-8}$$

Thus, by taking a sequence of M data points $\{x_i, y_i\}$ and forming the matrices A and B using Equation B-7 and B-8, the linear system is expressed by Equation B-6. This linear system can then be solved by one of several standard techniques to yield the least squares coefficient λ_j, j = 1, 5.

For the purpose of this project the two sequences $\{N_{H_i}, V_{g_i}\}$ at the lower and upper temperatures are calculated by data reduction program using the input current-voltage measurement described by Equation 113, Chapter IV. Then Equations B-7 and B-8 are used to set up the

linear (5 x 5) system. This system is solved to yield the fourth order polynomial coefficient. This procedure is done at both temperatures. In the data reduction program the coefficients λ_j, j = 1, 5 are referred to as RA1, RB1, RC1, RD1, and RE1 for the lower temperature and RA2, RB2, RC2, RD2, and RE2 for the upper temperature. Once the polynomial fits for $V_g(N_H)$ have been determined for both temperatures, then Equation 95, Chapter III, can be used to determine β.

3. CURVE FITTING TO DETERMINE $\alpha(N_H)$

The method chosen to determine $\alpha(N_H)$ is less well known, but not much more difficult than that chosen to determine β. Consider Figure 13 again. This plot is N_H vs V_g. Actually, to determine α the plot needed is V_g vs N_H. Then α is simply the slope of that plot multiplied by the appropriate constants.

Notice that the N_H vs V_g plot is slightly curved as the gate voltage approaches zero. Although this curvature is not readily visible to the eye, it is apparent when the curve fitting is done. The slope of N_H vs V_g decreases in magnitude as the gate voltage goes toward zero. At higher values of the gate voltage the slope approaches a constant value. Qualitatively, the inverse of the slope of this curve should start at one value, and decrease to some constant value as a function of N_H. This is shown in Figure B-1. The scales on this figure represent more an order of magnitude rather than exact numbers.

Section 2 of this appendix shows how one can fit $V_g(N_H)$ with a fourth order polynomial. If the technique were also used to find α, then α would have to have a shape that can be approximated by a polynomial. The curve shown in Figure B-1 cannot easily be approximated

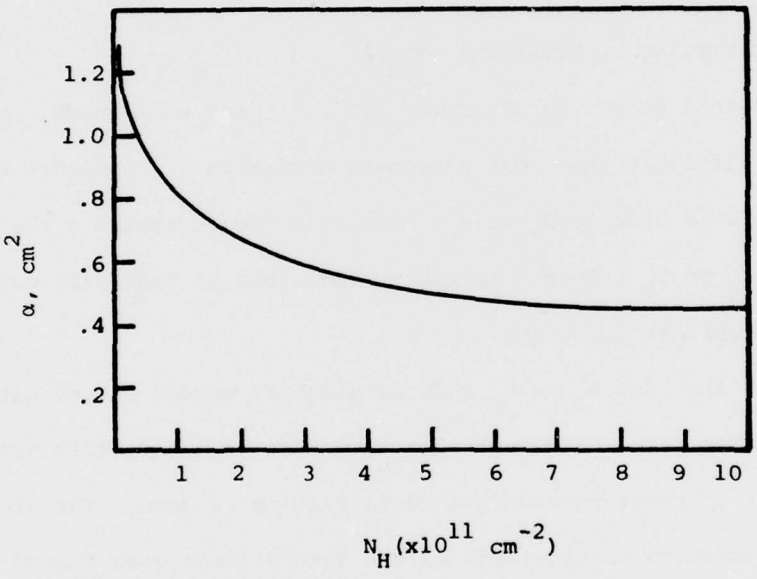

Figure B-1. A qualitative plot of $\alpha = (C_{ox}/q)\ (\partial V_g/\partial N_H)_T$ vs. N_H.

by a polynomial. It was for this reason that a different procedure was chosen to determine α.

One approach that was chosen was to use a series of the form

$$y = \sum_n a_n x^n$$

where n can be either negative or positive. This approximation allows an asymptotic behavior of y in x. The data used in this experiment had the largest error when x was small (N_H in this case). If n is negative, this expansion becomes extremely dependent on data taken near the origin. Thus, this technique was abandoned because of instabilities near the origin.

Another more fruitful approach is to look at Figure B-1 and examine its salient features. At large values of x (or N_H) the function α is constant. For values of x near the origin, the function α is curved. This curvature near the origin could be approximated by a quadratic. Therefore, one approach would be to curve fit y(x) by a power series, as was done with β, but use a different power series or polynomial over different parts of the range of data. Thus, x can be divided into as many subintervals as is necessary to obtain a good fit to the raw data. These polynomials should be continuous over the entire data range. This is often referred to as a piecewise polynomial approximation. Actually, one more constraint should be applied if piecewise polynomials are used. In curve fitting using polynomials, the function one obtains is y(x). Physically, the graph in Figure B-1 represents dy/dx vs x. Thus, in addition to forcing continuity on a piecewise polynomial, one should also use continuity of the first derivative as a constraint.

Thus far, the physical properties of the data under consideration lead one to piecewise polynomials in order to obtain the needed curvature of the derivative function, and continuity of the first derivative since the first derivative is the real function of interest. A class of functions has been developed that can be used in exactly this case (Ref. 56). An example of a suitable set of functions that can be used is "spline" functions. The entire range of data can be divided into many subintervals. Over each subinterval a different spline polynomial is used to curve fit the data. The overall polynomial described by the individual polynomials is continuous, as well as through its first and second derivatives.

The method by which one obtains these polynomials can be summed up as follows. Let the range of the data be $[a,b]$, and let it be divided into n intervals by the n + 1 points $\{a = x_1 < x_2 < x_3 \ldots x_{n+1} = b\}$ (Ref. B-1). Let τ be the entire polynomial covering the range $[a,b]$ comprised of the n polynomials $\{\tau_i\}$. The τ_i polynomial fits the range of data for $x_i < x < x_{i+1}$. Further, let the differential operator D be defined by $D \equiv d/dx$. Then the needed splines satisfy the equation

$$D^4\tau_i = 0, \quad x_i < x < x_{i+1}$$

or

$$D^4\tau = 0, \quad a \leq x \leq b \tag{B-9}$$

When Equation B-9 is used along with any appropriate boundary conditions such as continuity of the first and second derivatives, a set of basis functions has been defined. For this differential operator equation, the basis set is often referred to as splines.

The particular functions that satisfy Equation B-9 are 1, x, x^2 and x^3. Therefore, this basis set is referred to as cubic splines.

Each τ_i is made up of linear combinations of the four basis functions 1, x, x^2 and x^3. The particular linear combination varies with each interval. The overall polynomial τ is still made up of a linear combination of the four basis functions.

While cubic splines could have been used for this study, another set of splines, which are a simple extension of cubic splines, was available on he University of New Mexico IBM 360 system, and this other set was chosen. Recall that the curve shown in Figure B-1 has curvature near the origin, but flattens out as x increases. It would be nice, as was mentioned before, to use a cubic polynomial fit near the origin, and a linear polynomial as x increased. Then the derivative of the curve fit would be quadratic at first, and constant as x increases. The cubic splines previously talked about are cubic over all ranges of the data, and cannot easily become linear in the right hand region.

Another basis set has been developed to fit this curve fitting problem exactly. This basis set of splines is referred to as tension splines.

Consider again a data range $[a,b]$ split into n subintervals $\{a = x_1 < x_2 < x_3 < \ldots < x_{n+1} = b\}$. Also, consider n tension parameters, $\{\rho_i\}$, i = 1, n. Again a $\tau(x)$ can be found that is continuous through its first derivative, and satisfies the equation

$$\left(D^4 - \rho_i^2 D^2\right)\tau_i = 0, \; x_i < x < x_{i+1} \qquad \text{(B-10)}$$

This particular differential equation resembles Equation B-8 except for the addition of the $\rho_i^2 D^2$ term. This particular term represents a damping factor on the basis set. Notice that in Equation B-10, if $\rho_i \to 0$ over an interval, then τ_i for that interval satisfies Equation B-8. Thus, for the tension set at zero over any interval, the basis set for that interval should be a piecewise cubic polynomial.

Equation B-10 can be rewritten as

$$\left(D^4/\rho_i^2 - D^2\right)\tau_i = 0, \; x_i < x < x_{i+1} \tag{B-11}$$

Thus, if the tension $\rho_i \to \infty$ over some interval, Equation B-11 becomes

$$D^2\tau_i = 0 \tag{B-12}$$

The basis functions that satisfy Equation B-12 are 1 and x, or a linear spline fit.

Now, each ρ_i can be chosen independent of ρ_i in any other interval. Thus, the total approximating function $\tau(x)$ can resemble cubic splines over part of the interval, linear splines over part of the interval, and any admixture of the two, depending on how ρ_i is chosen. The actual basis functions which result from solving Equation B-10 are 1, x, sinh $\rho_i x$, and cosh $\rho_i x$. In evaluating the splines over the various intervals, linear combinations of these terms are used.

A complete derivation and discussion of the properties of tension splines can be found in Reference 57. This information is completely beyond the scope of this work. However, some of the general properties and a general description are given here that are pertinent to the development of the data reduction program.

The tension splines, as has been said before, are used to curve fit V_g as a function of N_H, or y(x). The data range is split into subintervals $\{x_1 < x_2 < x_3 < \ldots < x_{n+1}\}$, and a different function τ_i is used to approximate the function over each interval. The points x_i are referred to as knots. In actual application x_1 is usually less than the smallest x-value of the data, and x_{n+1} is larger than the largest x-value of the data. The x_1 knot can have a multiplicity of four, or represent four knots, as can x_{n+1}.

The n+1 knots split the data range into n subintervals. In each subinterval $x_i < x < x_{i+1}$, a tension parameter ρ_i is defined. One property of the tension splines is that each interval must contain at least one data point. Linear combinations of the splines are used over the entire data range for the curve fitting. If one interval has no data points, a singularity arises when solving for the least squares coefficients.

Each tension spline is formed by a linear combination of the four basis functions 1, x, sinh $\rho_i x$, and cosh $\rho_i x$. An individual spline is nonzero over a total of only four consecutive intervals, and at an arbitrary point x only four tension splines are nonzero. Figure B-2 is a representation of a data range extending over $[x_1, x_{n+1}]$. Both x_1 and x_{n+1} have a knot multiplicity of four. So four individual splines, N_1 to N_4 originate at x_1, but each one terminates at a different knot. Similarly, four splines terminate at the last knot, but each originates at a different knot. The splines are labeled N_i. In Figure B-2 there are seven knots and nine splines. In general there are two more splines than knots. Also note that in each interval there are only four nonzero knots, and the knots are not necessarily evenly spaced.

Once the knot sequence is defined and the tension array is specified, the splines N_i are determined. They are determined by requiring each spline to be continuous through its second derivative, as well as requiring of all the splines over the entire data range to be continuous through the second derivative. This means that any linear combination of four knots over one interval, when evaluated at a knot, should be equal to the linear combination of the four knots in the

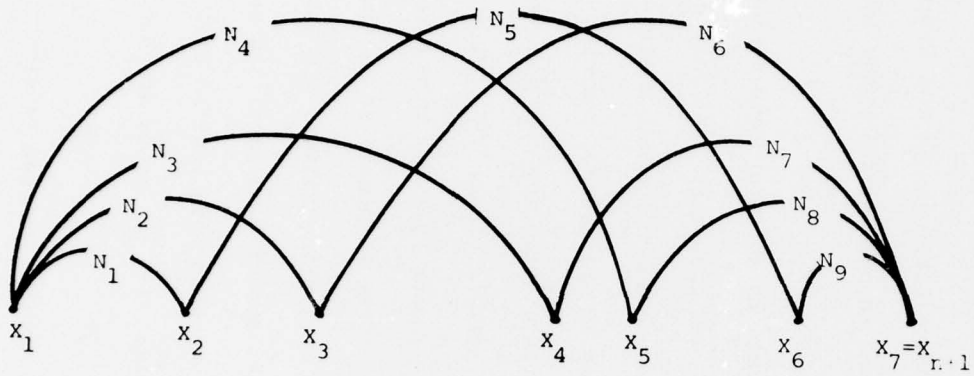

Figure B-2. A representation of a data range $[x_1, x_{n+1}]$ with 7 knots. There are nine splines. In general, there are two more splines than total numbers of knots.

next interval evaluated at that same knot. For instance, in Figure B-2, splines N_3 to N_6 evaluated at x_4 should equal splines N_4 to N_7 evaluated at x_4. This fact is a consequence of the property that the splines N_i as well as N_i'' go to zero at the knots defining their end points.

It may be instructive at this time to briefly summarize a few of these properties to get a better idea of how the tension splines are obtained. First of all, the curve fitting function must satisfy Equation B-10. Since τ_i must be a linear combination of the splines N_i over its range, each N_i must also satisfy Equation B-10. This is easily satisfied because the N_i's are linear combinations of the basis functions 1, x, $\sinh \rho_i x$, and $\cosh \rho_i x$. Also, each N_i must be continuous through its second derivative, and is nonzero over no more than four intervals. When a multiplicity occurs in the knots at the end points, the splines can be nonzero over less than four intervals. Thus, the three properties

(1) $(D^4 - \rho_j^2 D^2)N_i = 0$ over all intervals

(2) N_i and N_i'' continuous over the data range

(3) N_i nonzero over no more than four intervals

are the necessary and sufficient conditions to uniquely determine the N_i and N_i'' once a knot sequence and tension sequence are defined.

Once the splines have been determined, these serve as the new basis set which is used to curve fit the experimental data. A point of confusion that may arise here is that the four original functions found that satisfy Equation B-10 were 1, x, $\sinh \rho_i x$, and $\cosh \rho_i x$. The splines N_i are linear combinations of these four functions, and now form the basis set that is actually used in the curve fitting scheme. The τ_i are in turn linear combinations of the N_i splines.

In the data reduction program used here, the number of knots is fixed at four, so there are in all six splines, N_1 to N_6, which can be thought of as exactly analogous to 1, x, x^2, and x^3 in the fourth order curve fitting program. Once the splines have been determined, the appropriate least squares coefficients λ_1 to λ_6 must be determined to complete the curve fitting scheme. This is done in a fashion similar to the way Equation B-5 was obtained. The tension spline case has six coefficients instead of 5.

Recall that the first row in the linear system of Equation B-5 came from taking the partial derivative of the least squares error with respect to λ_1 to yield

$$\sum_{i=1}^{M} 2\left(\lambda_1 x_i^4 + \lambda_2 x_i^3 + \lambda_3 x_i^2 + \lambda_4 x_i + \lambda_5 - y_i\right)x_i^4 = 0 \qquad \text{(B-13)}$$

This equation is the basis function x^4 evaluated at the i^{th} data point times the E_i^{th} error, and summed over all data points. A similar result can be written for the spline functions. However, since the splines go to zero at the end knots, and only four splines are nonzero at a given point, some of the elements of the least squares matrix are zero. In general, the E_i^{th} tension spline error can be written as

$$E_i = \sum_{j=1}^{6} \lambda_j N_j(x_i) - y_i \qquad \text{(B-14)}$$

Only four of the terms are nonzero, however. For example, considering Figure B-2, if x_i lines between x_3 and x_4, the only nonzero splines are N_3, N_4, N_5, and N_6. The total squared error is then

$$\sum_{i=1}^{M} E_i^2 = \sum_{i=1}^{M} \left(\sum_{j=1}^{6} \lambda_j N_j(x_i) - y_i\right)^2 \qquad \text{(B-15)}$$

Again, taking the respective partial derivatives of B-15 with respect to λ_j, j = 1,6, the following equations result when placed in a matrix form.

$$
\begin{pmatrix}
\sum_i N_1^2(x_i) & \sum_i N_1(x_i)N_2(x_i) & \sum_i N_1(x_i)N_3(x_i) & \sum_i N_1(x_i)N_4(x_i) & 0 & 0 \\
\sum_i N_2(x_i)N_1(x_i) & \sum_i N_2^2(x_i) & \sum_i N_2(x_i)N_3(x_i) & \sum_i N_2(x_i)N_4(x_i) & \sum_i N_2(x_i)N_5(x_i) & 0 \\
\sum_i N_3(x_i)N_1(x_i) & \Sigma N_3(x_i)N_2(x_i) & \Sigma N_3^2(x_i) & \sum_i N_3(x_i)N_4(x_i) & \sum_i N_3(x_i)N_5(x_i) & \sum_i N_3(x_i)N_6(x_i) \\
\sum_i N_4(x_i)N_1(x_i) & \sum_i N_4(x_i)N_2(x_i) & \sum_i N_4(x\ )N_3(x_i)] & \sum_i N_4^2(x_i) & \sum_i N_4(x_i)N_5(x_i) & \sum_i N_4(x_i)N_6(x_i) \\
0 & \sum_i N_5(x_i)N_2(x_i) & \sum_i N_5(x_i)N_3(x_i) & \sum_i N_5(x_i)N_4(x_i) & \Sigma N_5^2(x_i) & \sum_i N_5(X_i)N_6(x_i) \\
0 & 0 & \sum_i N_6(x_i)N_3(x_i) & \sum_i N_6(x_i)N_4(x_i) & \sum_i N_6(x_i)N_5(x_i) & \sum_i N_6^2(x_i)
\end{pmatrix}
\begin{pmatrix} \lambda_1 \\ \lambda_2 \\ \lambda_3 \\ \lambda_4 \\ \lambda_5 \\ \lambda_6 \end{pmatrix}
=
\begin{pmatrix} \sum_i N_1(x_i)y_i \\ \sum_i N_2(x_i)y_i \\ \sum_i N_3(x_i)y_i \\ \sum_i N_4(x_i)y_i \\ \sum_i N_5(x_i)y_i \\ \sum_i N_6(x_i)y_i \end{pmatrix},
$$

or

$$AX = B \tag{B-17}$$

where

$$(a_{jk})^2 = \sum_{i=1}^{M} N_j(x_i)N_k(x_i) \tag{B-18}$$

$$(b_j) = \sum_{i=1}^{M} N_j(x_i)y_i \tag{B-19}$$

and

$$x_j = \lambda_j \tag{B-20}$$

The procedure for using tension splines is then similar to using any other basis set. Once the knots and tension arrays are defined, the $N_i(x)$ are determined. Using these expressions for $N_i(x)$, the linear matrix system described by Equation B-16 is filled up, and the least squares coefficients λ_j can be determined. These coefficients along with N_i then completely characterize the curve fitting function and its derivatives.

The data reduction program contains four subroutines that are used in handling the tension splines (Ref. A-2). The subroutines are called SETUP, INT, VALN, and SPLINE. The purpose of each of these routines is briefly described below.

The first subroutine is SETUP. The main input parameters to SETUP are the knot sequence, T(I), arranged in ascending order, the tension sequence, RHO(I), and the number of knots N. This subroutine takes these parameters in and establishes the spline functions N_i. The actual output of SETUP is two arrays VN0(I,J) and VN2(I,J). The elements of VN0(I,J) are the i^{th} spline N_i evaluated at the knot T(I+J-4), where J = 1, 5. Actually, VN0(I,1) = VN0(I,5) = 0. Similarly, VN2(I,J)

contains the second derivative of the i^{th} spline N_i evaluated at knot T(I+J-4). The values of the N_i splines and spline derivatives evaluated at all the knots completely characterize $N_i(x)$ for an arbitrary x. Thus, this routine actually sets up the splines N_i.

The subroutine INT is a search routine. If the value of y at some arbitrary value of x is needed, only four splines need be evaluated, since only four are nonzero. The routine INT locates x between two tabulated knot values, and returns a value ILEFT, the index in the knot array T(I) of the first knot to the left of x. By knowing ILEFT, it is possible to limit the spline evaluations to only those four needed for a given x value.

The subroutine VALN uses for its input x, a point at which the splines are to be evaluated, T, the knots, RH0, VN0, and VN2 defined above, and ILEFT found in INT. This subroutine takes in the value of x and actually calculates the spline values and derivative values of all nonzero splines at the point x. The output is a 4 x 4 array VN(I,J). The elements of VN(I,J) are the $(J-1)^{st}$ derivative of the N(ILEFT+4-I) spline evaluated at the point x. Thus, the first column contains all the nonzero spline values at x, and the second colunn contains all the first derivatives of the nonzero splines at x.

The last subroutine, SPLINE is used to form the linear combination of the spline least squares coefficients and the nonzero splines to actually determine a value of y(x) once an x has been specified. SPLINE actually calls INT and VALN to accomplish this operation. The output from SPLINE is TAU(I), a vector of length four. The I^{th} element of TAU contains the $(I-1)^{st}$ derivative of y(x).

Thus, to determine α in the data reduction program, a set of

tension splines is used to curve fit $V_g(N_H)$. The tension near the origin is relaxed. As N_H increases, the tension also increases. The tension splines are set up once in the entire program near the beginning, and a least squares fit is performed to find appropriate coefficients for the splines. When a value for α is needed, the splines are evaluated at the requested point, and the appropriate linear combination is determined.

APPENDIX C

DESCRIPTION OF THE DATA REDUCTION PROGRAM

1. INTRODUCTION

In this appendix the data reduction program used to analyze the micro-Hall data is presented and explained.

The first section deals entirely with the needed input parameters and their associated input forms, as well as the output parameters and their associated forms.

After presenting the input/output, a flow chart and listing of the program is presented. The entire flow of the program is then discussed using the flow chart and the listing for reference.

2. THE INPUT/OUTPUT

a. The Input

The input to the program basically consists of three distinct sections. The first two sections are one card each, but the last section is usually about 40 to 60 cards.

The first input card is a device identifier card containing any alphanumeric string of characters in columns 1 through 80 which uniquely identify the device. In most of the data run for this program, a typical name was SXXXRYYY. The position XXX defined a particular device by a three digit number. The character S implied the device was manufactured at Sandia Laboratories. The R was a preface that meant radiation dose. The remaining positions YYY denoted the total dose this device had been exposed to prior to taking the data set. The form the total dose coding took was $Y_1Y_2Y_3$ which stood for $Y_1 \cdot Y_2 \cdot 10^{Y_3}$. Thus S169R556 was device 169 manufactured by Sandia and irradiated to 5.5×10^6 Rad(Si) total dose.

The next card should contain 10 parameters in all. These first seven parameters are real variables and the last three are integer variables. The first seven parameters are read in by a 7G10.4 format, while the remaining three are read in under a 3I3 format. Any of the real data expressed in exponential notation must be right-hand justified in the data field of 10 allotted for it to prevent the inclusion of zeros into the exponential term. Similarly, the integer variables must also be right-hand justified.

The ten variables read in on the second card are:

N_D - donor density in the bulk, cm^{-3}

N_A - acceptor density in the bulk, cm^{-3}

PHS1 - initial value of the surface potential, kT

COX - oxide specific capacitance, $farads/cm^2$

T1 - lower temperature at which data were taken, K

T2 - upper temperature at which data were taken, K

MAGFLD - magnetic field strength, gauss

IND - conductivity type, 1 for n-channel, 2 for p-channel

NVGPT1 - number of points at which data were taken for the lower temperature

NVGPT2 - number of points at which data were taken for the upper temperature

Most of these variables are self explanatory. The variable PHS1 is the user supplied initial value of the surface potential at which N_{ss} should be evaluated. The method for choosing PHS1 is described later, but it can be noted here that PHS1 is in units of kT, and assumes values near 0 and 37 for n- and p-channel devices, respectively.

The variable IND is used to get the proper signs at some of the expressions. The value of IND is one for n channel and two for p channel.

The variables NVGPT1 and NVGPT2 are integers that state how many separate values of gate voltage were used in taking the data for the lower and upper temperatures, respectively.

All the remaining data cards contain the actual data used in calculating the Hall mobility and Hall surface carrier concentration. Altogether, there should be 2(NVGPT1) + 2(NVGPT2) cards remaining.

Figure C-1 shows how the data look for input. This last section is comprised of four large data blocks, the first two taken at the lower temperature and the last two taken at the upper temperature. Blocks one and three are formatted the same and take in similar information. The variables in blocks one and three are V_g, the gate voltage in volts, and I_{12}, V_{34}, I_{41}, I_{34}, V_{12}, I_{41}, V_{23}, respectively. The input format for these nine variables is 9G8.4. The gate voltage is read in volts (including a sign), but the currents and remaining voltages are read in units of microamps and millivolts, respectively. The subscripted currents and voltages are taken right from the data sheet described in Figure 28, Chapter V. Block one would contain NVGPT1 cards, and block three would contain NVGPT2 cards.

Blocks two and four also read in similar data. The six parameters on each card are I_{24}, V_{13}, $\bar{V}_{13}$, I_{13}, V_{24}, $\bar{V}_{24}$. Again, the voltages are expressed in millivolts and the currents in microamps. These data can also be taken directly from the data sheet shown in Figure 28. The bar over the voltage term implies a voltage reading taken under the influence of the magnetic field.

In blocks one and three, only the absolute ratio of voltages and currents is needed, so none of the voltages and currents need to have a sign associated with them. In blocks two and four, however, a difference

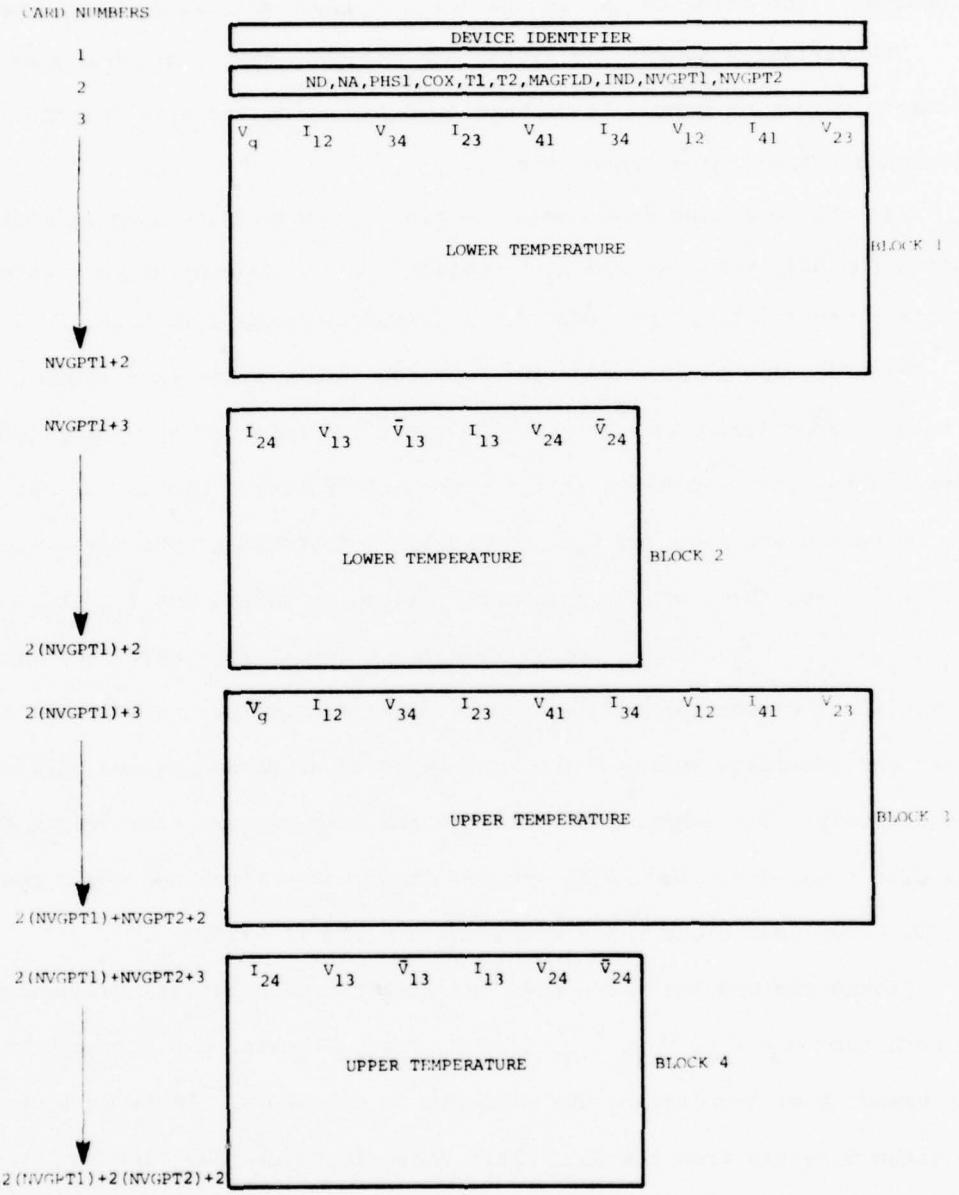

Figure C-1. A representation of the input cards to the data reduction program.

of two voltages is determined for the Hall effect, so these voltages must have a sign associated with them. However, the currents can be supplied as positive. In the data reduction program, once the difference $(V_{ij} - \bar{V}_{ij})$ is taken again only the magnitude is needed. The ratio of this difference to the opposite current leads to determination of N_H through Equation 113, Chapter IV. Since this ratio is the needed quantity, the signs can be dropped after the Hall voltage is calculated.

The value for C_{ox} can be found by applying a strong accumulation bias voltage on the gate of the transistor, tying all the source leads together and shorting them to the substrate, then measuring the capacitance. In this experiment, the oxide capacitance was determined by C-V measurements supplied by Sandia Laboratories on capacitors adjacent to the transistor under test.

One final term needs yet to be specified. A method must be devised to choose PHS1. The quantity PHS in the computer program represents $E_c - E_f$ in units of kT. For PHS = 0, the bands have been bent to the point that the Fermi level is touching the conduction band. For PHS = 042, the bands have been bent such that the Fermi level is touching the valance band (at 300 K). This quantity PHS is the same quantity Φ_s depicted in Figure 12, Chapter IV. The program always takes the values of PHS1, calculated N_{ss}, then decreases PHS1 by 0.2 kT to a new PHS. Thus, if the supplied value of PHS1 was zero, the program would increment PHS1 from zer to -6. If the supplied value of PHS1 was -35, the program would increment PHS to -41 by increments of 0.2. A total sweep of six is all that has been found useful.

The theory developed in Chapter III should be valid in very strong inversion, and to the point where $v_s \simeq -2u_b$, or the strong inversion point. Thus, v_s should increment from a value of $-2u_b$ to the band edges (see

Figure 12, Chapter III).

Figure C-2 displays curves of $E_f - E_i$ at various temperatures and device dopings (Ref. 58). Knowing the device doping, one can visually determine u_b at different values of T. Thus, for n channel devices, PHS1 is chosen around 0 and should increment to the strong inversion point. For a device doped to 10^{15} cm^{-3}, Figure C-2 shows $u_b \simeq 0.3$ eV at 300 K, or about 11.5 kT. The intrinsic level is displaced from mid gap by about 1.4 kT, and $E_g/2$ is about 21 kT, so PHS should increment from 0 to 21 - (1.4 + 11.5), or -8.1 kT. The minus sign arises from how PHS is defined.

Similarly, for a p-channel device, PHS should increment from 21 + (1.4 + 11.5) = 33.9 or -33.9 kT to -42 kT.

Thus, using PHS1 as 0 for an n-channel device and -33.9 for a p-channel device and incrementing 8 kT, N_{ss} could be determined from the band edges to the strong inversion point. Unfortunately, near the strong inversion point for both n- and p-channel devices, the experimental data that yield N_H are very unreliable. Thus, as was mentioned before, the actual useful range of this technique is more limited.

The method chosen to evade the strong inversion point is to choose PHS1 as 0 for n-channel devices, and increment PHS to -6 kT. For p-channel devices PHS1 is chosen as -37 and PHS increments to -43. The values for N_{ss} are calculated every 0.2 kT. The reliability of the answers can be established after they are printed out. For each value of PHS, a value for N_{ss} and r, the mobility ratio, is determined. These data are printed out along with N_H, the value of the Hall carrier concentration corresponding to that value of PHS being used at the time. If N_H lies outside the range of data actually supplied at the input, the curve fitting routines have been used to extrapolate data outside their useful regions, and

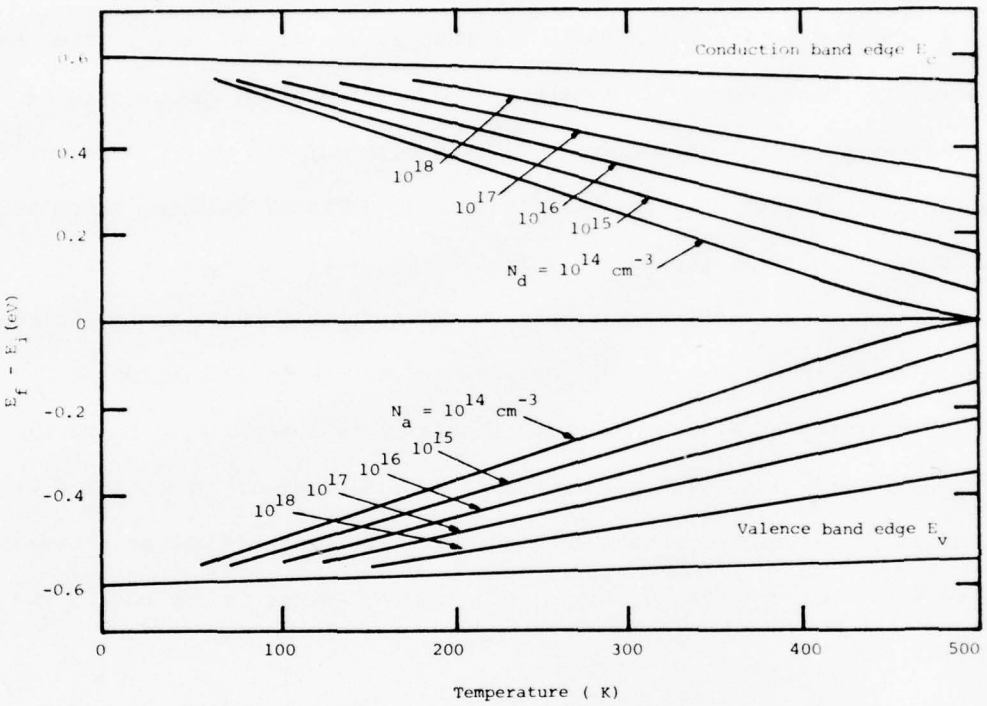

Figure C-2. $(E_F - E_i)$ at various temperatures and doping densities (see Ref. 58).

these values of N_{ss} and PHS are ignored. This same problem can occur at very strong inversion, or high values of gate voltage. It may be possible again to ask for extrapolated values of the data near the band edges.

A viable solution has been to fix PHS1 as was stated above. Then the answers are inspected to see if the N_H used at any given PHS is outside the supplied experimental data range. If this case exists, these values of N_{ss} and PHS are eliminated as answers. For these devices, sweeping about 6Kt was sufficient to get all the useful values of N_{ss}. If one uses the program and finds that more useful information is still available, PHS1 can be raised or lowered for both n- or p-channel devices at the user's discretion.

Examination of Figure C-2 shows that as T increases, $E_f - E_i$ decreases, so u_b decreases. The effect is reversed at T decreases. Thus, for a given conductivity material, one can scan further into the band gap by increasing the temperature, and further into the bands themselves by decreasing the temperature.

For this study, PHS1 was held at 0 for n-channel and at -37 for p-channel. The total range swept was 6 kT. For p-channel devices, this means that N_{ss} was actually determined about 1 kT into the valence band.

Figure C-3 is an example of a listing of a set of input cards.

b. Initial Handling of the Input

Once the data have been put onto cards in the form shown in Figure C-1, and the program is run, the data in blocks one to four are shifted around somewhat. All the raw data are stored in an array called DATA. It is dimensioned (50,30) and holds the experimental data from the lower temperature in columns 1 through 15, and the data from the upper temperature in columns 16 through 30. Thus, the user can use no more than 50 values of the gate voltage at any given temperature.

```
S160R000
    1.3E15      0.0000  -3.70E01    3.22E-8     2.60E2      2.96E2      4.41E3  2 22 21
  -1.75     .130    13.07     .148    14.49     .145    14.53     .147    14.68
  -2.0      .381    25.13     .574    25.24     .559    25.02     .566    25.27
  -2.5     1.534    30.44    1.517    29.61    1.470    29.07    1.491    29.29
  -3.0     2.410    31.11    2.382    30.35    2.308    29.75    2.340    29.91
  -3.5     3.209    31.34    3.172    30.60    3.073    29.96    3.072    29.96
  -4.0     3.937    31.42    3.902    30.71    3.778    30.05    3.830    30.18
  -4.5     4.623    31.47    4.572    30.77    4.428    30.11    4.488    30.22
  -5.0     5.258    31.50    5.199    30.80    5.035    30.14    5.105    30.26
  -5.5     5.862    31.57    5.792    30.84    5.611    30.22    5.693    30.32
  -6.0     6.451    31.58    6.373    30.91    6.190    30.37    6.281    30.42
  -6.5     7.024    31.77    6.947    30.98    6.750    30.50    6.848    30.53
  -7.0     7.564    31.83    7.483    31.04    7.278    30.60    7.382    30.60
  -8.0     8.571    31.94    8.483    31.16    8.267    30.79    8.360    30.75
  -9.0     9.495    32.01    9.406    31.24    9.176    30.92    9.295    30.85
 -10.0    10.350    32.05   10.255    31.30   10.015    31.01   10.134    30.93
 -11.0    11.138    32.09   11.041    31.36   10.793    31.09   10.925    31.00
 -12.0    11.878    32.11   11.730    31.39   11.525    31.14   11.665    31.00
 -13.0    12.552    32.14   12.420    31.43   12.230    31.20   12.375    31.10
 -14.0    13.249    32.13   13.147    31.45   12.890    31.23   13.022    31.16
 -15.0    13.862    32.16   13.758    31.48   13.484    31.28   13.631    31.16
 -16.0    14.437    32.15   14.328    31.48   14.053    31.29   14.204    31.17
 -17.0    14.788    32.16   14.681    31.51   14.603    31.33   14.756    31.21
   .133      .253    -.250      .133      .290      .813
   .510      .299    -.296      .512      .325    1.233
  1.337      .230    -.093     1.345      .298    1.284
  2.098      .270    -.314     2.110      .286    1.250
  2.791      .253    -.336     2.811      .282    1.211
  3.432      .251    -.338     3.449      .277    1.171
  4.021      .254    -.337     4.042      .283    1.136
  4.573      .253    -.337     4.593      .277    1.110
  5.091      .254    -.311     5.123      .305    1.107
  5.615      .323    -.405     5.649      .345    1.126
  6.117      .344    -.442     6.147      .370    1.134
  6.590      .354    -.375     6.621      .384    1.129
  7.474      .375    -.325     7.507      .403    1.110
  8.285      .383    -.273     8.313      .406    1.081
  9.030      .383    -.250     9.063      .407    1.056
  9.731      .382    -.237     9.770      .405    1.028
 10.388      .383    -.215    10.425      .402    1.000
 11.016      .374    -.173    11.054      .399    .975
 11.589      .372    -.153    11.628      .392    .948
 12.128      .368    -.135    12.168      .387    .923
 12.657      .365    -.132    12.698      .384    .903
 13.124      .362    -.137    13.168      .380    .881
  -1.75      .214   19.38      .211   19.30      .203   19.08      .209   19.33
  -2.00      .375   27.33      .369   26.48      .351   26.39      .357   26.68
  -2.50     1.423   30.34     1.393   29.77     1.287   29.27     1.285   29.52
  -3.00     2.311   31.29     2.283   30.40     2.168   29.83     2.183   30.04
  -3.50     2.951   31.47     2.921   30.64     2.839   30.02     2.874   30.21
  -4.00     3.265   31.47     3.243   30.74     3.117   30.10     3.159   30.28
  -4.50     3.799   31.51     3.737   30.80     3.638   30.16     3.688   30.33
  -5.00     4.329   31.57     4.274   30.85     4.146   30.21     4.205   30.37
  -5.50     4.843   31.58     4.784   30.91     4.639   30.34     4.709   30.44
  -6.00     5.327   31.75     5.284   30.98     5.112   30.48     5.188   30.57
  -6.50     5.797   31.83     5.733   31.06     5.569   30.60     5.647   30.68
  -7.00     6.243   31.92     6.186   31.13     6.015   30.71     6.098   30.75
  -8.00     7.101   32.02     7.031   31.24     6.851   30.88     6.943   30.88
  -9.00     7.891   32.03     7.815   31.31     7.628   31.00     7.724   31.08
 -10.00     8.632   32.13     8.554   31.38     8.354   31.04     8.455   31.06
 -11.00     9.325   32.13     9.243   31.42     9.038   31.15     9.148   31.12
 -12.00     9.982   32.17     9.900   31.46     9.682   31.21     9.797   31.16
 -13.00    10.603   32.17    10.517   31.49    10.275   31.25    10.413   31.20
 -14.00    11.192   32.17    11.104   31.51    10.875   31.29    11.040   31.24
 -15.00    11.743   32.19    11.657   31.52    11.423   31.31    11.547   31.25
 -16.00    12.275   32.21    12.187   31.53    11.947   31.35    12.075   31.28
   .188      .341    -.117      .183      .233      .880
   .501      .426    -.203      .503      .425    1.102
  1.151      .333    -.334     1.133      .378    1.071
  1.750      .315    -.338     1.790      .316    1.019
  2.307      .301    -.331     2.320      .300      .981
  2.829      .283    -.331     2.845      .291      .950
  3.304      .283    -.330     3.324      .287      .927
  3.763      .291    -.334     3.786      .287      .921
  4.208      .321    -.271     4.239      .334      .939
  4.632      .353    -.225     4.663      .366      .957
  5.040      .375    -.187     5.073      .386      .964
  5.442      .383    -.176     5.483      .399      .963
  6.190      .397    -.160     6.219      .410      .952
  6.883      .402    -.110     6.918      .415      .935
  7.533      .403    -.077     7.569      .411      .915
  8.143      .403    -.032     8.181      .408      .894
  8.721      .397    -.070     8.760      .402      .875
  9.266      .394    -.021     9.309      .397      .853
  9.784      .387    -.049     9.829      .390      .832
 10.271      .384    -.041    10.319      .384      .811
 10.739      .383    -.039    10.791      .379      .795
```

[Numbers in this printout illustrate form only and do not have to be read to understand the figure.]

Figure C-3. An example of a set of input cards.

As soon as the experimental data are read in, they are immediately printed out to allow visual inspection to make sure they were entered properly.

c. The Output

The output has several stages or sections to it. Some sections allow one to scan the original input data. Others allow one to follow the intermediate calculations, and finally the answers are printed out.

As was mentioned before, immediately after the experimental data are read in, they are printed right back out again. This allows one to scan all the input data for correctness, and supplies a permanent record of them. The device identifier is used as the page heading.

Next, the program calculates N_H at the values of V_g for the lower temperature, as well as N_H, $\sigma_{\square}$, R (sheet resistivity), and μ_H at each value of V_g for the upper temperature. The values are stored destructively over the experimental values in the array DATA in columns 1 through 7. All of these values are then printed out. Close examination of the way in which either N_H, $\sigma_{\square}$, R, or μ_H varies with V_g is a sensitive way to catch mistakes in the input.

After these calculations are performed, then V_g as a function of N_H is curve fit through the polynomial fit. This is done at both temperatures. The five coefficients of these polynomials at the two separate temperatures are the next quantities printed out. If the fourth-order polynomial is used, all 10 coefficients are nonzero. If the first-order polynomial is used, the first three coefficients in each group of five are zero. These are the coefficients used to determine β.

Having curve fit $V_g(N_H)$ for β using polynomials, the next problem is to curve fit $V_g(N_H)$ using tension splines to determine α. As was

mentioned in Appendix B, there are six splines and six corresponding coefficients. These are the next variables printed out. If NORDER is set at 1, this implies the data are not reliable near the origin. In this case α is determined by a polynomial and this print is skipped.

Both α and β as functions of N_H provide some insight into how well the curve fitting is progressing. At this point in the program both the polynomial and tension spline curve fits have been done, so a table is tabulated for β and α at various value of N_H. This is done purely for visual inspection.

Next the process of choosing a PHS and calculating N_{ss} begins. At this point, each time a new value for R is calculated for a given PHS, it is printed out. This allows one to scan the action of the program to see how well the contraction on R is progressing. This can be most useful if the program does not run.

Finally, the last page of output is a tabulation of the calculated values. The page has again the device identifier as a header. Note that the last column printed out is N_H at a given value of PHS. The second page printed out contains the actual calculated values of N_H at various values of V_g. These are the values of N_H that must be compared to see if reliability can be placed in the answers. If the N_H at a given PHS on the last data page lies in the range of N_H (at the upper temperature) listed on the second data page, the answers are valid.

Figure C-4 is an example of the output testing.

3. OPERATING PRINCIPLES

Now that the input/output of the program has been discussed, and the curve fitting explained (Appendix B), it is time to examine the whole program to see how it fits together.

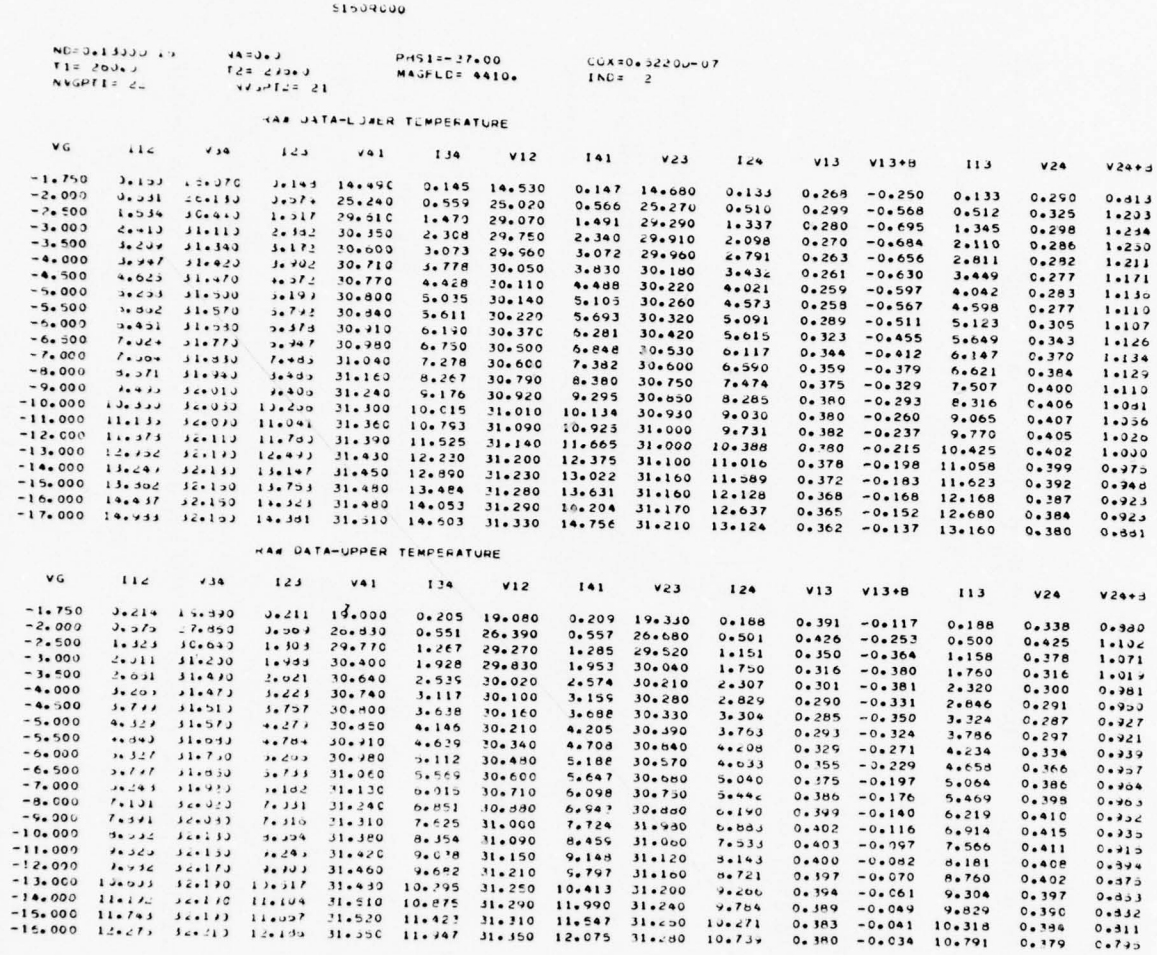

S1504000

ND=0.13000 E 19 VA=0.0 PHS1=-37.00 COX=0.52200-07
T1= 200.0 T2= 2000.0 MAGFLD= 4410. IND= 2
NVGPT1= 21 NVGPT2= 21

VAN DATA-LOWER TEMPERATURE

VG	I12	V34	I23	V41	I34	V12	I41	V23	I24	V13	V13+B	I13	V24	V24+B
-1.750	0.133	15.070	0.143	14.490	0.145	14.530	0.147	14.680	0.133	0.268	-0.250	0.133	0.290	0.813
-2.000	0.331	25.130	0.374	25.240	0.559	25.020	0.566	25.270	0.510	0.299	-0.568	0.512	0.325	1.203
-2.500	1.534	30.410	1.517	29.510	1.470	29.070	1.491	29.290	1.337	0.280	-0.695	1.345	0.298	1.234
-3.000	2.413	31.110	2.382	30.350	2.308	29.750	2.340	29.910	2.098	0.270	-0.684	2.110	0.286	1.230
-3.500	3.209	31.340	3.172	30.600	3.073	29.960	3.072	29.960	2.791	0.263	-0.656	2.811	0.282	1.211
-4.000	3.997	31.420	3.902	30.710	3.778	30.050	3.830	30.180	3.432	0.261	-0.630	3.449	0.277	1.171
-4.500	4.823	31.470	4.672	30.770	4.428	30.110	4.488	30.220	4.021	0.259	-0.597	4.042	0.283	1.136
-5.000	5.633	31.530	5.497	30.800	5.035	30.140	5.105	30.260	4.573	0.258	-0.567	4.598	0.277	1.110
-5.500	6.852	31.570	6.742	30.840	5.611	30.220	5.693	30.320	5.091	0.289	-0.511	5.123	0.305	1.107
-6.000	8.431	31.630	8.378	30.910	6.190	30.370	6.281	30.420	5.615	0.323	-0.455	5.649	0.343	1.126
-6.500	7.024	31.770	8.947	30.980	6.750	30.500	6.848	30.530	6.117	0.344	-0.412	6.147	0.370	1.134
-7.000	7.504	31.830	7.483	31.040	7.278	30.600	7.382	30.600	6.590	0.359	-0.379	6.621	0.384	1.129
-8.000	8.371	31.940	8.483	31.160	8.267	30.790	8.380	30.750	7.474	0.375	-0.329	7.507	0.400	1.110
-9.000	9.443	32.010	9.405	31.240	9.176	30.920	9.295	30.850	8.285	0.380	-0.293	8.316	0.406	1.091
-10.000	10.333	32.050	10.230	31.300	10.015	31.010	10.134	30.930	9.030	0.380	-0.260	9.065	0.407	1.056
-11.000	11.133	32.070	11.041	31.360	10.793	31.090	10.925	31.000	9.731	0.382	-0.237	9.770	0.405	1.026
-12.000	11.973	32.110	11.780	31.390	11.525	31.140	11.665	31.000	10.388	0.380	-0.215	10.425	0.402	1.000
-13.000	12.752	32.140	12.443	31.430	12.220	31.200	12.375	31.100	11.016	0.378	-0.198	11.058	0.399	0.975
-14.000	13.247	32.150	13.147	31.450	12.890	31.230	13.022	31.160	11.589	0.372	-0.183	11.623	0.392	0.948
-15.000	13.302	32.130	13.753	31.480	13.484	31.280	13.631	31.160	12.128	0.368	-0.168	12.168	0.387	0.923
-16.000	14.437	32.150	14.321	31.480	14.053	31.290	14.204	31.170	12.637	0.365	-0.152	12.680	0.384	0.923
-17.000	14.933	32.150	14.881	31.510	14.603	31.330	14.756	31.210	13.124	0.362	-0.137	13.160	0.380	0.861

VAN DATA-UPPER TEMPERATURE

VG	I12	V34	I23	V41	I34	V12	I41	V23	I24	V13	V13+B	I13	V24	V24+B
-1.750	0.214	15.830	0.211	15.000	0.205	19.080	0.209	19.330	0.188	0.391	-0.117	0.188	0.338	0.980
-2.000	0.575	27.850	0.564	26.830	0.551	26.390	0.557	26.680	0.501	0.426	-0.253	0.500	0.425	1.102
-2.500	1.323	30.640	1.303	29.770	1.267	29.270	1.285	29.520	1.151	0.350	-0.364	1.158	0.378	1.071
-3.000	2.011	31.230	1.983	30.400	1.928	29.830	1.953	30.040	1.750	0.316	-0.380	1.760	0.316	1.019
-3.500	2.631	31.430	2.621	30.640	2.535	30.020	2.574	30.210	2.307	0.301	-0.381	2.320	0.300	0.981
-4.000	3.203	31.473	3.223	30.740	3.117	30.100	3.155	30.280	2.829	0.290	-0.331	2.846	0.291	0.950
-4.500	3.744	31.513	3.757	30.800	3.638	30.160	3.688	30.330	3.304	0.285	-0.350	3.324	0.287	0.927
-5.000	4.329	31.573	4.277	30.850	4.146	30.210	4.205	30.390	3.763	0.293	-0.324	3.786	0.297	0.921
-5.500	4.843	31.643	4.784	30.910	4.629	30.340	4.708	30.840	4.208	0.329	-0.271	4.234	0.334	0.939
-6.000	5.327	31.710	5.293	30.980	5.112	30.480	5.188	30.570	4.633	0.355	-0.229	4.658	0.366	0.957
-6.500	5.797	31.830	5.733	31.060	5.569	30.600	5.647	30.680	5.040	0.375	-0.197	5.064	0.386	0.964
-7.000	6.243	31.930	6.182	31.130	6.015	30.710	6.098	30.750	5.446	0.386	-0.176	5.469	0.398	0.963
-8.000	7.131	32.020	7.031	31.240	6.851	30.880	6.943	30.860	6.190	0.399	-0.140	6.219	0.410	0.952
-9.000	7.941	32.043	7.810	31.310	7.625	31.000	7.724	31.980	6.883	0.402	-0.116	6.914	0.415	0.935
-10.000	8.695	32.133	8.594	31.380	8.354	31.090	8.459	31.060	7.533	0.403	-0.097	7.566	0.411	0.913
-11.000	9.325	32.133	9.243	31.420	9.038	31.150	9.148	31.120	8.143	0.400	-0.082	8.181	0.408	0.894
-12.000	9.932	32.173	9.803	31.460	9.682	31.210	9.797	31.160	8.721	0.397	-0.070	8.760	0.402	0.875
-13.000	10.533	32.190	10.317	31.480	10.295	31.250	10.413	31.200	9.266	0.394	-0.061	9.304	0.397	0.853
-14.000	11.172	32.170	11.104	31.510	10.875	31.290	11.990	31.240	9.784	0.389	-0.049	9.829	0.390	0.832
-15.000	11.743	32.193	11.697	31.520	11.423	31.310	11.547	31.290	10.271	0.383	-0.041	10.318	0.384	0.811
-16.000	12.273	32.213	12.139	31.550	11.947	31.350	12.075	31.280	10.739	0.380	-0.034	10.791	0.379	0.795

Figure C-4. An example of an output listing.

NH(T-LOW)	VG(T-LOW)	NH(T-HIGH)	VG(T-HIGH)	CONDUCTIVITY	R	MOBILITY
0.7033D 11	-1.750	0.9856D 11	-1.750	0.3950-05	2793.	151.7
0.1612D 12	-2.000	0.2032D 12	-2.000	0.4613D-05	1355.	141.7
0.3765D 12	-2.500	0.4517D 12	-2.500	0.9594D-05	609.4	132.6
0.6019D 12	-3.000	0.6906D 12	-3.000	0.1431D-04	398.6	129.4
0.8344D 12	-3.500	0.9344D 12	-3.500	0.1873D-04	294.6	123.1
0.1061D 13	-4.000	0.1220D 13	-4.000	0.2297D-04	225.5	117.6
0.1299D 13	-4.500	0.1431D 13	-4.500	0.2674D-04	192.4	110.6
0.1523D 13	-5.000	0.1674D 13	-5.000	0.3042D-04	164.4	113.4
0.1755D 13	-5.500	0.1928D 13	-5.500	0.3382D-04	142.7	109.5
0.1986D 13	-6.000	0.2176D 13	-6.000	0.3724D-04	126.5	106.8
0.2221D 13	-6.500	0.2418D 13	-6.500	0.4041D-04	113.8	104.3
0.2452D 13	-7.000	0.2665D 13	-7.000	0.4349D-04	103.3	101.9
0.2916D 13	-8.000	0.3160D 13	-8.000	0.4929D-04	87.11	97.36
0.3390D 13	-9.000	0.3659D 13	-9.000	0.5423D-04	75.23	92.51
0.3864D 13	-10.00	0.4139D 13	-10.00	0.5970D-04	66.49	90.01
0.4329D 13	-11.00	0.4642D 13	-11.00	0.6445D-04	59.30	86.66
0.4802D 13	-12.00	0.5119D 13	-12.00	0.6893D-04	53.77	84.04
0.5274D 13	-13.00	0.5611D 13	-13.00	0.7318D-04	49.06	81.40
0.5751D 13	-14.00	0.6135D 13	-14.00	0.7896D-04	44.87	80.33
0.6218D 13	-15.00	0.6659D 13	-15.00	0.8104D-04	41.33	75.93
0.6599D 13	-16.00	0.7140D 13	-16.00	0.8464D-04	38.55	73.99
0.7235D 13	-17.00	32.16	14.88	31.51	14.60	31.33

A1= 0.1683D-30 B1=-0.2432D-37 C1= 0.1199D-24 D1=-0.2369D-11 E1= -1.603
A2= 0.3122D-31 B2=-0.3163D-38 C2= 0.1110D-25 D2=-0.2049D-11 E2= -1.571

-1.560	-.1774	-.3902	-1.996	-.5202	-16.18

NH	BETA	ALPHA
0.1999999D 12	0.3262599D 09	-0.6776061
0.3999998D 12	0.1298128D 10	-0.6714037
0.5999999D 12	0.1708650D 10	-0.6664416
0.7999995D 12	0.2065824D 10	-0.6626701
0.9999994D 12	0.2377171D 10	-0.6600515
0.1199999D 13	0.2649737D 10	-0.6585595
0.1399999D 13	0.2890091D 10	-0.6581792
0.1599999D 13	0.3104322D 10	-0.6589068
0.1799999D 13	0.3298043D 10	-0.6607496
0.1999993D 13	0.3476363D 10	-0.6635048
0.2199999D 13	0.3644031D 10	-0.6651202
0.2399999D 13	0.3805139D 10	-0.6658310
0.2599999D 13	0.3963421D 10	-0.6661171
0.2799999D 13	0.4122109D 10	-0.6661714
0.2999999D 13	0.4283953D 10	-0.6660308
0.3199999D 13	0.4451226D 10	-0.6656001
0.3399997D 13	0.4625726D 10	-0.6645888
0.3599997D 13	0.4808776D 10	-0.6623144
0.3799997D 13	0.5001216D 10	-0.6588105
0.3999999D 13	0.5203414D 10	-0.6567505

Figure C-4. (continued)

Figure C-4. (continued)

VALUE FOR R	ITERATION
0.0455	1
VALUE FOR R	ITERATION
0.0097	1
0.0084	2
VALUE FOR R	ITERATION
0.0020	1
0.0009	2
VALUE FOR R	ITERATION
0.4593	1
VALUE FOR R	ITERATION
0.4593	1
VALUE FOR R	ITERATION
0.4534	1
0.4523	2
VALUE FOR R	ITERATION
0.4632	1
0.4618	2
VALUE FOR R	ITERATION
0.4738	1
0.4726	2
VALUE FOR R	ITERATION
0.4657	1
0.4645	2
VALUE FOR R	ITERATION
0.4733	1
VALUE FOR R	ITERATION
0.4645	1
VALUE FOR R	ITERATION
0.4455	1
0.4420	2
VALUE FOR R	ITERATION
0.4252	1
0.4209	2
VALUE FOR R	ITERATION
0.4054	1
0.4004	2

Figure C-4. (continued)

S160R000

PHS	NSS	R	VG	NIND	NM
-37.00	0.6527D 12	0.4704	-1.797	0.5192D 11	0.1104D 12
-37.20	0.7155D 12	0.4832	-1.830	0.6108D 11	0.1264D 12
-37.40	0.8071D 12	0.4912	-1.870	0.7161D 11	0.1458D 12
-37.60	0.9157D 12	0.4981	-1.915	0.8366D 11	0.1680D 12
-37.80	0.1034D 13	0.5045	-1.966	0.9739D 11	0.1930D 12
-38.00	0.1117D 13	0.5142	-2.021	0.1130D 12	0.2197D 12
-38.20	0.1381D 13	0.5096	-2.095	0.1306D 12	0.2562D 12
-38.40	0.1544D 13	0.5143	-2.169	0.1504D 12	0.2924D 12
-38.60	0.1695D 13	0.5200	-2.251	0.1727D 12	0.3321D 12
-38.80	0.1936D 13	0.5210	-2.347	0.1977D 12	0.3794D 12
-39.00	0.2219D 13	0.5208	-2.457	0.2256D 12	0.4332D 12
-39.20	0.2559D 13	0.5193	-2.582	0.2567D 12	0.4944D 12
-39.40	0.2953D 13	0.5170	-2.723	0.2914D 12	0.5636D 12
-39.60	0.3332D 13	0.5166	-2.876	0.3299D 12	0.6386D 12
-39.80	0.3836D 13	0.5133	-3.054	0.3726D 12	0.7258D 12
-40.00	0.4269D 13	0.5133	-3.241	0.4199D 12	0.8180D 12
-40.20	0.4452D 13	0.5200	-3.425	0.4722D 12	0.9081D 12
-40.40	0.5119D 13	0.5155	-3.669	0.5299D 12	0.1028D 13
-40.60	0.5978D 13	0.5084	-3.953	0.5936D 12	0.1168D 13
-40.80	0.6968D 13	0.5009	-4.273	0.6637D 12	0.1325D 13
-41.00	0.7712D 13	0.4993	-4.595	0.7407D 12	0.1483D 13
-41.20	0.8403D 13	0.4993	-4.939	0.8252D 12	0.1653D 13
-41.40	0.9671D 13	0.4923	-5.369	0.9177D 12	0.1864D 13
-41.60	0.1142D 14	0.4818	-5.878	0.1019D 13	0.2114D 13
-41.80	0.1332D 14	0.4726	-6.436	0.1129D 13	0.2389D 13
-42.00	0.1537D 14	0.4645	-7.044	0.1249D 13	0.2688D 13
-42.20	0.1600D 14	0.4703	-7.537	0.1378D 13	0.2931D 13
-42.40	0.1815D 14	0.4645	-8.225	0.1518D 13	0.3269D 13
-42.60	0.2328D 14	0.4420	-9.259	0.1669D 13	0.3777D 13
-42.80	0.2944D 14	0.4209	-10.42	0.1831D 13	0.4351D 13
-43.00	0.3705D 14	0.4004	-11.75	0.2004D 13	0.5006D 13

Figure C-4. (continued)

There is one main driver program and fifteen subroutines. The sequence numbers are alphanumeric. All sequence numbers containing the preface A are in the main driver. The remaining 15 routines have statement ment numbers prefaced with B through P, respectively.

The basic approach is to discuss the main program, and see how it operates. The subroutines that are difficult to understand have already been discussed. After the main program is described, each subroutine is briefly mentioned.

Figure C-5 is a flow charge of the main driver program, which for continuity is listed in Figure C-6 at the end of this section. Whenever possible, the calculations on the program are coordinated with equations from the text.

a. The Main Program

The overall approach taken by the main program is to:

1. Take in the experimental data and device constants.
2. Calculate N_H, μ_H, $\sigma_{\square}$ and R from the experimental data.
3. Curve fit $V_g(N_H)$ at both temperatures for β determination using polynomials.
4. Curve fit $V_g(N_H)$ at the upper temperature for α determination using tension splines.
5. Select a Φ_s.
6. Calculate all parameters necessary to determine C_1, C_2, C_3, and C_4 at this Φ_s and the upper temperature.
7. Do a contraction to determine r, w, and N_{ss}.
8. Save these three answers in an array.
9. Select a new Φ_{ss}, then go to Step 6.
10. Print out answers.

With this approach in mind, consider now the flow chart and the program together.

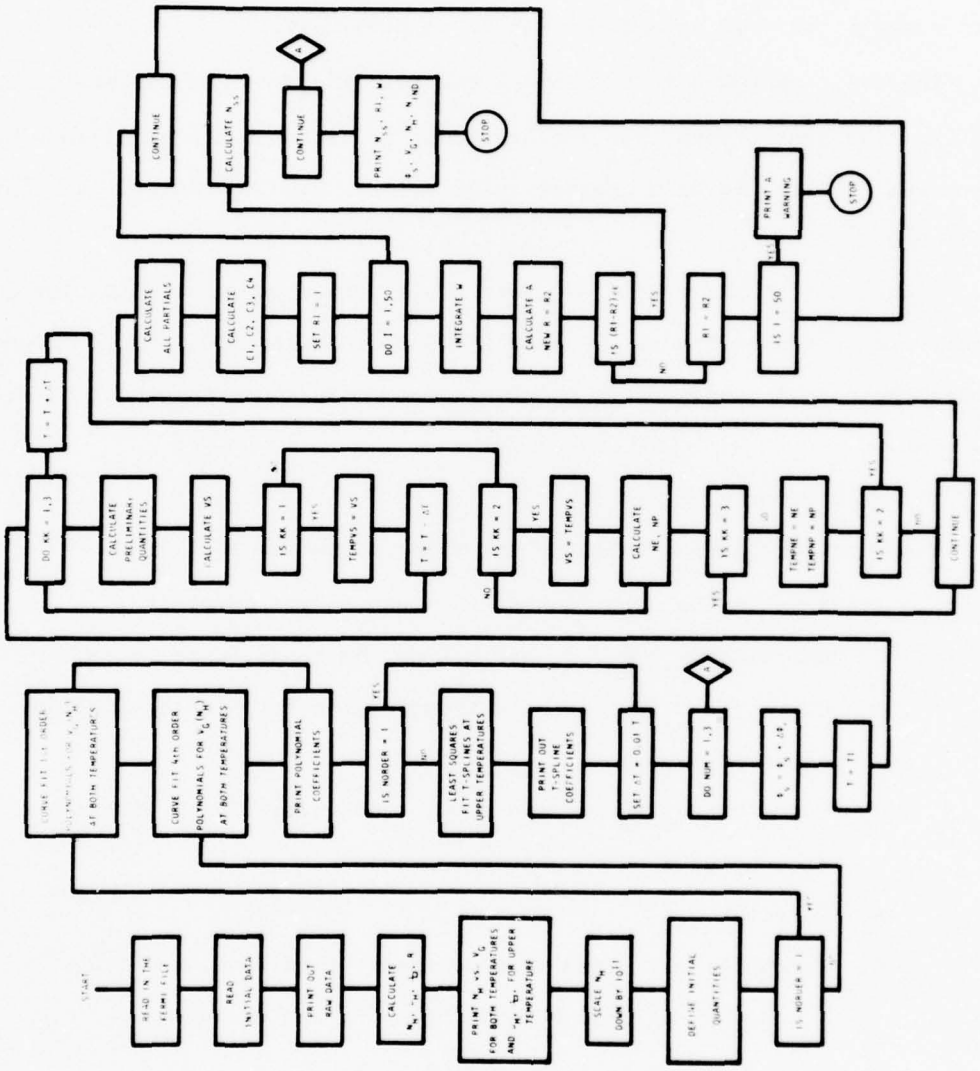

Figure C-5. A flow chart of the program

The first step is to read in the Fermi array for finding the Fermi integrals. These cards are actually part of the data deck, but are kept with the source program since they never change. Lines A250 to A270 read in the Fermi array. The form of the Fermi array is as follows: There are 501 cards, each card containing three numbers. The first number is the argument of the Fermi integral, x, and the second and third numbers are $F_{1/2}(x)$ and $F_{3/2}(x)$. The arguments go from -50.0 to +50.0 in increments of 0.2, giving rise to the 501 cards mentioned.

Since some IBM 360 computers do not automatically zero all arrays initially, any array that may not be completely filled is often initialized to zero. Lines A310 to A340 zero the DATA array.

Next, the device identifier, device characteristic parameters, and the actual experimental data are read in and printed out again immediately so they can be scanned. This is done in lines A750 to A900. Notice that the lower temperature data are stored in columns 1 through 15 of DATA, and the upper temperature data are stored in columns 16 through 30.

Lines A940 and A1040 are simply definitions of physical constants that recur. Notice that A1030 defines R1=1. This is the initial guess to the mobility ratio. In subsequent statements, a new R1 will be set equal to previously calculated R1 so contraction may occur. In lines A1050 to A1120, N_H is being calculated for the lower temperature. Line A1060 is a combination of Equations 111 and 102, Chapter IV, and A1120 is Equation 113, Chapter IV.

In lines A1150 to A1210 the N_H calculation is repeated for the upper temperature. Line A1220 stores R_s in the data array. This was calculated in A1150. Lines 1260 to 1280 calculate $\sigma_{\square}$ using Equations 107 and 108, Chapter IV, while Line 1320 calculates μ_H through Equation 110, Chapter IV.

Notice that in all the above calculations the answers are destructively read back into the DATA array. All of the useful information for the program is now in columns 1 through 7 of DATA. The variables N_H, V_g at the lower temperatures, and N_H, V_g, $\sigma_{\square}$, R_s and μ_H at the upper temperature are in columns 1 through 7, respectively.

After these calculations are performed, the resulting values are printed out. In general, the number of data points at the two temperatures is different. Line A1340 finds which has the most data points, and that number is the number used to determine how many rows are printed out.

In curve fitting $V_g(N_H)$, the quantity N_H is on the order of 10^{11}. From Appendix B, it can be seen that the (1,1) element of the A matrix in Equation B-5 contains an x_i^8. Since N_H is x here, this presents a problem in terms of the computer. To prevent an overflow, all the values of N_H are scaled by 10^{11}. This is done in lines A1480 and A1490.

Again, the arrays to be used at this point are zeroed in lines A1600 to A1670.

Examination of Equation B-5 shows that the A matrix is not only symmetric, but all the I, J^{th} elements of A where I + J = K, are equal. Thus, A(2,3) = A(3,2) = A(4,1) = A(1,4). Here, K=5. Lines A1720 to A1820 do two things. First, they calculate the nine values that comprise the elements of the AA array, $\sum_{i=1}^{M} x_i^k$, k=0,1,...8. The values are stored in a working vector XX. Second, they fill up the BB vector defined by Equation B-10, Appendix B.

From lines A1830 to A1890 the AA array is filled with the values in XX. AgainAgain, by looking at Equation B-5, Appendix B, one can see that a similar array would be derived if one approximated $V_g(N_H)$ with a first order polynomial instead of a fourth order polynomial. The difference

would be that the linear system solved would be a 2x2 instead of a 5x5, and the A array would have as its elements A(4,4), A(4,5), A(5,4), and A(5,5) described in Equation B-5. To actually solve for a first order polynomial, these values must be transferred in the A array, as well as the last two elements of the B vector. When the data exhibit leakage current at low values of N_H, a first-degree polynomial is preferred over a fourth order polynomial in determining $V_g(N_H)$. If a fourth order polynomial is used, and much of the lower data have to be thrown away, then the polynomial may not have sufficient data to maintain a nicely varying curve fit for small values of N_H. Similarly, the tension splines may also experience too much relaxation in the lower data interval. For this reason, data that are unreliable for small values of N_H, $V_g(N_H)$ are curve fit by a first order polynomial. The tension spline fits are by-passed, and both α and β are determined by the first order polynomial. This, of course, forces α to a constant.

Line A1940 determines the order of fit. If it is first order, the matrix AA and vector BB are modified for first order fit. If the order is fourth, both are left alone since they are already set up for a fourth order fit. The rearrangement is done in lines A1960 to A2010.

In lines A2050 and A2060 the (2x2) system is solved by calling the subroutines DECOMP and SOLVE. The least squares coefficients are returned, having been desctructively read back into the array BB.

In lines A2110 and A2120 the same thing is done for the 5x5 system.

Lines A2130 and A2140 determine a variable DUM1 that is zero for a first order fit and one for a fourth order fit.

In lines A2240 to A2360 the polynomial least squares coefficients are defined at both the upper and lower temperatures. Notice that the

variable DUM1 is used to make the proper coefficients go to zero when the order is one. Also, the coefficients are rescaled now, to allow the use of N_H in its proper order of magnitude. The polynomial least squares fit ends here, and the coefficients are printed out in A2460 and A2470.

Again, the order is checked. If the data at the lower end are not reliable, the tension splines are not used, and the entire tension spline setup and least squares evaluation are skipped. The coefficients are not printed out, since they do not exist, and control transfers to A3100.

If tension splines are to be used, however, the next step is to determine the knot array. This is done in A2520 to A2550. This definition of the knots puts about the same number of data points in each interval.

In A2600 to A2630 the working arrays AA and BB are again zeroed. After this, the subroutine SETUP is called. Recall from Appendix B that this subroutine uniquely determines the six splines, N(I), from the knot array and tension array. The tension array here is defined in SETUP. This is done in line A2680. After this, the variable ILEFT is initialized. Again, if it is not initialized, it may assume some arbitrary number in some compilers. Lines A2740 to A2910 fill up the matrix A and the vector B described in Equation B-16. This is the linear system used to find the least squares coefficients for the splines.

Once the linear system has been established, lines A2960 and A2970 call DECOMP and SOLVE. Again, these two subroutines solve the matrix equation AX = B. The answers are returned in the vector BB through SOLVE. Line A3000 finally fills the coefficient array of the six tension splines, called COEF. The coefficients are then printed out in A3010.

At this point, all the curve fitting of the experimental data is done for either order, one or four. A chart is next tabulated for α and β as functions of N_H in A3100 to A3160. This chart allows the results

of the curve fitting to be visually inspected and checked for any unusual anomaly that might have developed.

Now that the curve fitting is done, the next steps are to determine all the partial derivatives needed to calculate C_1, C_2, C_3 and C_4 at a fixed Φ_s. Line A3320 fixes Φ_s.

Recall from Chapter IV, Table 4c, that it was decided to determine $(\partial N_i/\partial T)_{v_s}$ and $(\partial N_d/\partial T)_{v_s}$ by differencing. This is equivalent to finding $(\partial N_e/\partial T)_{v_s}$ and $(\partial N_p/\partial T)_{v_s}$ where N_e and N_p are the quantities ΔN and ΔP defined by Equations 154 and 155. The upper limit in Equations 154 and 155 is v_s. But the data reduction program sweeps Φ_s. The method chosen to do the differencing goes as follows. First, define a ΔT. This is done in line A3210. Next, fix Φ_s, and determine the corresponding value of v_s at the temperature at which one is working (296 K in most cases).

Then set the temperature to a $T + \Delta T$, and calculate all the bulk parameters. Once this is done, Equations 154 and 155 can be integrated to the value of v_s previously found. The integrals then yield $N_e(T+ T)$ and $N_p(T + \Delta T)$. Next, reset the temperature to T, and recalculate the bulk parameters used in Equations 154 and 155. Then reintegrate the same v_s to yield $N_e(T)$ and $N_p(T)$.

Lines A3500 to A3940 do the calculation to obtain $\Delta N_e/\Delta T$ and $\Delta N_p/\Delta T$. Notice that the loop ending in statement number 340 is gone through three times. The first time through, Φ_s is fixed and a value for v_s is determined. This is done at the temperature at which all of these calculations are being made. Once v_s has been found, the loop starts the second time. This is done at line A3730. The second time through the loop, the temperature is shifted slightly, and all the bulk parameters shift value slightly. Those parameters needed to integrate for N_e and N_p are calcu-

lated at $T + \Delta T$ in lines A3590 to A3870. Then $N_e(T + \Delta T)$ and $N_p(T + \Delta T)$ are found in lines A3890 and A3900. These values are stored in temporary storage in lines A3910 and A3920. Then the loop again begins the third time. The temperature is reset to T and the bulk parameters are again recalculated. Then N_e and N_p are recalculated. Finally, in lines A3990 and A4000 the derivatives $(\partial N_e/\partial T)_{v_s}$ and $(\partial N_p/\partial T)_{v_s}$ are found by differencing.

In lines A4040 to A4130 more bulk parameters needed to find the rest of the partial derivatives are calculated. Equations 170 to 183, Chapter IV, are used for the bulk calculations.

Finally, the remaining partial derivatives are evaluated. Lines A4170 and A4180 represent Equations 164 and 165, Chapter IV. Lines A4190 and A4200 are the evaluations of Equations 166 and its hole counterpart. Equations 160 and 161 are evaluated in A4210 and A4220. The factor of 1×10^7 is a joules to ergs conversion. Equation 167 and its hole counterpart are evaluated in A4230 and A4240. Finally, lines A4250 and A4260 evaluate Equations 169 and 170, respectively.

All of the partial derivatives are expressed in terms of hole and electron concentrations. The variables C_1, C_2, C_3 and C_4 are defined in terms of induced and depleted carrier concentrations. For n-channel devices, the induced carrier concentration, $N_i = N_e$, and the depleted carrier concentration $N_d = N_p$. For p-channel devices this is reversed. Lines A4300 to A4480 define the induced and depleted carrier concentrations according to the polarity of the device under examination.

In lines A4530 to A4560 the constants C_1, C_2, C_3 and C_4, as defined by Equations 96 through 99, Chapter III, are evaluated.

Lines A4570 to A4590 define some dummy variables that are useful in tracing problems in the program, and can be ignored in these computations.

Once the four constants C_1, C_2, C_3, and C_4 are known for the value of Φ_s, it is then possible to evaluate w. Thus, Equation 100b can be integrated to yield a value for r. The function w is integrated in line A4640, and r is evaluated in line A4680. This value for r, and the iteration number in trying to get r to converge is printed so the relative contraction rate may be visually inspected. For most of the data here, r converged in one to three iterations.

In line A4730 the relative error on r is examined. If it is within a reasonable tolerance, then N_{ss} is calculated. Either Equations 100A or 100c can be used to evaluate N_{ss}, corresponding to the two lines A4810 and A4820.

If, for some reason, r does not converge after 50 iterations, calculations are terminated and a warning is printed out in line A4750.

If r has converged, N_{ss} is calculated and stored in an answer array, ANS. Along with N_{ss} the current values for Φ_s, r, V_g, N_i and N_H are all stored.

Notice that lines A3500 to A5010 were all done at a fixed Φ_s. At this point, program control goes back to A3260 where a new Φ_s is determined, and the entire set of calculations proceeds again.

Once all the values for Φ_s have been considered, the answer array is printed out. First, the device identifier is put on a new page in line A5030. Then the answers are written out in the order Φ_s, N_{ss}, r, V_g, N_i and N_H for each value of Φ_s. Notice that this table gives a numerical curve for $V_g(\Phi_s)$. After these answers are printed out, then Φ_s, N_{ss}, r and V_g are also punched on cards for each value of Φ_s. These cards then contain the answers and can be used for any further curve fitting or analysis one wishes to do.

b. The Subroutines

Next, consider briefly the subroutines. Some of this has already been discussed elsewhere and will not be mentioned here.

FUNCNH - This subroutine is a statement function of Equation 155,

Chapter IV. It must be integrated to yield N_p or ΔP.

FUNCNE - This subroutine is a statement function of Equation 154, Chapter IV. It must be integrated to yield N_e or ΔN.

G - This subroutine is a statement function of G(v) where G is defined by Equations 148 and 149.

F32 and F12 - These subroutines evaluate the Fermi integrals $F_{3/2}$ and $F_{1/2}$ at a point X.

SIMP - This subroutine is a simple Simpson's integrator.

W, A, B - These function subroutines define w, α, and β. The functions w, α, and β are defined by Equations 76, 77 and 92, respectively, in Chapter III.

The remaining subroutines are discussed in Appendix B.

4. SUMMARY

This appendix has been devoted to two separate areas. Section 2 describes the format that the input data must assume to be used in this program. The total number of input cards needed and individual card formats were explicitly stated.

Section 3 contains a narrative synopsis of how the program operates.

The information in this chapter should be sufficient to allow a prospective user to operate the program.

One final note is that the output of the program will be 30 cards. The number of lines is about 2000 if the listing is not suppressed. The average time needed to run it on a G-level compiler is 220 seconds. This information is needed for any estimated accounting necessary as a job card.

```
C     MICRO HALL MAIN DRIVER PROGRAM                                    A  10
      REAL*8 A,ANS,AREAW,ARG1,B,BOLTZ,C1,C2,C3,C4,COX,EA,EC,ED,EF,EFFMN,  A  20
     1EFFMP,EG,EI,EPSIL,ETA,EV,F,F12,F32,FERMI,FUNCNE,FUNCNH,G,GAMMA,PB,  A  30
     2PHS,PHS1,P1,PLANK,Q,R1,R2,RA1,RA2,RB1,RB2,RC1,RC2,RD1,RD2,RE1,RE2,  A  40
     3SIGN,SQRT2,T,T1,T2,T12,T32,T52,TEMPNE,TEMPNP,TEMPVS,UB,VS,W,WAF,WC  A  50
     4F,WCI,WDF,WVF,WVI,ZETA,LOG2,MAGFLD,DGAMDT                          A  60
      REAL*8 DABS,DECDT,DEFDT,DEGDT,DEIDT,DELTAT,DEVDT,DEXP,DLOG,DNDEDO,  A  70
     1DNDEDT,DNEDOT,DNEDTO,DNEDTP,DNEDTV,DNEDVT,DNINDO,DNPDOT,DNPDTE,DNP  A  80
     2DTO,DNPDTV,DNPDVT,DODTNE,DODTNP,DSQRT,DTDONI,DUBDT,DUM1,DUM2,DUM3,  A  90
     3DVSDT,DWCFDT                                                       A 100
      REAL*8 KAPPA,KT,L,LAMBE,LAMBH,NA,NB,ND,NE,NI,NIND,NP,NSS,NSS1      A 110
      REAL*8 DATA,XX,BB,WORK,AA,COND,COEF,RHO,TAU,TKNOT,VN,VNO,VN2,X     A 120
      INTEGER IPUT(9),INAME(20)                                          A 130
      COMMON C1,C2,C3,C4,COX,DUBDT,ETA,FERMI(501,3),L,LAMBE,LAMBH,NA,NB,  A 140
     1ND,NI,PB,Q,R1,RA1,RA2,RB1,RB2,RC1,RC2,RD1,RD2,RE1,RE2,SQRT2,T,T1,T  A 150
     22,UB,WAF,WCF,WDF,WVF,COEF(9),RHO(7),TKNOT(7),TAU(4),VN(4,4),VNO(7,  A 160
     35),VN2(7,5),IND,NVGPT1,NVGPT2,NORDER                               A 170
      DIMENSION ANS(51,6), DATA(50,30), XX(9), AA(9,9), BB(9), WORK(9)   A 180
      EXTERNAL FUNCNH,FUNCNE,G,F32,F12,W,A,B                             A 190
C                                                                        A 200
C                                                                        A 210
C       READ IN THE FERMI ARRAY. THE ARGUMENT IS IN COLUMN 1. F1/2 AND   A 220
C       F3/2 ARE IN COLUMNS 2 AND 3.                                     A 230
C                                                                        A 240
      DO 110 I=1,501                                                     A 250
      READ (5,430) (FERMI(I,J),J=1,3)                                    A 260
110   CONTINUE                                                           A 270
C                                                                        A 280
C       ZERO THE DATA ARRAY.                                             A 290
C                                                                        A 300
      DO 120 I=1,50                                                      A 310
      DO 120 J=1,30                                                      A 320
      DATA (I,J)=0.D0                                                    A 330
120   CONTINUE                                                           A 340
C                                                                        A 350
C     READ IN AND PRINT OUT THE DEVICE IDENTIFIER AND ALL RAW DATA.      A 360
C     THERE SHOULD BE 2+2*NVGPT1+2*NVGPT2 CARDS SET UP AS FOLLOWS.       A 370
C                                                                        A 380
C       CARD1--DEVICE IDENTIFIER. ANY ALPHA-NUMERIC STRING IN COL 1-80.  A 390
C                                                                        A 400
C       CARD2--10 PARAMETERS READ IN WITH A 7G10.4 FORMAT FOR THE        A 410
C         FIRST 7 REAL VARIABLES AND A 3I3 FORMAT FOR THE NEXT THREE     A 420
C         INTEGER VARIABLES. THE PARAMETERS ARE AS FOLLOWS.              A 430
C         1. ND-DONOR DENSITY,PER CUBIC CM.                              A 440
C         2. NA-ACCEPTOR DENSITY,PER CUBIC CM.                           A 450
C         3. PHS1-INITIAL SURFACE POTENTIAL,UNITS OF KT.                 A 460
C         4. COX-OXIDE CAPACITANCE,FARADS/SQUARE CM.                     A 470
C         5. T1-LOWER TEMPERATURE,DEGREES K.                             A 480
C         6. T2-HIGHER TEMPERATURE,DEGREES K.                            A 490
C         7. MAGFLD-MAGNETIC FIELD STRENGTH,GAUSS                        A 500
C         8. IND=  +1 FOR N-CHANNEL,+2 FOR P-CHANNEL                     A 510
C         9. NVGPT1-THE NUMBER OF DIFFERENT VALUES OF VG THAT THE LOWER  A 520
C            TEMPERATURE DATA WAS TAKEN AT.                              A 530
C         10. NVGPT2-THE NUMBER OF DIFFERENT VALUES OF VG THAT THE       A 540
C            UPPER TEMPERATURE DATA WAS TAKEN AT.                        A 550
```

Figure C-6. A listing of the program.

```
C                                                                       A 560
C       CARDS 3-NVGPT1+2--NINE PARAMETERS IN A FORMAT OF 9G8.4. THE     A 570
C            PARAMETERS ARE VG,I12,V34,I23,V41,I34,V12,I41,V23 AT THE   A 580
C            LOWER TEMP. IN THESE AND ALL REMAINING CASES VG IS IN VOLTS A 590
C            BUT THE OTHER PARAMETERS ARE IN MICROAMPS AND MILLIVOLTS.  A 600
C                                                                       A 610
C       CARDS NVGPT1+3 TO 2*NVGPT1+2--SIX PARAMETERS IN A FORMAT OF     A 620
C            6G8.4. THE PARAMETERS ARE I24,V13,V13 WITH MAGNETIC FIELD, A 630
C            I13,V24,V24 WITH MAGNETIC FIELD AT THE LOWER TEMPERATURE.  A 640
      CONTINUE                                                          A 645
C                                                                       A 650
C       CARDS 2*NVGPT1+3 TO 2*NVGPT1+NVGPT2+2--NINE PARAMETERS IN THE   A 660
C            FORMAT OF 9G8.4.  THE NINE PARAMETERS ARE VG,I12,V34,I23,  A 670
C            V41,I34,V12,I41,V23 AT THE UPPER TEMPERATURE.              A 680
C                                                                       A 690
C       CARDS 2*NVGPT1+NVGPT2+3 TO 2*NVGPT1+2*NVGPT2+2--SIX PARAMETERS  A 700
C            IN THE FORMAT OF 6G8.4. THE PARAMETERS ARE I24,V13,V13     A 710
C            WITH MAGNETIC FIELD,I13,V24,V24 WITH MAGNETIC FIELD AT THE A 720
C            UPPER TEMPERATURE                                          A 730
C                                                                       A 740
      READ (5,440) INAME                                                A 750
      WRITE (6,450) INAME                                               A 760
      READ (5,460) ND,NA,PHS1,COX,T1,T2,MAGFLD,IND,NVGPT1,NVGPT2        A 770
      WRITE (6,470) ND,NA,PHS1,COX,T1,T2,MAGFLD,IND,NVGPT1,NVGPT2       A 780
      READ (5,480) ((DATA(I,J),J=1,9),I=1,NVGPT1)                       A 790
      READ (5,490) ((DATA(I,J),J=10,15),I=1,NVGPT1)                     A 800
      READ (5,480) ((DATA(I,J),J=16,24),I=1,NVGPT2)                     A 810
      READ (5,490) ((DATA(I,J),J=25,30),I=1,NVGPT2)                     A 820
      WRITE (6,500)                                                     A 830
      WRITE (6,510)                                                     A 840
      DO 130 I=1,NVGPT1                                                 A 850
130   WRITE (6,520) (DATA(I,J),J=1,15)                                  A 860
      WRITE (6,530)                                                     A 870
      WRITE (6,510)                                                     A 880
      DO 140 I=1,NVGPT2                                                 A 890
140   WRITE (6,520) (DATA(I,J),J=16,30)                                 A 900
C                                                                       A 910
C       DEFINE INITIAL CONSTANTS                                        A 920
C                                                                       A 930
      BOLTZ=1.380622D-16                                                A 940
      EFFMN=(1.10D0)*(9.11D-28)                                         A 950
      EFFMP=(0.59D0)*(9.11D-28)                                         A 960
      EPSIL=8.854185D-21                                                A 970
      KAPPA=11.7D0                                                      A 980
      LOG2=DLOG(2.D0)                                                   A 990
      PI=3.14159264D0                                                   A1000
      PLANK=6.626196D-27                                                A1010
      Q=1.602192D-19                                                    A1020
      R1=1.D0                                                           A1030
      SQRT2=DSQRT(2.D0)                                                 A1040
      DO 150 I=1,NVGPT1                                                 A1050
      DUM1=(DABS(DATA(I,11)-DATA(I,12))/DATA(I,10)+DABS(DATA(I,14)-DATA( A1060
     11,15))/DATA(I,13))/(2.D-3)                                        A1070
      DATA (I,2)=DATA(I,1)                                              A1080
C                                                                       A1090
```

Figure C-6 (continued)

```
C       CALCULATE NH AT THE LOWER TEMPERATURE AT NVGPT1 GATE VALUES        A1100
C                                                                          A1110
      DATA (I,1)=MAGFLD*1.D-8/(Q*DUM1)                                     A1120
150   CONTINUE                                                             A1130
      DO 160 I=1,NVGPT2                                                    A1140
      DUM1=(DABS(DATA(I,26)-DATA(I,27))/DATA(I,25)+DABS(DATA(I,29)-DATA(   A1150
     1I,30))/DATA(I,28))/(2.D-3)                                           A1160
      DATA (I,4)=DATA(I,16)                                                A1170
C                                                                          A1180
C       CALCULATE NH AT THE UPPER TEMPERATURE                              A1190
C                                                                          A1200
      DATA (I,3)=MAGFLD*1.D-8/(Q*DUM1)                                     A1210
      DATA (I,6)=DUM1                                                      A1220
C                                                                          A1230
C       CALCULATE THE CONDUCTIVITY AT THE UPPER TEMPERATURE                A1240
C                                                                          A1250
      DUM1=(DATA(I,17)/DATA(I,18)+DATA(I,19)/DATA(I,20)+DATA(I,21)/DATA(   A1260
     1I,22)+DATA(I,23)/DATA(I,24))/4.D3                                    A1270
      DATA (I,5)=DUM1*LOG2/PI                                              A1280
C                                                                          A1290
C       CALCULATE THE MOBILITY AT THE UPPER TEMPERATURE                    A1300
C                                                                          A1310
      DATA (I,7)=1.D8*DATA(I,5)*DATA(I,6)/MAGFLD                           A1320
160   CONTINUE                                                             A1330
      K=MAXO(NVGPT1,NVGPT2)                                                A1340
      WRITE (6,540)                                                        A1350
      DO 170 I=1,K                                                         A1360
C                                                                          A1370
C       PRINT OUT NH AND VG AT THE LOWER TEMPERATURE AND NH,VG,            A1380
C         CONDUCTIVITY,TOTAL SHEET RESISTANCE,AND MOBILITY FOR THE UPPER   A1390
C         TEMPERATURE                                                      A1400
C                                                                          A1410
170   WRITE (6,550) (DATA(I,J),J=1,7)                                      A1420
      WRITE (6,560)                                                        A1430
      DO 180 I=1,K                                                         A1440
C                                                                          A1450
C       SCALE NH FOR THE POLYNOMIAL CURVE FITTING                          A1460
C                                                                          A1470
      DATA (I,1)=DATA(I,1)/1.D11                                           A1480
      DATA (I,3)=DATA(I,3)/1.D11                                           A1490
180   CONTINUE                                                             A1500
C                                                                          A1510
C       BEGIN POLYNOMIAL LEAST SQUARES CURVE FITTING                       A1520
C                                                                          A1530
C                                                                          A1540
C       ZERO THE WORKING ARRAYS USED IN SOLVING THE LINEAR SYSTEM          A1550
C         A*X=B. HERE A IS A SYMMETRIC SQUARE MATRIX, AND X AND B ARE      A1560
C         VECTORS. THE VECTOR X CONTAINS THE LEAST SQUARES POLYNOMIAL      A1570
C         COEFFICIENTS AFTER THE SYSTEM HAS BEEN SOLVED.                   A1580
C                                                                          A1590
      DO 270 N=1,2                                                         A1600
      DO 190 I=1,9                                                         A1610
      BB(I)=0.D0                                                           A1620
      IPVT(I)=0                                                            A1630
      WORK(I)=0.D0                                                         A1640
```

Figure C-6 (continued)

```
      XX(I)=0.D0                                                        A1650
      DO 190 J=1,9                                                      A1660
190   AA(I,J)=0.D0                                                      A1670
C                                                                       A1680
C       CALCULATE THE VALUES FOR THE INDIVIDUAL ELEMENTS OF THE A AND B A1690
C         ARRAY. THE VALUES FOR A ARE STORED IN THE TEMPORARY ARRAY XX. A1700
C                                                                       A1710
      XX(1)=NVGPT1                                                      A1720
      M=NVGPT1                                                          A1730
      IF (N.EQ.2) XX(1)=NVGPT2                                          A1740
      IF (N.EQ.2) M=NVGPT2                                              A1750
      DO 220 KK=1,M                                                     A1760
      DO 200 K=1,8                                                      A1770
200   XX(K+1)=XX(K+1)+DATA(KK,2*N-1)**K                                 A1780
      DO 210 K=1,4                                                      A1790
210   BB(K)=BB(K)+DATA(KK,2*N)*DATA(KK,2*N-1)**(5-K)                    A1800
      BB(5)=BB(5)+DATA(KK,2*N)                                          A1810
220   CONTINUE                                                          A1820
      DO 230 I=1,5                                                      A1830
      DO 230 J=1,5                                                      A1840
      INDEX=11-(I+J)                                                    A1850
C                                                                       A1860
C       FILL THE ELEMENTS OF THE ARRAY A WITH THE VALUES STORED IN XX   A1870
C                                                                       A1880
230   AA(I,J)=XX(INDEX)                                                 A1890
C                                                                       A1900
C       IF NORDER=1, A FIRST ORDER POLYNOMIAL IS USED TO FIT VG(NH).    A1910
C         IF NORDER=4,A FOURTH ORDER POLYNOMIAL IS USED.                A1920
C                                                                       A1930
      NORDER=4                                                          A1940
      IF (NORDER.EQ.4) GO TO 240                                        A1950
      AA(1,1)=AA(4,4)                                                   A1960
      AA(2,2)=AA(5,5)                                                   A1970
      AA(1,2)=AA(4,5)                                                   A1980
      AA(2,1)=AA(1,2)                                                   A1990
      BB(1)=BB(4)                                                       A2000
      BB(2)=BB(5)                                                       A2010
C                                                                       A2020
C       SOLVE THE 2 X 2 SYSTEM A*X=B.                                   A2030
C                                                                       A2040
      CALL DECOMP (9,2,AA,COND,IPVT,WORK)                               A2050
      CALL SOLVE (9,2,AA,BB,IPVT)                                       A2060
      GO TO 250                                                         A2070
C                                                                       A2080
C       SOLVE THE 5 X 5 SYSTEM A*X=B.                                   A2090
C                                                                       A2100
240   CALL DECOMP (9,5,AA,COND,IPVT,WORK)                               A2110
      CALL SOLVE (9,5,AA,BB,IPVT)                                       A2120
250   IDUM1=NORDER/4                                                    A2130
      DUM1=IDUM1                                                        A2140
C                                                                       A2150
C       RESCALE THE COEFFICIENTS. DUM1=0 FOR A FIRST ORDER POLYNOMIAL.  A2160
C         DUM1=1 FOR A FOURTH ORDER POLYNOMIAL. COEFFICIENTS ENDING IN 1 A2170
C         OR 2 RESPECTIVLY REFER TO THE LOWER AND UPPER TEMPERATURES    A2180
C         RESPECTIVELY. THE POLYNOMIAL HAS THE FORM                     A2190
```

Figure C-6 (continued)

```
C                 Y=A*X**4+B*X**3+C*X**2+D*X+E                          A2200
C         WHERE Y IS VG AND X IS NH. THE COEFFICIENTS A,ETC REFER TO    A2210
C         RA1 ETC.                                                      A2220
C                                                                       A2230
      IF (N.EQ.2) GO TO 260                                             A2240
      RA1=BB(1)*1.D-44*DUM1                                             A2250
      RB1=BB(2)*1.D-33*DUM1                                             A2260
      RC1=BB(3)*1.D-22*DUM1                                             A2270
      RD1=BB(NORDER)*1.D-11                                             A2280
      RE1=BB(NORDER+1)                                                  A2290
      GO TO 270                                                         A2300
260   RA2=BB(1)*1.D-44*DUM1                                             A2310
      RB2=BB(2)*1.D-33*DUM1                                             A2320
      RC2=BB(3)*1.D-22*DUM1                                             A2330
      RD2=BB(NORDER)*1.D-11                                             A2340
      RE2=BB(NORDER+1)                                                  A2350
270   CONTINUE                                                          A2360
C                                                                       A2370
C       END POLYNOMIAL LEAST SQUARES FIT.                               A2380
C                                                                       A2390
      I=1                                                               A2400
      J=2                                                               A2410
C                                                                       A2420
C       PRINT OUT THE LEAST SQUARES POLYNOMIAL COEFFICIENTS FOR THE     A2430
C         LOWER AND UPPER TEMPERATURES RESPECTIVELY.                    A2440
C                                                                       A2450
      WRITE (6,570) I,RA1,I,RB1,I,RC1,I,RD1,I,RE1                       A2460
      WRITE (6,570) J,RA2,J,RB2,J,RC2,J,RD2,J,RE2                       A2470
      WRITE (6,560)                                                     A2480
C                                                                       A2490
C       DETERMINE THE KNOT ARRAY FOR THE TENSION SPLINES.               A2500
C         IF NORDER=1, THE TENSION SPLINES DO NOT HAVE TO BE            A2504
C         EVALUATED. IN THIS CASE, ALPHA IS DETERMINED BY A LINEAR      A2505
C         POLYNOMIAL FIT TO THE DATA.                                   A2506
C                                                                       A2510
      IF(NORDER.EQ.1) GO TO 325                                         A2515
      TKNOT(1)=0.D0                                                     A2520
      TKNOT(2)=DATA((NVGPT2/3+2),3)                                     A2530
      TKNOT(3)=DATA((2*NVGPT2/3),3)                                     A2540
      TKNOT(4)=DATA(NVGPT2,3)+1.D0                                      A2550
C                                                                       A2560
C       ZERO THE WORKING ARRAYS NEEDED TO LEAST SQUARES FIT THE         A2570
C         COEFFICIENTS FOR THE TENSION SPLINES.                         A2580
C                                                                       A2590
      DO 280 I=1,9                                                      A2600
      BB(I)=0.D0                                                        A2610
      DO 280 J=1,9                                                      A2620
280   AA(I,J)=0.D0                                                      A2630
C                                                                       A2640
C       CALL THE SUBROUTINE THAT SETS UP THE TENSION SPLINE BASIS       A2650
C         FUNCTIONS ONCE THE KNOT SEQUENCE HAS BEEN DEFINED.            A2660
C                                                                       A2670
      CALL SETUP                                                        A2680
      ILEFT=1                                                           A2690
C                                                                       A2700
```

Figure C-6 (continued)

```
C       FILL UP THE ARRAYS AA AND BB IN THE LINEAR SYSTEM AA*X=BB. THIS    A2710
C         LINEAR SYSTEM IS SOLVED IN ORDER TO LEAST SQUARES FIT THE        A2720
C         TENSION SPLINES TO THE DATA.                                     A2730
C                                                                          A2740
      DO 310 KK=1,NVGPT2                                                   A2750
      X=DATA(KK,3)                                                         A2760
C                                                                          A2770
C       CALL THE SUBROUTINE THAT LOCATES WHICH KNOTS A VALUE X LIES        A2780
C         BETWEEN.                                                         A2790
C                                                                          A2800
      CALL INT (X,ILEFT)                                                   A2810
C                                                                          A2820
C       EVALUATE ALL NON-ZERO SPLINES AT THE POINT X.                      A2830
C                                                                          A2840
      CALL VALN (X,ILEFT)                                                  A2850
      ILP3=ILEFT+3                                                         A2860
      DO 300 II=ILEFT,ILP3                                                 A2870
      DO 290 JJ=ILEFT,ILP3                                                 A2880
290   AA(II,JJ)=AA(II,JJ)+VN(ILEFT+4-II,1)*VN(ILEFT+4-JJ,1)                A2890
300   BB(II)=BB(II)+DATA(KK,4)*VN(ILEFT+4-II,1)                            A2900
310   CONTINUE                                                             A2910
C                                                                          A2920
C       SOLVE THE LINEAR SYSTEM FOR THE LEAST SQUARES VALUES OF THE        A2930
C         SPLINE COEFFICIENTS.                                             A2940
C                                                                          A2950
      CALL DECOMP (9,6,AA,COND,IPVT,WORK)                                  A2960
      CALL SOLVE (9,6,AA,BB,IPVT)                                          A2970
      DO 320 I=1,9                                                         A2980
320   COEF(I)=BB(I)                                                        A2990
C                                                                          A3000
C       PRINT OUT THE SIX VALUES OF THE LEAST SQUARES SPLINE COEF.         A3010
C                                                                          A3020
      WRITE (6,580) (COEF(I),I=1,6)                                        A3030
      WRITE (6,560)                                                        A3040
      WRITE (6,590)                                                        A3050
325   CONTINUE                                                             A3055
C                                                                          A3060
C       TABULATE A CHART FOR BETA(B) AND ALPHA(A) FOR VARIOUS VALUES       A3070
C         OF NH. THIS IS DONE STRICTLY FOR VISUAL INSPECTION.              A3080
C                                                                          A3090
      DO 330 I=2,40,2                                                      A3100
      RI=I                                                                 A3110
      DUM1=RI*1.E11                                                        A3120
      DUM2=B(DUM1)                                                         A3130
      DUM3=A(DUM1)                                                         A3140
330   WRITE (6,600) DUM1,DUM2,DUM3                                         A3150
      WRITE (6,610)                                                        A3160
C                                                                          A3170
C       DETERMINE A DELTA T USED TO NUMERICALLY CALCULATE PARTIAL NE-      A3180
C         PARTIAL T WITH VS HELD CONSTANT.                                 A3190
C                                                                          A3200
      DELTAT=1.D-4*T2                                                      A3210
C                                                                          A3220
C       THIS LOOP FIXES A VALUE OF THE SURFACE POTENTIAL,AND CALCULATES    A3230
C         NSS,R,AND W AT THIS VALUE OF THE SURFACE POTENTIAL.              A3240
```

Figure C-6 (continued)

```
C                                                                       A3250
      DO 390 NUM=1,31                                                   A3260
C                                                                       A3270
C       FIX THE VALUE OF THE SURFACE POTENTIAL. THE INITIAL VALUE OF    A3280
C         PHS IS PHS1,WHICH IS READ IN IN UNITS OF KT. NOTE THAT PHS    A3290
C         SWEEPS THROUGH 6 KT.                                          A3300
C                                                                       A3310
      PHS=PHS1-(NUM-1)*.20D0                                            A3320
C                                                                       A3330
C       THIS LOOP DOES THE FOLLOWING CALCULATIONS.                      A3340
C         1--SET T=UPPER TEMPERATURE.                                   A3350
C         2--CALCULATE ALL BULK PARAMETERS AS WELL AS VS, THE UPPER     A3360
C            LIMIT IN THE INTEGRAL CALCULATING THE EXCESS SURFACE HOLE  A3370
C            AND ELECTRON CONCENTRATIONS. STORE THIS VALUE OF VS        A3380
C            IN TEMPVS.                                                 A3390
C         3--RESET T=UPPER TEMPERATURE+DELTAT.                          A3400
C         4--RECALCULATE THE BULK PARAMETERS, BUT SET VS=TEMPVS.        A3410
C         5--CALCULATE THE ELECTRON AND HOLE SURFACE DENSITIES.         A3420
C            STORE THESE VALUES IN TEMPNE AND TEMPNP RESPECTIVELY.      A3430
C         6--RESET T=UPPER TEMPERATURE AGAIN.                           A3440
C         7--RECALCULATE ALL THE BULK PARAMETERS INCLUDING VS, WHICH    A3450
C            SHOULD NOW HAVE THE SAME VALUE IT ASSUMED IN STEP 1.       A3460
C         8--CALCULATE A NEW VALUE FOR THE ELECTRON AND HOLE DENSITIES  A3470
C            NE AND NP RESPECTIVELY.                                    A3480
C                                                                       A3490
      DO 340 KK=1,3                                                     A3500
      T=T2                                                              A3510
      IF (KK.EQ.2) T=T2+DELTAT                                          A3520
      T12=DSQRT(T)                                                      A3530
      T32=T12*T12*T12                                                   A3540
      T52=T32*T12*T12                                                   A3550
C                                                                       A3560
C       CALCULATE MORE BULK PARAMETERS.                                 A3570
C                                                                       A3580
      KT=BOLTZ*T                                                        A3590
      EG=(1.1551-0.00023*T)*1.602192D-12                                A3600
      GAMMA=EG/(2.D0*BOLTZ)                                             A3610
      ZETA=2.D0*((2.D0*PI*BOLTZ/(PLANK*PLANK))**1.5)*((EFFMN*EFFMP)**.75 A3620
     1)                                                                 A3630
      ARG1=(ND-NA)/(2.D0*ZETA*T32*DEXP(-GAMMA/T))                       A3640
      UB=(ARG1/DABS(ARG1))*DLOG(DABS(ARG1)+DSQRT((ARG1*ARG1)+1.D0))     A3650
      EI=(EG/2.D0)-0.75D0*KT*DLOG(EFFMN/EFFMP)                          A3660
      EF=EI+KT*UB                                                       A3670
      EC=EG                                                             A3680
      WCF=(EC-EF)/KT                                                    A3690
      VS=WCF+PHS                                                        A3700
      IF (KK.EQ.2) VS=TEMPVS                                            A3710
      TEMPVS=VS                                                         A3720
      IF (KK.EQ.1) GO TO 340                                            A3730
      ED=0.9586*EG                                                      A3740
      EA=0.041398*EG                                                    A3750
      EV=0.D0                                                           A3760
      LAMBE=4.D0*PI*((2.D0*EFFMN*KT/(PLANK*PLANK))**1.5)                A3770
      LAMBH=4.D0*PI*((2.D0*EFFMP*KT/(PLANK*PLANK))**1.5)                A3780
      WCI=(EC-EI)/KT                                                    A3790
```

Figure C-6 (continued)

```
      WVI=(EV-EI)/KT                                                    A3800
      WVF=(EV-EF)/KT                                                    A3810
      WAF=(EA-EF)/KT                                                    A3820
      WDF=(ED-EF)/KT                                                    A3830
      NB=LAMBE*F12(-WCF)                                                A3840
      PB=LAMBH*F12(WVF)                                                 A3850
      NI=LAMBE*F12(-WCI)                                                A3860
      L=(KAPPA*EPSIL*KT/(2.D0*Q*Q*NI))**0.5                             A3870
      SIGN=(-1.D0)**IND                                                 A3880
      CALL SIMP (FUNCNE,VS,1.D-5,NE)                                    A3890
      CALL SIMP (FUNCNH,VS,1.D-5,NP)                                    A3900
      IF (KK.EQ.3) GO TO 340                                            A3910
      TEMPNE=NE                                                         A3920
      TEMPNP=NP                                                         A3930
340   CONTINUE                                                          A3940
C                                                                       A3950
C       CALCULATE THE DERIVATIVE OF NE AND NP WITH RESPECT TO T HOLDING A3960
C         VS CONSTANT.                                                  A3970
C                                                                       A3980
      DNEDTV=(TEMPNE-NE)/DELTAT                                         A3990
      DNPDTV=(TEMPNP-NP)/DELTAT                                         A4000
C                                                                       A4010
C       DETERMINE MORE NEEDED BULK PARAMETERS AT THE UPPER TEMPERATURE. A4020
C                                                                       A4030
      DEGDT=2.3D-4*1.602192D-12                                         A4040
      DGAMDT=DEGDT/(2.D0*BOLTZ)                                         A4050
      DUBDT=((NA-ND)*DEXP(GAMMA/T)*(1.5D0+GAMMA/T-DGAMDT))/(T52*2.D0*ZET A4060
     1A*DSQRT((ARG1*ARG1)+1.D0))                                        A4070
      DEIDT=(DEGDT/2.D0)-0.75D0*BOLTZ*DLOG(EFFMN/EFFMP)                 A4080
      DEFDT=DEIDT+(BOLTZ*UB+KT*DUBDT)                                   A4090
      DECDT=DEGDT                                                       A4100
      DEVDT=0.D0                                                        A4110
      DWCFDT=-(WCF/T)+(DECDT-DEFDT)/KT                                  A4120
      DVSDT=DWCFDT-(PHS/T)                                              A4130
C                                                                       A4140
C       CALCULATE ALL THE REMAINING NEEDED PARTIAL DERIVATIVES.         A4150
C                                                                       A4160
      DNEDVT=-FUNCNE(VS)                                                A4170
      DNPDVT=-FUNCNH(VS)                                                A4180
      DNEDTO=DNEDVT*DVSDT+DNEDTV                                        A4190
      DNPDTO=DNPDVT*DVSDT+DNPDTV                                        A4200
      DNEDOT=Q*1.D7*DNEDVT/KT                                           A4210
      DNPDOT=Q*1.D7*DNPDVT/KT                                           A4220
      DODTNE=-DNEDTO/DNEDOT                                             A4230
      DODTNP=-DNPDTO/DNPDOT                                             A4240
      DNEDTP=(DNEDOT*DODTNP)+DNEDTO                                     A4250
      DNPDTE=(DNPDOT*DODTNE)+DNPDTO                                     A4260
      IF (IND.EQ.1) GO TO 350                                           A4270
C                                                                       A4280
C       SET UP THE PROPER PARTIAL DERIVATIVE DEFINITIONS FOR P-CHANNEL  A4290
C         DEVICES.                                                      A4300
C                                                                       A4310
      NIND=NP                                                           A4320
      DNINDO=DNPDOT                                                     A4330
      DNDEDO=DNEDOT                                                     A4340
```

Figure C-6 (continued)

```
      DTDONI=1.D0/DODTNP                                                A4350
      DNDEDT=DNEDTP                                                     A4360
      GO TO 360                                                         A4370
C                                                                       A4380
C       SET UP THE PROPER PARTIAL DERIVATIVE DEFINITIONS FOR N CHANNEL  A4390
C         DEVICES                                                       A4400
C                                                                       A4410
350   NIND=NE                                                           A4420
      DNINDO=DNEDOT                                                     A4430
      DNDEDO=DNPDOT                                                     A4440
      DTDONI=1.D0/DODTNE                                                A4450
      DNDEDT=DNPDTE                                                     A4460
360   CONTINUE                                                          A4470
      WRITE (6,620)                                                     A4480
C                                                                       A4490
C       DETERMINE C1,C2,C3 AND C4 NECESSARY IN CALCULATING W. NOTE THAT A4500
C         W MUST BE INTEGRATED IN ORDER TO OBTAIN NSS.                  A4510
C                                                                       A4520
      C1=DNINDO                                                         A4530
      C2=(((-1)**IND)*DNINDO)-(COX/Q)+((-1)**IND)*DNDEDO                A4540
      C3=DTDONI                                                         A4550
      C4=(((-1)**IND)*DTDONI*DNDEDT)-COX/Q                              A4560
      DUM1=B(NIND)                                                      A4570
      DUM2=A(NIND)                                                      A4580
      DUM3=W(NIND)                                                      A4590
      DO 370 I=1,50                                                     A4600
C                                                                       A4610
C       INTEGRATE W.                                                    A4620
C                                                                       A4630
      CALL SIMP (W,1.D8,NIND,AREAW)                                     A4640
C                                                                       A4650
C       DETERMINE R.                                                    A4660
C                                                                       A4670
      R2=NIND/AREAW                                                     A4680
      WRITE (6,630) R2,I                                                A4690
C                                                                       A4700
C       CHECK TO SEE IF R HAS CONVERGED.                                A4710
C                                                                       A4720
      IF (DABS(R1-R2).LE.5.D-3) GO TO 380                               A4730
370   R1=R2                                                             A4740
      WRITE (6,640)                                                     A4750
      GO TO 420                                                         A4760
C                                                                       A4770
C       ONCE R HAS CONVERGED,CALCULATE NSS. THIS CAN BE DONE WITH       A4780
C         EITHER OF TWO EXPRESSIONS.                                    A4790
C                                                                       A4800
380   NSS1=(C1*A(NIND)*W(NIND))+C2                                      A4810
      NSS=C3*B(NIND)+C4                                                 A4820
C                                                                       A4830
C       STORE THE FOLLOWING DATA IN THE ANSWER ARRAY AT EACH VALUE OF   A4840
C         THE SURFACE POTENTIAL.                                        A4850
C         1--SURFACE POTENTIAL.                                         A4860
C         2--NSS                                                        A4870
C         3--R                                                          A4880
C         4--VG                                                         A4890
```

Figure C-6 (continued)

```
C          5--N-INDUCED.(INDUCED CARRIER CONCENTRATION.) THIS IS NE FOR     A4900
C             N-CHANNEL AND NP FOR P-CHANNEL.                               A4910
C          6--NB,THE HALL CARRIER CONCENTRATION.                            A4920
C                                                                           A4930
      ANS(NUM,1)=PHS                                                        A4940
      ANS(NUM,2)=NSS1                                                       A4950
      ANS(NUM,3)=R2                                                         A4960
      ANS(NUM,4)=RA2*(NIND/R2)**4+RB2*(NIND/R2)**3+RC2*(NIND/R2)**2+RD2*    A4970
     1(NIND/R2)+RE2                                                         A4980
      ANS(NUM,5)=NIND                                                       A4990
      ANS(NUM,6)=NIND/R2                                                    A5000
390   CONTINUE                                                              A5010
C                                                                           A5020
C       WRITE THE DEVICE IDENTIFIER NAME ON THE FINAL ANSWER PAGE.          A5030
C                                                                           A5040
      WRITE (6,450) INAME                                                   A5050
      WRITE (6,650)                                                         A5060
C                                                                           A5070
C       WRITE OUT THE FINAL ANSWER ARRAY AND PUNCH THE ANSWERS ON CARDS     A5080
C                                                                           A5090
      DO 400 I=1,NUM                                                        A5100
400   WRITE (6,660) (ANS(I,J),J=1,6)                                        A5110
      WRITE (7,440) INAME                                                   A5120
      DO 410 I=1,NUM                                                        A5130
410   WRITE (7,670) (ANS(I,J),J=1,4)                                        A5140
420   CONTINUE                                                              A5150
      STOP                                                                  A5160
C                                                                           A5170
C                                                                           A5180
C                                                                           A5190
C                                                                           A5200
C                                                                           A5210
430   FORMAT (G20.13,5X,G20.13,5X,G20.13)                                   A5220
440   FORMAT (20A4)                                                         A5230
450   FORMAT (1H1,37X,20A4,//)                                              A5240
460   FORMAT (7G10.4,3I3)                                                   A5250
470   FORMAT (9X,3HND=,G10.4,5X,3HNA=,G10.4,5X,5HPHS1=,G10.4,5X,4HCOX=,G    A5260
     110.4,/,9X,3HI1=,G10.4,5X,3HI2=,G10.4,5X,7HMAGFLD=,G10.4,3X,4HIND=,    A5270
     2I3,/,9X,7HNVGPT1=,I3,9X,7HNVGPT2=,I3,/)                               A5280
480   FORMAT (9G8.4)                                                        A5290
490   FORMAT (6G8.4)                                                        A5300
500   FORMAT (31X,26HRAW DATA-LOWER TEMPERATURE,/)                          A5310
510   FORMAT (9X,2HVG,6X,3HI12,5X,3HV34,5X,3HI23,5X,3HV41,5X,3HI34,5X,3H    A5320
     1V12,5X,3HI41,5X,3HV23,5X,3HI24,5X,3HV13,3X,5HV13+B,5X,3HI13,5X,3HV    A5330
     224,4X,5HV24+B,/)                                                      A5340
520   FORMAT (5X,15F8.3)                                                    A5350
530   FORMAT (1X,/,31X,26HRAW DATA-UPPER TEMPERATURE,/)                     A5360
540   FORMAT (1H1,6X,9HNH(T-LOW),8X,9HVG(T-LOW),11X,10HNH(T-HIGH),8X,10H    A5370
     1VG(T-HIGH),9X,12HCONDUCTIVITY,11X,1HR,14X,8HMOBILITY,/)               A5380
550   FORMAT (1X,5X,G10.4,6(9X,G10.4))                                      A5390
560   FORMAT (1X,//)                                                        A5400
570   FORMAT (6X,1HA,I1,1H=,G11.4,5X,1HB,I1,1H=,G11.4,5X,1HC,I1,1H=,G11.    A5410
     14,5X,1HD,I1,1H=,G11.4,5X,1HE,I1,1H=,G11.4)                            A5420
580   FORMAT (6X,6(G10.4,5X))                                               A5430
590   FORMAT (1X,17X,2HNH,12X,4HBETA,14X,5HALPHA,/)                         A5440
```

Figure C-6 (continued)

```
600   FORMAT (12X,2(G15.7,5X),G15.7)                                    A5450
610   FORMAT (1H1)                                                      A5460
620   FORMAT (1HO,20X,11HVALUE FOR R,20X,9HITERATION)                   A5470
630   FORMAT (1H ,20X,G10.4,21X,I3)                                     A5480
640   FORMAT (1HO,40HR IS EITHER NOT A CONTRACTION OR IS SLOW,11H CONVER A5490
     1GING)                                                             A5500
650   FORMAT (1X,19X,3HPHS,18X,3HNSS,16X,1HR,19X,2HVG,19X,4HNIND,17X,2HN A5510
     1H,/)                                                              A5520
660   FORMAT (1H ,17X,G10.4,5(10X,G10.4))                               A5530
670   FORMAT (4(G15.6,5X))                                              A5540
      END                                                               A5550-
      FUNCTION FUNCNH (V)                                               B  10
C                                                                       B  20
C       THIS FUNCTION SUBROUTINE DEFINES THE FUNCTION THAT MUST BE      B  30
C         INTEGRATED TO YIELD THE EXCESS HOLE CONCENTRATION AT THE      B  40
C         SILICON SURFACE.                                              B  50
C                                                                       B  60
      REAL*8 C1,C2,C3,C4,COX,DUBDT,ETA,FERMI,L,LAMBE,LAMBH,NA,NB,ND,NI,P B  70
     1B,Q,R1,RA1,RA2,RB1,RB2,RC1,RC2,RD1,RD2,RE1,RE2,SQRT2,T,T1,T2,UB,WA B  80
     2F,WCF,WDF,WVF,COEF,RHO,TAU,TKNOT,VN,VN0,VN2                       B  90
      REAL*8 F12,FUNCNH,G,SIGN,V                                        B 100
      COMMON C1,C2,C3,C4,COX,DUBDT,ETA,FERMI(501,3),L,LAMBE,LAMBH,NA,NB,B 110
     1ND,NI,PB,Q,R1,RA1,RA2,RB1,RB2,RC1,RC2,RD1,RD2,RE1,RE2,SQRT2,T,T1,T B 120
     22,UB,WAF,WCF,WDF,WVF,COEF(9),RHO(7),TKNOT(7),TAU(4),VN(4,4),VN0(7,B 130
     35),VN2(7,5),IND,NVGPT1,NVGPT2,NORDER                              B 140
      SIGN=(-1.D0)**IND                                                 B 150
      FUNCNH=L*((LAMBH*F12(WVF-V)-PB)/G(V))*SIGN                        B 160
      RETURN                                                            B 170
C                                                                       B 180
C                                                                       B 190
      END                                                               B 200-
      FUNCTION FUNCNE (V)                                               C  10
C                                                                       C  20
C       THIS FUNCTION SUBROUTINE DEFINES THE FUNCTION THAT MUST BE      C  30
C         INTEGRATED TO YIELD THE EXCESS ELECTRON CONCENTRATION AT THE  C  40
C         SILICON SURFACE.                                              C  50
C                                                                       C  60
      REAL*8 C1,C2,C3,C4,COX,DUBDT,ETA,FERMI,L,LAMBE,LAMBH,NA,NB,ND,NI,P C  70
     1B,Q,R1,RA1,RA2,RB1,RB2,RC1,RC2,RD1,RD2,RE1,RE2,SQRT2,T,T1,T2,UB,WA C  80
     2F,WCF,WDF,WVF,COEF,RHO,TAU,TKNOT,VN,VN0,VN2                       C  90
      REAL*8 F12,FUNCNE,G,SIGN,V                                        C 100
      COMMON C1,C2,C3,C4,COX,DUBDT,ETA,FERMI(501,3),L,LAMBE,LAMBH,NA,NB,C 110
     1ND,NI,PB,Q,R1,RA1,RA2,RB1,RB2,RC1,RC2,RD1,RD2,RE1,RE2,SQRT2,T,T1,T C 120
     22,UB,WAF,WCF,WDF,WVF,COEF(9),RHO(7),TKNOT(7),TAU(4),VN(4,4),VN0(7,C 130
     35),VN2(7,5),IND,NVGPT1,NVGPT2,NORDER                              C 140
      SIGN=(-1.D0)**IND                                                 C 150
      FUNCNE=L*((LAMBE*F12(V-WCF)-NB)/G(V))*SIGN                        C 160
      RETURN                                                            C 170
C                                                                       C 180
C                                                                       C 190
      END                                                               C 200-
      FUNCTION G (V)                                                    D  10
C                                                                       D  20
C       THIS FUNCTION SUBROUTINE DEFINES  THE DENOMINATOR THAT APPEARS  D  30
C         IN THE FUNCTIONS FUNCNE AND FUNCNH.                           D  40
```

Figure C-6 (continued)

```
C                                                                       D  50
      REAL*8 C1,C2,C3,C4,COX,DUBDT,ETA,FERMI,L,LAMBE,LAMBH,NA,NB,ND,NI,P D  60
     1B,Q,R1,RA1,RA2,RB1,RB2,RC1,RC2,RD1,RD2,RE1,RE2,SQRT2,T,T1,T2,UB,WA D  70
     2F,WCF,WDF,WVF,COEF,RHO,TAU,TKNOT,VN,VNO,VN2                       D  80
      REAL*8 D1,D2,D3,D4,DEXP,DLOG,DSQRT,F12,F32,G,V,DABS,DM            D  90
      COMMON C1,C2,C3,C4,COX,DUBDT,ETA,FERMI(501,3),L,LAMBE,LAMBH,NA,NB, D 100
     1ND,NI,PB,Q,R1,RA1,RA2,RB1,RB2,RC1,RC2,RD1,RD2,RE1,RE2,SQRT2,T,T1,T D 110
     22,UB,WAF,WCF,WDF,WVF,COEF(9),RHO(7),TKNOT(7),TAU(4),VN(4,4),VNO(7, D 120
     35),VN2(7,5),IND,NVGPT1,NVGPT2,NORDER                              D 130
      D1=DLOG((1.D0+.5D0*DEXP(WDF-V))/(1.D0+.5D0*DEXP(WDF)))            D 140
      D2=DLOG((1.D0+.5D0*DEXP(V-WAF))/(1.D0+.5D0*DEXP(-WAF)))           D 150
      D3=2.D0*(F32(WVF)-F32(WVF-V))/(3.D0*F12(WVF+UB))                  D 160
      D4=2.D0*(F32(V-WCF)-F32(-WCF))/(3.D0*F12(-UB-WCF))                D 170
      DM=DABS(((ND*D1+NA*D2)/NI)-D3+D4)                                 D 180
      G=DSQRT(DM)                                                       D 190
      RETURN                                                            D 200
C                                                                       D 210
C                                                                       D 220
      END                                                               D 230-
      FUNCTION F32 (X)                                                  E  10
C                                                                       E  20
C       THIS FUNCTION SUBROUTINE DETERMINES THE FERMI INTEGRAL F3/2 AT   E  30
C         THE ARGUMENT X. A TABLE,FERMI(501,3), HAS THE VALUE OF F1/2   E  40
C         AND F3/2 IN COLUMNS 2 AND 3. THE ARGUEMENT IS STORED IN       E  50
C         COLUMN 1 AND GOES FROM -50 TO 450 BY INCREMENTS OF 0.2. THIS  E  60
C         SUBROUTINE LOCATES X BETWEEN TWO ARGUEMENTS VALUES IN THE     E  70
C         TABLE AND DOES A LINEAR INTERPOLATION TO FIND THE             E  80
C         VALUE OF F3/2 BETWEEN THE TWO KNOWN, TABULATED VALUES.        E  90
C                                                                       E 100
      REAL*8 C1,C2,C3,C4,COX,DUBDT,ETA,FERMI,L,LAMBE,LAMBH,NA,NB,ND,NI,P E 110
     1B,Q,R1,RA1,RA2,RB1,RB2,RC1,RC2,RD1,RD2,RE1,RE2,SQRT2,T,T1,T2,UB,WA E 120
     2F,WCF,WDF,WVF,COEF,RHO,TAU,TKNOT,VN,VNO,VN2                       E 130
      REAL*8 F32,R,X                                                    E 140
      COMMON C1,C2,C3,C4,COX,DUBDT,ETA,FERMI(501,3),L,LAMBE,LAMBH,NA,NB, E 150
     1ND,NI,PB,Q,R1,RA1,RA2,RB1,RB2,RC1,RC2,RD1,RD2,RE1,RE2,SQRT2,T,T1,T E 160
     22,UB,WAF,WCF,WDF,WVF,COEF(9),RHO(7),TKNOT(7),TAU(4),VN(4,4),VNO(7, E 170
     35),VN2(7,5),IND,NVGPT1,NVGPT2,NORDER                              E 180
C                                                                       E 190
C       BEGIN A BINARY SEARCH TO LOCATE WHICH TABULATED ARGUEMENT VALUE  E 200
C         IS JUST LESS THAN X.                                          E 210
C                                                                       E 220
      ILFT=250                                                          E 230
      R=250                                                             E 240
      DO 20 I=1,8                                                       E 250
      R=.5*R                                                            E 260
      ICOUNT=R+1                                                        E 270
      IF (X.GE.FERMI(ILFT,1)) GO TO 10                                  E 280
      ILFT=ILFT-ICOUNT                                                  E 290
      GO TO 20                                                          E 300
10    ILFT=ILFT+ICOUNT                                                  E 310
20    CONTINUE                                                          E 320
      IF (X.LE.FERMI(ILFT,1)) ILFT=ILFT-1                               E 330
      IRT=ILFT+1                                                        E 340
C                                                                       E 350
C       PERFORM THE LINEAR INTERPOLATION OF THE TABULATED DATA TO       E 360
```

Figure C-6 (continued)

```
C          DETERMINE F3/2(X).                                                    E 370
C                                                                                E 380
      F32=(((X-FERMI(ILFT,1))*(FERMI(IRT,3)-FERMI(ILFT,3)))/(FERMI(IRT,1        E 390
     1)-FERMI(ILFT,1)))+FERMI(ILFT,3)                                           E 400
      RETURN                                                                    E 410
C                                                                               E 420
C                                                                               E 430
      END                                                                       E 440-
      FUNCTION F12 (X)                                                          F  10
C                                                                               F  20
C       THIS FUNCTION SUBROUTINE DETERMINES THE FERMI INTEGRAL F1/2 AT          F  30
C         THE ARGUMENT X. A TABLE,FERMI(501,3), HAS THE VALUE OF F1/2           F  40
C         AND F3/2 IN COLUMNS 2 AND 3. THE ARGUEMENT IS STORED IN               F  50
C         COLUMN 1 AND GOES FROM -50 TO +50 BY INCREMENTS OF 0.2. THIS          F  60
C         SUBROUTINE LOCATES X BETWEEN TWO ARGUEMENTS VALUES IN THE             F  70
C         TABLE AND DOES A LINEAR INTERPOLATION TO FIND THE                     F  80
C         VALUE OF F1/2 BETWEEN THE TWO KNOWN, TABULATED VALUES.                F  90
C                                                                               F 100
      REAL*8 C1,C2,C3,C4,COX,DUBDT,ETA,FERMI,L,LAMBE,LAMBH,NA,NB,ND,NI,P        F 110
     1B,Q,R1,RA1,RA2,RB1,RB2,RC1,RC2,RD1,RD2,RE1,RE2,SQRT2,T,T1,T2,UB,WA        F 120
     2F,WCF,WDF,WVF,COEF,RHO,TAU,TKNOT,VN,VNO,VN2                               F 130
      REAL*8 F12,R,X                                                            F 140
      COMMON C1,C2,C3,C4,COX,DUBDT,ETA,FERMI(501,3),L,LAMBE,LAMBH,NA,NB,        F 150
     1ND,NI,PB,Q,R1,RA1,RA2,RB1,RB2,RC1,RC2,RD1,RD2,RE1,RE2,SQRT2,T,T1,T        F 160
     22,UB,WAF,WCF,WDF,WVF,COEF(9),RHO(7),TKNOT(7),TAU(4),VN(4,4),VNO(7,        F 170
     35),VN2(7,5),IND,NVGPT1,NVGPT2,NORDER                                      F 180
C                                                                               F 190
C       BEGIN A BINARY SEARCH TO LOCATE WHICH TABULATED ARGUEMENT VALUE         F 200
C         IS JUST LESS THAN X.                                                  F 210
C                                                                               F 220
      ILFT=250                                                                  F 230
      R=250                                                                     F 240
      DO 20 I=1,8                                                               F 250
      R=.5*R                                                                    F 260
      ICOUNT=R+1                                                                F 270
      IF (X.GE.FERMI(ILFT,1)) GO TO 10                                          F 280
      ILFT=ILFT-ICOUNT                                                          F 290
      GO TO 20                                                                  F 300
10    ILFT=ILFT+ICOUNT                                                          F 310
20    CONTINUE                                                                  F 320
      IF (X.LE.FERMI(ILFT,1)) ILFT=ILFT-1                                       F 330
      IRT=ILFT+1                                                                F 340
C                                                                               F 350
C       PERFORM THE LINEAR INTERPOLATION OF THE TABULATED DATA TO               F 360
C         DETERMINE F1/2(X).                                                    F 370
C                                                                               F 380
      F12=(((X-FERMI(ILFT,1))*(FERMI(IRT,2)-FERMI(ILFT,2)))/(FERMI(IRT,1        F 390
     1)-FERMI(ILFT,1)))+FERMI(ILFT,2)                                           F 400
      RETURN                                                                    F 410
C                                                                               F 420
C                                                                               F 430
      END                                                                       F 440-
      SUBROUTINE SIMP (F,A,B,ANS)                                               G  10
C                                                                               G  20
C       THIS SUBROUTINE IS A SIMPSON'S INTEGRATER. IT INTEGRATES THE            G  30
```

Figure C-6 (continued)

```
C          FUNCTION F FROM A TO B AND RETURNS THE ANSWER AS 'ANS'.                G  40
C                                                                                 G  50
      REAL*8 C1,C2,C3,C4,COX,DUBDT,ETA,FERMI,L,LAMBE,LAMBH,NA,NB,ND,NI,P          G  60
     1B,Q,R1,RA1,RA2,RB1,RB2,RC1,RC2,RD1,RD2,RE1,RE2,SQRT2,T,T1,T2,UB,WA         G  70
     2F,WCF,WDF,WVF,COEF,RHO,TAU,TKNOT,VN,VNO,VN2                                G  80
      REAL*8 A,ANS,B,F,H,H2,SUM1,SUM2,X                                          G  90
      COMMON C1,C2,C3,C4,COX,DUBDT,ETA,FERMI(501,3),L,LAMBE,LAMBH,NA,NB,         G 100
     1ND,NI,PB,Q,R1,RA1,RA2,RB1,RB2,RC1,RC2,RD1,RD2,RE1,RE2,SQRT2,T,T1,T         G 110
     22,UB,WAF,WCF,WDF,WVF,COEF(9),RHO(7),TKNOT(7),TAU(4),VN(4,4),VNO(7,         G 120
     35),VN2(7,5),IND,NVGPT1,NVGPT2,NORDER                                       G 130
      X=A                                                                        G 140
      SUM1=0.D0                                                                  G 150
      SUM2=0.D0                                                                  G 160
      H=(B-A)/200.D0                                                             G 170
      H2=2.D0*H                                                                  G 180
      DO 10 I=1,100                                                              G 190
      SUM1=SUM1+F(X)                                                             G 200
      SUM2=SUM2+F(X+H)                                                           G 210
10    X=X+H2                                                                     G 220
      ANS=(2.D0*SUM1+4.D0*SUM2-F(A)+F(B))*H/3.D0                                 G 230
      RETURN                                                                     G 240
C                                                                                G 250
C                                                                                G 260
      END                                                                        G 270-
      FUNCTION W (N)                                                             H  10
C                                                                                H  20
C       THIS FUNCTION SUBROUTINE DEFINES W, THE PARTIAL OF NH WITH               H  30
C         RESPECT TO NIND,THE INDUCED SURFACE CARRIER CONCENTRATION.             H  40
C         THE VARIABLES A(N) AND  B(N) ARE KNOWN FROM THE EXPERIMENTAL           H  50
C         DATA. THUS W CAN BE INTEGRATED OVER THE RANGE COVERED BY N IN          H  60
C         THE ORIGINAL EXPERIMENTAL DATA.                                        H  70
C                                                                                H  80
      REAL*8 C1,C2,C3,C4,COX,DUBDT,ETA,FERMI,L,LAMBE,LAMBH,NA,NB,ND,NI,P         H  90
     1B,Q,R1,RA1,RA2,RB1,RB2,RC1,RC2,RD1,RD2,RE1,RE2,SQRT2,T,T1,T2,UB,WA         H 100
     2F,WCF,WDF,WVF,COEF,RHO,TAU,TKNOT,VN,VNO,VN2                                H 110
      REAL*8 A,B,N,W                                                             H 120
      COMMON C1,C2,C3,C4,COX,DUBDT,ETA,FERMI(501,3),L,LAMBE,LAMBH,NA,NB,         H 130
     1ND,NI,PB,Q,R1,RA1,RA2,RB1,RB2,RC1,RC2,RD1,RD2,RE1,RE2,SQRT2,T,T1,T         H 140
     22,UB,WAF,WCF,WDF,WVF,COEF(9),RHO(7),TKNOT(7),TAU(4),VN(4,4),VNO(7,         H 150
     35),VN2(7,5),IND,NVGPT1,NVGPT2,NORDER                                       H 160
      W=(C3*B(N)+C4-C2)/(C1*A(N))                                                H 170
      RETURN                                                                     H 180
C                                                                                H 190
C                                                                                H 200
      END                                                                        H 210-
      FUNCTION A (N)                                                             I  10
C                                                                                I  20
C       THIS FUNCTION SUBROUTINE DEFINES A OR ALPHA FROM THE ORIGINAL            I  30
C         EXPERIMENTAL DATA. HERE, A IS THE PARTIAL OF VG WITH RESPECT           I  40
C         TO NH HOLDING T CONSTANT. IT IS EVALUATED THROUGH TENSION              I  50
C         SPLINES.                                                               I  60
C                                                                                I  70
      REAL*8 C1,C2,C3,C4,COX,DUBDT,ETA,FERMI,L,LAMBE,LAMBH,NA,NB,ND,NI,P         I  80
     1B,Q,R1,RA1,RA2,RB1,RB2,RC1,RC2,RD1,RD2,RE1,RE2,SQRT2,T,T1,T2,UB,WA         I  90
     2F,WCF,WDF,WVF,COEF,RHO,TAU,TKNOT,VN,VNO,VN2                                I 100
```

Figure C-6 (continued)

```
      REAL*8 A,ALPHA,DVGDNH,N,NH,NH2,NH3,X                                I 110
      COMMON C1,C2,C3,C4,COX,DUBDT,ETA,FERMI(501,3),L,LAMBE,LAMBH,NA,NB,  I 120
     1ND,NI,PB,Q,R1,RA1,RA2,RB1,RB2,RC1,RC2,RD1,RD2,RE1,RE2,SQRT2,T,T1,T  I 130
     22,UB,WAF,WCF,WDF,WVF,COEF(9),RHO(7),TKNOT(7),TAU(4),VN(4,4),VNO(7,  I 140
     35),VN2(7,5),IND,NVGPT1,NVGPT2,NORDER                               I 150
      NH=N/R1                                                            I 160
C                                                                        I 170
C        THE NEXT TWO CARDS MAKE ALPHA EQUAL TO A CONSTANT WHEN THE      I 180
C         POLYNOMIAL FIT HAS BEEN REDUCED TO FIRST ORDER. THE TENSION    I 190
C         SPLINES ARE NOT USED IN THIS CASE.                             I 200
C                                                                        I 210
      IF (NORDER.EQ.1) A=COX*RD2/Q                                       I 220
      IF (NORDER.EQ.1) RETURN                                            I 230
C                                                                        I 240
      CALL SPLINE (NH/1.D11)                                             I 250
      DVGDNH=TAU(2)/1.D11                                                I 260
      A=COX*DVGDNH/Q                                                     I 270
      RETURN                                                             I 280
C                                                                        I 290
C                                                                        I 300
      END                                                                I 310-
      FUNCTION B (N)                                                     J  10
C                                                                        J  20
C       THIS FUNCTION SUBROUTINE DEFINES B OR BETA FROM THE EXPERIMENTAL  J  30
C         DATA. HERE,B IS THE PARTIAL OF VG WITH RESPECT TO T AT A       J  40
C         CONSTANT NH. IT IS DETERMINED THROUGH THE POLYNOMIAL FIT       J  50
C                                                                        J  60
      REAL*8 C1,C2,C3,C4,COX,DUBDT,ETA,FERMI,L,LAMBE,LAMBH,NA,NB,ND,NI,P  J  70
     1B,Q,R1,RA1,RA2,RB1,RB2,RC1,RC2,RD1,RD2,RE1,RE2,SQRT2,T,T1,T2,UB,WA  J  80
     2F,WCF,WDF,WVF,COEF,RHO,TAU,TKNOT,VN,VNO,VN2                        J  90
      REAL*8 B,BETA,N,NH,NH2,NH3,NH4,X                                   J 100
      COMMON C1,C2,C3,C4,COX,DUBDT,ETA,FERMI(501,3),L,LAMBE,LAMBH,NA,NB,  J 110
     1ND,NI,PB,Q,R1,RA1,RA2,RB1,RB2,RC1,RC2,RD1,RD2,RE1,RE2,SQRT2,T,T1,T  J 120
     22,UB,WAF,WCF,WDF,WVF,COEF(9),RHO(7),TKNOT(7),TAU(4),VN(4,4),VNO(7,  J 130
     35),VN2(7,5),IND,NVGPT1,NVGPT2,NORDER                               J 140
      NH=N/R1                                                            J 150
      NH2=NH*NH                                                          J 160
      NH3=NH2*NH                                                         J 170
      NH4=NH3*NH                                                         J 180
      B=COX*((RA2-RA1)*NH4+(RB2-RB1)*NH3+(RC2-RC1)*NH2+(RD2-RD1)*NH+(RE2  J 190
     1-RE1))/((T2-T1)*Q)                                                 J 200
      RETURN                                                             J 210
C                                                                        J 220
C                                                                        J 230
      END                                                                J 240-
      SUBROUTINE SETUP                                                   K  10
C                                                                        K  20
C       THIS SUBROUTINE ALONG WITH INT,VALN,AND SPLINE ARE USED TO SET   K  30
C         UP A MINIMAL SUPPORT BASIS SET OF TENSION SPLINES. THIS BASIS  K  40
C         SET ALONG WITH AN APPROPRIATE SET OF COEFFICIENTS FOR THE      K  50
C         FUNCTIONS IS USED TO CURVE FIT THE EXPERIMENTAL DATA. THIS IS  K  60
C         SIMILAR TO A FOURIER EXPANSION EXCEPT THAT AT ANY POINT IN     K  70
C         THE INTERVAL OVER WHICH THE CURVE FITTING IS BEING DONE, ONLY  K  80
C         FOUR OF THE BASIS FUNCTIONS ARE NON-ZERO.                      K  90
C         USING THIS BASIS SET AND THESE COEFFICIENTS A CONTINOUS        K 100
```

Figure C-6 (continued)

```
C         ANALYTICAL EXPRESSION FOR VG(NH), AS WELL AS THE DERIVATIVE     K 110
C         OF VG WITH RESPECT TO NH IS DERIVED. THIS SUBROUTINE AS WELL    K 120
C         AS THE NEXT THREE WERE WRITTEN BY S. PRUESS,DEPT. OF MATH.,     K 130
C         UNIV. OF N.M.,(505)277-3332. ALL QUESTIONS REGARDING ITS USE    K 140
C         SHOULD BE REFERRED TO HIM.                                      K 150
C                                                                         K 160
C                                                                         K 170
C       THIS PARTICULAR SUBROUTINE COMPUTES THE KNOT VALUES AND KNOT      K 180
C         SECOND DERIVATIVES VALUES FOR THE BASIS FUNCTIONS N(I),         K 190
C         I=1,2,...N+2. HERE, N IS THE NUMBER OF KNOTS, FIXED AT FOUR.    K 200
C                                                                         K 210
C         THE INPUTS TO SETUP ARE AS FOLLOWS.                             K 220
C            1--TKNOT, THE KNOT ARRAY                                     K 230
C            2--RHO, THE TENSION ARRAY.                                   K 240
C         THE OUTPUTS FROM THIS ROUTINE ARE AS FOLLOWS.                   K 250
C            1--VNO, THE TWO DIMENSIONAL ARRAY CONTAINING THE KNOT        K 260
C              VALUES. VNO(I,J)=N(I) EVALUATED AT THE (I+J-4) KNOT.       K 270
C            2--VN2, THE TWO DIMENSIONAL ARRAY OF KNOT SECOND DERIVATIVE  K 280
C              VALUES. VN2(I,J) CONTAINS THE SECOND DERIVATIVE OF N(I)    K 290
C              EVALUATED AT THE (I+J-4)TH KNOT.                           K 300
C         THE ARRAYS VNO AND VN2 COMPLETELY CHARACTERIZE THE BASIS SET.   K 310
      CONTINUE                                                            K 315
C                                                                         K 320
      REAL*8 C1,C2,C3,C4,COX,DUBDT,ETA,FERMI,L,LAMBE,LAMBH,NA,NB,ND,NI,P    330
     1B,Q,R1,RA1,RA2,RB1,RB2,RC1,RC2,RD1,RD2,RE1,RE2,SQRT2,T,T1,T2,UB,WA  K 340
     2F,WCF,WDF,WVF,COEF,RHO,TAU,TKNOT,VN,VNO,VN2                         K 350
      COMMON C1,C2,C3,C4,COX,DUBDT,ETA,FERMI(501,3),L,LAMBE,LAMBH,NA,NB,  K 360
     1ND,NI,PB,Q,R1,RA1,RA2,RB1,RB2,RC1,RC2,RD1,RD2,RE1,RE2,SQRT2,T,T1,T  K 370
     22,UB,WAF,WCF,WDF,WVF,COEF(9),RHO(7),TKNOT(7),TAU(4),VN(4,4),VNO(7,  K 380
     35),VN2(7,5),IND,NVGPT1,NVGPT2,NORDER                                K 390
      REAL*8 D(7),E(7),HI(7),RH,R2,A11,A21,A22,A23,P,DSINH,DCOSH          K 400
      N=4                                                                 K 410
      NP2=N+2                                                             K 420
      RHO(1)=0.05D0                                                       K 430
      RHO(2)=0.40D0                                                       K 440
      RHO(3)=0.3D0                                                        K 450
      RHO(4)=0.D0                                                         K 460
      DO 10 I=1,NP2                                                       K 470
      DO 10 J=1,5                                                         K 480
      VNO(I,J)=0                                                          K 490
10    VN2(I,J)=0                                                          K 500
      NM1=N-1                                                             K 510
      DO 30 I=1,NM1                                                       K 520
      HI(I)=TKNOT(I+1)-TKNOT(I)                                           K 530
      RH=RHO(I)*HI(I)                                                     K 540
      HI(I)=1/HI(I)                                                       K 550
      R2=RHO(I)**2                                                        K 560
      IF (RH.GT..1) GO TO 20                                              K 570
      D(I)=(1-R2/15)/(3*HI(I))                                            K 580
      E(I)=(1-7.*R2/60)/(6*HI(I))                                         K 590
      GO TO 30                                                            K 600
20    P=DSINH(RH)*RHO(I)                                                  K 610
      A11=HI(I)/R2                                                        K 620
      D(I)=DCOSH(RH)/P-A11                                                K 630
      E(I)=A11-1/P                                                        K 640
```

Figure C-6 (continued)

```
30    CONTINUE                                                          K 650
      VNO(1,4)=1                                                        K 660
      VNO(1,5)=0                                                        K 670
      VN2(1,4)=HI(1)/E(1)                                               K 680
      VN2(1,5)=0                                                        K 690
      VNO(2,4)=1                                                        K 700
      VN2(2,4)=HI(2)/E(2)                                               K 710
      VN2(2,3)=-(HI(1)+HI(2)+(D(1)+D(2))*VN2(2,4))/E(1)                 K 720
      IF (N.EQ.2) GO TO 60                                              K 730
      VN2(3,4)=HI(3)/E(3)                                               K 740
      A11=E(2)/(D(1)+D(2)-E(1)*E(1)/D(1))                               K 750
      A21=HI(2)+HI(3)+(D(2)+D(3))*VN2(3,4)                              K 760
      VNO(3,3)=(A21+A11*(HI(2)-E(2)*VN2(3,4)))/(HI(2)+A11*(HI(1)+HI(2)+E  K 770
     1(1)*HI(1)/D(1)))                                                  K 780
      VN2(3,3)=(HI(2)*VNO(3,3)-A21)/E(2)                                K 790
      VNO(3,4)=1                                                        K 800
      VN2(3,2)=(VNO(3,3)*HI(1)-VN2(3,3)*E(1))/D(1)                      K 810
      IF (N.EQ.3) GO TO 60                                              K 820
      IF (N.EQ.4) GO TO 50                                              K 830
      DO 40 I=4,NM1                                                     K 840
      A11=D(I-3)+D(I-2)+E(I-3)*(1+HI(I-2)/HI(I-3))                      K 850
      A21=E(I-2)-HI(I-2)*E(I-3)/HI(I-3)                                 K 860
      P=A21/A11                                                         K 870
      A22=D(I-2)+D(I-1)-P*E(I-2)                                        K 880
      A23=E(I-1)-HI(I-1)*E(I)/HI(I)                                     K 890
      R2=-HI(I-1)-HI(I-2)*(1+P)                                         K 900
      P=E(I-1)/A22                                                      K 910
      VN2(I,4)=(HI(I-1)-P*R2)/(D(I-1)+D(I)+E(I)*(1+HI(I-1)/HI(I))-P*A23)  K 920
      VN2(I,3)=(R2-A23*VN2(I,4))/A22                                    K 930
      VN2(I,2)=(HI(I-2)-E(I-2)*VN2(I,3))/A11                            K 940
      VNO(I,2)=E(I-3)*VN2(I,2)/HI(I-3)                                  K 950
      VNO(I,3)=1                                                        K 960
40    VNO(I,4)=E(I)*VN2(I,4)/HI(I)                                      K 970
50    VN2(N,2)=HI(N-3)/E(N-3)                                           K 980
      A11=E(N-2)/(D(N-1)+D(N-2)-E(N-1)*E(N-1)/D(N-1))                   K 990
      A21=HI(N-2)+HI(N-3)+(D(N-2)+D(N-3))*VN2(N,2)                      K1000
      VNO(N,3)=(A21+A11*(HI(N-2)-E(N-2)*VN2(N,2)))/(HI(N-2)+A11*(HI(N-1)  K1010
     1+HI(N-2)+E(N-1)*HI(N-1)/D(N-1)))                                  K1020
      VN2(N,3)=(HI(N-2)*VNO(N,3)-A21)/E(N-2)                            K1030
      VNO(N,2)=1                                                        K1040
      VN2(N,4)=(VNO(N,3)*HI(N-1)-VN2(N,3)*E(N-1))/D(N-1)                K1050
60    VNO(N+1,2)=1                                                      K1060
      VN2(N+1,2)=HI(N-2)/E(N-2)                                         K1070
      VN2(N+1,3)=-(HI(N-1)+HI(N-2)+(D(N-1)+D(N-2))*VN2(N+1,2))/E(N-1)   K1080
      VNO(N+2,2)=1                                                      K1090
      VNO(N+2,1)=0                                                      K1100
      VN2(N+2,2)=HI(N-1)/E(N-1)                                         K1110
      VN2(N+2,1)=0                                                      K1120
      RETURN                                                            K1130
C                                                                       K1140
C                                                                       K1150
      END                                                               K1160-
      SUBROUTINE INT (X,ILEFT)                                          L  10
C                                                                       L  20
C       THIS SUBROUTINE DETERMINES ILEFT SUCH THAT TAUT(ILEFT).LE.X     L  30
```

Figure C-6 (continued)

```
C          .LT.TKNOT(ILEFT+1). NOTE THAT X MUST LIE WITHIN THE RANGE OF    L  40
C          THE LARGEST AND SMALLEST DATA POINTS.                           L  50
C                                                                          L  60
      REAL*8 C1,C2,C3,C4,COX,DUBDT,ETA,F   MI,L,LAMBE,LAMBH,NA,NB,ND,NI,P  L  70
     1B,Q,R1,RA1,RA2,RB1,RB2,RC1,RC2,RD   D2,RE1,RE2,SQRT2,T,T1,T2,UB,WA  L  80
     2F,WCF,WDF,WVF,COEF,RHO,TAU,TKNOT,   NO,VN2                         L  90
      COMMON C1,C2,C3,C4,COX,DUBDT,ETA,     (501,3),L,LAMBE,LAMBH,NA,NB,  L 100
     1ND,NI,PB,Q,R1,RA1,RA2,RB1,RB2,RC     RD1,RD2,RE1,RE2,SQRT2,T,T1,T  L 110
     22,UB,WAF,WCF,WDF,WVF,COEF(9),RH      NOT(7),TAU(4),VN(4,4),VNO(7,  L 120
     35),VN2(7,5),IND,NVGPT1,NVGPT2,N                                    L 130
      INTEGER ILEFT,K,N,NM1                                              L 140
      REAL*8 X                                                           L 150
      N=4                                                                L 160
      K=MAXO(ILEFT,1)                                                    L 170
      IF (X.GE.TKNOT(K)) GO TO 20                                        L 180
      DO 10 ILEFT=1,K                                                    L 190
      IF (X.LT.TKNOT(ILEFT+1)) RETU                                      L 200
10    CONTINUE                                                           L 210
20    NM1=N-1                                                            L 220
      DO 30 ILEFT=K,NM1                                                  L 230
      IF (X.LT.TKNOT(ILEFT+1)) RETURN                                    L 240
30    CONTINUE                                                           L 250
      ILEFT=NM1                                                          L 260
      RETURN                                                             L 270
C                                                                        L 280
C                                                                        L 290
      END                                                                L 300-
      SUBROUTINE VALN (X,I)                                              M  10
C                                                                        M  20
C       THIS SUBROUTINE COMPUTES THE FUNCTION AND DERIVATIVE VALUES AT   M  30
C         AN ARBITRARY POINT X OF ALL POSSIBLE NON-ZERO N(I) WHERE N(I)  M  40
C         ARE THE BASIS FUNCTIONS. TO DO THIS CALCULATION THE KNOT       M  50
C         ARRAY,TENSION ARRAY,ILEFT,VNO,AND VN2 ARE FED IN.              M  60
C         THE OUTPUT IS IN VN(I,J) WHICH CONTAINS THE (J-1)ST DERIVATIVE M  70
C         OF THE (ILEFT+4-K)TH BASIS FUNCTION.                           M  80
C                                                                        M  90
      REAL*8 C1,C2,C3,C4,COX,DUBDT,ETA,FERMI,L,LAMBE,LAMBH,NA,NB,ND,NI,P M 100
     1B,Q,R1,RA1,RA2,RB1,RB2,RC1,RC2,RD1,RD2,RE1,RE2,SQRT2,T,T1,T2,UB,WA M 110
     2F,WCF,WDF,WVF,COEF,RHO,TAU,TKNOT,VN,VNO,VN2                       M 120
      COMMON C1,C2,C3,C4,COX,DUBDT,ETA,FERMI(501,3),L,LAMBE,LAMBH,NA,NB, M 130
     1ND,NI,PB,Q,R1,RA1,RA2,RB1,RB2,RC1,RC2,RD1,RD2,RE1,RE2,SQRT2,T,T1,T M 140
     22,UB,WAF,WCF,WDF,WVF,COEF(9),RHO(7),TKNOT(7),TAU(4),VN(4,4),VNO(7, M 150
     35),VN2(7,5),IND,NVGPT1,NVGPT2,NORDER                              M 160
      INTEGER I,J,K                                                      M 170
      REAL*8 TMX,TMXH,XMT,XMTH,SRT,SRX,SRH,X,H,CRT,CRX,H26,RH,DCOSH,DSIN M 180
     1H                                                                 M 190
      H=TKNOT(I+1)-TKNOT(I)                                              M 200
      R2=RHO(I)**2                                                       M 210
      TMX=TKNOT(I+1)-X                                                   M 220
      TMXH=TMX/H                                                         M 230
      XMT=X-TKNOT(I)                                                     M 240
      XMTH=XMT/H                                                         M 250
      RH=RHO(I)*H                                                        M 260
      IF (RH.LT..1) GO TO 20                                             M 270
      SRH=DSINH(RH)                                                      M 280
```

Figure C-6 (continued)

```
      SRT=DSINH(TMX*RHO(I))                                                  M 290
      CRT=DCOSH(TMX*RHO(I))                                                  M 300
      SRX=DSINH(XMT*RHO(I))                                                  M 310
      CRX=DCOSH(XMT*RHO(1))                                                  M 320
      DO 10 K=1,4                                                            M 330
      J=I+4-K                                                                M 340
      VN(K,4)=RHO(I)*(VN2(J,K+1)*CRX-VN2(J,K)*CRT)/SRH                       M 350
      VN(K,3)=(VN2(J,K+1)*SRX+VN2(J,K)*SRT)/SRH                              M 360
      VN(K,2)=VN(K,4)/R2+(VN0(J,K+1)-VN0(J,K)+(VN2(J,K)-VN2(J,K+1))/R2)/     M 370
     1H                                                                      M 380
10    VN(K,1)=VN(K,3)/R2+(VN0(J,K)-VN2(J,K)/R2)*TMXH+(VN0(J,K+1)-VN2(J,K     M 390
     1+1)/R2)*XMTH                                                           M 400
      RETURN                                                                 M 410
20    H26=H*H/6                                                              M 420
      SRH=1+R2*H26                                                           M 430
      DO 30 K=1,4                                                            M 440
      J=I+4-K                                                                M 450
      VN(K,4)=(VN2(J,K+1)*(1+R2*XMT**2/2)-VN2(J,K)*(1+R2*TMX**2/2))/(H*S     M 460
     1RH)                                                                    M 470
      VN(K,3)=(VN2(J,K+1)*XMTH*(1+XMT**2*R2/6)+VN2(J,K)*TMXH*(1+TMX**2*R     M 480
     12/6))/SRH                                                              M 490
      VN(K,2)=(VN2(J,K+1)*(XMT**2/2-H26+R2/24*(XMT**4-2*(XMTH**2+H**4/15     M 500
     1)))-VN2(J,K)*(TMX**2/2-H26+R2/24*(TMXH**4-2*(TMXH**2+H**4/15)))+VN     M 510
     20(J,K+1)-VN0(J,K))/H                                                   M 520
30    VN(K,1)=(VN0(J,K+1)*XMTH+VN0(J,K)*TMXH+XMTH*VN2(J,K+1)*H26*(XMTH**     M 530
     12-1)*(1+R2/10*H26*(3*XMTH**2-7))+TMXH*VN2(J,K)*H26*(TMXH**2-1)*(1+     M 540
     2R2/10*H26*(3*TMXH**2-7)))                                              M 550
      RETURN                                                                 M 560
C                                                                            M 570
C                                                                            M 580
      END                                                                    M 590-
      SUBROUTINE SPLINE (X)                                                  N  10
C                                                                            N  20
C       THE TENSION SPLINES ARE BEING USED TO CURVE FIT VG AS A FUNCTION     N  30
C         OF NH.  THIS ROUTINE CALCULATES THE LINEAR COMBINATIONS OF THE     N  40
C         BASIS FUNCTIONS AND THE APPROPRIATE COEFFICIENTS TO ACTUALLY       N  50
C         ARRIVE AT A VALUE FOR VG AT A GIVEN NH. THE OUTPUT IS THE          N  60
C         VECTOR TAU(J) WHICH CONTAINS THE (J-1)ST DERIVATIVE AT THE         N  70
C         POINT X.                                                           N  80
C                                                                            N  90
      REAL*8 C1,C2,C3,C4,COX,DUBDT,ETA,FERMI,L,LAMBE,LAMBH,NA,NB,ND,NI,P     N 100
     1B,Q,R1,RA1,RA2,RB1,RB2,RC1,RC2,RD1,RD2,RE1,RE2,SQRT2,T,T1,T2,UB,WA    N 110
     2F,WCF,WDF,WVF,COEF,RHO,TAU,TKNOT,VN,VN0,VN2                           N 120
      COMMON C1,C2,C3,C4,COX,DUBDT,ETA,FERMI(501,3),L,LAMBE,LAMBH,NA,NB,     N 130
     1ND,NI,PB,Q,R1,RA1,RA2,RB1,RB2,RC1,RC2,RD1,RD2,RE1,RE2,SQRT2,T,T1,T    N 140
     22,UB,WAF,WCF,WDF,WVF,COEF(9),RHO(7),TKNOT(7),TAU(4),VN(4,4),VN0(7,     N 150
     35),VN2(7,5),IND,NVGPT1,NVGPT2,NORDER                                   N 160
      INTEGER N,ILEFT,J,K                                                    N 170
      REAL*8 X                                                               N 180
      N=4                                                                    N 190
      ILEFT=1                                                                N 200
      CALL INT (X,ILEFT)                                                     N 210
      CALL VALN (X,ILEFT)                                                    N 220
      DO 10 K=1,4                                                            N 230
10    TAU(K)=0                                                               N 240
```

Figure C-6 (continued)

```
      DO 20 K=1,4                                                        N 250
      DO 20 J=1,4                                                        N 260
20    TAU(J)=TAU(J)+COEF(ILEFT+K-1)*VN(5-K,J)                            N 270
      RETURN                                                             N 280
C                                                                        N 290
C                                                                        N 300
      END                                                                N 310-
      SUBROUTINE DECOMP (NDIM,N,A,COND,IPVT,WORK)                        O  10
C                                                                        O  20
C       THIS SUBROUTINE AND THE NEXT ARE USED TO SOLVE THE LINEAR        O  30
C         SYSTEM A*X=B. THESE ROUTINES WERE WRITTEN BY C. MOLER,DEPT. OF O  40
C         MATH.,UNIV. OF N.M.,(505)277-4110. QUESTIONS REGARDING ITS USE O  50
C         SHOULD BE REFERRED TO HIM.                                     O  60
C                                                                        O  70
C                                                                        O  80
C     THIS SUBROUTINE DECOMPOSES A REAL*8 MATRIX BY GAUSSIAN ELIMINATION O  90
C     AND ESTIMATES THE CONDITION OF THE MATRIX.                         O 100
C                                                                        O 110
C     USE SOLVE TO COMPUTE SOLUTIONS TO LINEAR SYSTEMS.                  O 120
C                                                                        O 130
C     INPUT..                                                            O 140
C                                                                        O 150
C        NDIM = DECLARED ROW DIMENSION OF THE ARRAY CONTAINING  A.       O 160
C                                                                        O 170
C        N = ORDER OF THE MATRIX.                                        O 180
C                                                                        O 190
C        A = MATRIX TO BE TRIANGULARIZED.                                O 200
C                                                                        O 210
C     OUTPUT..                                                           O 220
C                                                                        O 230
C        A  CONTAINS AN UPPER TRIANGULAR MATRIX  U  AND A PERMUTED       O 240
C          VERSION OF A LOWER TRIANGULAR MATRIX  I-L  SO THAT            O 250
C          (PERMUTATION MATRIX)*A = L*U .                                O 260
C                                                                        O 270
C        COND = AN ESTIMATE OF THE CONDITION OF  A .                     O 280
C           FOR THE LINEAR SYSTEM  A*X = B, CHANGES IN  A  AND  B        O 290
C           MAY CAUSE CHANGES  COND  TIMES AS LARGE IN  X .              O 300
      CONTINUE                                                           O 315
C          COND = 1.0D+32  IF EXACT SINGULARITY IS DETECTED.             O 310
C                                                                        O 320
C        IPVT = THE PIVOT VECTOR.                                        O 330
C           IPVT(K) = THE INDEX OF THE K-TH PIVOT ROW                    O 340
C           IPVT(N) = (-1)**(NUMBER OF INTERCHANGES)                     O 350
C                                                                        O 360
C     WORK SPACE..  THE VECTOR  WORK  MUST BE DECLARED AND INCLUDED      O 370
C                   IN THE CALL.  ITS INPUT CONTENTS ARE IGNORED.        O 380
C                   ITS OUTPUT CONTENTS ARE USUALLY UNIMPORTANT.         O 390
C                                                                        O 400
C     THE DETERMINANT OF A CAN BE OBTAINED ON OUTPUT BY                  O 410
C        DET(A) = IPVT(N) * A(1,1) * A(2,2) * ... * A(N,N).              O 420
C                                                                        O 430
      INTEGER NDIM,N                                                     O 440
      REAL*8 A(NDIM,N),COND,WORK(N)                                      O 450
      INTEGER IPVT(N)                                                    O 460
      REAL E,EK,T,ANORM,YNORM,ZNORM                                      O 470
```

Figure C-6 (continued)

```
      INTEGER NM1,I,J,K,KP1,KB,KM1                                      0 480
      REAL*8 DABS,DSIGN                                                 0 490
      IF (N.EQ.1) GO TO 150                                             0 500
      NM1=N-1                                                           0 510
C                                                                       0 520
C     COMPUTE 1-NORM OF A                                               0 530
C                                                                       0 540
      ANORM=0.0D0                                                       0 550
      DO 20 J=1,N                                                       0 560
      T=0.0D0                                                           0 570
      DO 10 I=1,N                                                       0 580
      T=T+DABS(A(I,J))                                                  0 590
10    CONTINUE                                                          0 600
      IF (T.GT.ANORM) ANORM=T                                           0 610
20    CONTINUE                                                          0 620
C                                                                       0 630
C     GAUSSIAN ELIMINATION WITH PARTIAL PIVOTING                        0 640
C                                                                       0 650
      DO 70 K=1,NM1                                                     0 660
      KP1=K+1                                                           0 670
C                                                                       0 680
C        FIND PIVOT                                                     0 690
C                                                                       0 700
      M=K                                                               0 710
      DO 30 I=KP1,N                                                     0 720
      IF (DABS(A(I,K)).GT.DABS(A(M,K))) M=I                             0 730
30    CONTINUE                                                          0 740
      IPVT(K)=M                                                         0 750
      IF (M.NE.K) IPVT(N)=-IPVT(N)                                      0 760
      T=A(M,K)                                                          0 770
      A(M,K)=A(K,K)                                                     0 780
      A(K,K)=T                                                          0 790
C                                                                       0 800
C        SKIP STEP IF PIVOT IS ZERO                                     0 810
C                                                                       0 820
      IF (T.EQ.0.0D0) GO TO 70                                          0 830
C                                                                       0 840
C        COMPUTE MULTIPLIERS                                            0 850
C                                                                       0 860
      DO 40 I=KP1,N                                                     0 870
      A(I,K)=-A(I,K)/T                                                  0 880
40    CONTINUE                                                          0 890
C                                                                       0 900
C        INTERCHANGE AND ELIMINATE BY COLUMNS                           0 910
C                                                                       0 920
      DO 60 J=KP1,N                                                     0 930
      T=A(M,J)                                                          0 940
      A(M,J)=A(K,J)                                                     0 950
      A(K,J)=T                                                          0 960
      IF (T.EQ.0.0D0) GO TO 60                                          0 970
      DO 50 I=KP1,N                                                     0 980
      A(I,J)=A(I,J)+A(I,K)*T                                            0 990
50    CONTINUE                                                         01000
60    CONTINUE                                                         01010
70    CONTINUE                                                         01020
```

Figure C-6 (continued)

```
C                                                                       01030
C     COND = (1-NORM OF A)*(AN ESTIMATE OF 1-NORM OF A-INVERSE)         01040
C     ESTIMATE OBTAINED BY ONE STEP OF INVERSE ITERATION FOR THE        01050
C     SMALL SINGULAR VECTOR.  THIS INVOLVES SOLVING TWO SYSTEMS         01060
C     OF EQUATIONS, (A-TRANSPOSE)*Y = E  AND  A*Z = Y  WHERE  E         01070
C     IS A VECTOR OF +1 OR -1 CHOSEN TO CAUSE GROWTH IN Y.              01080
C     ESTIMATE = (1-NORM OF Z)/(1-NORM OF Y)                            01090
C                                                                       01100
C     SOLVE (A-TRANSPOSE)*Y = E                                         01110
C                                                                       01120
      DO 100 K=1,N                                                      01130
      T=0.0D0                                                           01140
      IF (K.EQ.1) GO TO 90                                              01150
      KM1=K-1                                                           01160
      DO 80 I=1,KM1                                                     01170
      T=T+A(I,K)*WORK(I)                                                01180
80    CONTINUE                                                          01190
90    EK=1.0D0                                                          01200
      IF (T.LT.0.0D0) EK=-1.0D0                                         01210
      IF (A(K,K).EQ.0.0D0) GO TO 160                                    01220
      WORK(K)=-(EK+T)/A(K,K)                                            01230
100   CONTINUE                                                          01240
      DO 120 KB=1,NM1                                                   01250
      K=N-KB                                                            01260
      T=0.0D0                                                           01270
      KP1=K+1                                                           01280
      DO 110 I=KP1,N                                                    01290
      T=T+A(I,K)*WORK(K)                                                01300
110   CONTINUE                                                          01310
      WORK(K)=T                                                         01320
      M=IPVT(K)                                                         01330
      IF (M.EQ.K) GO TO 120                                             01340
      T=WORK(M)                                                         01350
      WORK(M)=WORK(K)                                                   01360
      WORK(K)=T                                                         01370
120   CONTINUE                                                          01380
C                                                                       01390
      YNORM=0.0D0                                                       01400
      DO 130 I=1,N                                                      01410
      YNORM=YNORM+DABS(WORK(I))                                         01420
130   CONTINUE                                                          01430
C                                                                       01440
C     SOLVE A*Z = Y                                                     01450
C                                                                       01460
C                                                                       01480
      ZNORM=0.0D0                                                       01490
      DO 140 I=1,N                                                      01500
      ZNORM=ZNORM+DABS(WORK(I))                                         01510
140   CONTINUE                                                          01520
C                                                                       01530
C     ESTIMATE CONDITION                                                01540
C                                                                       01550
      COND=ANORM*ZNORM/YNORM                                            01560
      IF (COND.LT.1.0D0) COND=1.0D0                                     01570
      RETURN                                                            01580
```

Figure C-6 (continued)

```
C                                                                       01590
C     1-BY-1                                                            01600
C                                                                       01610
150   IPVT(1)=1                                                         01620
      COND=1.0D0                                                        01630
      IF (A(1,1).NE.0.0D0) RETURN                                       01640
C                                                                       01650
C     EXACT SINGULARITY                                                 01660
C                                                                       01670
160   COND=1.0D+32                                                      01680
      RETURN                                                            01690
      END                                                               01700-
      SUBROUTINE SOLVE (NDIM,N,A,B,IPVT)                                P  10
C                                                                       P  20
      INTEGER NDIM,N,IPVT(N)                                            P  30
      REAL*8 A(NDIM,N),B(N)                                             P  40
C                                                                       P  50
C     SOLUTION OF LINEAR SYSTEM, A*X = B .                              P  60
C     DO NOT USE IF DECOMP HAS DETECTED SINGULARITY.                    P  70
C                                                                       P  80
C     INPUT..                                                           P  90
C     NDIM = DECLARED ROW DIMENSION OF ARRAY CONTAINING A .             P 100
C                                                                       P 110
C     N = ORDER OF MATRIX.                                              P 120
C                                                                       P 130
C     A = TRIANGULARIZED MATRIX OBTAINED FROM DECOMP .                  P 140
C                                                                       P 150
C     B = RIGHT HAND SIDE VECTOR.                                       P 160
C                                                                       P 170
C     IPVT = PIVOT VECTOR OBTAINED FROM DECOMP .                        P 180
C                                                                       P 190
C     OUTPUT..                                                          P 200
C                                                                       P 210
C     B = SOLUTION VECTOR, X .                                          P 220
C                                                                       P 230
      INTEGER KB,KM1,NM1,KP1,I,K,M                                      P 240
      REAL*8 T                                                          P 250
C                                                                       P 260
C     FORWARD ELIMINATION                                               P 270
C                                                                       P 280
      IF (N.EQ.1) GO TO 50                                              P 290
      NM1=N-1                                                           P 300
      DO 20 K=1,NM1                                                     P 310
      KP1=K+1                                                           P 320
      M=IPVT(K)                                                         P 330
      T=B(M)                                                            P 340
      B(M)=B(K)                                                         P 350
      B(K)=T                                                            P 360
      DO 10 I=KP1,N                                                     P 370
      B(I)=B(I)+A(I,K)*T                                                P 380
10    CONTINUE                                                          P 390
20    CONTINUE                                                          P 400
C                                                                       P 410
C     BACK SUBSTITUTION                                                 P 420
C                                                                       P 430
```

Figure C-6 (continued)

```
      DO 40 KB=1,NM1                                                    P 440
      KM1=N-KB                                                          P 450
      K=KM1+1                                                           P 460
      B(K)=B(K)/A(K,K)                                                  P 470
      T=-B(K)                                                           P 480
      DO 30 I=1,KM1                                                     P 490
      B(I)=B(I)+A(I,K)*T                                                P 500
30    CONTINUE                                                          P 510
40    CONTINUE                                                          P 520
50    B(1)=B(1)/A(1,1)                                                  P 530
      RETURN                                                            P 540
      END                                                               P 550-
```

-50.00000000000	0.1681989519314D-21	0.2565762115842D-21
-49.80000000000	0.2054560623530D-21	0.3133809414352D-21
-49.60000000000	0.2509658084209D-21	0.3827619764031D-21
-49.40000000000	0.3065561800181D-21	0.4675036553130D-21
-49.20000000000	0.3744600714424D-21	0.5710067580350D-21
-49.00000000000	0.4574049682713D-21	0.6974249831080D-21
-48.80000000000	0.5587224998752D-21	0.8518316410038D-21
-48.60000000000	0.6824822572989D-21	0.1040423252669D-20
-48.40000000000	0.8336552548685D-21	0.1270768224043D-20
-48.20000000000	0.1018313590396D-20	0.1552110576226D-20
-48.00000000000	0.1243874341071D-20	0.1895740920423D-20
-47.80000000000	0.1519397473431D-20	0.2315449565442D-20
-47.60000000000	0.1855949743585D-20	0.2828079941619D-20
-47.40000000000	0.2267049200175D-20	0.3454045550901D-20
-47.20000000000	0.2769208144017D-20	0.4218950569980D-20
-47.00000000000	0.3382596352239D-20	0.5153008239201D-20
-46.80000000000	0.4131851205169D-20	0.6293862505427D-20
-46.60000000000	0.5047067254405D-20	0.7687297346601D-20
-46.40000000000	0.6165004977655D-20	0.9389233148899D-20
-46.20000000000	0.7530562693848D-20	0.1146792087331D-19
-46.00000000000	0.9198602969656D-20	0.1400693307359D-19
-45.80000000000	0.1123610986873D-19	0.1710801176710D-19
-45.60000000000	0.1372492566953D-19	0.2089565751381D-19
-45.40000000000	0.1676501498827D-19	0.2552187380512D-19
-45.20000000000	0.2047848441281D-19	0.3117231719516D-19
-45.00000000000	0.2501448687978D-19	0.3807324798322D-19
-44.80000000000	0.3055521234968D-19	0.4650313045539D-19
-44.60000000000	0.3732205388889D-19	0.5679874789335D-19
-44.40000000000	0.4559030356074D-19	0.6937327841445D-19
-44.20000000000	0.5568855562496D-19	0.8473287644854D-19
-44.00000000000	0.6802355806050D-19	0.1034924254072D-18
-43.80000000000	0.8309074555471D-19	0.1264052739810D-18
-43.60000000000	0.1014952897423D-18	0.1543909493409D-18
-43.40000000000	0.1239764053961D-18	0.1885725591872D-18
-43.20000000000	0.1514370402888D-18	0.2303218639289D-18
-43.00000000000	0.1849801411684D-18	0.2813143277060D-18
-42.80000000000	0.2259529524054D-18	0.3435963575694D-18
-42.60000000000	0.2760011264869D-18	0.4196674292445D-18
-42.40000000000	0.3371348196000D-18	0.5125803953362D-18
-42.20000000000	0.4118094269026D-18	0.6260640015243D-18
-42.00000000000	0.5030242000465D-18	0.7646725275513D-18
-41.80000000000	0.6144427077137D-18	0.9339685583685D-18
-41.60000000000	0.7505399771964D-18	0.1140746220389D-17

Figure C-6 (continued)

-41.40000000000	0.9167822266241D-18	0.1393303841733D-17
-41.20000000000	0.1119846406356D-17	0.1701776978836D-17
-41.00000000000	0.1367888366881D-17	0.2078545174405D-17
-40.80000000000	0.1670870423517D-17	0.2538728770703D-17
-40.60000000000	0.2040961473682D-17	0.3100795716212D-17
-40.40000000000	0.2493025736400D-17	0.3787302718020D-17
-40.20000000000	0.3045219742885D-17	0.4625800483801D-17
-40.00000000000	0.3719721554688D-17	0.5649939382507D-17
-39.80000000000	0.4543621496287D-17	0.6900819896135D-17
-39.60000000000	0.5550010175790D-17	0.8428642058828D-17
-39.40000000000	0.6779307490741D-17	0.1029472007861D-16
-39.20000000000	0.8280885994408D-17	0.1257394299253D-16
-39.00000000000	0.1011505381986D-16	0.1535778010627D-16
-38.80000000000	0.1235547679942D-16	0.1875795183252D-16
-38.60000000000	0.1509213705589D-16	0.2291091324647D-16
-38.40000000000	0.1843494688706D-16	0.2798333029246D-16
-38.20000000000	0.2251816308259D-16	0.3417876841341D-16
-38.00000000000	0.2750577895843D-16	0.4174586203139D-16
-37.80000000000	0.3359811066003D-16	0.5098829273770D-16
-37.60000000000	0.4103984224862D-16	0.6227697663794D-16
-37.40000000000	0.5012985267069D-16	0.7606494995595D-16
-37.20000000000	0.6123321977266D-16	0.9290555028724D-16
-37.00000000000	0.7479587993407D-16	0.1134746231542D-15
-36.80000000000	0.9136254266472D-16	0.1385976450598D-15
-36.60000000000	0.1115985619306D-15	0.1692828515452D-15
-36.40000000000	0.1363166602794D-15	0.2067616992533D-15
-36.20000000000	0.1665095684248D-15	0.2525382893470D-15
-36.00000000000	0.2033898946378D-15	0.3084497251512D-15
-35.80000000000	0.2484388246191D-15	0.3767398440058D-15
-35.60000000000	0.3034656076674D-15	0.4601492646470D-15
-35.40000000000	0.3706802181282D-15	0.5620253745206D-15
-35.20000000000	0.4527821102336D-15	0.6864566675409D-15
-35.00000000000	0.5530686307489D-15	0.8384368240694D-15
-34.80000000000	0.6755674432964D-15	0.1024065118012D-14
-34.60000000000	0.8251982825310D-15	0.1250791193822D-14
-34.40000000000	0.1007970534217D-14	0.1527714036863D-14
-34.20000000000	0.1231224576010D-14	0.1865947135497D-14
-34.00000000000	0.1503926571159D-14	0.2279064489681D-14
-33.80000000000	0.1837028553975D-14	0.2783645365425D-14
-33.60000000000	0.2243908267998D-14	0.3399939657364D-14
-33.40000000000	0.2740906420588D-14	0.4152680561984D-14
-33.20000000000	0.3347982929858D-14	0.5072077175971D-14
-33.00000000000	0.4089518518461D-14	0.6195026854973D-14
-32.80000000000	0.4995293845751D-14	0.7566595987587D-14
-32.60000000000	0.6101685499600D-14	0.9241828611509D-14
-32.40000000000	0.7453124877970D-14	0.1128795545592D-13
-32.20000000000	0.9103892628011D-14	0.1378709206419D-13
-32.00000000000	0.1112027830410D-13	0.1683953427909D-13
-31.80000000000	0.1358326277771D-13	0.2056778334614D-13
-31.60000000000	0.1659176031853D-13	0.2512146217229D-13
-31.40000000000	0.2026659294678D-13	0.3068332004119D-13
-31.20000000000	0.2475534258116D-13	0.3747656676896D-13
-31.00000000000	0.3023827783864D-13	0.4577383063796D-13
-30.80000000000	0.3693559349759D-13	0.5590809961241D-13
-30.60000000000	0.4511525335079D-13	0.6828608493373D-13

Figure C-6 (continued)

-30.40000000000	0.5510879154302D-13	0.834045434097BD-13
-30.20000000000	0.673145062982BD-13	0.1018702134517D-12
-30.00000000000	0.8222357544975D-13	0.1244241649417D-12
-29.80000000000	0.1004347416510D-12	0.1519715401516D-12
-29.60000000000	0.1226793570816D-12	0.1856178792917D-12
-29.40000000000	0.1498507536588D-12	0.2267134885243D-12
-29.20000000000	0.1830401180619D-12	0.2769076310419D-12
-29.00000000000	0.2235803122547D-12	0.3382147160382D-12
-28.80000000000	0.2730993992393D-12	0.413095141900BD-12
-28.60000000000	0.3335860235150D-12	0.5045540380715D-12
-28.40000000000	0.4074692717646D-12	0.6162618683385D-12
-28.20000000000	0.4977162207764D-12	0.7527017356797D-12
-28.00000000000	0.6079510898813D-12	0.9193493603837D-12
-27.80000000000	0.7426007827510D-12	0.1122892532027D-11
-27.60000000000	0.9070726631248D-12	0.1371500114529D-11
-27.40000000000	0.1107971703442D-11	0.1675149276079D-11
-27.20000000000	0.1353365726444D-11	0.2046026200611D-11
-27.00000000000	0.1653109391073D-11	0.2499015090391D-11
-26.80000000000	0.2019239932944D-11	0.3052295507097D-11
-26.60000000000	0.2466460551109D-11	0.3728071964260D-11
-26.40000000000	0.3012730852373D-11	0.4553465051561D-11
-26.20000000000	0.3679988063457D-11	0.5561599854176D-11
-26.00000000000	0.4495027972479D-11	0.6792935346355D-11
-25.80000000000	0.5490580975308D-11	0.8296888125445D-11
-25.60000000000	0.6706626437012D-11	0.1013381560978D-10
-25.40000000000	0.8191998148411D-11	0.1237743835530D-10
-25.20000000000	0.1000634534691D-10	0.1511779865545D-10
-25.00000000000	0.1222528048078D-10	0.1846487416793D-10
-24.80000000000	0.1492954288022D-10	0.2255299161453D-10
-24.60000000000	0.1823609689690D-10	0.2754621766850D-10
-24.40000000000	0.2227497290220D-10	0.3364494338769D-10
-24.20000000000	0.2720836155737D-10	0.4109326444011D-10
-24.00000000000	0.3323437439858D-10	0.5019211390600D-10
-23.80000000000	0.4059499929576D-10	0.6130463929004D-10
-23.60000000000	0.4958581780960D-10	0.7487747887537D-10
-23.40000000000	0.6056787465225D-10	0.9145534488135D-10
-23.20000000000	0.7398217587543D-10	0.1117035513110D-09
-23.00000000000	0.9036739796575D-10	0.1364347122976D-09
-22.80000000000	0.1103815189610D-09	0.1666413550352D-09
-22.60000000000	0.1348282401887D-09	0.2035357526208D-09
-22.40000000000	0.1646892595953D-09	0.2485985759141D-09
-22.20000000000	0.2011636926009D-09	0.3036383169520D-09
-22.00000000000	0.2457162234218D-09	0.3708638687478D-09
-21.80000000000	0.3001359203702D-09	0.4529731743114D-09
-21.60000000000	0.3666080768438D-09	0.5532615026227D-09
-21.40000000000	0.4478019627563D-09	0.6757536970218D-09
-21.20000000000	0.5469780100324D-09	0.8253657034162D-09
-21.00000000000	0.6681187361435D-09	0.1008101861078D-08
-20.80000000000	0.8160886828422D-09	0.1231295873704D-08
-20.60000000000	0.9968296515224D-09	0.1503905131213D-08
-20.40000000000	0.1217599498744D-08	0.1836870192752D-08
-20.20000000000	0.1487263372521D-08	0.2243554882655D-08
-20.00000000000	0.1816649291214D-08	0.2740277531154D-08
-19.80000000000	0.2218985442519D-08	0.3346976054307D-08
-19.60000000000	0.2710426291600D-08	0.4087997954467D-08

Figure C-6 (continued)

-19.40000000000	0.331070632207 5D-08	0.499308252103 9D-08
-19.20000000000	0.404392994149 4D-08	0.609855334395 8D-08
-19.00000000000	0.493953987982 7D-08	0.744877608652 2D-08
-18.80000000000	0.603349944192 1D-08	0.909793908026 0D-08
-18.60000000000	0.736973658623 3D-08	0.111122276975 1D-07
-18.40000000000	0.900190781233 2D-08	0.135724812902 5D-07
-18.20000000000	0.109955526917 6D-07	0.165774367911 9D-07
-18.00000000000	0.134307255304 2D-07	0.202476916592 1D-07
-17.80000000000	0.164052098682 3D-07	0.247305437582 0D-07
-17.60000000000	0.200384448518 2D-07	0.302059028444 8D-07
-17.40000000000	0.244763211566 8D-07	0.368935108789 1D-07
-17.20000000000	0.298970390209 4D-07	0.450617609225 8D-07
-17.00000000000	0.365182636078 5D-07	0.550384685470 0D-07
-16.80000000000	0.446058650022 0D-07	0.672240280481 8D-07
-16.60000000000	0.544845937737 5D-07	0.821074814632 9D-07
-16.40000000000	0.665511207560 6D-07	0.100286145288 2D-06
-16.20000000000	0.812899646170 9D-07	0.122489582576 1D-06
-16.00000000000	0.992929467476 2D-07	0.149608824890 9D-06
-15.80000000000	0.121282954630 2D-06	0.182732423816 5D-06
-15.60000000000	0.148142967762 9D-06	0.223189547655 0D-06
-15.40000000000	0.180951511791 9D-06	0.272603922388 1D-06
-15.20000000000	0.221025964041 8D-06	0.332958691865 9D-06
-15.00000000000	0.269975449576 5D-06	0.406676072172 7D-06
-14.80000000000	0.329765451438 0D-06	0.496714541019 3D-06
-14.60000000000	0.402796729296 4D-06	0.606876711593 0D-06
-14.40000000000	0.492001715185 1D-06	0.741008951517 9D-06
-14.20000000000	0.600942256680 9D-06	0.905069116146 4D-06
-14.00000000000	0.734054350010 0D-06	0.110545238969 4D-05
-13.80000000000	0.896619732623 5D-06	0.135020075193 9D-05
-13.60000000000	0.109518710175 6D-05	0.164913668623 7D-05
-13.40000000000	0.133773005385 7D-05	0.201425738460 7D-05
-13.20000000000	0.163398678412 6D-05	0.246021622992 2D-05
-13.00000000000	0.199585269255 0D-05	0.300491087818 7D-05
-12.80000000000	0.243785749520 0D-05	0.367020154196 8D-05
-12.60000000000	0.297274860274 9D-05	0.448278830108 0D-05
-12.40000000000	0.363720368719 8D-05	0.547528264853 1D-05
-12.20000000000	0.444270104095 0D-05	0.668751627436 3D-05
-12.00000000000	0.542650269174 3D-05	0.816813941018 9D-05
-11.80000000000	0.662835288539 7D-05	0.997652428486 8D-05
-11.60000000000	0.809626417350 6D-05	0.121853978432 4D-04
-11.40000000000	0.988925466360 3D-05	0.148832564248 3D-04
-11.20000000000	0.120793142601 9D-04	0.181784222835 2D-04
-11.00000000000	0.147543248507 4D-04	0.222031389016 5D-04
-10.80000000000	0.180218404838 0D-04	0.271189280504 0D-04
-10.60000000000	0.220128988927 8D-04	0.331230717394 1D-04
-10.40000000000	0.268872883416 2D-04	0.404565291251 9D-04
-10.20000000000	0.328422295074 3D-04	0.494136060074 3D-04
-10.00000000000	0.401152820384 8D-04	0.603537648225 6D-04
-9.800000000000	0.489989399532 1D-04	0.737160488759 9D-04
-9.600000000000	0.598498509901 7D-04	0.900366993563 7D-04
-9.400000000000	0.731036297035 5D-04	0.109970671640 8D-03
-9.200000000000	0.892923379437 7D-04	0.134317913637 2D-03
-9.000000000000	0.109065833028 5D-03	0.164055459644 1D-03
-8.800000000000	0.133217838458 1D-03	0.200376826040 0D-03
-8.600000000000	0.162717780490 0D-03	0.244738879283 7D-03

Figure C-6 (continued)

-8.400000000000	0.198749663766BD-03	0.298922293499ID-03
-8.200000000000	0.242759539288 9D-03	0.365100938028 3D-03
-8.000000000000	0.296513459329 1D-03	0.445930051456 6D-03
-7.800000000000	0.362168229425 4D-03	0.544652487994 7D-03
-7.600000000000	0.442357723183 6D-03	0.665228689333 4D-03
-7.400000000000	0.540298540250 7D-03	0.812495369950 6D-03
-7.200000000000	0.659918134196 1D-03	0.992359242364 9D-03
-7.000000000000	0.806012242190 8D-03	0.121203349446 8D-02
-6.800000000000	0.984436044311 4D-03	0.148032641608 0D-02
-6.600000000000	0.120233760453 4D-02	0.180799361905 9D-02
-6.400000000000	0.146844234160 0D-02	0.220816772917 3D-02
-6.200000000000	0.179339959574 4D-02	0.269688283778 8D-02
-6.000000000000	0.219020460269 4D-02	0.329371324118 3D-02
-5.800000000000	0.267471192024 3D-02	0.402255318751 9D-02
-5.600000000000	0.326625958872 0D-02	0.491256613648 9D-02
-5.400000000000	0.398842710675 9D-02	0.599934117391 6D-02
-5.200000000000	0.486995472051 9D-02	0.732630038946 1D-02
-5.000000000000	0.594585658896 6D-02	0.894641040908 4D-02
-4.800000000000	0.725876608997 4D-02	0.109242618168 0D-01
-4.600000000000	0.886055779135 3D-02	0.133385925807 7D-01
-4.400000000000	0.108142972329 3D-01	0.162853459037 6D-01
-4.200000000000	0.131965762794 3D-01	0.198813691987 2D-01
-4.000000000000	0.161002977741 1D-01	0.242688790473 9D-01
-3.800000000000	0.196379775330 3D-01	0.296208366848 6D-01
-3.600000000000	0.239456328203 1D-01	0.361473990304 2D-01
-3.400000000000	0.291873207088 1D-01	0.441036302454 1D-01
-3.200000000000	0.355603876027 1D-01	0.537986761079 5D-01
-3.000000000000	0.433014271261 7D-01	0.656066148930 7D-01
-2.800000000000	0.526929756094 6D-01	0.799791992026 3D-01
-2.600000000000	0.640708101360 4D-01	0.974606867691 7D-01
-2.400000000000	0.778316901468 3D-01	0.1187049161118
-2.200000000000	0.944412084198 4D-01	0.1444947045823
-2.000000000000	0.1144412525796	0.1757635200976
-1.800000000000	0.1384563688215	0.2136191924198
-1.600000000000	0.1671980976754	0.2593691773301
-1.400000000000	0.2014661528512	0.3145465675519
-1.200000000000	0.2421451963164	0.3809356716797
-1.000000000000	0.2901960011023	0.4605955901362
-0.800000000000	0.3466400666035	0.5558798614805
-0.600000000000	0.4125373136045	0.6694500089094
-0.400000000000	0.4889573305710	0.8042807674070
-0.200000000000	0.5769456665295	0.9636549803099
-0.355271367880 1D-14	0.677487664486 8	1.151144634098
0.200000000000	0.791513454344 4	1.371296328097
0.400000000000	0.919274403640 5	1.627789873937
0.600000000000	1.062898605642	1.924996313595
0.800000000000	1.221355080651	2.267449182029
1.000000000000	1.395450671015	2.659798092749
1.200000000000	1.585336310174	3.106760842193
1.400000000000	1.791020866005	3.613078625010
1.600000000000	2.012390169791	4.183474171149
1.800000000000	2.249228746819	4.822628154368
2.000000000000	2.501242056020	5.535132164184
2.200000000000	2.768077560296	6.325488230960
2.400000000000	3.049343528121	7.198084338669

Figure C-6 (continued)

2.600000000000	3.344624995619	8.157187152682
2.800000000000	3.653496735042	9.206937079958
3.000000000000	3.975533363429	10.35134677938
3.200000000000	4.310316895949	11.59430230839
3.400000000000	4.657442122411	12.93956619696
3.600000000000	5.016520240509	14.39078185846
3.800000000000	5.387181015087	15.95147886319
4.000000000000	5.769073962843	17.62507870623
4.200000000000	6.161868699305	19.41490079194
4.400000000000	6.565254672635	21.32416843253
4.600000000000	6.978940401231	23.35601471804
4.800000000000	7.402653581150	25.51348816178
5.000000000000	7.836138070532	27.79955806092
5.200000000000	8.279154791003	30.21711953791
5.400000000000	8.731479604755	32.76899824818
5.600000000000	9.192902404626	35.45795475241
5.800000000000	9.663226042153	38.28668856151
6.000000000000	10.14226530941	41.25784186799
6.200000000000	10.62984598376	44.37400298155
6.400000000000	11.12580393990	47.63770948830
6.600000000000	11.62998433015	51.05145115415
6.800000000000	12.14224083184	54.61767259246
7.000000000000	12.66243495897	58.33877571592
7.200000000000	13.19043543450	62.21712199119
7.400000000000	13.72611761926	66.25503451391
7.600000000000	14.26936299302	70.45479992052
7.800000000000	14.82005868333	74.81867015163
8.000000000000	15.37809703817	79.34886408090
8.200000000000	15.94337523803	84.04756902172
8.400000000000	16.51579494395	88.91694212307
8.600000000000	17.09526197784	93.95911166474
8.800000000000	17.68168603209	99.17617826118
9.000000000000	18.27498040528	104.5702159822
9.200000000000	18.87506176164	110.1432733982
9.400000000000	19.48184991170	115.8973745560
9.600000000000	20.09526761198	121.8345198928
9.800000000000	20.71524038195	127.9568870912
10.00000000000	21.34169633635	134.2658318833
10.20000000000	21.97456603145	140.7638888053
10.40000000000	22.61378232388	147.4527719088
10.60000000000	23.25928024068	154.3343754307
10.80000000000	23.91099685959	161.4105744266
11.00000000000	24.56887119858	168.6832253689
11.20000000000	25.23284411372	176.1541667134
11.40000000000	25.90285820456	183.8252194363
11.60000000000	26.57885722647	191.6981875439
11.80000000000	27.26078850911	199.7748585522
12.00000000000	27.94859783069	208.0570039723
12.20000000000	28.64223459731	216.5463296995
12.40000000000	29.34164877711	225.2442264816
12.60000000000	30.04679183865	234.1523702934
12.80000000000	30.75761644337	243.2722227225
13.00000000000	31.47407644159	252.6107813346
13.20000000000	32.19612682183	262.1621300221
13.40000000000	32.92372366334	271.9309393386

Figure C-6 (continued)

13.60000000000	33.65682409128	281.9188668193
13.80000000000	34.39538623462	292.1275572880
14.00000000000	35.13936918647	302.5586431529
14.20000000000	35.88873296654	313.2137446896
14.40000000000	36.64343848580	324.0944703141
14.60000000000	37.40344751293	335.2024168448
14.80000000000	38.16872264270	346.5391697553
15.00000000000	38.93922726587	358.1063034176
15.20000000000	39.71492554073	369.9053813363
15.40000000000	40.49578236606	381.9379563752
15.60000000000	41.28176335544	394.2055709254
15.80000000000	42.07283481280	406.7097573660
16.00000000000	42.86896370920	419.4520377675
16.20000000000	43.67011766066	432.4339245892
16.40000000000	44.47626490707	445.6569206187
16.60000000000	45.28737429206	459.1225192068
16.80000000000	46.10341524376	472.8322044451
17.00000000000	46.92435775651	486.7874513388
17.20000000000	47.75017237325	500.9897259742
17.40000000000	48.58083016878	515.4404856802
17.60000000000	49.41630273372	530.1411791858
17.80000000000	50.25656215910	545.0932467727
18.00000000000	51.10158102167	560.2981204225
18.20000000000	51.95133236979	575.7572239611
18.40000000000	52.80578970985	591.4719731975
18.60000000000	53.66492699329	607.4437760599
18.80000000000	54.52871860415	623.6740327265
19.00000000000	55.39713934706	640.1641357542
19.20000000000	56.27016443572	656.9154702028
19.40000000000	57.14776948183	673.9294137558
19.60000000000	58.02993048444	691.2073368386
19.80000000000	58.91662381969	708.7506027328
20.00000000000	59.80782623093	726.5605674883
20.20000000000	60.70351481920	744.6385810313
20.40000000000	61.60366703409	762.9859852711
20.60000000000	62.50826066487	781.6041162026
20.80000000000	63.41727383199	800.4943030072
21.00000000000	64.33068497885	819.6578683513
21.20000000000	65.24847286385	839.0961284811
21.40000000000	66.17061655273	858.8103933168
21.60000000000	67.09709541118	878.8019665432
21.80000000000	68.02788909765	899.0721456989
22.00000000000	68.96297755649	919.6222222627
22.20000000000	69.90234101120	940.4534817389
22.40000000000	70.84595995800	961.5672037395
22.60000000000	71.79381515959	982.9646620655
22.80000000000	72.74588763903	1004.647124786
23.00000000000	73.70215867392	1026.615854314
23.20000000000	74.66260979071	1048.872107485
23.40000000000	75.62722275921	1071.417135628
23.60000000000	76.59597958724	1094.252184638
23.80000000000	77.56886251543	1117.378495049
24.00000000000	78.54585401229	1140.797302099
24.20000000000	79.52693676922	1164.509835802
24.40000000000	80.51209369609	1188.517321011

Figure C-6 (continued)

24.60000000000	81.50130791612	1212.820977484
24.80000000000	82.49456276198	1237.422019949
25.00000000000	83.49184177121	1262.321658162
25.20000000000	84.49312868207	1287.521096872
25.40000000000	85.49840742949	1313.021536378
25.60000000000	86.50766214108	1338.824171590
25.80000000000	87.52087713334	1364.930193083
26.00000000000	88.53803690787	1391.340786655
26.20000000000	89.55912614777	1418.057133482
26.40000000000	90.58412971410	1445.080410171
26.60000000000	91.61303264242	1472.411789814
26.80000000000	92.64582013950	1500.052437040
27.00000000000	93.68247757998	1528.003518063
27.20000000000	94.72299050330	1556.266190737
27.40000000000	95.76734461053	1584.841609599
27.60000000000	96.81552576141	1613.730924922
27.80000000000	97.86751997142	1642.935282761
28.00000000000	98.92331340892	1672.455824996
28.20000000000	99.98289239238	1702.293689381
28.40000000000	101.0462433876	1732.450009589
28.60000000000	102.1133530053	1762.925915254
28.80000000000	103.1842079983	1793.722532011
29.00000000000	104.2587952589	1824.840981548
29.20000000000	105.3371018169	1856.282381635
29.40000000000	106.4191148369	1888.047846176
29.60000000000	107.5048216158	1920.138485241
29.80000000000	108.5942095811	1952.555405109
30.00000000000	109.6872662879	1985.299708309
30.20000000000	110.7839794174	2018.372493652
30.40000000000	111.8843367745	2051.774856275
30.60000000000	112.9883262858	2085.507887671
30.80000000000	114.0959359974	2119.572675731
31.00000000000	115.2071540732	2153.970304779
31.20000000000	116.3219687929	2188.701855402
31.40000000000	117.4403685500	2223.768405491
31.60000000000	118.5623418500	2259.171028271
31.80000000000	119.6878773086	2294.910794332
32.00000000000	120.8169636503	2330.988770670
32.20000000000	121.9495897059	2367.406020912
32.40000000000	123.0857444116	2404.163605348
32.60000000000	124.2254168070	2441.262580968
32.80000000000	125.3685960333	2478.704001486
33.00000000000	126.5152713324	2516.488917375
33.20000000000	127.6654320444	2554.618375895
33.40000000000	128.8190676071	2593.093421123
33.60000000000	129.9761675536	2631.915093980
33.80000000000	131.1367215117	2671.084432264
34.00000000000	132.3007192019	2710.602470671
34.20000000000	133.4681504361	2750.470240831
34.40000000000	134.6390051166	2790.688771329
34.60000000000	135.8132732343	2831.259087734
34.80000000000	136.9909448678	2872.182212625
35.00000000000	138.1720101818	2913.459165618
35.20000000000	139.3564594261	2955.090963393
35.40000000000	140.5442829344	2997.078619713

Figure C-6 (continued)

35.60000000000	141.7354711227	3039.423145457
35.80000000000	142.9300144888	3082.125548641
36.00000000000	144.1279036104	3125.186834440
36.20000000000	145.3291291445	3168.608005216
36.40000000000	146.5336818263	3212.390060539
36.60000000000	147.7415524676	3256.533997211
36.80000000000	148.9527319565	3301.040809290
37.00000000000	150.1672112557	3345.911488109
37.20000000000	151.3849814016	3391.147022304
37.40000000000	152.6060335038	3436.748397831
37.60000000000	153.8303587435	3482.716592989
37.80000000000	155.0579483729	3529.052603445
38.00000000000	156.2887937139	3575.757392247
38.20000000000	157.5228861576	3622.831939855
38.40000000000	158.7602171633	3670.277219154
38.60000000000	160.0007782572	3718.094200476
38.80000000000	161.2445610321	3766.283851623
39.00000000000	162.4915571460	3814.847137883
39.20000000000	163.7417583217	3863.785022052
39.40000000000	164.9951563458	3913.098464451
39.60000000000	166.2517430677	3962.788422948
39.80000000000	167.5115103989	4012.855852973
40.00000000000	168.7744503127	4063.301707542
40.20000000000	170.0405548424	4114.126937268
40.40000000000	171.3098160817	4165.332490386
40.60000000000	172.5822261829	4216.919312766
40.80000000000	173.8577773571	4268.888347934
41.00000000000	175.1364618726	4321.240537086
41.20000000000	176.4182720550	4373.976819109
41.40000000000	177.7032002860	4427.098130595
41.60000000000	178.9912390027	4480.605405859
41.80000000000	180.2823806972	4534.499576954
42.00000000000	181.5766179159	4588.781573692
42.20000000000	182.8739432586	4643.452323653
42.40000000000	184.1743493781	4698.512752207
42.60000000000	185.4778289794	4753.963782528
42.80000000000	186.7843748194	4809.806335608
43.00000000000	188.0939797058	4866.041330274
43.20000000000	189.4066364968	4922.669683203
43.40000000000	190.7223381007	4979.692308937
43.60000000000	192.0410774750	5037.110119898
43.80000000000	193.3628476256	5094.924026402
44.00000000000	194.6876416072	5153.134936674
44.20000000000	196.0154525215	5211.743756862
44.40000000000	197.3462735176	5270.751391054
44.60000000000	198.6800977912	5330.158741286
44.80000000000	200.0169185837	5389.966707562
45.00000000000	201.3567291824	5450.176187865
45.20000000000	202.6995229193	5510.788078170
45.40000000000	204.0452931709	5571.803272459
45.60000000000	205.3940333579	5633.222662733
45.80000000000	206.7457369443	5695.047139025
46.00000000000	208.1003974371	5757.277589416
46.20000000000	209.4580083862	5819.914900044
46.40000000000	210.8185633832	5882.959955117

Figure C-6 (continued)

46.60000000000	212.1820560616	5946.413636928
46.80000000000	213.5484800958	6010.276825866
47.00000000000	214.9178292014	6074.550400429
47.20000000000	216.2900971339	6139.235237234
47.40000000000	217.6652776888	6204.332211033
47.60000000000	219.0433647012	6269.842194720
47.80000000000	220.4243520450	6335.766059348
48.00000000000	221.8082336330	6402.104674135
48.20000000000	223.1950034159	6468.858906480
48.40000000000	224.5846553826	6536.029621973
48.60000000000	225.9771835591	6603.617684406
48.80000000000	227.3725820087	6671.623955785
49.00000000000	228.7708448312	6740.049296339
49.20000000000	230.1719661627	6808.894564533
49.40000000000	231.5759401753	6878.160617079
49.60000000000	232.9827610766	6947.848308944
49.80000000000	234.3924231093	7017.958493365
50.00000000000	235.8049205511	7088.492021855

END OF FILE

READY

Figure C-6 (continued)

5. GUIDE TO EXECUTING THE SURFACE PROGRAM WITH CDC 6600

SURFACE is a program designed to calculate the number of interface states at a semiconductor-oxide boundary. The algorithms used in the program are derived from the equations and methods which are previously explained in this report.

The purpose of this section is to aid the user in successfully executing the program. It is written specifically for CDC 6600 users at the Air Force Weapons Laboratory, Kirtland Air force Base, New Mexico. The following CDC manuals contain necessary reference information:

Scope Reference Manual

Scope Users Guide

INTERCOM Reference Manual (for user utilizing the sharing system)

FORTRAN Extended Reference Manual

This document contains two major sections:

a. Files - contains a description of the source code, and a description and the format for the input files.

b. Execution - contains brief descriptions of SCOPE control commands; commands for execution using cards; commands for execution using INTERCOM.

a. Files:

1) Source File: The source program was written at UNM for the IBM-360 model computer. It is coded in FORTRAN and contains numerous comments in each subroutine explaining the purpose of the routine.

Since IBM-FORTRAN and CDC-FORTRAN are not identical, a number of changes had to be made to make it compatible with the CDC-6600 model computer:

a) The most significant change dealt with precision. The model 360 computer uses a 32 bit word and the original program was written with all variables and constants in double precision. The 6600 computer uses a 60 bit word so the source code and data were put into single precision form.

b) The CDC and IBM models also use different internal codes for special characters. For example, all "=" signs were read as "#" signs by the CDC computer and had to be changed.

c) A number of other minor changes were made in order to make the code CDC compatible.

d) Only two logic changes were made.

1 The program has a curve fitting routine in it. This routine is capable of doing a linear (first order) fit or a fourth order fit. In the original program the flag which determined the order of curve fitting was "hard coded"--so that if the user wanted to change the curve fitting he had to replace a source card and recompile. The new program allows the user to enter

this flag as INPUT so no recompilation is necessary.

2 The original program had the Fermi integral and the device data as one input file. This has been changed so that they are now separate input files. This makes program execution much easier when data are stored on tape or disk. However, the files can still be entered on cards if that is desired.

2) Input Files and Output Files: The following are the descriptions of the input files.

Fermi File: The Fermi File is a table of values for the Fermi integral

$$F_j(n) = \int_0^\infty \frac{x^j dx}{1 + \exp(x-n)}$$

The mathematics require values of this integral for $F_{1/2}$ and $F_{3/2}$ at various arguments n. Having a routine which did this integration each time it was needed was found to be too time consuming. Therefore, a separate program was run once to do the integral at periodic steps through the possible range of arguments. The values obtained are the entries in the Fermi table. Each table entry has the argument and $F_{1/2}$ and $F_{3/2}$ for that argument.

There are 501 entries for arguments -50 to +50 by 0.2. The argument value is normalized to units of kT. This gives values for the Fermi integral from just below the valance band to just above the conduction band. A binary search is used to find the argument entry in the table. If a value is needed for an argument between two table arguments, a linear interpolation is used. Both of these tasks are performed in the F32 Function Subroutine.

Card #	Fortran Variable	Columns	Input Variable	Description
Each of	FERMI(I,1)	1-20	G20.13	Argument
501 cards		21-25	5x	Blank
I = 1, 501	FERMI(I,2)	26-45	G20.13	$F_{1/2}$
		46-50	5x	Blank
	FERMI(I,3)	51-70	G20.13	$F_{3/2}$

Data File: The first two cards are header cards with pertinent information about the data. The remaining cards contain the raw data for one device at one radiation dosage.

Card #	Fortran Variable	Columns	Input Format	Description
1	INAME	1-80	20A4	Unique identification for this particular device
2	ND	1-10	G10.4	Donor Density (per cubic cm.)
	NA	11-20	G10.4	Acceptor Density (per cubic cm.)
	PHS1	21-30	G10.4	Initial Surface Potential (Units of kT)
	COX	31-40	G10.4	Oxide Capacitance (Farads/sq.cm.)
	T1	41-50	G10.4	Lower Temperature (Kelvin)
	T2	51-60	G10.4	Upper Temperature (Kelvin)
	MAGFLD	61-70	G10.4	Magnetic Field Strength (Gauss)
	IND	71-73	I3	+1 for N-channel +2 for P-channel
	NVGPT1	74-76	I3	Number of different values of VG at which Lower Temperature was taken
	NVGPT2	77-79	I3	Number of different values of VG at which Upper Temperature was taken
	NORDER	80	I1	NORDER=1 First Order Polynomial is used to fit VG(NH) or NORDER=4 Fourth Order Polynomial is used to fit VG(NH)

The raw data are then fed into a two dimensional array called

DATA (I,J)

Card #	Variable	Columns	Format	Description
The next NVGPT1 cards I=1 to NVGPT1	DATA(I,1)	1-8	G8.4	VG-Gate voltage (volts)
	DATA(I,2)	9-16	G8.4	I12-indicates current through terminals 1 to 2 (milliamps)
	DATA(I,3)	17-24	G8.4	V34-indicates voltage across terminals 3 & 4 (millivolts)
	DATA(I,4)	25-32	G8.4	I23
	DATA(I,5)	33-40	G8.4	V41
	DATA(I,6)	41-48	G8.4	I34
	DATA(I,7)	49-56	G8.4	V12
	DATA(I,8)	57-64	G8.4	I41
	DATA(I,9)	65-72	G8.4	V23
The next NVGPT1 cards	DATA(I,10)	1-8	G8.4	I24 Mag. field off
	DATA(I,11)	9-16	G8.4	V13 Mag. field off
	DATA(I,12)	17-24	G8.4	V13 Mag. field on
	DATA(I,13)	25-32	G8.4	I13 Mag. field off
	DATA(I,14)	33-40	G8.4	V24 Mag field off
	DATA(I,15)	41-48	G8.4	V24 Mag field on
Above Data at lower temperature				
The next NVGPT2 cards	DATA(I,J) I=1, NVGPT2 J=16,24		9G8.4	Same as J=1 to 9 except data for upper temperature
The next NVGPT2 cards	DATA(I,J) I=1,NVGPT2 J=25,30		6G8.4	Same as J=1,15 except for upper temperature

b. Execution of the Program:

1) Control Card Description: Compiling and executing the program can be done in a number of ways. In this section two ways are explained. The first tells how to compile and execute using cards for all input files. The second explains how to execute the program using the Intercom time sharing system. The use of the time sharing system frees the user from handling cards once the initial files are made. It is an easy and useful system; however, to use it the user must familiarize himself with the Intercom Language--see the CDC Intercom Reference Manual.

Both the card method and the time sharing method require knowledge of SCOPE Commands. The following is a very brief summary of some of the more frequent control commands necessary for running the program. However, do not rely on this summary alone. See the Scope Reference Manual and the Scope Users Guide for complete information regarding these commands.

The three cards you must have to run any program are the JOBCARD, ACCOUNT Card and Delimiter Card.

JOBCARD:

The first card of any program is the JOBCARD. It consists of a JOB name followed by a period. (There are parameters you may add to adjust program running time and priority, etc. See your Scope Manual.)

Example: MYPROG.

ACCOUNT Card:

Col. 1 - All control cards start in Column 1. The ACCOUNT card gives accounting information so that the proper person or department will be charged for the computer time used.

Example: ACCOUNT (parameters)

Check with the Computing Center for the proper use of the parameters. They will keep you informed of any changes in the format.

NOTE: All examples of a control card deck assume a JOB card and an ACCOUNT card precede the deck.

Delimiter Cards:

Delimiter cards are used to separate groups of cards used for different Input files. A delimiter card is also used to signal the end of your job.

- Delimiter cards used to separate input groups are cards with a multipunched 7, 8, and 9 in the first column. They are indicated in this document simply by "789"; however, the numbers are punched only in column 1.

- Delimiter cards for "End of Job" are a multipunched 6, 7, 8, and 9 in the first column. They are indicated in the document by "6789."

Other Cards

a) The FTN card. The FTN card calls in the FORTRAN Extended compiler. There are a number of parameters which the user may define or may leave to the default specifications.

Examples: FTN.

FTN(I=COMEIN,B=OBJECT,OPT=2)

The first example indicates FORTRAN compilation using all the default specifications. In the second example I=COMEIN indicates the source file in the file COMEIN (Default I=INPUT). B=OBJECT indicates that the executable object deck will be put

in a file called OBJECT. (Default B=LGO)

OPT=2 indicates that the level of optimization is 2 (fast execution) (Default OPT=1).

b) ATTACH card--The ATTACH card makes a permanent disk file available for the use of your job.

Example:

ATTACH (DATA,DEVICE1,ID=UNMABC,CY=3)

DEVICE1 is the permanent file name.

DATA is the logical file name (the name of the file for this job only).

CY=3 indicates that the third cycle is to be used. Each time you catalog a file with the name DEVICE1, another cycle is created (up to 99). Omitting the CY=x parameter defaults to the highest numbered cycle.

ID=UNMABC--An ID identification is given to every user by the Computing Center. It is used for accounting and also for storing your permanent files together.

c) CATALOG card--The CATALOG card makes a logical file used by a JOB (or created by the JOB) a permanent disk file.

Example:

CATALOG(OUT1,DEVICE2,ID=UNMABC,RP=100)

OUT1 is logical file created by this program.

DEVICE2 is a permanent file name under which the logical file will be stored.

ID = See ID under ATTACH.

RP = 100--RP means retention period in days. In this example the Permanent file will be scratched after 100 days.

d) REQUEST card--Allows user to request a disk or tape storage unit for a file.

Example:

REQUEST(DEVICE2,*PF)

DEVICE2--is the file name to be stored on the device.

*PF indicates that the file will be a permanent disk file.

e) REWIND card--the REWIND card sets a file to its initial position. It is used, normally, when a file has been used in one step and must be reused later in the job.

Example:

REWIND(FERMI,TOM)

Files FERMI and TOM are rewound to their initial positions.

f) COPY card--The COPY card allows the user to copy information from one file to another.

2) Executing the Program from Cards

The program is looking for two input files (FERMI and DATA) and puts out two output files (OUT1,OUT2). (See FILES.) To read the two input files in card form the cards must be copied to a file with the name FERMI or DATA. This file must be rewound so that the cards are positioned at their starting points when execution begins:

CONTROL CARDS

```
     JOB CARD
     ACCOUNT CARD
     FTN
     COPYCR (INPUT,FERMI)
     COPYCR (INPUT,DATA)
     REWIND (FERMI,DATA)
            (,,OUTPUT)
     789
          Source Deck goes here
     789
          Fermi Deck goes here
     789
          Data Deck goes here
    6789
```

FTN. The FTN card assumes that input to the compiler is on file INPUT (unless stated otherwise). This causes the computer to skip down to the first 789 delimiter and read all the cards up to the next delimiter as FORTRAN statements. B = RUN puts the object file in a file called RUN (arbitrary name). COPYCR (INPUT,FERMI).

This tells the computer to read all the cards between the second and third delimiters and put them in a temporary file named FERMI.

COPYCR (INPUT,DATA). This takes all the cards between 3rd and 4th delimiters and puts them on a file named DATA.

REWIND (FERMI,DATA). Positions the newly created temporary files at their starting points.

RUN (,,OUTPUT). RUN (same name as in B = lfn on FTN card) tells the computer to execute the compiled program which is on the file RUN.

The first card of the program lists the files used

PROGRAM SURF (FERMI,DATA, OUT1,OUT2,etc.)

The (,,OUTPUT) replaces OUT1 with OUTPUT so that the main print file OUT is channeled to the general OUTPUT file. The two preceding commas are necessary since RUN(OUTPUT) will replace FERMI with OUTPUT.

The second OUTPUT file OUT2 is typically a punch card output (see FILES). If this is desired, use RUN (,,OUTPUT,PUNCH).

This will associate OUT1 with OUTPUT and OUT2 with the punch file PUNCH.

NOTE: Order is important with these control cards. If FTN precedes the COPYCR cards then the SOURCE cards must precede both data files. If COPYCR (INPUT,FERMI) precedes COPYCR (INPUT,DATA), then the FERMI file cards must precede the data file cards.

3) Execution of the Program Using the Time Sharing Mode-Intercom

Utilizing the time sharing terminals is the easiest way to execute the program once the user's files have been established. The advantages are:

a) No cards need be stored or handled.

b) A card reader is not required.

c) The text editor can be used to change any of the files or create new data files directly (without punching cards).

d) An object file can be created so that the program need not be recompiled until the source code is changed.

e) The output can be channeled to a file any part of which can be viewed at the terminal with the Intercom PAGE command mode or Text Editor Mode. The user then, if he chooses, may have all or part of the output channeled to a line printer for a hard copy.

The following is a listing of procedures.

a) Preliminaries: To Use the Intercom time sharing system, the user must notify the Computing Center in order to obtain a terminal ID number and a password, if he does not have one already. Call the Consulting Office (505-264-0831) for assistance. To use the system effectively you must become familiar with the basic Intercom control language including the TEXT EDITOR.

b) Establishing the files from cards: Cards are entered in batch queue using appropriate Scope control cards. The

card file, which is to be made a disk file on the Intercom System, is entered as data.

```
JOBCARD
ACCOUNT (parameters)
REQUEST (DISK,*PF)
COPYCR (INPUT,DISK)
CATALOG (DISK,SOURCE,ID=ABCUNM,RP=999)
789
  Card file goes here.
6789
```

REQUEST - allocates disk space for file

DISK - arbitrary temporary file name

COPYCR - copies the card file to the temporary file DISK

CATALOG - makes the temporary file DISK a permanent file,

SOURCE (arbitrary name).

ID - users ID

RP - 999 when the retention period is 999, the file is *never* scratched.

c) Getting into Intercom - Telephone Hookup:

If a telephone hookup is used, dial one of the tie-in numbers (call Consulting for these numbers) and wait for the tone. NOTE: If the terminal can be used offline it will have an ON LINE button. Make sure terminal is on line.

Press the space bar and then the RETURN key.

The Computer will respond with a heading and date and then

PLEASE, LOGIN

You type

LOGIN,password,ID

Example:

LOGIN,12345678,ABCUNM

The system responds, "READY."

You are now in COMMAND MODE.

d) Running the Program

If you have established the files correctly as in 3,b) you should have at least two files--the Source file and the Fermi file.

Example: Let us say that you have given them the permanent file names of SOURCE and FERMI respectively.

You may also have one or more data files and an object file.

Example: Let us say there is one data file called DATA.

1) Creating another data file.

Type in EDITOR--this puts the system in Text Editor mode. System responds with two dots ".." when in Editor mode, with READY when in command mode.

Type in F,CH=80.

F allows the format to be changed.

CH=80 allows 80 characters for each line (this is card image).

Type in CREATE.

System responds with line number=

Example:

100=

Type in a line of Data (as if you were using a key-punch and cards). When you finish the line, hit the return key--system will respond with new line number automatically incremented.

If you make a mistake in the line you were entering you may backspace and retype from the error.

When you finish entering all the information type an = sign following the system = sign.

Example:

400==

This will get you out of CREATE mode and allow you to use other commands.

To save the finished file

Type SAVE,lfn,N

lfn is a Logical File Name which you choose

N means no sequence--do not store file with the antecedent sequence numbers

Example:

SAVE,DATAFILE,N

To make this new Data File a permanent file,

Type CATALOG(lfn,pfn,ID=xxxxxx,RP=xxx)

lfn = logical file name

pfn = permanent file name

ID = user ID

RP = retention period

Example:

CATALOG(DATAFILE,DATA,ID=ABCUNM,RP=20)

In this example we have already created a permanent file called DATA from cards

Therefore the system responds

PF = DATA

CYCLE = 002

You now have two sets of data in a file called Data-- the first having a cycle of 1, the second having a cycle of 2.

2) Creating control cards to compile and execute the program.

Create a file as immediately above.

The control cards are

JOBCARD

ACCOUNT(parameters)

ATTACH(lfn,pfn,ID=xxxxxx,CY=xxx)

FTN(parameters)

CATALOG(lfn,pfn,ID=xxxxxx,RP=xx)

EOF

EOR

JOBCARD

Explained previously.

ACCOUNT

EOF

takes the place of the multipunch 789 and 6789 cards

EOR

ATTACH--brings in the required file.

There must be one for each file used.

CY = Cycle #

CATALOG--catalogs new files created (output from program).

FTN--brings in FORTRAN compiler--compiles and executes the program.

Example:

```
ATTACH(PROG,SOURCE,ID=ABCUNM)
ATTACH(FERMI,FERMI,ID=ABCUNM)
ATTACH(DATA,DATA,ID=ABCUNM)CY=1)
FTN(I=PROG)
CATALOG(OUT1,DATAOUT,ID=ABCUNM,RP=30)
```

First two cards bring in source and FERMI files, third card brings in data file (Cycle 1). If CY=x is omitted as in the first two, the highest numbered cycle is used. Therefore, to run the program with Cycle 2 data specify CY=2 or omit CY=x altogether.

The FTN card--See your CDC FORTRAN Extend Manual.

I=PROG--Specifies source file to be compiled. Name must be identical with lfn of the ATTACH card for the source file.

The Program is looking to read two sets of data. One is a file called FERMI, the other is a file called DATA. The lfn names for the second and third cards must be FERMI and DATA.

The program's main output goes to lfn OUT1.

The catalog card is needed, otherwise file OUT1 will be lost when job terminates. The lfn of the catalog card must be OUT1, the pfn is arbitrary.

Once you have created the control card file using the Text Editor, save it with the save command as before

SAVE,lfn,N.

Example:

SAVE,CONTROL,N

NOTE: You may wish to catalog this control file as a permanent file, so that successive executions need only change the cycle number of the data ATTACH card.

3) To execute the program,

Type in BATCH,lfn,INPUT,HERE

BATCH--tells the system to use batch mode for the file lfn

INPUT--means its card image input

HERE--indicates output is to be returned to the terminal you are using.

lfn--logical file containing control commands

Example:

BATCH,CONTROL,INPUT,HERE

When the execution of the program is completed, the output file OUT1 will be in a permanent file DATAOUT (according to the CATALOG card in #2 above). This file may be made local using the ATTACH command and inspected using the PAGE command (see your INTERCOM manual).

ABBREVIATIONS AND SYMBOLS

Å	angstroms
ac	alternating current
°C	degrees centigrade
CRT	cathode ray tube computer display terminal
C-V	capacitance-voltage
dc	direct current
D.I.	deionized
DVM	digital volt meter
eV	electron volt
FET	field effect transistor
HF	high frequency
kG	kilogauss
K	temperature, Kelvin
LF	low frequency
MHz	megahertz
MOS	metal-oxide-semiconductor
MOSFET	metal-oxide-semiconductor field effect transistor
N_2	nitrogen
QS	quasi static
RPM	revolutions per minute
SCCM	standard cubic centimeters per minute

ABBREVIATIONS AND SYMBOLS (continued)

a	voltage sweep rate
B	susceptance
C_a	accumulation region capacitance
C_d	depletion region capacitance
C_{HF}	measured high frequency capacitance
C'_{HF}	high frequency capacitance with series resistance effects removed
C_i	inversion region capacitance
C_{LF}	measured low frequency capacitance
C_{meas}	measured capacitance at the terminals of an MOS capacitor
C_{ox}	oxide capacitance
C_{sc}	space charge capacitance
C_{ss}	surface state capacitance
D	a differential operator
$D_C(E)$, $D_V(E)$	density of states function in the conduction and valence band respectively
E	energy
E_A	acceptor energy level
E_c	conduction band energy level
E_D	donor energy level
E_f	Fermi energy level
E_g	band gap energy
E_i	intrinsic energy level error in i^{th} data point evaluation
E_v	valence band energy level
f	geometrical correction factor used in Hall calculations electron occupation probability
G	conductance

AD-A064 143 NEW MEXICO UNIV ALBUQUERQUE BUREAU OF ENGINEERING R--ETC F/G 9/1
INVESTIGATION OF INTERFACE STATES USING METAL-OXIDE-SILICON TRA--ETC(U)
AUG 78 J WHITEFIELD, H D SOUTHWARD F29601-75-C-0036
UNCLASSIFIED EE-247(77)AF-352-1 AFWL-TR-77-140-VOL-1 NL

4 OF 4
AD
A064143

END
DATE
FILMED
4-79
DDC

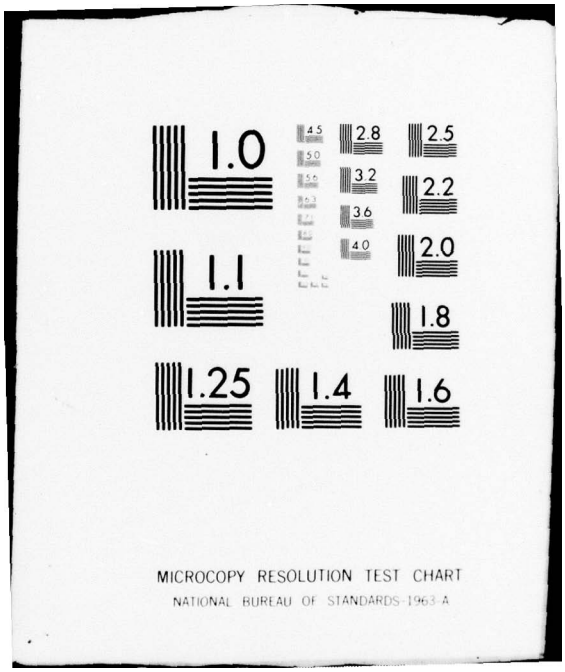
1.0
1.1
1.25
1.4
1.6
1.8
2.0
2.2
2.5
2.8
3.2
3.6
4.0
4.5
5.0
5.6
6.3
MICROCOPY RESOLUTION TEST CHART
NATIONAL BUREAU OF STANDARDS-1963-A

ABBREVIATIONS AND SYMBOLS (continued)

h	Plank's constant
i	time varying current
I	dc current
I_{SD}	source-drain current
I_{ij}	current flowing from terminal i to terminal j
k	Boltzmann's constant
L	effective Debye length
L_C	effective charge distance
L_D	depletion region width Debye length
L_{Dmax}	maximum depletion region width
m_n^* , m_p^*	effective mass for holes and electrons
n	electron concentration
n_A^-	ionized acceptor concentration
n_b	bulk electron concentration
n_D^+	ionized donor concentration
n_i	intrinsic electron concentration
N_A	acceptor concentrations
$\langle N_A \rangle$	average acceptor concentrations
N_c	effective density of states in the conduction band
N_D	donor concentration
N_d	depleted surface carrier concentration
N_H	Hall carrier concentration
N_i	induced surface carrier concentration
N_{ss}	interface state density
ΔN	excess surface electron density
p	hole concentration

ABBREVIATIONS AND SYMBOLS (continued)

p_b	bulk hole concentration
P_s	Ettinghausen coefficient
ΔP	excess surface hole concentration
q	absolute value of the electronic charge
Q_{ox}	charge on the oxide surface
Q_{sc}	net charge in a space charge region
Q_{ss}	charge trapped in surface states
Q_t	charge trapped in the oxide
r	Hall mobility ratio
R_c	generation-recombination resistance between the valence and conduction band
R_s	series substrate resistance Hall coefficient
R_v	generation-recombination resistance from the surface states to the valence band
T	temperature
t	thickness time
t_{ox}	oxide thickness
u	dimensionless potential
u_b, u_s	value of u in the bulk and at the surface
v	dimensionless potential barrier
v_s	value of v at the surface
V	potential barrier
V_a	applied voltage
V_E	Ettinghausen-Seebeck voltage
V_{fb}	flat band voltage
V_g	gate voltage

ABBREVIATIONS AND SYMBOLS (continued)

V_H	Hall voltage
V_{ox}	voltage across an oxide
V_s	potential barrier at the surface of a semiconductor
V_{SD}	source-drain voltage
V_{th}	threshold voltage
w	rate of change of the Hall carrier concentration with respect to the induced surface carrier concentration
$w_{P,Q}$	dimensionless energy difference between two levels P and Q
X_c	capacitive reactance
Y	admittance
Z	impedance
α	defined in Equation 77, determined from experimental data
β	defined in Equation 92, determined from experimental data
β_o	defined in Equation 80
γ	a computational constant defined by Equation 180
ε_o	permittivity of free space
θ	Seebeck coefficient
κ_{ox}	dielectric constant of the oxide
κ_s	dielectric constant of silicon
λ_i	a coefficient in either a polynomial or spline expansion
μ_H	Hall mobility
μ_σ	conductivity mobility
ξ	electric field a dummy computational variable defined in Equation 180

ξ_s	value for the electric field at the semiconductor surface
ρ	charge density
ρ_A	charge density due to ionized acceptors
ρ_D	charge density due to ionized donors
ρ_S	sheet resistivity
ρ_i	tension coefficient
$\sigma_\square$	sheet conductivity
τ_i	the i^{th} polynomial or sum of splines in an expansion approximation
ϕ	potential
ϕ_b, ϕ_s	values for ϕ in the bulk and at the surface of the semiconductor
Φ	potential, measured with a different zero potential than ϕ
Φ_s	value of Φ at the surface of the semiconductor
ω	frequency